The University Of Sheffield.

Dystroglycan in the nucleus and the cell cycle

By:

Laura Jacobs

A thesis submitted in partial fulfilment of the requirements for the degree of Doctor of Philosophy

The University of Sheffield
Faculty of Science
Department of Biomedical Science

September 2016

ABSTRACT

Dystroglycan is a ubiquitously expressed adhesion receptor and signalling scaffold found at the plasma membrane. DG function at the PM is disrupted in multiple human diseases including muscular dystrophy and epithelial carcinomas. More recently DG has also been identified in the nucleus of many cell types, however its nuclear functions and the mechanisms of its nuclear localisation are relatively poorly understood. In support of a growing number of reports, in this thesis βDG was found to localise at the nuclear envelope, nucleoplasm and distinct nuclear foci in multiple prostate cell lines, normal and cancerous. Furthermore, in fibroblasts lacking DG, nuclear morphology was severely disrupted, supporting a role for DG in nuclear structure. The nuclear levels of βDG are variable suggesting a dynamic regulation. DG protein levels and localisation have previously been reported to be regulated in a cell cycle dependent manner. Upon investigation via immunoblots, the nuclear levels of βDG also appear to slightly fluctuate in a cell cycle dependent manner, with an increase in the nuclear levels of a phosphorylated form (pY892) of βDG weakly correlating with cells in S phase following quantification, however this observation was not supported via immunofluorescence analysis and requires additional investigation. To further understand the precise mechanisms of nuclear translocation of βDG we investigated a role for regulatory post-translational modification, specifically phosphorylation at residue T788 within the c-terminal of βDG. Whilst mutations at residue T788 did not clearly affect the nuclear localisation of βDG, preliminary evidence suggests that this residue may be important in protein stability. Finally, it was observed that βDG antibodies colocalised to the centrosome in immunofluorescence studies however this localisation was demonstrated to be an antibody artefact. Studying the functions and regulation of βDG at intracellular locations is important to better understand the numerous roles of this multifunctional protein in maintaining cellular homeostasis and may provide further insights into its contribution to disease progression.

ACKNOWLEDGEMENTS

This thesis could not have been completed without the support of many people. Firstly, my thanks go to Prof. Steve Winder for always having the time to guide me through this project with patience and humour. Thanks to my advisors Dr. Martin Zeidler and Dr. Colby Eaton for their advice and encouragement throughout the project and also to Prof. Kathryn Ayscough for her keen analysis and support. Thanks to Dr. Mark Jones and Dr. Darren Robinson for their expertise and time helping me with the flow cytometry and microscopy respectively. To the many members of the BMS department especially of the KA/SW labs, both past and present whom I now consider as great friends as well as colleagues a huge thank you for the teaching and the chats, the coffee and the reagents. Ellen and Iwona thanks for sharing your experience and kindness to help at any time. Aga, thanks (I think) for improving my caffeine tolerance. Thanks to Chris and Rob, for your enthusiastic help and for the ability to take conversations in unexpected but always interesting directions. Thanks to Emma for taking on the role of events organiser and to Harriet for your enthusiasm and positivity. Kate, thanks for helping me out with you can do attitude and for being a great friend and landlord. Tracy, you are a constant source of support and I can always rely on you to tell it how it is! Joe thanks for the belief, encouragement and reminding me that it's important to keep the balance. Daniel, who taught me so much in the lab with patience and support and is always a great person to have just one more beer with. Sarah, your positive attitude has been a constant inspiration, thanks for the laughs and the cat videos and for weathering the rants.

Outside of the lab there are people that have made my time in Sheffield great. Sarah and Ryan, thanks for keeping me in the real world but also letting me vent and of course the wine. Travis and Simon I can always rely on you to lighten the mood. Kate, thanks for being a great house mate and friend always with words, I'll always be in awe of your organisation skills. Tom, thank you for the pep talks and encouragement and, of course, all the food. Anna and Natalie, you have been amazing as always. Anna, thanks for knowing when to tell me to just get on with it and when to take a break. Natalie, thanks for knowing exactly how to make me laugh.

And finally and most importantly thank you to my family. This project was driven largely by their unconditional love and support. This thesis is dedicated to my family. To my grandparents who always filled me with their belief and love. Mum, Dad and Clare thank you for learning the words, for understanding my long absences and for your endless encouragement.

ABBREVIATIONS

AR Androgen Receptor

BMD Becker muscular dystrophy

CaP Prostate cancer

CDK Cyclin Dependent Kinase

CRM1 Chromosome Region Maintenance 1

CIP Calf Intestinal Phosphatase

CNX Calnexin

DAPC Dystrophin Associated Protein Complex

DG Dystroglycan

DHT 5α-Dihydrotestosterone/ 17beta-hydroxy-5alpha-androstan-3-one

DMD Duchenne Muscular Dystrophy

ECM Extracellular Matrix

EDMD Emery Dreifuss Muscular Dystrophy

ER Endoplasmic Reticulum

ERK Extracellular Signal Regulated Kinase

ERM Ezrin, Radixin, Moesin Proteins

ETV1 ETS Translocation Variant 1

FBS Fetal Bovine Serum

$G_{0/1/2}$ $GAP_{0/1/2}$ Phase

GAPDH Glyceraldehyde-3-Phosphate Dehydrogenase

GFP Green Fluorescent Protein

Grb2 Growth Factor Receptor-bound Protein 2

ICD Intra Cellular Domain

INFS Integrative Nuclear FGFR1 Signalling

INM Inner Nuclear Membrane

INTERNET Integral Trafficking from the ER to the Nuclear Envelope Transport

KASH Klarsicht, ANC-1, Syne Homology

kDa Kilo Dalton

LARGE Like-acetylglucosaminyltransferase

LINC Linker of Nucleoskeleton and Cytoskeleton

LGMD Limb Girdle Muscular Dystrophy

MAPK Mitogen Activated Protein Kinase

MCM Mini-Chromosome Maintenance Complex

MMP Matrix Metalloproteinase

MTOC Microtubule Organising Centre

NAE Nuclear envelope associated endosomes

NE Nuclear envelope

NEBD Nuclear Envelope Breakdown

NEM N-Ethylmalemide

NES Nuclear Export Signal

NLS Nuclear Localisation Signal

nNOS neuronal Nitric Oxide Synthase

NPC Nuclear Pore Complex

ONM Outer Nuclear Membrane

PBS Phosphate Buffered Saline

PCM Pericentriolar Material

PDGFR Platelet Derived Growth Factor Receptor

PDZ Post synaptic density protein (PSD95), Drosophila disc large tumour suppressor (Dlg1) and zona occludens-1 (ZO-1)

PKC Protein Kinase C

PM Plasma membrane

PNGaseF Peptide- *N*- Glycosidase F

PTM Post Translational Modification

RIP Regulated Intramembrane Proteolysis

SGC Sarcoglycan Complex

SH1/2/3 Src Homology 1/2/3 domain

SUMO Small Ubiquitin-like Modifier

SUN Sad and UNC-84

TM Trans-membrane

WW WWP repeating motif

CONTENTS

1. Introduction

The human body consists of vast numbers of highly specialised cells, that together form complex tissues with specific tasks. It is critical for a cell to interact with its surrounding environment and neighbouring cells and respond accordingly to regulate its growth, division, movement and activity. The complex behaviour of a cell is a result of a network of incredibly diverse molecular components. These molecules are highly regulated by the cell to ensure their correct spatial and temporal expression and activity. Disruptions to the levels, processing, and functions of these molecules can cause an imbalance in the cell homeostasis, resulting in perturbed tissue integrity and ultimately a vast array of human diseases. Studying the regulation, interactions and functions of these molecules is fundamental in the understanding of the human body and disease processes.

1.1 The Biosynthesis and Structure of Dystroglycan

Initially isolated as cranin, a laminin binding glycoprotein in neural cells (Smalheiser et al. 1987), the same protein was later isolated and characterised in skeletal muscle (Ibraghimov-Beskronaya et al. 1992) and the brain (Gee et al. 1993) and subsequently named dystroglycan (DG). Dystroglycan is encoded for by the *DAG1* gene which is comprised of two exons separated by a single intron (Ibraghimov-Beskronaya et al. 1993). Following the transcriptional and translational processing of the *DAG1* gene the product is a single 895 amino acid polypeptide (in humans) that is post-translationally cleaved in the endoplasmic reticulum (ER) between Gly653/ Ser654 to form two subunits, α- and β-dystroglycan (Ibraghimov-Beskronaya et al. 1993, Holt et al. 2000) (Fig 1.1).

αDG is a peripheral membrane protein with globular immunoglobulin like N- and C- terminal domains that are linked by a mucin-like linker domain (Brancaccio et al, 1995, Brancaccio et al. 1997, Bozic et al 2004) (Fig 1.1). The linker domain is highly glycosylated O- linked glycans, which are important for its interaction with its ligands in the ECM (Talts et al. 1999, Tisi et al, 2000). The molecular weight of αDG is predicted to be 72 KDa, however the mature protein runs on SDS PAGE gels between 120-180 KDa, depending on the tissue, as a result of its highly glycosylated state (Durbeej et al, 1998, Ervasti et al. 1991, Yamada et al, 1994). βDG has a globular, N-glycosylated, extracellular N-terminal domain, a short transmembrane domain and a cytoplasmic, largely disordered and proline rich, C-terminal domain (Fig 1.1). The βDG core peptide is predicted to have a molecular weight of 26 KDa, however the mature protein runs at 43 KDa on SDS-PAGE as a consequence of its proline rich composition and post-translational

modifications (Ibraghimov-Beskrovnaya et al 1992, Holt et al 2000). In its mature form DG is a type 1 transmembrane domain protein in which the α and β subunits interact non-covalently.

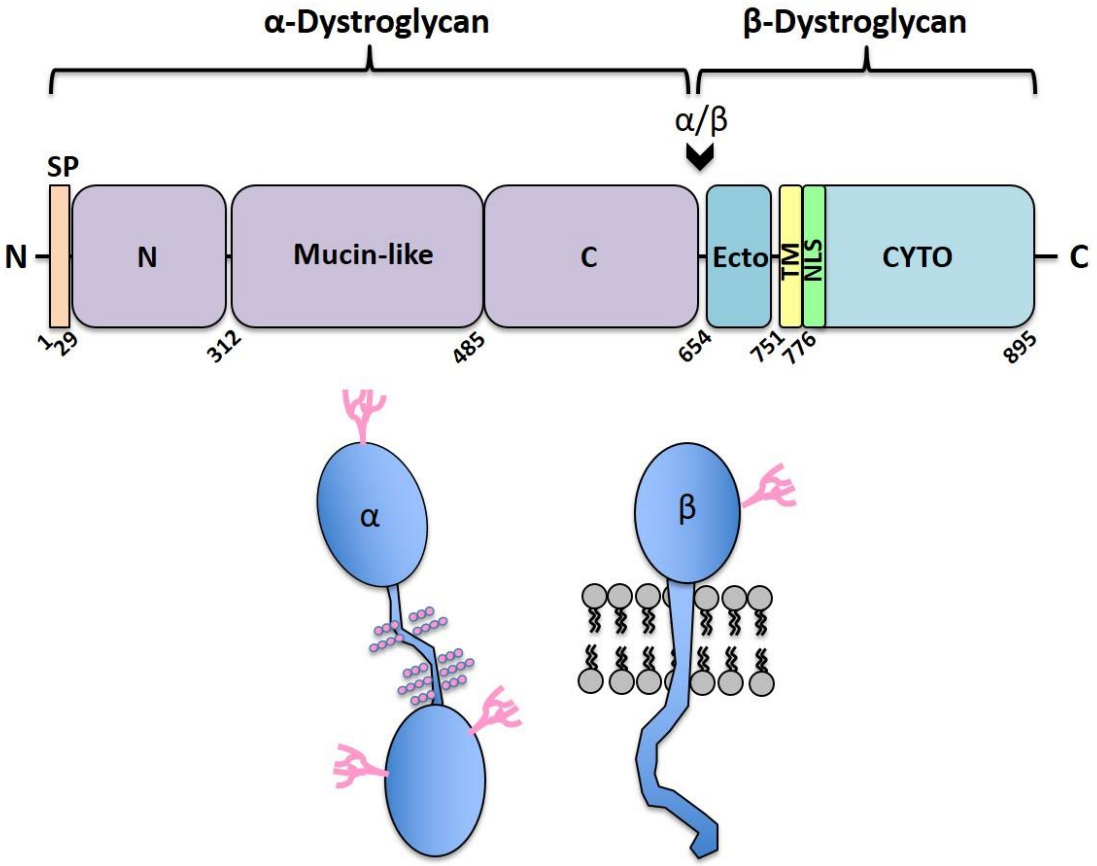

Figure 1.1: The domain structure of human dystroglycan. (Top) Schematic diagram of the domains of α and β dystroglycan. SP: Signal peptide, Ecto: N terminal- Ectodomain, TM: transmembrane, NLS: Nuclear localisation signal, Cyto: Cytoplasmic domain. Amino acid positions are denoted beneath the structure. Arrowhead indicates site of cleavage between α and β dystroglycan. Domains are not to scale. (Bottom) Cartoon diagram of the extracellular α and transmembrane β dystroglycan subunits with glycosylation modifications in pink.

Dystroglycan orthologues can be found widely across Metazoa although not in the choanoflagellates, the unicellular relatives of the metazoan (Adams et al. 2015). There is a high degree of homology between human DG and vertebrate orthologues, with a 94% identity between mice and humans whilst other animal models have varying degrees of homology; *Xenopus* (69%), Zebrafish (59%), *Drosophila* (33%) and *C. elegans* (24%) (Adams et al. 2015). Dystroglycan is expressed ubiquitously in mammalian tissues, with high expression in skeletal muscle and heart tissue (Ibraghimov-Beskronaya et al. 1993).

1.2 DYSTROGLYCAN IN THE DYSTROPHIN ASSOCIATED GLYCOPROTEIN COMPLEX (DAPC)

In its characterisation in skeletal muscle dystroglycan was identified as a binding partner of dystrophin in the dystrophin associated glycoprotein complex (DAPC) (Ervasti et al. 1991, Ibraghimov-Beskrovnaya et al. 1992) and it is within this context that DG is best understood (Fig 1.2). αDG interacts with components of the extracellular matrix including laminin α1 and α2 (Ervasti et al. 1993), biglycan (Bowe et al. 2000), agrin (Deyst et al. 1995) and perlecan (Peng et al. 1998). βDG is a transmembrane component of the DAPC, interacting with the c-terminal of αDG via its extracellular N-terminal domain (Sciandra et al. 2001, Bozzi et al. 2003) and various binding partners, including dystrophin via its cytoplasmic C-terminal domain (Jung et al. 1995, Yoshida et al. 1990) (Fig 1.2). Dystrophin is a member of the spectrin family of proteins and binds to the actin cytoskeleton through its N-terminal actin binding domain and βDG through its cysteine rich and C-terminal domains (Suzuki et al. 1992, Rentschler et al. 1999, Corrado et al. 1994). As such, the DAPC provides a physical tether between the extracellular environment and the actin cytoskeleton (Ervasti et al. 1993).

In muscle tissue a number of other proteins were co-purified with dystrophin and dystroglycan and have been characterised as the other major components of the DAPC and are briefly described below (Ervasti et al. 1991, Ibraghimov-Beskrovnaya et al. 1992) (Fig 1.2). The transmembrane sarcoglycans (α,β,γ,δ) form the sarcoglycan subcomplex (SGC) (Holt et al. 1998). The SGC interacts with DG and is proposed to strengthen the interaction between the DG subunits, as well as DG's interaction with dystrophin (Iwata et al. 1993, Roberds et al. 1993). The stabilising role of the SGC was proposed following observations of destabilised interactions between these components in animal models lacking the SGC (Iwata et al. 1993, Roberds et al. 1993), however how the interactions are stabilised by the SGC remains unclear. The SGC also provides a scaffold for other DAPC components, such as dystrobrevin (Yoshida et al. 2000). Sarcospan binds to the SGC (Crosbie et al. 1999) and is proposed to have a role in clustering DAPCs to form membrane micro-domains (Miller et al. 2007). α-Dystrobrevin, a muscle specific dystrobrevin isoform, is proposed to interact with the SGC and dystrophin and acts to recruit syntrophins (Nawrotzki et al. 1998, Newey et al. 2000). Syntrophins can interact with both dystrophin and dystrobrevins (Newey et al. 2000, Suzuki et al. 1995) and are able to recruit and bind a number of adaptor proteins, such as Grb2, and signal transduction molecules, such as microtubule associated serine/threonine kinase (MAST), to their PDZ domains (Bhat et al. 2013, Oak et al. 2002, Lumeng et al. 1999). Neural nitric oxide synthase (nNOS) is another signalling molecule that has been identified to interact with syntrophins and

dystrophin and contributes towards a functional DAPC and can modulate calcium homeostasis (Lai et al. 2009, Ito et al. 2013).

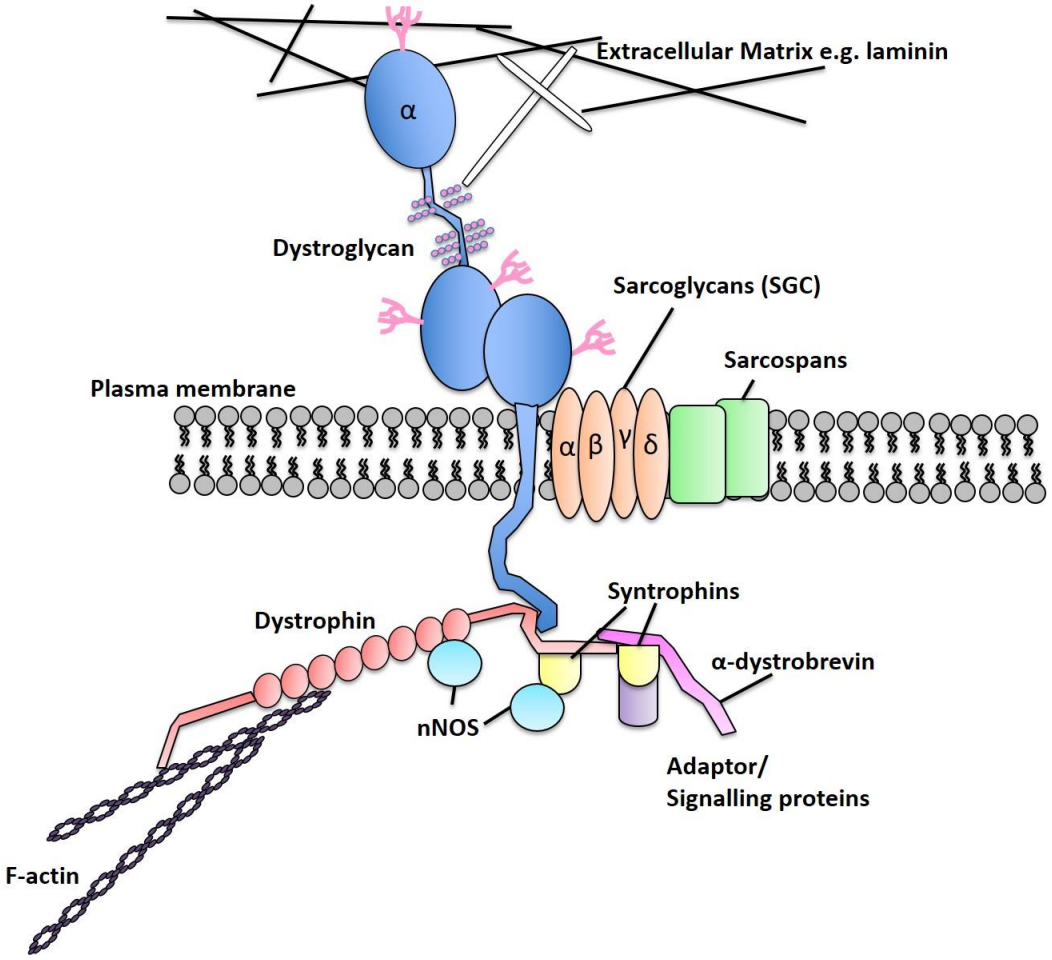

Figure 1.2: The dystrophin associated glycoprotein complex. A schematic representation of the DAPC linking the ECM to the actin cytoskeleton. Extracellular αDG binds to components of the ECM and to the transmembrane βDG which binds to dystrophin which in turn binds to F-actin. Additional transmembrane components of the complex includes α,β,γ and δ Sarcoglycans making up the SGC and sarcospan. Syntrophins, α-dystrobrevin and nNOS are intracellular members of the DAPC. The DAPC also acts as a scaffold for various adaptor and signalling proteins. The scale and relative positions are for simplicity and not to scale.

The DAPC is a critical adhesion complex and confers protection to muscle cells during their contraction and relaxation (Ervasti et al. 1993, Campbell. 1995, Petrof 1998). Indeed, the loss or mutation of members of the DAPC leads to muscular dystrophies of varying severity (Mercuri et al. 2013, Campbell 1995, Holt et al. 1998). However, the DAPC is not simply a physical connection between a cell and its environment and multiple components of the DAPC have networks of interacting partners with roles in signal transduction, a number of which shall be discussed in the following sections. Importantly, the composition of complexes within which DG is found varies both within and between tissues. Thus DG containing complexes have both important structural adhesion and signal transduction scaffold roles in multiple tissues.

1.3 DYSTROGLYCAN POST-TRANSLATIONAL MODIFICATIONS AND PROTEIN INTERACTIONS

Dystroglycan is a complex protein and undergoes a plethora of post-translational modifications (PTM) that are important for its localisation, stability and interaction with a number of binding partners.

1.3.1 Alpha-dystroglycan is highly glycosylated and interacts with the ECM

The α-dystroglycan subunit is highly glycosylated, the N and C-terminal domains contain multiple N-glycosylation sites whilst the mucin-like domain is heavily O-glycosylated harbouring at least 21 potential sites of glycosylation (Stalnaker et al. 2010, Yoshida-Moriguchi et al. 2015). There is evidence of multiple, heterogeneous glycosyl structures including O-manosyl and O-linked –*N*-acetylglucosamine (Chiba et al. 1997, Tran et al. 2012). The glycosylation of α-DG requires the initial presence of the N-terminal domain which is later cleaved by furin at residue 312 (Kanagawa et al. 2004, Singh et al. 2004) (Fig 1.3). The extent to which αDG is glycosylated depends upon both the developmental stage and the tissue in which it is expressed, this is reflected in the range of molecular weights (from 100-200KDa) that αDG presents as in western blots of lysates from different tissues (Barresi et al. 2006, Durbeej et al, 1998, Ervasti et al. 1991, Yamada et al, 1994). A number of ECM components that contain a laminin G (LG) binding module (Hohenester et al. 1999) including laminins (Ervasti et al. 1993, Chiba et al. 1997), agrins (Bowe et al.1994) and perlecan (Talts et al. 1999, Peng et al. 1998) interact with α-DG through the O-glycans decorating the mucin-like domain whilst biglycan binds to the N-terminal domain of αDG (Bowe et al. 2000). Preventing the correct O-mannosylation (Chiba et al. 1997), including its phosphorylation (Yoshida-Moriguchi et al. 2010) and other glycosylation events (Combs et al. 2005) of the mucin-like domain of αDG inhibits its ability to act as an ECM receptor (Ervasti et al. 1993), indeed hypoglycosylation of αDG is implicated in multiple diseases (See section 1.5) (Barresi et al. 2006). Disrupting the N-glycosylation, however does not disrupt α-DG's ECM receptor function (Ervasti et al. 1993) and the interaction between the α- and βDG subunits occurs in a glycosylation-independent manner (Di Stasio et al. 1999, Sciandra et al. 2001). It is thought that the heterogeneity in glycosylation of αDG across tissues enables the fine tuning of binding to relevant ECM components (Yoshida-Moriguchi et al. 2015). αDG also acts as a receptor for various pathogens including *Mycobacterium leprae* (Rambukkana et al. 1998), Lassa Virus and lymphocytic choromeningitis viruses (Cao et al. 1998), again in a glycosylation dependent manner (Kunz et al. 2005) and a DG-like protein in ticks, *I. scapulatris* dystroglycan-like protein (ISDLP) is important for the migration from the gut of *Borrelia burgdorferi,* the causative agent of Lymes disease (Coumou et al. 2016).

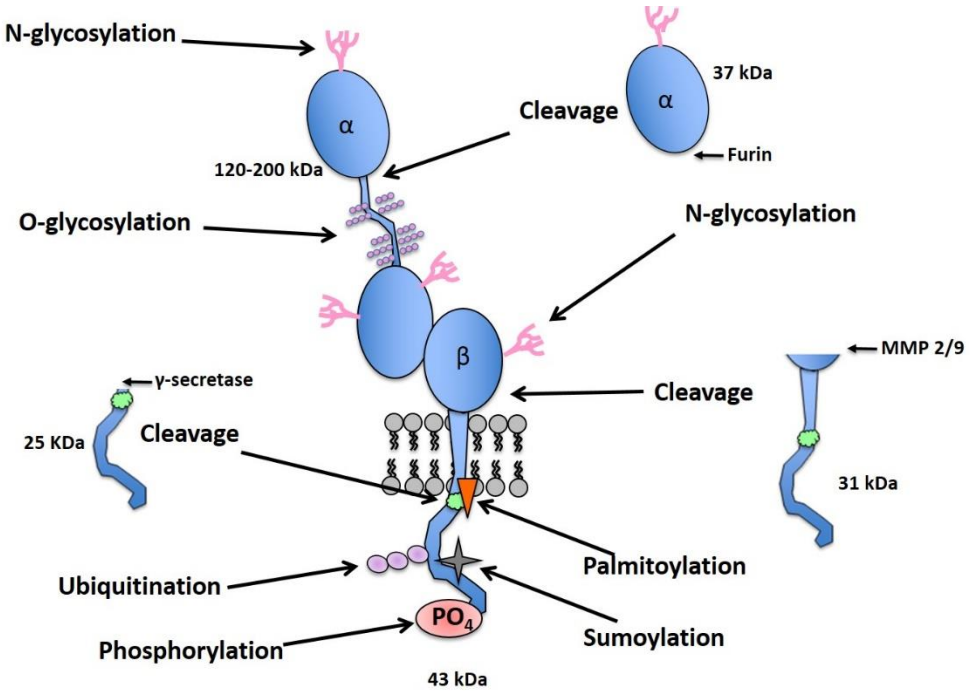


```
         660         670         680         690         700
---SIVVEWT NNTLPLEPCP KEQIAGLSRR IAEDDGKPRP AFSNALEPDF

         710         720         730         740         750
KATSITVTGS GSCRHLQFIP VVPPRRVPSE APPTEVPDRD PEKSSEDDVY

         760         770         780         790         800
LHTVIPAVVV AAILLIAGII AMICYRKKRK GKLTLEDQAT FIKKGVPIIF

         810         820         830         840         850
ADELDDSKPP PSSSMPLILQ EEKAPLPPPE YPNQSVPETT PLNQDTMGEY

         860         870         880         890    895
TPLRDEDPNA PPYQPPPPFT APMEGKGSRP KNMTPYRSPP PYVPP
```

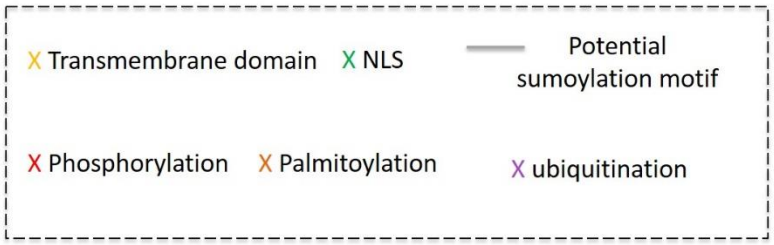

Figure 1.3 Posttranslational modifications of dystroglycan. (Top) Cartoon depicting known and predicted PTM of DG including proteolytic cleavage by and the resulting fragments, glycosylation, ubiquitination, sumoylation and phosphorylation. (Bottom) PTM annotated sequence of β-dystroglycan. yellow residues: Transmembrane domain, Green residues: NLS, orange residue: reported site of palmitoylation, Purple residues: Potential/ reported sites of ubiquitination, red residues: Reported sites of phosphorylation by mass spectrometry studies, validated Y892 phosphorylation site is enlarged. Grey underline: Potential sumoylation motif.

1.3.2 Beta-Dystroglycan: a highly modified structural scaffold and signal transducer

βDG is a complex subunit that is dynamically regulated by multiple PTM (Fig 1.3) and interacts with a growing number of protein partners (Fig 1.4), overthrowing the notion that dystroglycan is a simple adhesion receptor.

1.3.2.1 Post-translational modifications of βDG

Like the α subunit, βDG is also glycosylated with a small number of N-glycosylation sites identified in its ectodomain, although the functional relevance of these modifications is as yet unknown (Holt et al. 1998, Mitchell et al. 2013, Zielinska et al. 2010) (Fig 1.3). A little studied PTM of βDG is palmitoylation. During a global study of palmitoylated proteins in neural cells Cys_{774}, situated at the transmembrane domain boundary of βDG, was identified as a site of palmitoylation (Kang et al. 2008) and was also identified in mass spectrometry analysis of βDG in LNCaP cells (Leocadio, 2014) (Fig 1.3). Whilst there have been no further studies into this modification, palmitoylation has been demonstrated to play a role in the retention of proteins at the plasma membrane (Linder et al. 2007). Furthermore, it is a reversible modification and as such may be an important regulator of βDG localisation (Linder et al. 2007).

One of the best studied PTM of βDG is phosphorylation. Phosphorylation at a tyrosine residue (Y892 in human, Y890 in mice) within the extreme C-terminus of the cytoplasmic domain of βDG is an important regulator of βDG (Fig 1.3). Phosphorylation at Y892 is catalysed by c-Src (Sotgia et al 2001). Phosphorylation of βDG is proposed to occur in an adhesion dependent manner following an observed electrophoretic shift of βDG as detected by anti-DG and phospho-tyrosine antibodies in adhered compared to suspended HeLa cells (James et al 2000). The site of phosphorylation was identified at Y892 through a combination of site specific monoclonal antibodies and peptide spot arrays of the cytoplasmic domain of βDG (James et al 2000). Interestingly, phosphorylation at Y892 within the PPxY motif has been shown to modulate the interaction of βDG with its WW and SH2 domain containing binding partners. (James et al. 2000, Ilsley et al. 2001, Sotgia et al. 2001)(see below). Furthermore, it has been shown that phosphorylation at residue Y892 results in the internalisation of βDG from the plasma membrane and targeting to the late endosomes (Sotgia et al. 2003, Miller et al. 2012) as well as potentially its ubiquitination and subsequent degradation (Miller et al. 2012). Phosphorylation at Y892 is also induced by lassa virus binding and helps to facilitate virus internalisation (Moraz et al. 2013). Y892 is the only site to have been confirmed to be phosphorylated by site specific methods (James et al. 2000). However, in cells treated with src inhibitors, whilst phosphorylation at Y892 was inhibited, βDG was still detected by an anti-phospho tyrosine antibody, indicative of additional tyrosine residues that could be phosphorylated by non-src kinases (Moraz et al. 2013). Furthermore, there is evidence in the form of 2D gel electrophoresis combined with phospho- specific antibodies (James et al. 2000),

high-throughput mass spectrometry analysis (Hornbeck et al. 2014) and in silico analysis of consensus sites (Gould et al. 2010), for the phosphorylation of additional tyrosine, threonine and serine residues within the cytoplasmic tail of βDG (Fig 1.3). As yet the functional roles of these putative phospho-sites are unknown but hint at additional levels of regulation for βDG.

As mentioned above there are reports of the ubiquitination of DG (Miller et al. 2012). Dystrophic mdx mice in which DAPC components are lost from the PM saw a restoration of βDG at the PM upon treatment with the proteasomal inhibitor MG-132 (Bonuccelli et al. 2003). Additionally, in lysates obtained from in vitro models, MG-132 treatment resulted in increased levels of βDG and its fragments (see below) (Leocadio et al. 2016). Whilst not direct evidence of DG ubiquitination, these studies hint at a role for the ubiquitin proteasome system in DG fate. Importantly, ubiquitination at sites within βDG has been identified by mass spectrometry studies (Kim et al. 2011, Lee et al. 2011) and βDG is detected upon pull-down with Multi-Dsk (Miller et al. 2012), a high affinity resin specifically detecting ubiquitinated proteins (Wilson et al. 2012). Interestingly, the species of βDG isolated with MultiDsk was detected with a pY892 specific antibody, suggesting interplay between these forms of modifications (Miller et al. 2012). The importance of ubiquitination on βDG interaction, modifications and turnover requires further investigation but is crucial given the vital functional roles of DG. It should also be noted that there is preliminary evidence of the sumoylation of βDG (S. Winder, personal communication). Small Ubiquitin-like Modifiers (SUMO) proteins are structurally similar to ubiquitin and have roles in localisation, protein stability and transcriptional activity of modified target proteins (Flotho et al. 2013).

Finally, βDG can be proteolytically cleaved into a 31 KDa and a 26 KDa fragment by MMP-2 and -9 and γ-secretase or furin respectively (Yamada et al. 2001., Leocadio et al. 2016) The cleavage of βDG by MMPs is proposed to occur within the ectodomain as the fragment retains the transmembrane domain and is detected by antibodies recognising the cytoplasmic C-terminal tail (Yamada et al. 2001, Bozzi et al. 2009, Zhong et al. 2006). The 26 KDa fragment is a result of regulated intramembrane proteolysis (RIP) within the transmembrane domain, again this fragment is detected by C-terminal targeted antibodies (Hemming et al. 2008, Leocadio et al. 2016). Cleavage of proteins by γ-secretase is often preceded by the N-terminal proteolysis of their targets by an additional protease (Wolfe, 2010, Hemming et al. 2008), for example MMPs, thus suggesting a sequential processing of the fragments of βDG. There is also some evidence for the cleavage of βDG by furin at a juxtamembrane site, as seen in the increase in the levels of the 26 KDa fragment upon treatment with a furin 1 inhibitor (Decanoyl-RVKR-CMK) (Leocadio et al. 2016). The fate of these C-terminal fragments of βDG is unclear, however they can be detected to varying extents within the nuclear and cytoplasmic

fractions of biochemically fractionated cells (Mathew et al. 2013, Mitchell et al. 2013, Leocadio et al. 2016). Furthermore, nothing is known about the fate of the N-terminal portions of the cleaved DG as there are no antibodies targeted to these regions. The 26KDa fragment retains the putative palmitoylated Cys residue and therefore there is still the possibility that it may be retained at the PM. It is unclear if the fragments are simply targeted for degradation, indeed the fragments increased upon MG-132 treatment (Leocadio et al. 2016). However, the fragments may also have functional roles. The fragments both contain multiple sites of interactions with binding partners (Gould et al. 2010, Sotgia et al. 2001, James et al. 2000) and their nuclear targeting results in altered gene expression (See section 1.6.4) (Mathew et al. 2013). The principle of PM protein fragments being cleaved to perform signalling roles in not unfamiliar, with well characterised examples being the EGF receptor and Notch (Wang and Hung, 2012). Thus understanding the fate of the cytoplasmic fragments of βDG may provide further levels of regulation and functions to an already complex protein. Furthermore, the cleavage and loss of βDG from the plasma membrane has been implicated in multiple diseases including muscular dystrophies (Matsumura et al. 2015) and cancer (Singh et al. 2004, Cross et al. 2008, Mitchell et al. 2013, Leocadio et al. 2016) and thus gaining an understanding into βDG proteolytic cleavage may provide important insights into disease mechanisms (see section 1.5).

1.3.2.2 βDG as a scaffold for multiple binding partners

βDG also forms multiple interactions with a plethora of binding partners which enables it to fulfil its mechanical role as well as establishing βDG as a signal transduction hub (Moore et al. 2010) (Fig 1.4). The complexes DG forms vary across the tissues and depend upon its post-translational modifications, its adhesion state and other binding interactions, indeed these events are often inextricably linked (Moore et al. 2010, Ilsley et al. 2001, Sotgia et al. 2003). Within its cytoplasmic tail βDG contains consensus binding sites for WW (Ilsley et al. 2001, James et al. 2000, Sotgia et al. 2000), SH2 (Sotgia et al. 2001) and SH3 domain containing proteins (Russo et al. 1995, Yang et al. 1995) (Fig 1.4). In its role as an adhesion receptor βDG interacts with the C-terminal WW domain of dystrophin or utrophin, an approximately 30 aa region containing two conserved tryptophans, via the proline rich PPxY motif at its extreme C-terminus (Huang et al 2000, Pereboev et al 2001, Ilsley et al. 2001, Ilsley et al. 2002, Jung et al. 1995, James et al. 2000). In the case of dystrophin and utrophin the WW domain is necessary but not sufficient for interaction with βDG and also requires interaction with the EF-hand-like region for stabilisation and orientation of the interaction (Rentschler et al. 1999, Jung et al. 1995). The DG-Dystrophin/utrophin interaction is a good example of the tissue specificity and PTM regulated fine tuning of many βDG interactions.

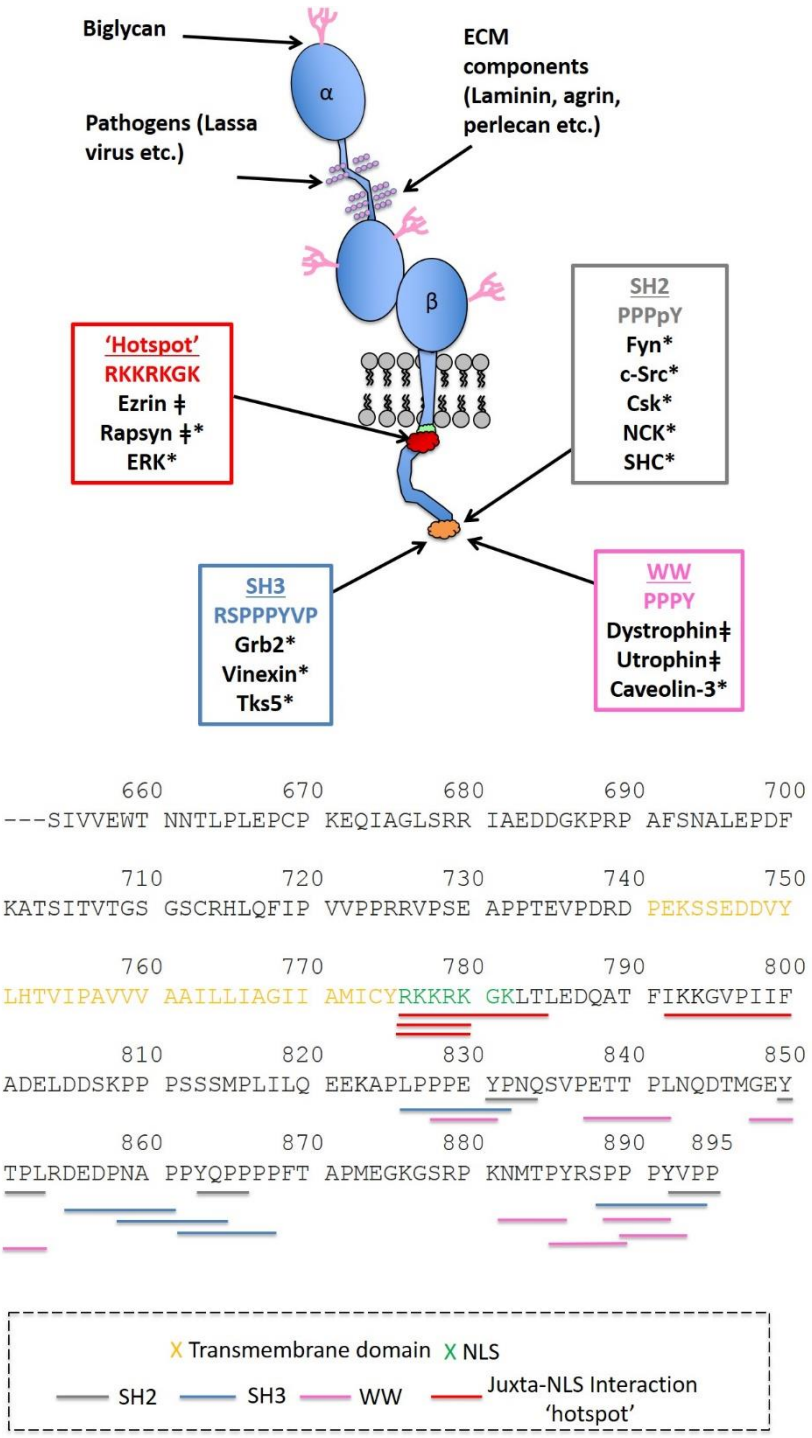

Figure 1.4 Dystroglycan and putative sites of protein interaction. (Top) Cartoon of dystroglycan with identified sites of protein interactions with SH2, SH3 and WW domain proteins interacting at the C-terminus of βDG and the proteins interacting at the 'hotspot' overlapping with the NLS. Proteins are indicated as having roles in signal transduction (*) or cytoskeleton binding and stabilisation(ǂ) (Adapted from Leocadio 2014). Interaction sequence within βDG is indicated. (Bottom) Annotated sequence of β-dystroglycan with putative sites of interaction as determined by ELM underlined. Yellow residues: Transmembrane domain, Green residues: NLS, grey underline: SH2 motifs. Blue underline: SH3 motifs. Pink underline: WW motifs, Red underline: site of multiple interactions 'hotspot' including ERK, Ezrin and Rapsyn.

The dystrophin gene has multiple promoters and can produce multiple isoforms of varying lengths and tissue specificity which can form DAPC like complexes (Muntoni et al. 2003). Full length dystrophin can be expressed from three tissue specific promoters and is expressed in the muscle and cardiac tissue with small amounts in the brain (Torelli et al. 1999), the hippocampus (Gorecki et al. 1992) and the purkinje fibres (Bies et al. 1992). Alternative promoters result in shorter isoforms such as Dp140 which is expressed in the brain, retina and kidneys (Lidov et al. 1995) whilst a short Dp71 isoform is expressed largely in non-muscle tissues (Bar et al. 1990). Alternatively, utrophin is a ubiquitously expressed homologue of dystrophin with high level of homology (Pearce et al. 1993) that fulfils the cytoskeletal linker role in non-muscle tissues as well as muscle tissues (Durbeej et al. 1999, James et al. 1996, Thi Man et al. 1995, Winder et al. 1995) binding DG in the same manner as dystrophin (Ilsley et al. 2001). Moreover residue Y892, a key site of phosphorylation within βDG, lies within the PPxY binding motif of DG. Immunoprecipitation experiments with phosphorylated and unphosphorylated βDG as well as binding studies using peptide arrays of the cytoplasmic domain of βDG indicate that phosphorylation at Y892 of βDG disrupts its interaction with dystrophin and utrophin (Ilsley et al. 2001, James et al. 2000, Pereboev et al 2001). As discussed above this phosphorylation occurs in an adhesion dependent manner (Ilsley et al. 2001, Sotgia et al. 2003), thus demonstrating the role of βDG in facilitating internal response to external stimuli. It is likely that additional, unknown factors contribute to the phosphorylation status of pY892 and within a cell βDG may be phosphorylated and dephosphorylated in a stochastic manner. Importantly, phosphorylation and disruption of dystrophin/utrophin interactions at this site enables a variety of outcomes for βDG including its internalisation (Sotgia et al. 2003, Miller et al. 2012), degradation (Miller et al. 2012, Lipscomb et al. 2016) or interaction with different binding partners (Sotgia et al. 2001) all of which can affect the adhesion and signalling properties of a cell.

In addition to dystrophin and utrophin, Caveolin-3, a protein with roles in membrane domain organisation, was identified as interacting with the PPxY site through its WW domain although is insensitive to phosphorylation at Y892 (Sotgia et al. 2000, Ilsley et al. 2001). The phosphorylation of Y892 not only promotes the release of WW domain partners but also creates an SH2 binding site pYxPP. A number of SH2 domain containing proteins including tyrosine kinases c-Src, Fyn, Csk and the adaptor proteins NCK and SHC have been shown to interact with βDG at this site (Sotgia et al. 2001). Moreover, an interaction site, RxxxPxxP, for SH3 domain proteins has also been found to overlap with the C-terminal WW and SH2 binding sites (Moore et al. 2010). Grb2, an adaptor protein with roles in the Ras-MAP kinase signalling cascade, has been shown to bind at this site through its SH3 domain (Russo et al. 2000, Yang et al. 1995). Vinexin, a binding partner of vinculin found at focal adhesions (Thompson et al.

2010), and Tsk5 a scaffolding protein with roles in podosome formation (Thompson et al. 2008) can also bind to the C-terminal of βDG via their SH3 domains.

In addition to the C-terminal region a cytoplasmic site, close to the trans-membrane domain, has been identified as a 'hot-spot' for the interaction of binding partners with βDG (Moore et al. 2010) (Fig 1.4). An NLS which binds importins has been identified at this site (Lara-Chacon et al. 2010, Oppizzi et al. 2008) (Discussed further in section 1.6). βDG has been shown to interact with ERM (Ezrin, Radixin, Moesin) family member, Ezrin and its binding site was identified as RKKRK, overlapping with the NLS (Spence et al. 2004a). ERM family proteins can link actin and microtubule networks to plasma membrane proteins and as such have key roles in cell adhesion, polarity and shape but also in signal transduction (Louvet-Vallee, 2000). It has been shown in REF52 cells that following ezrin binding to DG, a Rho GEF; Dbl was recruited to the plasma membrane where it locally activated the Rho GTPase Cdc42 and subsequently drove filopodia formation (Batchelor et al. 2007). Additionally, DG has been shown to act as a scaffold for Ras-MAP kinase pathway components MEK and ERK. DG is not a substrate nor does it affect the activity of these kinases, however it appears to sequester these components at different locations at the membrane (Spence et al. 2004b). Again the binding site for ERK (RKKRKxxLxL) overlaps with the NLS and ezrin interaction site on βDG (Moore et al. 2010). Rapsyn, which interacts with and clusters nicotinic acetylcholine receptors at the neuromuscular junctions also interacts with βDG at the juxta-NLS site (Kahl et al. 2003) (Fig 1.4).

The above selection of βDG interactions demonstrates how βDG can act as a scaffold for proteins involved in a variety of important processes including membrane organisation and remodelling (Thompson et al. 2010, Thompson et al. 2008, Batchelor et al. 2007, Spence et al. 2004a, Kahl et al. 2003), mechanical strength (James et al. 2000, Ilsley et al. 2001) and multiple signalling pathways (Spence et al. 2004b, Sotgia et al. 2001, Yang et al. 1995). The overlapping sites of interaction likely provide a means of regulating the binding partners and functions of βDG through competitive interactions and can be fine-tuned by PTM in response to the external environment (Moore et al. 2010, Sotgia et al. 2001, Ilsley et al. 2001). Moreover, it is important to note that other components of the DGC act as signalling scaffolds, such as syntrophin and dystrophin (Bhat et al. 2013, Oak et al. 2002, Lumeng et al. 1999) and that the DGC itself associates with other signalling hubs such as the integrin-talin-vinculin signalling hub in cardiac muscle (Anastasi et al. 2009). Furthermore, there is crosstalk between the signalling hubs as is seen in the case of the inhibitory modulation of βDG on the ERK activation of α6β1 integrin (Ferletta et al. 2003). The presence of additional putative interaction sites with the

cytoplasmic region of βDG and its localisation at multiple cellular locations (See section 1.6) hints at further unknown interactions and roles for this complex protein.

1.4 DYSTROGLYCAN: IMPORTANT ROLES IN DEVELOPMENT AND TISSUE HOMEOSTASIS

DG has been implicated in a broad range of processes including cell adhesion (Ervasti et al. 1993, Thompson et al, 2010, Galvagni et al. 2016), polarity (Deng et al, 2003, Weir et al. 2006, Schroder et al. 2007), migration and invasion (Thompson et al. 2008, Batchelor et al. 2007, Mitchell et al. 2012, Galvagni et al. 2016), neuromuscular junction composition (Deyst et al. 1995, Cohen et al. 1995, Peng et al. 1998, Kahl et al. 2003), proliferation (Hosokawa et al. 2001, Sgambato et al. 2006, Higginson et al. 2008, Mitchell et al. 2012), differentiation (Schroder et al. Sgambato et al. 2006) and cell death (Langenbach et al. 2002) Furthermore, the functions of DG are by no means completely understood and new roles are constantly emerging.

DG has important roles in development and tissue homeostasis. The vital role of DG during development is seen in the embryonic lethality at embryonic day 6.5 of *DAG1* deletion in mice in which there is disruption of the formation of Reichart's membrane and subsequent implantation defects (Williamson et al. 1997). DG has also been proposed to have roles in basement membrane formation (Henry and Campbell, 1998) maybe through the organisation of laminins in the ECM (Cohen et al. 1997. Henry et al. 2001). Chimeric mice demonstrated progressive muscular dystrophy (Côté et al. 1999). *Drosophila* have multiple DG isoforms but just one containing a mucin-like region (Schneider et al. 2006) however RNAi silencing of DG results in muscle degeneration, neuronal and eye abnormalities (Shcherbata et al. 2007) and disrupting the binding capabilities of DG can result in oocyte arrest (Yatsenko et al. 2009). Dystroglycan null zebrafish are viable, however they display a number of defects including dystrophic muscles and abnormal brain and eye structure (Gupta et al. 2011). The loss or disruption of DG in animal models has clear implications in maintaining healthy muscles but its ubiquitous nature also underlies important functions in other tissues (Sciandra et al. 2015). Blocking the binding of dystroglycan to laminins resulted in defects in branching of epithelial organs including the lungs, kidney and salivary glands (Durbeej et al. 1995, Durbeej et al. 2001). Conditional knockouts in mice have shown that DG is also important for the development and organisation of multiple neuronal structures such as branching of oligodendria (Eyermann et al. 2012) and formation of the myelin sheath and NMJ, (Côté et al. 1999, Saito et al. 2003, Kahl et al. 2003, Jacobson et al. 1998) and clustering of sodium channels at the nodes of Ranvier (Saito et al. 2003).

1.5 DYSTROGLYCAN IN DISEASE

Given the wide range of cellular roles of DG and the severe defects seen in animal models in which DG function is abrogated, it is of no surprise that DG has been implicated in multiple human diseases.

1.5.1 Dystroglycan in Muscular Dystrophies

Muscular dystrophies are a group of heterogeneous diseases characterised by the progressive degeneration of muscle tissue. Many muscular dystrophies are a consequence of mutated DAPC components or nuclear membrane proteins (Mercuri et al. 2013). Given its important roles in muscle it is unsurprising that a large body of the studies on DG are with regards to its context in the DAPC and muscular dystrophies. Indeed, the initial characterisation was a consequence of a study of binding partners for dystrophin (Ibraghimov-Beskronaya et al. 1993), which is lost from the sarcolemma in the X-linked, inherited Duchenne Muscular Dystrophy (DMD) (Koenig et al. 1987, Campbell, 1995). In DMD the absence of dystrophin results in the loss of multiple components of the DAPC, including DG, from the sarcolemmal membrane (Campbell, 1995, Ervasti et al. 1990). Subsequently there is a weakening of muscle fibres and increased fibrosis of the muscle tissue resulting in eventual loss of ambulation (Mercuri et al. 2013). DMD patients also have respiratory and cardiac weakness (Mercuri et al. 2013). Interestingly it has been observed that there is an increase in the 31 kDa fragment of βDG as a consequence of MMP-2/9 cleavage of its ectodomain in DMD and sarcoglycanopathies but not other muscular dystrophies (Matsumura et al. 2005). Thus the proteolytic cleavage of βDG is another mechanism through which the ECM- cell interaction is disrupted and can contribute to muscle degeneration in DMD patients.

More than 200 mutations, including point mutations, deletions and duplications within the DMD gene have been reported, resulting in DMD or the related Becker Muscular Dystrophy (BMD) which retains a short form of dystrophin and displays a milder phenotype than DMD (Koenig et al. 1989). A large proportion of current research into therapeutic approaches for the treatment of DMD aims at restoring shorter, yet functional versions, of dystrophin in muscle cells, which in turn should recruit other DAPC components to the sarcolemma. For example, exon skipping is being developed for use in patients in which a deletion has caused a frame shift mutation and subsequently prevents the expression of functional dystrophin (Kole et al. 2015). Targeting of antisense oligonucleotides to splice sites within the pre-mRNA results in the ‘skipping’ of the mutated exons, restoring the reading frame and enabling the production

of a shorter but functional dystrophin protein (Kole et al. 2015). Other approaches aim to upregulate expression of utrophin, a dystrophin homologue, which can also form functional complexes at the sarcolemma (Miura et al. 2006). Other components of the DAPC are also potential therapeutic targets for the treatment of DMD and BMD. Overexpressing DG in a DMD model, the *Mdx* mouse, did not improve the DMD phenotype or restore DAPC components to the membrane (Hoyte et al. 2004) however another approach is aiming to retain DG at the plasma membrane rather than altering the overall levels of the protein. The hypothesis is that by targeting PTM of DG, such as phosphorylation or ubiquitination, which control its degradation and internalisation there will be an increased level of DG at the PM, which may recruit other components of the DAPC and therefore partially restore some of its function and reduce the dystrophic phenotype (Miller et al. 2012, Lipscomb et al. 2016). Dystroglycan is also implicated more directly in a number of muscular dystrophies termed dystroglycanopathies (See below).

1.5.1.1 Primary Dystroglycanopathies

Mutations in *DAG1* itself in humans are rare with only four reported cases to date, a telling indicator of the crucial roles that DG fulfils. The first patient identified was a 16 year old girl with a heterozygous deletion of ~2MB in chromosome 3 (Frost et al. 2010). The patient presented white matter abnormalities, learning difficulties and facial hypotonia and mild myopathy (Frost et al. 2010). Upon further investigation it was shown that that patient had a 60% reduction in *DAG1* mRNA levels compared to wild-type tissue, however the deletion also includes the sequence for 62 protein coding genes and 3 miRNAs, thus the symptoms may not be attributed solely to the DG deficiency (Frost et al. 2010). A second patient had a homozygous missense mutation converting Thr192 to a methionine (Hara et al. 2011). This mutation disrupted the receptor capabilities of DG by inhibiting its O-glycosylation by LARGE by disrupting its binding site within the N-terminus of αDG (Hara et al. 2011, Kanagawa et al. 2004). The patient had Limb-girdle Muscular Dystrophy and mental retardation. The same mutation in mice caused consistent skeletal muscle abnormalities and neurological impairment (Hara et al. 2011). Two siblings were found to have a homozygous missense mutation in the *DAG1* resulting in a cysteine to phenylalanine substitution at residue 669 within the ectodomain of βDG (Geis et al. 2013). As a result the patients had severe muscle-eye-brain (MEB) disease as well as macrocephaly and multicystic white matter disease (Geis et al. 2013). The above cases demonstrate the effects of reduced levels of DG or preventing PTM, such as glycosylation, of DG on health and development. In the most recently reported patients (5 patients from a consanguineous family) however, there was an absence of both α and β DG core proteins (Riemersma et al. 2015). A homozygous single base pair deletion at nucleotide 743 resulted in a frameshift and a premature stop codon at residue 248 (p.Ala248Glufs*19)

with subsequent biochemical analysis detecting a small PCR product but no alternative spice products, no core protein as detected by immunoblot and no laminin binding in a laminin overlay assay of cultured patient myotubes (Riemersma et al. 2015). The patients had Walker-Warburg syndrome (WWS) displaying congenital muscular dystrophy, hydrocephaly and ocular malformations with infantile death at ages from a couple of hours to 3.5 months as a result of respiratory failure or aspiration pneumonia, tragically reinforcing the crucial and wide-reaching functions of DG (Riemersma et al. 2015).

1.5.1.2 Secondary Dystroglycanopathies

As previously described, the PTM of DG are crucial to its function. Interestingly, a number of diseases have been linked to genes which affect the PTM of DG as opposed to *DAG1* itself and have been termed secondary dystroglycanopathies (Godfrey et al. 2011). Secondary dystroglycanopathies are more common than primary, with 18 genes identified as the causative factors behind secondary dystroglycanopathies to date (Table 1.1) (Taniguchi-Ikeda et al. 2016). The majority of these genes have roles in the modification of αDG with the glycosyl moieties that are so important in its receptor function. Diseases that are represented within the secondary dystroglycanopathies include a number of LGMD, MEB, Fukuyama congenital muscular dystrophy (FCMD), and WWS. These heterogenous groups of muscular dystrophies occasionally occur in conjunction with ocular and brain abnormalities (Godfrey et al. 2011, Yoshida-Moriguchi et al. 2015). Different mutations within the same gene can cause different diseases as is the case with *FKTN*, mutation in which can cause FCMD, WWS and LGMD (Kobayashi et al. 1998, De Bernabe et al. 2003, Puckett et al. 2009). In the case of some genes such as *POMT1* and *POMT2* the severity of the disease correlated positively with hypoglycosylation of αDG, however this does not hold true for all genes (Jimenez-Mallebrera et al. 2009). Furthermore, the enzymes encoded by the dystroglycanopathy genes often have multiple substrates and therefore the resulting disease phenotypes and their varying severity are likely to be a combination of DG and non-DG mediated effects (Yoshida-Moriguchi et al. 2015).

Table 1.1 Proteins identified as mutated in secondary dystroglycanopathies (Adapted from Godfrey et al. 2011, Yoshida-Moriguchi et al. 2015 and Taniguchi-Ikeda et al. 2016)

Protein (*Gene*)	Protein Function
β3-N-Acetylgalactosaminyltrans-ferase 2 (*B3GALNT2*)	β3-N-Acetylgalactosaminyltransferase
β3-N-Acetylglucosaminyltransfe-rase (*B3GNT1*)	β3-N-Acetylglucosaminyltransferase
β-1,4-Glucuronyltransferase 1 (*B4GAT1*)	Xylose, β-1,4-Glucuronyltransferase
Dolichyl-phosphate mannosyltransferase polypeptide 1 (*DPM1*)	Component of the dolichol-phosphatase mannose synthase complex
Dolichyl-phosphate mannosyltransferase polypeptide 2 (*DPM2*)	Component of the dolichol-phosphatase mannose synthase complex
Dolichyl-phosphate mannosyltransferase polypeptide 3 (*DPM3*)	Component of the dolichol-phosphatase mannose synthase complex
Dolichol Kinase (*DOLK*)	Catalyses phosphorylation of dolichol
Fukutin (*FKTN*)	Not known (indirect implication in modifications of phosphorylated O-linked mannose)
Fukutin-related protein (*FKRP*)	Not known
GDP- mannose pyrophosphorylase (*GMPPB*)	GDP- mannose pyrophosphorylase (GTP- to GDP-Mannose)
Isoprenoid synthase domain containing (*ISPD*)	Cytidyltransferase (Glycerolphospholipid metabolim) and implicated in O-mannosylation
Like-glycosyltransferase (*LARGE*)	β3-Glucuronylltransferase (synthesis of glycoprotein and glycosphingolipid sugar chains)
Protein-O-mannose kinase (*POMK*)	Phosphorylation of O-mannose
Protein- O- mannosyl transferase 1 (*POMT1*)	Forms heterodimeric mannosyl transferase enzyme complex (α1-O linkage of mannose to proteins)
Protein- O- mannosyl transferase 2 (*POMT2*)	Forms heterodimeric mannosyl transferase enzyme complex (α1-O linkage of mannose to proteins)
Protein- O- linked mannose beta 1,2-N-acetylglucosaminyltrans-ferase (*POMGNT1*)	Pathway specific protein O-mannose β1,2GlcNAc transferase
Protein- O- linked mannose N-acetylglucosaminyltransfe-rase 2(*POMGNT2*)	Pathway specific protein O-mannose β4 GlcNAc transferase
Transmembrane protein 5 (*TMEM5*)	Not known (potential glycosyltransferase function)

1.5.2 Cancer

1.5.2.1 ECM-Cell interactions in cancer

Alterations in ECM components, ECM receptors and components of the acto-myosin cytoskeleton results in the loss of normal tissue architecture, increased proliferation and invasion and metastasis of surrounding tissue, all features of cancer progression (Hu et al. 2008, Olson et al. 2009, Zutter et al. 1995). Indeed, mutations in these groups of proteins are highly represented in exome studies of cancer patients (Shah et al. 2012). Additionally, the composition and properties of the ECM are altered in cancer patients, with increased cross-linking, deposition and proteolysis of ECM components (Levental et al. 2009, Provenzano et al. 2006, Xu et al. 2001), with ECM modifiers frequently reported as upregulated in cancer patients and models.

There is a complex, reciprocal relationship between the ECM and the cell, the tight regulation of which is lost upon oncogenic transformation (Van Dijk et al. 2013). Cell proliferation, survival, differentiation, adhesion and migration can all be regulated by the composition and mechanical properties of the ECM (Beattie et al. 2010, Bae et al. 2014, Baker et al. 2013, Levental et al. 2009, Calvacanti- Adam et al. 2006). Furthermore invasion of cells requires degradation of the surrounding ECM and, in the case of mesenchymal migration, there is often the formation of specialised invadosome structures which are enriched in and regulated by adhesion molecules (Ridley et al. 2003, Beaty et al. 2014, Kelly et al. 1994, Brooks et al. 1996). The interaction between the cell and the ECM is also regulated by the subsets, levels and activities of adhesion receptors expressed at the PM (Hua et al. 1993, Zutter et al. 1995, Desgrosellier et al. 2010).

Integrins are extremely well characterised adhesion receptors, binding to ECM components such as collagen and fibronectin, and can contribute to the malignant transformation of cells through a number of processes. Integrin levels vary in cancers, with αvβ3 levels upregulated in some cancers whilst α2β1 is downregulated in a number of cancers, with both instances correlating with poor prognosis (Desgrosellier et al. 2010, Takayama et al. 2005). Moreover, the vesicular recycling of integrin at the PM is reported as altered in cancers through a number of mechanisms, including altered levels of proteins involved in its vesicular transport (Cheng et al. 2004, Caswell et al. 2007), and its PTM regulation such as phosphorylation by c-src, which modulates the interaction with important intracellular binding partners and signalling molecules (Oxley et al. 2008). Consequently the adhesion mediated integrin signalling pathways are disrupted, including the ERK MAPK regulation of cell cycle progression (Moro et al. 1998, Walker et al. 2005). Furthermore, invadopodia are integrin- rich structures and integrins are implicated in the early stages of their formation, stabilising the structure and

promoting its maturation (Beaty et al. 2014, Beaty et al. 2013, Destaing et al. 2010). Normal growth requires a balance of signals from different adhesion receptors, including integrins but also, syndecans, and other glycoprotein receptors such as CD44, CD36 and DG (Desgrosellier et al. 2010, Hua et al. 1993, Durbeej et al. 1998, Chung et al. 2016). Investigating the distinct contributions of the different adhesion receptors is important in the understanding of mechanisms of cancer progression.

1.5.2.2 Dystroglycan in cancer

As a ubiquitously expressed adhesion receptor the interaction of DG with the ECM provides an important physical tether between the cell and its environment (Ervasti et al. 1993) but also regulates ECM organisation (Williamson et al. 1997, Henry et al. 2001b), cytoskeletal organisation (Spence et al. 2004a, Thompson et al. 2008) and signal transduction events (Spence et al 2004b, Ferletta et al 2003, Yang et al. 1885, Sotgia et al.2001) and ultimately cell proliferation, differentiation, polarity, survival and migration (Fig 1.5). All of the above processes are crucial in normal tissue homeostasis and when aberrant are drivers of cancer development and progression.

Dystroglycan has been shown to be important for normal branching epithelial morphogenesis in tissues such as the kidney and salivary gland (Durbeej et al. 19997), moreover the loss of DG has been reported in numerous adenocarcinomas (Cross et al. 2008). Epithelial carcinomas including oesophageal (Parberry-Clark et al. 2011, Cross et al. 2008), colon (Losasso et al. 2000, Sgambato et al. 2003), skin and squamous cell (Jing et al. 2004, Herzog et al. 2004, Shang et al. 2008), cervical (Sgambato et al. 2006), renal cell (Sgambato et al. 2010), breast (Henry et al. 2001, Muschler et al. 2002, Sgambato et al. 2003, Cross et al. 2008) and prostate (Henry et al. 2001, Sgambato et al. 2007b, Mathew et al. 2013) cancer have reported a reduction in DG protein expression from the PM in comparison to benign tissue. Moreover, this progressive loss of DG correlated to higher grade, more aggressive tumours and the ability to metastasise (Mathew et al. 2013, Mitchell et al. 2013, Sgambato et al. 2010, Esser et al. 2013). A number of groups have examined the impact of βDG expression on the growth and behaviour of cancer cells. Sgambato et al. observed that overexpression of DG had an inhibitory effect on cell growth and reduced tumourigenicity in mice, an effect also observed in breast cancer cell lines (Sgambato et al, 2007, Sgambato et al., 2006). This work was expanded upon in a study by Mitchell *et al* in which shRNA depletion of DG in prostate cancer cell lines saw an increase in growth on soft agar and a reduction in invasive capability whilst overexpression of DG abolished growth on soft agar and increased invasion (Mitchell et al., 2013). Consequently, a model was proposed in which initial loss of functional DG in the primary tumour promotes tumour growth and disruption of ECM organisation but at later stages an increase in DG may be required for

MET and anchorage of invading cells at secondary sites (Mitchell et al. 2013). This is supported by the re-expression of DG in some metastatic samples in an immunohistochemical study (Mitchell et al, 2013, Mathew et al.2013). One group has also reported a potential role for DG in angiogenesis based upon the observation of dynamic expression levels of DG in vascular endothelial cells regulating proliferation, migration and formation of tubes in matrigel assays (Hosokawa et al. 2002). Combined the above information suggests a potential role for DG in epithelial carcinoma progression although the precise mechanisms through which it achieves this requires further validation. It is therefore important to understand not only the functions of DG which could contribute to this process but also the mechanisms behind its regulation.

The loss of functional DG in carcinomas does not appear to be a consequence of reduced transcription or mutations of *DAG1*, rather it is a consequence of altered PTM (Singh et al. 2004, Bao et al. 2009) (Fig 1.5). A number of groups are therefore addressing the question of the underlying mechanisms of reduced DG and the contributions of these to cancer progression.

Once again the glycosylation status of αDG is highly implicated in its disease contribution, with hypoglycosylation of the α subunit reported in prostate (Bao et al. 2009, Shimojo et al. 2011, Esser et al. 2013), breast (Muschler et al, 2002, Singh et al. 2004), colon (Singh et al. 2004, Losasso et al. 20000) and clear cell renal cell carcinoma (Miller et al. 2015). Furthermore, glycosylation inversely correlates with the Gleason scores of prostate cancers (Esser et al 2012). Reduced glycosylation of αDG perturbs its binding to laminin and other ECM components and disrupts downstream signalling cascades (Chiba et al. 1997, Yoshida-Moriguchi et al. 2015). The loss of anchoring to laminin has been reported to be widespread in cancers and was characteristic of aggressive cancer subtypes (Akhavan et al. 2012). The importance of this interaction in cancer was further demonstrated by Bao et al. in prostate cancer cells in which reduced levels of laminin binding glycans, including of DG, resulted in increased cell migration and tumour formation compared to their glycosylated counterparts (Bao et al. 2009). The reduced glycosylation and increased invasion correlated with reduced expression of glycosyltransferases β3GnT1 and LARGE, key enzymes in the glycosylation of αDG which, along with ISPD, have been reported as downregulated in a number of human cancers, correlating with reduced DG glycosylation and poor prognosis (Bao et al. 2009, Esser et al. 2013, Miller et al. 2015). In prostate cancer the loss of LARGE was a consequence of the important EMT transcription factors snail and zeb1 (Huang et al. 2015). Increased invasion of cells as a consequence of hypoglycosylation is reduced upon overexpression of β3GnT1 or LARGE and a more specific role of αDG demonstrated by increasing migration by blocking the αDG-laminin interaction with the DG blocking antibody IIH6 (Bao et al. 2009).

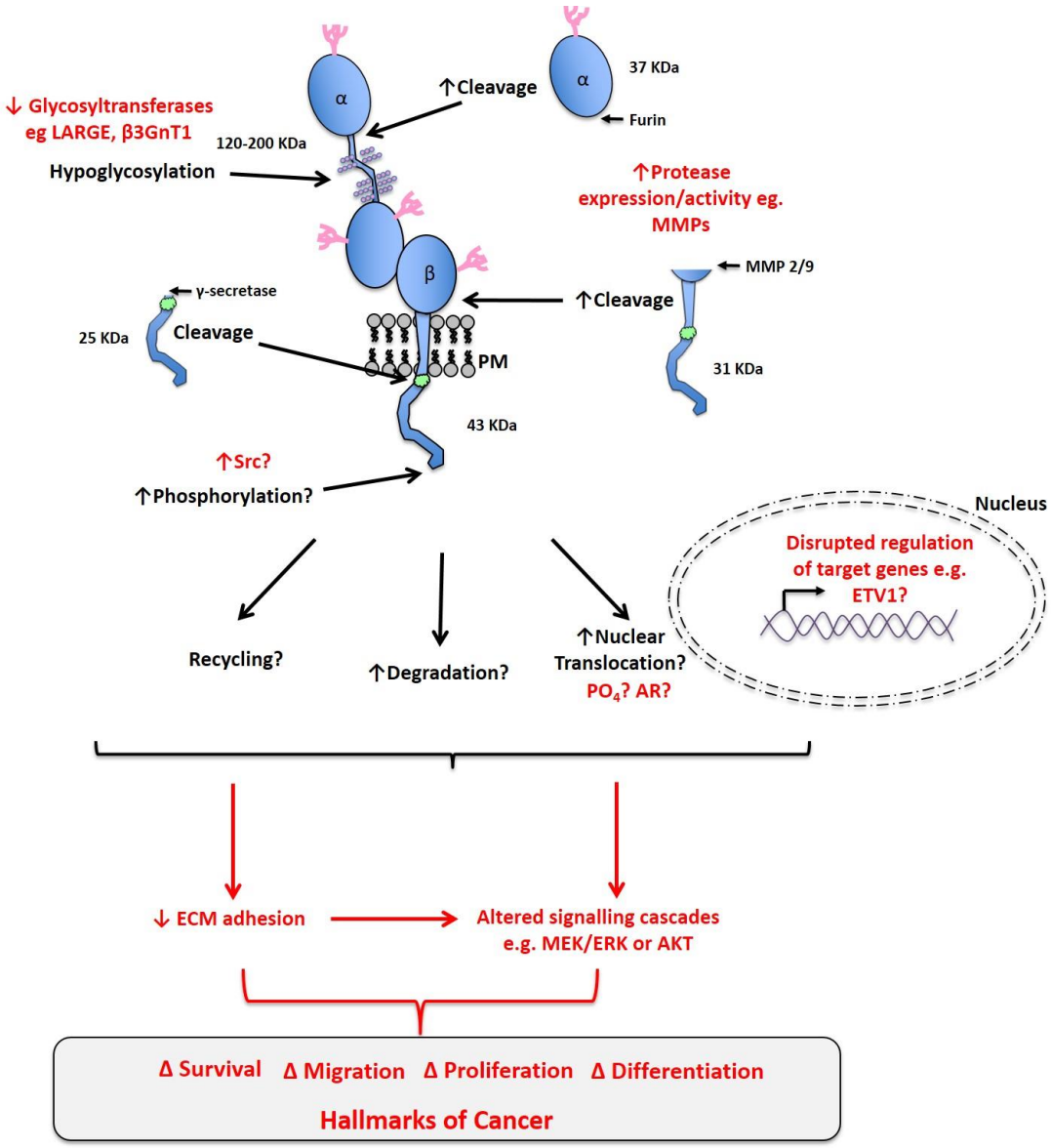

Figure 1.5: Aberrant modifications and potential contributions of DG in cancer. Cartoon of dystroglycan with known aberrant modifications and processing of DG highlighted in red. Increased levels of Src and subsequent phosphorylation and abnormal androgen receptor (AR) signalling have all been hypothesised as potential causes of disrupted DG regulation including potential changes to its interactions, recycling, degradation and nuclear translocation. These changes may ultimately alter the regulation of genes, ECM adhesion and signalling pathways and consequently alter the ability of the cell to survive, migrate, proliferate and differentiate, all of which can contribute to cancer progression,

Whilst hypoglycosylation of DG is a clear feature of many cancers, if and how this contributes to the disease progression is more difficult to unravel. The signalling cascades modulated by DG binding to the ECM are likely to be perturbed upon hypoglycosylation of the α subunit, indeed levels of phospho-ERK and phospho-AKT were increased in cells in which αDG, β3GnT1 or LARGE were depleted by RNAi (Bao et al. 2009). DG can sequester ERK and MEK of the MAPK cascade and has been shown to modulate integrin signalling pathways (Spence et al. 2004, Ferletta et al. 2003), thus loss of DG function may contribute to cancer progression by disrupting the fine balance of signalling from ECM receptors. Furthermore, laminin can be internalised by endocytosis and this process is disrupted in cancers in which DG function is perturbed and restored by DG re-expression. (Leonoudakis et al. 2014) The majority of the internalised laminin was transported through the late endosome for degradation, however, other than ECM remodelling, the functional significance of this is unclear both in normal cells as well as cancer (Leonoudakis et al. 2014).

As mentioned previously, hypoglycosylation of αDG makes the ectodomain more vulnerable to cleavage by MMPs, resulting in a ~31kDa fragment, which can be further cleaved to a 26 kDa cytoplasmic fragment by gamma secretase and furin (Cross et al. 2008, Singh et al. 2004, Leocadio et al. 2016). The 31 KDa fragment has been detected at increased levels in multiple cancers including breast, colon, prostate, skin and squamous cell carcinomas, with smaller 26 kDa and 17kDa fragments also variably detected (Singh et al. 2004, Mathew et al. 2013, Cross et al. 2008, Shang et al. 2008, Herzog et al. 2004). Moreover, the production of the 31 and 26 kDa fragments were regulated in a cell density dependent manner (Mitchell et al. 2013). Interestingly, treating cells with resveratrol, a potent activator of the notch signalling pathway, resulted in an increase in the formation of the 26kDa fragment, indicating a potential role for the notch signalling pathway, which is known to detect cell-density changes, in the proteolysis of βDG (Leocadio et al. 2016). MMPs are upregulated in a number of cancers (Morgia et al. 2005), tumours are inherently dense populations of cells and abrogated notch signalling is widely reported in the neoplastic transformation of cells (Yuan et al. 2015), all of which, alongside hypoglycosylation may account for increased proteolytic cleavage of DG in cancer cells. There is also increased shedding of the N-terminal of αDG in a furin dependent manner, but independent of βDG cleavage (Singh et al. 2004) Proteolytic cleavage of DG again leads to reduced adhesion and disrupted signalling cascades the implications of which in cancer have been discussed above, however the fate and potential functions of the cytoplasmic fragments of βDG are not clearly understood.

Recent studies have shown the targeting of a population of these fragments to the nucleus in prostate cancer cells (Mathew et al. 2013, Leocadio et al. 2016), if these fragments are then

targeted for degradation or have a signalling function is unknown. A recent microarray comparing nuclear targeted to nuclear excluded c-terminal βDG in metastatic prostate cancer LNCaP cells saw the differential expression of 34 genes (Mathew et al. 2013). ETV1, a transcription factor involved in a number of cellular processes including promoting proliferation and differentiation, was up-regulated by 4.44 fold in cells with increased nuclear localisation of the C-terminal fragment of βDG. This is of particular interest because overexpression of ETV1 is reported in approximately 40% of CaP and correlates with increased invasiveness (Hsu et al, 2004, Cai et al, 2007). Thus DG appears to be able to modulate gene expression, though it has no identified DNA binding sites itself.

Many of the aforementioned studies on glycosylation, proteolytic cleavage, localisation and nuclear translocation of fragments of DG in cancer have been carried out in prostate cancer cell lines and tissues. Both subunits of DG are lost from the basement membrane and intracellular junctions in mid to high grade prostate cancer and are re-expressed at sites of secondary metastasis (Cross et al. 2008, Henry et al.2001, Mathew et al. 2013, Mitchell et al. 2013). In addition to the nuclear targeting of the cytoplasmic fragments it was reported that there was a potential increase of Y892 phosphorylated βDG in the nucleus of cancer cells compared to wild type tissue (Mathew et al. 2013). Interestingly, DG is dynamically regulated in prostate cells with regards to the androgen receptor (AR) (Sgambato et al. 2007b). The AR is a critical regulator of proliferation, differentiation and cell survival and mutations or increased levels of the AR can lead to androgen independent signalling and the development and progression of prostate cancer (Feldman et al. 2001, Knudsen et al, 2006). Anti-androgen treatment of androgen responsive cells resulted in the decreased expression of DG whilst androgen treatment resulted in a dose dependent increase as well as translocation of βDG to the nucleus (Sgambato et al. 2007b, Mathew et al. 2013). The promoter sequence of DG also contains a putative androgen responsive element (ARE), suggesting DG may be regulated by AR at both the DNA and protein level, though this requires further validation (Sgambato et al. 2007b).

Combined, the above information suggests a potential role for DG not only in muscular dystrophies but also epithelial cancer progression, often through abrogation of its complex PTM (Barresi et al. 2006) It is therefore important to understand not only the functions of DG which could contribute to the disease processes but also the mechanisms behind its regulation. Furthermore, the majority of studies focus on DG at the cell membrane, with much emphasis on the disrupted interaction with the ECM. DG is observed in the nucleus of a variety of tissues including muscle and epithelial cells, both normal and in disease states. It is therefore important to gain a greater understanding of the regulation of DG at both the membrane and nucleus and

to consider that aberrant processing may impact nuclear levels and functions of DG and may contribute towards the disease state.

1.6 NUCLEAR DYSTROGLYCAN

Whilst initially surprising, the localisation of βDG in the nucleus of many cell lines and tissues of many origins, both cancerous and normal, has now been reported by multiple groups (Oppizzi et al. 2008, Martinez-Vieyra et al. 2013, Mitchell et al. 2013, Mathew et al. 2013). The nuclear localisation of βDG hints at yet more roles for this enigmatic, multifunctional protein and there is a growing field of research aimed at understanding its nuclear functions and regulation.

1.6.1 The Nucleus

The nucleus contains the DNA and coordinates cellular activities such as growth, division and protein synthesis. The nucleus is a membrane bound organelle, separating the highly regulated nuclear contents and processes from the surrounding cytoplasm (Prunuske et al. 2006). The nucleus also contains organelles such as the nucleolus, dense structures that are sites of ribosome and rRNA synthesis and assembly. In interphase the nucleoli can be described as three main structures; the fibrillar centers (FCs), the dense fibrillar component (DFC) and the granular component (GC) (Hernandez-Verdun 2011).The nuclear envelope consists of the nuclear membranes, the nuclear lamina and the nuclear pore complexes (Hertzer et al. 2010) (Fig 1.6). The nuclear membrane is made of two phospholipid bilayers; the outer nuclear membrane (ONM) which is contiguous with ER and the inner nuclear membrane (INM) (Purunske et al. 2006). Both the INM and ONM contain differing populations of integral and associated membrane proteins (Foisner et al. 2003, Manilal et al. 2008, Worman et al. 1988, Hertzer et al. 2010). Embedded within the NE are the nuclear pore complexes, large complexes of nucleoporin proteins, which act as channels for communication between the nucleoplasm and cytoplasm (Alber et al. 2007). Beneath the INM is a protein meshwork referred to as the nuclear lamina (Gruenbaum et al. 2005). The nuclear lamina consists predominantly of intermediate filaments formed by A and B type lamins, the lamins form coiled-coil dimers which associated to form higher order network structures (Gruenbaum et al. 2005, Stuurman et al. 1998, Shimi et al. 2015). The lamins are connected to the INM through their interactions with proteins embedded within the INM such as emerin, lamin binding receptor (LBR) and lamin-associated peptides 1 and 2 (LAP1 and -2) (Gruenbaum et al. 2005, Foisner et al. 2003, Worman et al.1988, Sakaki et al. 2001) (Fig 1.6). The nuclear lamina serves as a scaffold at the nuclear periphery, where it plays a structural role in maintaining the shape of the nucleus and the spacing of the NPCs but also has active roles in organising chromatin,

DNA replication and regulating transcription factors (Gruenbaum et al. 2005, Dorner et al. 2007, Prokocimer et al.2009).

A mechanical link between the external cytoskeleton and the nucleus is formed by the Linker of the nucleoskeleton to the cytoskeleton (LINC) complex (Mejat et al. 2010). A prototypical LINC complex consists of transmembrane SUN proteins in the INM which can interact with the nuclear lamina and associated proteins within the INM such as emerin, and with the ONM KASH proteins in the perinuclear space (Razafsky et al. 2009, Haque et al. 2010, Haque et al. 2006) (Fig 1.6). The KASH proteins, such as nesprins of which there are many isoforms, project into the cytoplasm where they interact with cytoskeletal and signalling proteins, directly or through linkers or motor proteins such as plectin or dynein (Zhang et al. 2002, Wilhelmsen et al. 2005, Razafsky et al. 2009). Thus the LINC complex forms a bridge between the nucleus and the cytoskeleton and has important roles in transducing extracellular mechanical forces to the nucleus and regulating cellular functions such as cell division, cytoskeleton organisation and organelle position (Mejat et al. 2010, Razafsky et al. 2009, Chang et al. 2015).

Mutations in the genes of a number of nuclear envelope proteins have been identified as the cause of a heterogenous array of human diseases, for example emerin is mutated in X-linked EDMD (Bione et al. 1994), and over 200 mutations in *LMNA,* the gene encoding A-type lamins have been identified (Mejat et al. 2009) resulting in several laminopathies including autosomal dominant-EDMD (Bonne et al. 1999), Limb Girdle Muscular dystrophy (LGMD) (Muchir et al. 2000) and Hutchinson-Gilford progeria syndrome (HGPS) (Eriksson et al. 2003). Interestingly a common phenotype within NE diseases is muscle defects and the ongoing work into understanding of the structural and signalling roles is providing valuable insight into these diseases (Mejat et al. 2010).

Correct nuclear functions are vital for maintaining a healthy, viable cell, therefore the spatial and temporal regulation of proteins with nuclear roles is tightly regulated (Handwerger et al. 2006). The complexities of selectively transporting sufficient levels of the necessary proteins to the desired locations within the nucleus are amplified as a result of the rapid shuttling of proteins between the cytoplasm and the nucleus, the need of the nucleus to respond to external signals transmitted by the cell and the vast changes in nuclear morphology and processes, such as DNA replication, required for a cell to divide (Foisner et al. 2003).

1.6.2 Nuclear Translocation Pathways

The compartmentalisation of different processes is a key principle of the eukaryotic cell, and in the case of the nucleus, separates the transcription and synthesis of DNA from the translational processes in the cytoplasm. The nuclear envelope (NE) forms the barrier whilst the tightly controlled nuclear pore complexes (NPC) form selective routes for transport and

communication between the two compartments (Cautain et al. 2015). Proteins smaller than 40 kDa can traverse through the NPC via diffusion however larger proteins require the assistance of adaptor proteins (carriers). Importins and exportins (Karyopherins) are the carriers that facilitate the transport into and out of the nucleus respectively (Cautain et al. 2015). The importins and exportins recognise specific transport sequences within the cargo protein known as nuclear localisation signal (NLS) or nuclear export signals (NES), enabling the transport across the pore (Lange et al. 2007, Wen et al 1995). The characterised NLS are either classical or non-classical, with the classical members being either a short, highly basic signal of ~4-5 residues (monopartite) or two stretches of basic residues separated by a linker region generally between 10-12 residues long (Kalderon et al. 1984, Lange et al. 2007, Lange et al. 2010). Non-classical NLS include PY-NLS in which a central arginine residue is flanked N-terminally by a hydrophobic motif and C-terminally by a PY sequence and these proteins often do not require an adaptor but bind directly to the transporter (Cautain et al. 2015, Suel et al. 2008). NES are often leucine rich with the consensus sequence $\phi 1\text{-}X_{(2\text{-}3)}\text{-}\ \phi 2\text{-}\ X_{(2\text{-}3)}\text{-}\ \phi 3\text{-}X\text{-}\ \phi 4$, (where ϕ is a hydrophobic residue, L, V, I, F, or M and X is any residue but preferentially small, charged or polar) but can be more complex, requiring 3D structural features of the protein to be recognised (La Cour et al. 2004, Cautain et al. 2015) . The recognition signals for many of the karyopherin family remain to be characterised. The majority of the nuclear transport receptors are members of the karyopherin β family, such as the import receptors Importinβ, which can either bind directly to the NLS or via an adaptor which are members of the Impα family (Lange et al. 2007, Cautain et al. 2015). In the case of export receptors, chromosome region maintenance 1 (CRM1) is one of the best characterised and is also a karyopherin β family protein (Fornerod et al. 1997).

In the case of nuclear import of a classical NLS cargo protein, Imp-α and -β form a heterodimer in the cytoplasm, following which Imp-α binds to the cargo protein and the complex then translocates through the nuclear pore, where Imp-β interacts with components of the NPC, into the nucleoplasm, whereby the complex dissociates (Isgro et al. 2005, Cautain et al. 2015, Lange et al. 2007) (Fig 1.7). Using CRM1 as a classical example in the case of nuclear export, CRM1 binds to cargo within the nucleoplasm, occasionally through adaptors, transporting the complex through the NPC to be dissociated in the cytosol (Fornerod et al. 1997, Cautain et al. 2015) (Fig 1.7). The loading and unloading of cargo proteins from the transport complexes requires metabolic energy and is regulated by RAN GTPases (Moore, 1998). RanGEFs are predominantly nuclear whilst Ran GAPs are predominantly cytoplasmic in localisation, thus creating a RanGTP gradient between the two compartments (Moore, 1998, Gorlich et al. 1996).

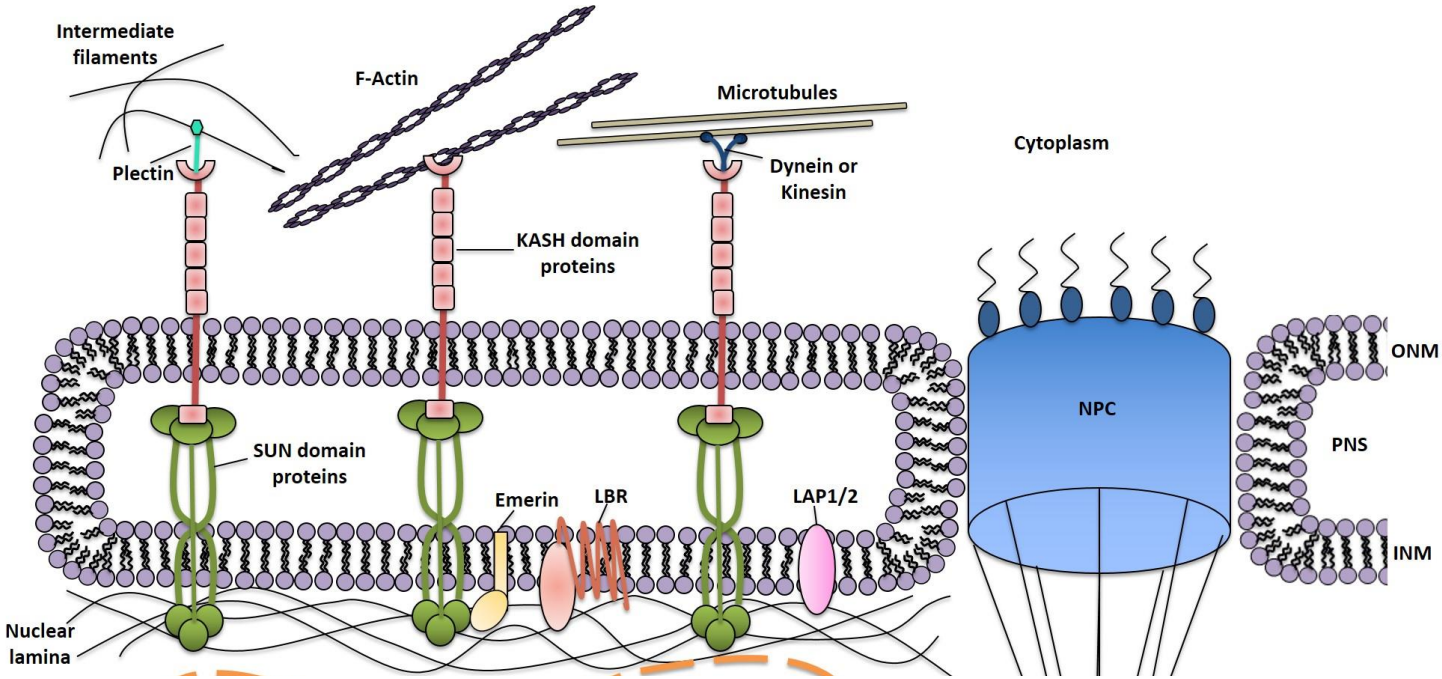

Figure 1.6. The nuclear envelope. Schematic diagram of the components of the nuclear envelope and associated proteins. The nuclear membrane can be divided into the ONM and INM and is under laid by the nuclear lamina meshwork which provides structural support and signalling functions. The nuclear pore complex crosses the nuclear envelope allowing the transport of molecules. Distinct populations can be found in the ONM and INM which can interact in the PNS as is the case with the LINC complex KASH domain proteins of the ONM and the INM Sun proteins. The LINC complex physically tethers the nucleus to the cytoskeleton through KASH proteins interacting directly or through linker proteins with the cytoskeleton and with the nuclear lamina and INM proteins through SUN proteins. A number of INM proteins including emerin, LBR and LAP proteins interact with each other and the nuclear lamina and sometimes the chromatin providing structural and signalling roles.

The RanGTP in the nucleus promotes the dissociation of the import complex, whilst it promotes the formation of the export complexes (Gorlich et al. 1996, Lindsay et al. 2001). Importins α- and β- are recycled back out of the nucleus in complex with RanGTP, and in the case of importin- α, with export transporters such as exportin-2 or CAS, and are released through the action of RanGAPs in the cytoplasm to start a new import cycle (Moore, 1998, Kutay et al. 1997) (Fig 1.7).

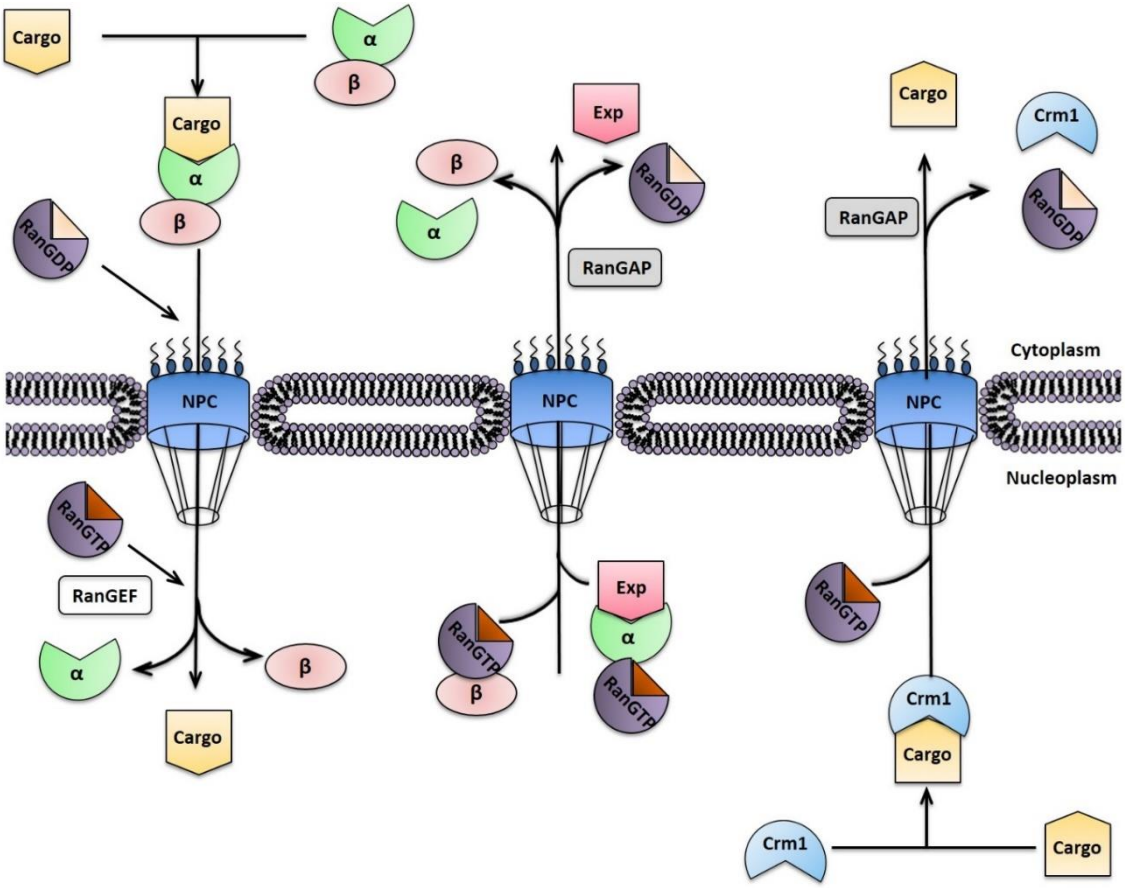

Figure 1.7: The nucleo-cytoplasmic transport of proteins. A schematic diagram depicting the nuclear import of a protein cargo with a classical NLS through the nuclear pore in complex importins α and β. Once in the nucleus high levels of RanGTP, catalysed by RanGEFs, cause the dissociation of the complex and release of the cargo. Importin β and importin α are transported back into the cytoplasm in a RanGTP dependent manner, and in the case of importin α in complex with a nuclear export transporter (Exp). In the cytoplasm the importins are released through the activity of RanGAPs for further cycles of transport. Nuclear proteins can be bound by nuclear export proteins such as Crm1 at their NES, in an interaction promoted by RanGTP. Hydrolysis of RanGTP in the cytoplasm by RanGAPs promotes the release of the cargo protein.

A number of membrane receptors are trafficked to the nucleus, either as full length receptors or as proteolytically cleaved fragments, where they also have nuclear functions, however, the mechanisms of transport are poorly defined (Chen et al. 2015). Receptor tyrosine kinases (RTKs) such as EGFR, MET and FGFR have been shown to be transported to the nucleus and a large proportion of the understanding of the nuclear translocation of cell surface receptors comes from the study of these proteins (Bryant et al. 2005, Chen et al. 2015, Lo et al. 2006). Membrane receptors can be internalised from the membrane into vesicles by clathrin-dependent or independent mechanisms from which they can be recycled, degraded or undergo retrograde transport back through the golgi and the ER (Wang et al. 2010a. Chen et al. 2015). At least two methods of traffic of endocytic membrane receptors from the ER to the nucleus have been identified: integral trafficking from the ER to the nuclear envelope transport (INTERNET) or integrative nuclear FGFR1 signalling (INFS) (Chen et al. 2015, Myers et al. 2003, Wang et al. 2012). Receptors trafficked via INTERNET remain membrane bound, for example EGFR has been shown to traffic from the ER to the ONM where it binds to a NPC and through to the INM from which it can be transported into the nucleoplasm in a Sec61 dependent manner (Wang et al. 2010a, Wang et al. 2010b, Wang et al. 2012). This process requires the binding of importin-β to the NLS of EGFR (Lo et al. 2006). In INFS the receptors become soluble following release from the ER and are translocated to the nucleus through the NPC in an importin α/β dependent manner (Chen et al. 2015, Myers et al. 2003). Additionally, a number of membrane proteins are cleaved by caspases or through RIP after which the intracellular domain can perform signalling functions, often within the nucleus to which it is transported in an importin α/β dependent manner (Chen et al. 2015). Some receptors are also proposed to enter the nucleus by 'piggy-backing' with another protein, such as the case with some cytokines through the NLS in their cognate interleukin ligands (Jans et al. 1998). A recent study by Chaumet et al. has identified an alternative route of nuclear transport for surface proteins in a process mediated by nuclear envelope-associated endosomes (NAE) (Chaumet et al. 2015). Through this route the LRP1 receptor was internalised into endosomes which then associated with, and fused to the outer membrane of the NE, where it released its contents into the NE lumen (Chaumet et al.2015). The receptor was then released into the nucleoplasm through a process that was shown to require the NE proteins SUN1 and SUN2 as well as the Sec61 translocon (Chaumet et al. 2015). The authors could find no interaction with importin-β and also demonstrated that the process was golgi independent (Chaumet et al. 2015).

1.6.3 Nuclear translocation of βDG

Oppizzi and colleagues were first to report a functional bipartite NLS located directly C-terminal to the transmembrane domain in βDG (Oppizzi et al. 2008). The study in breast cancer cells demonstrated variable levels of full length glycosylated βDG within the nucleus, as determined by immunoblots following cellular fractionation, in a manner that was independent of the glycosylation status or ligand binding capability of αDG (Oppizzi et al. 2008). The NLS was further characterised by Lara-Chacon et al. in myoblasts who determined that residues $_{776}$RKKRKGK$_{782}$ were necessary and sufficient for the nuclear localisation of βDG through a combination of site directed mutagenesis studies as well as the fusion of this sequence to a tetra-GFP molecule (Lara-Chacon et al. 2010). Furthermore, this group demonstrated that DG was undergoing rapid nucleocytoplasmic shuttling and the nuclear localisation was prevented upon blocking the nuclear pore complex with *Agaricus bisporus* lectin (ABL), which binds to the N-acetyl glucosamine of nucleoporins with high affinity (Lara-Chacon et al. 2010). An α/β importin heterodimer bound the cytoplasmic NLS of βDG with a Kd of 0.8 nM and mediated the nuclear translocation of βDG in a Ran dependent manner, suggesting the nuclear import of βDG occurs through a classical importin mediated pathway through the NPC (Lara-Chacon et al. 2010).

Multiple groups have also shown that C-terminal fragments of βDG target strongly to the nucleus within the nucleoplasm (Oppizzi et al. 2008, Lara-Chacon et al. 2010, Mitchell et al. 2013, Mathew et al. 2013, Leocadio et al. 2016), as has also been seen with the nuclear targeting of numerous ICD of RTK receptors and cleavage products of other proteins such as Notch (Guruharsha et al. 2012, Chen et al. 2015). The production of the 31kDa and 26kDa cytoplasmic fragment of βDG increases in a cell density dependent manner. Additionally, the nuclear 31kDa DG fragment may undergo a sequential proteolysis event by γ-secretase to form the 26kDa fragment (Mitchell et al. 2013, Leocadio et al. 2016). The nuclear translocation of a cytoplasmic fragment of βDG can be prevented by mutating the NLS within it (Mitchell et al. 2013, Mathew et al. 2013). It is possible that the fragments of βDG in the nucleus may be targeted to the nuclear proteasome or exported to the cytoplasmic proteasomes for degradation or they may have a functional role (See section 1.6.4).

An important question when addressing the nuclear localisation of a protein that also has roles at the plasma membrane is if it is internalised from the PM to the nucleus or if it is a separate population. Whilst still not clear in the case of βDG, biotinylation experiments followed by fractionation suggest a pool of nuclear βDG, at least some of which has been at the PM (Vasquez-Limeta et al. 2014).

Another important observation is that the nuclear levels of βDG are variable within a population, independent of αDG, suggesting that it is dynamically regulated (Oppizzi et al 2008, Mitchell et al. 2013, Mathew et al. 2013, Martinez-Vieyra et al. 2013). A number of groups have therefore addressed different aspects of the regulation of nuclear translocation of βDG. Phosphorylation is known to be an important regulator of nuclear translocation of proteins (Nardozzi et al. 2010). Given the importance of phosphorylation at Y892 for the interactions (Ilsley et al. 2001, James et al. 2000, Sotgia et al. 2001) and internalisation of βDG from the PM (Sotgia et al. 2003, Miller et al. 2012) it was hypothesised that it may also be important for the nuclear localisation of βDG. Initial studies suggest that the effect of phosphorylation on nuclear translocation is complex. A non-phosphorylatable Y892F form of a GFP-tagged c-terminal fragment of βDG accumulated in the nucleus, although no change in nuclear levels were seen when the same mutation was introduced into full length flag-tagged mouse DG (Lara-Chacon et al. 2010, Leocadio, 2014). In immunohistochemical studies of prostate samples from normal and cancerous tissues from patients a pY892 form of βDG was identified at the BM and cell junctions but also in the nucleus (Mathew et al. 2013). Peroxyvanadate (PV) treatment and consequent increased tyrosine phosphorylation also caused an increase in nuclear accumulation of βDG, although it must be considered that PV treatment will have broad targets within the cell. (Lara-Chacon et al., 2010). Therefore, phosphorylation at different sites may have both promoting and inhibitory roles in nuclear translocation. In addition to sites of tyrosine phosphorylation within the sequence of βDG there are also phosphorylated serine and threonine residues identified by mass spectrometry, potential regulatory roles of which are as yet unknown (Hornbeck et al. 2014) Alternatively, βDG is subject to other PTM such as ubiquitination or sumoylation with as yet unclear functions on the fate of βDG. PTM can contribute to the nuclear localisation of proteins by facilitating or destabilising interactions with binding partners, for example import or export machinery or protein partners which may sequester the protein in the cytoplasm (Nardozzi et al, 2010, Gill, 2004). It will therefore be important to identify PTM that play a role in the nuclear translocation of βDG.

The nuclear or cytoplasmic retention or translocation of proteins can be affected by their binding partners. As previously described the binding site of ezrin overlaps with the site of importin binding at the NLS of βDG (Spence et al. 2004a, Lara-Chacon et al. 2010). However, rather than competing with importins to prevent nuclear accumulation of βDG, overexpression or increased activation of ezrin resulted in an increase in the nuclear levels of βDG and occurred in a manner that required the actin binding function of ezrin (Vasquez-Limeta et al. 2014). Furthermore, disruption of the actin cytoskeleton resulted in lower levels of nuclear accumulation of βDG, suggesting that the cytoskeleton, which can be reorganised depending

upon the cellular requirements, could contribute to the nuclear translocation of a pool of βDG (Vasquez-Limeta et al. 2014).

Additionally, it has been shown that androgen stimulation of the androgen sensitive prostate cancer cell line, LNCaP, resulted in the nuclear accumulation of βDG (Mathew et al. 2013). *DAG1* contains an ARE and DG levels are regulated by androgens (Sgambato et al. 2007b). It is possible that βDG is targeted to the nucleus in complex with the AR, which translocates to the nucleus to act upon target genes, however the inability to detect an interaction between the androgen receptor and βDG, the delayed response of nuclear translocation after treatment and the fact that the same result was achieved through serum addition to starved cells suggest that nuclear translocation of βDG could be a consequence of the mitogenic effects of androgen in LNCaP as opposed to a direct response to the androgen pathway itself (Mathew. 2011).

Interestingly, Sgambato and colleagues have reported that DG mRNA and protein expression are cell cycle regulated (Sgambato et al, 2006). Furthermore, delays in cell cycle progression at S phase, G_2/M and G_0/G_1 transitions following reduction of βDG levels have been reported (Sgambato et al, 2006, Higginson et al, 2008, Villarreal-Silva et al., 2011). It has also been proposed that DG may play a mechanical role in the contractile ring and tethering the membrane to the cytoskeleton during cell division following the observation that in REF52 cells DG colocalised with ezrin to the cleavage furrow and midbody during cytokinesis (Higginson et al., 2008). This observation also indicates that DG localisation as well as expression can be regulated in a cell cycle dependent manner. If the nuclear levels of DG fluctuate in a cell cycle dependent manner requires further investigation, furthermore a reason as to why DG would be required in the nucleus at specific stages of the cell cycle is unknown. The nucleus undergoes dynamic structural and signalling changes as the cell cycle progresses which DG may contribute to. However, a great deal of investigation is required to establish if this is indeed the case.

Thus, whilst our understanding of the mechanisms of the nuclear translocation of βDG is improving, there still remain many questions regarding the triggers, such as the proliferation status or in response to external stimuli, and mechanisms, such as binding partners or PTM, that regulate the nuclear translocation of βDG.

1.6.4 Nuclear functions of βDG

Within the nucleus βDG has been identified at the INM of the NE, dispersed throughout the nucleoplasm and at distinct nuclear structures including the nucleoli, splicing speckles and cajal bodies through immunofluorescence and EM studies in multiple cell lines including HeLa cells, C2C12 myoblasts, LNCaP, PNT1A and PC3 prostate cancer cells as well as in epithelial and carcinoma prostate tissue from patients (Lara-Chacon et al. 2010, Martinez-Vieyra et al. 2013, Mitchell et al. 2013, Mathew et al. 2013). As the studies of nuclear DG grows, so too does the

evidence towards nuclear functions for DG and, in accordance with the diverse localisation of βDG within the nucleus, seem to hint at both static and dynamic functions of βDG.

βDG is not the only member of the DAPC to have been found in the nucleus. Indeed, the first reports of βDG in the nucleus came from studies with the aim of investigating DAPC components in the nucleus following the observation of a short isoform of dystrophin, Dp71 in the nucleus of HeLa (cervical), C2C12 (muscle) and N1E-115 (neuroblast) cells (Gonzalez et al. 2000). Further studies in HeLa, C2C12 and PC12 cells identified not only Dp71 but also βDG, α and β-dystrobrevin, α,β,ε-sarcoglycan and α and β-syntrophin in the nucleus, including at the nuclear envelope (Villarreal-Silva et al. 2010, Gonzalez-Ramirez et al. 2008, Fuentes-Mera et al. 2006, Martinez-Vieyra et al. 2013). α-dystrobrevin and Dp71 also translocate to the nucleus in an importin α/β dependent manner, although only βDG contains a classical NLS and it is possible that other components of the DAPC can enter the nucleus in complex with these components (Aguilar et al. 2015, Suarez-Sanchez et al. 2014). Furthermore, multiple interactions between the DAPC components were identified via immunoprecipitations of the nuclear fractions, prompting the hypothesis of the existence of a nuclear DAPC (Villarreal-Silva et al. 2010, Gonzalez-Ramirez et al. 2008, Fuentes-Mera et al. 2006, Martinez-Vieyra et al. 2013). Depleting the levels of Dp71 resulted in reduction of other nuclear DAPs, similar to loss of dystrophin at the PM in DMD patients and demonstrating its importance for stability of the complex (Villarreal-Silva et al. 2010).

Given the structural role of the DAPC at the PM, the possibility for similar roles within the nucleus was exciting. Multiple components of the nuclear DAPC can interact with the nuclear matrix which underlies the nuclear envelope (Fuentes-Mera et al. 2006, Martinez-Vieyra et al. 2013, Aguilar et al. 2015). Through immunoprecipitations βDG was shown to interact with nuclear lamina proteins, lamin B1 and lamin A/C, and lamin binding protein, emerin, in C2C12 myoblasts (Martinez-Vieyra et al. 2013). Support for a structural role for βDG within the nucleus was seen upon RNAi depletion of βDG whereby lamin B1 and emerin levels were reduced and mislocalised (Martinez-Vieyra et al. 2013). Moreover, the βDG depleted cells displayed aberrant nuclear morphology including disrupted morphology of the NE, nucleoli, cajal bodies and splicing speckles (Martinez-Vieyra et al. 2013). It is interesting to consider if the role of βDG at the nucleoli, cajal bodies and splicing speckles is solely structural or if it can also contribute to their functions in ribosomal assembly, pre-mRNA splicing and rRNA processing. Similar disrupted morphology phenotypes were displayed upon depletion of α-dystrobrevin or Dp71 (Aguilar et al. 2015, Hernandez-Ibarra et al. 2015, Villarreal-Silva et al. 2010). Interestingly preliminary studies suggest an interaction between βDG and SUN1 a component of the LINC complex located within the inner nuclear membrane (M. Laredo and S.

Winder personal communication), the functional significance of this interaction is currently under investigation but could be another route through which DG contributes to the mechanical properties of the cell. Additionally, in βDG depleted cells there was an increased distance between the nuclear envelope and the centrosomes (Martinez-Vieyra et al. 2013). The association between the centrosome and NE is mediated in part by NE proteins. Interestingly, βDG antibodies detect punctate structures within a variety of cells, which may be the centrosome or primary cilia (Personal communication S. Winder) and the potential of an uncharacterised role for βDG at another subcellular structure with links to the nucleus would be interesting to investigate. The above information indicates that, βDG, along with other DAPC components, has a role in maintaining nuclear structure and may contribute to nuclear envelope mediated functions.

Just as DG has multifunctional roles at the plasma membrane, there is emerging evidence that the same is true within the nucleus. As previously discussed, the differential regulation of 34 genes was detected in a microarray comparing the expression of genes in LNCaP cells expressing either a cytoplasmic fragment of βDG which targets to the nucleus or is excluded from the nucleus via mutation of its NLS (Mathew et al. 2013). No DNA binding sites have been identified in DG, however the microarray results highlight the exciting possibility that nuclear βDG may regulate the transcription of genes, maybe through sequestering a transcription factor. The idea of the proteolytically cleaved fragments of surface proteins interacting with transcription factors within the nucleus is by no means new and has been reported for numerous receptors including RTKs. For example, the ICD of Erb4 interacts with STAT5 within the nucleus and modulates the transcription of β-casein (Williams et al. 2004). Alternatively, βDG may regulate nuclear functions through the signalling pathways that it modulates. Given that both DG and ERK translocate to the nucleus it is possible that they may interact there in a manner which modulates signalling activity (Chen et al., 1992.). Erk may even play a role in the translocation of DG as its binding site overlaps that of DG's NLS as is seen with ezrin as described above (Moore et al. 2010, Vasquez-Limeta et al. 2014). Therefore, although there is no direct evidence, it is tempting to speculate that nuclear DG may have a signalling role. Given DG's crucial roles within development and tissue homeostasis and its ability to contribute to multiple disease states it is important to better understand the functions and mechanisms of regulation of nuclear dystroglycan.

1.7 PROJECT OUTLINE

Originally identified as an adhesion receptor at the plasma membrane, DG is now acknowledged as a multifunctional molecule also acting as a scaffold for numerous signal transduction pathways (Ervasti et al. 1993, Sotgia et al. 2001, Spence et al. 2004). Importantly, the level of functional DG at the cell membrane is reduced in many human diseases including muscular dystrophies and epithelial cancers (Barresi et al. 2006). More recently βDG has been identified in the nucleus of numerous cell types (Oppizzi et al. 2008, Lara-Chacon et al. 2010, Mathew et al. 2013), hinting at yet more roles for this versatile protein. Yet the mechanisms of translocation and function of βDG in the nucleus are relatively unknown. Interestingly the reported levels of nuclear βDG are variable within a population of cells, suggesting that it is dynamically regulated (Mitchell et al. 2013, Martinez-Vieyra et al. 2013). DG is highly regulated by its PTM, with phosphorylation of βDG implicated in its subcellular localisation (Sotgia et al. 2003, Miller et al. 2012). There are multiple sites of phosphorylation identified within βDG with as yet uncharacterised functions (Hornbeck et al. 2014), therefore one aim of this project is to investigate the role of phosphorylation on the regulation and nuclear localisation of βDG. There is also emerging evidence that the nuclear level of βDG fluctuates as the cell cycle progresses (Mathew. 2011). DG expression and the cell cycle have been shown to be intrinsically linked (Higginson et al. 2008, Sgambato et al, 2007b, Villarreal-Silva et al, 2011). Therefore, a second aim of this project is to investigate the potential cell cycle dependent nuclear translocation of βDG. Finally, DG antibodies have been reported to detect structures within the cell which may be the centrosomes. Furthermore, centrosome number and position has been shown to be disrupted upon DG depletion (Martinez-Vieyra et al. 2013), which may be a consequence of the role of βDG at the nuclear envelope. Consequently, a further aim of this project is to investigate a novel localisation of βDG at the centrosome.

1.7.1 Project aims

1. To characterise the different βDG antibodies used in the study of dystroglycan
2. To investigate the role of specific phosphorylation events of the regulation and nuclear localisation of βDG in prostate cell lines.
3. To investigate the localisation of βDG and its nuclear translocation throughout cell cycle progression in prostate cell lines.
4. To study the localisation of βDG at the centrosomes.
5. To use dystroglycan null fibroblasts to investigate potential nuclear functions of DG including nuclear morphology and centrosome position.

2. Materials and Methods

2.1 BACTERIAL TECHNIQUES

2.1.1 BACTERIAL GROWTH CONDITIONS

Escherichia Coli (E. coli) strains DH5α (Lucigen) and XL-10 Gold (Stratagene) were grown at 37°C in 5 ml 2x YT liquid media (Appendix A) with the appropriate antibiotic; ampicillin (100µg/ml) or kanamycin (30µg/ml) as required for selection.

2.1.2 PREPARATION OF COMPETENT BACTERIA

A single colony of DH5α was used to inoculate 10 ml of 2x YT. The starter culture was grown overnight at 37°C in a shaking incubator. The following morning 1ml of the starter culture was used to inoculate 100ml of 2xYT which was then incubated at 37°C in a shaking incubator until OD_{600} was 0.4-0.6 AU as determined on the spectrophotometer (Jenway). The bacteria was pelleted by centrifuging the culture at 700g for 10 minutes at 4°C (Sigma 12169-H rotor). The supernatant was discarded and the pellets resuspended in 10ml ice cold 100mM $CaCl_2$ and incubated on ice for 2 hours. The bacterial cells were centrifuged again at 700xg, 10 minutes at 4°C. The supernatant was discarded and the pellet resuspended in 2ml ice cold $CaCl_2$ supplemented with glycerol to a final concentration of 15%. The bacterial glycerol solution was divided into 100µl aliquots and snap frozen in liquid nitrogen prior to storage at -80°C for up to 6 months

2.1.3 TRANSFORMATION OF COMPETENT BACTERIA

Aliquots of *E.coli* (50 µl) were thawed on ice. DH5α and XL-10 Gold were used for plasmid purification. In the case of the commercial super competent XL-10 Gold cells 2 µl B-mercaptoethanol was added to each aliquot and swirled gently. Cells were incubated on ice for 10 minutes. 100-150ng of plasmid DNA was added to the cells. Cells were incubated on ice for 30 minutes, heat shocked at 42°C for 30 seconds and then incubated on ice for 2 minutes. 500 µl of pre-warmed non-selective media, NZY^+ broth, was added to the cells and placed at 37°C for 1 hour in a shaking incubator to recover. Cells were then harvested in a benchtop centrifuge (3000g, 2 minutes) and the non-selective media removed. Cells were resuspended

in 200 µl non-selective media and plated on agar plates containing the required selection antibiotic (Table B.1) and incubated overnight at 37°C.

2.1.4 GLYCEROL STOCKS OF BACTERIAL CULTURES

Bacteria was transformed with the required plasmid and grown on an agar plate with antibiotic selection overnight. A single colony was picked and grown overnight at 37°C in 5ml 2x YT with antibiotic selection. 750µl of the overnight culture was added to an equal volume of 50% glycerol and stored at -80°C

2.2 MOLECULAR BIOLOGY TECHNIQUES

2.2.1 PLASMID PURIFICATION BY MINI- OR MAXIPREP

Plasmids were purified from transformed *E.coli* for small and large scale preparations by mini- and maxiprep kits (Qiagen) respectively, according to the manufacturer's instructions. Briefly, the cells are lysed with an alkaline lysis solution following which the DNA is bound to an anion exchange membrane or resin. A medium salt wash is used to remove impurities The purified plasmid DNA was eluted and then subject to isopropanol precipitation in order to desalt and concentrate the DNA, the eluted DNA is dissolved in sterile dH_2O or 10mM Tris-HCl pH 8.5 and the concentration determined using A_{260} via a nanodrop (NanoDropLite, Thermo Scientific) and stored at 4°C for immediate use or -20°C for long term storage.

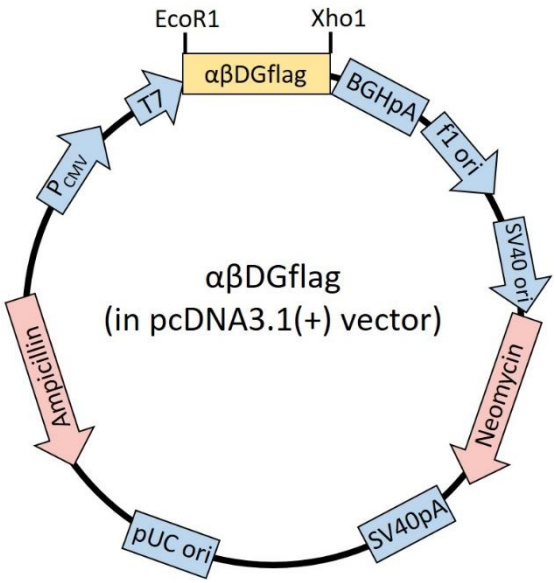

Figure 2.1. Plasmid map of pcDNA3.1 (+) vector including the αβDGflag insert. The αβDGflag insert is flanked by EcoR1 and Xho1 restriction sites in the multiple cloning region as designed by D. Leocadio (Leocadio, D. 2014). The multiple cloning site is under the T7 promoter. The plasmid contains neomycin and ampicillin resistance. BGHpA: Bovine Growth Hormone polyadenylation sequence.

2.2.2 SITE-DIRECTED MUTAGENESIS (SDM)

Site-directed mutagenesis was carried out using the QuikChange Lightning Site-Directed Mutagenesis Kit (Agilent Technologies). T788A and T788D mutations were introduced into the full length sequence of mouse αβDG. The αβDG with a flag tag was in a pcDNA3.1+ plasmid as generated by D. Leocadio Victoria (Figure 2.1). The two complimentary mutagenic oligonucleotide primers were designed according to the kit guidelines (Table B.2). The reaction mixture was set up as follows:

Component	Amount
10x Reaction Buffer	5 µl
αβDGflag pcDNA 3.1 (+)	20 ng
Forward Primer	125 ng
Reverse Primer	125 ng
dNTP Mix	1 µl
QuikSolution Reagent	1.5 µl
QuikChange Lightning Enzyme	1 µl
dH_2O	Make up to 50 µl

The reaction was then cycled under the following parameters:

Segment	Cycles	Temperature	Time
1	1	95°C	2 minutes
2	18	95°C	20 seconds
		60°C	10 seconds
		68°C	4.5 minutes (30 seconds/kb plasmid length)
3	1	68°C	5 minutes
4	1	4°C	10 minutes/ Hold

2µl (20 Units) of restriction enzyme Dpn1 (New England Biosciences) was added to the resulting amplification reaction and incubated for 15 minutes at 37°C in order to digest any remaining parental plasmid. 2µl of Dpn1 treated amplification reaction was then transformed into XL-10 gold competent cells as per the manufacturer's instructions and grown on agar plates with antibiotic selection (Table B.1). Colonies were then selected for overnight cultures and subsequent minipreps for restriction digests and sequencing.

2.2.3 Restriction Enzyme digest of Plasmid DNA

Prior to sending plasmids for sequencing there were analysed by restriction enzyme digests to assess for positive clones. Digestion with the restriction enzymes EcoR1 and Xho1 (New England Biosciences) would be expected to produce a 2.09 Kb insert containing fragment as well as the remaining plasmid fragment at 5.4Kb. The restriction digest per reaction was set up as follows (1Unit/ 0.1µg DNA):

Component	Amount
EcoR1	1-5U
Xho1	1-5U
10x Buffer 4	2 µl (1x)
100x BSA	0.2 µl (1x)
Plasmid DNA	0.1-0.5µg
dH_2O	Make up to 20 µl

The mixture was then incubated for 2 hours at 37°C.

2.2.4 DNA Sequencing

Isolated plasmid DNA at a concentration of 100ng/µl in a total volume of 5 µl was sent for sequencing at Source Bioscience for verification. Bovine growth hormone (BGH) and T7 stock primers were used.

2.2.5 DNA electrophoresis

DNA samples were mixed with 10x loading buffer and run on a 0.8% agarose gel containing ethidium bromide (0.5µg/ml) alongside 2.5 µl 1Kb Hyper ladder (New England Biosciences, NO4685). The gel was run at 100V in 1x TAE buffer (40mM Tris-Acetate, 1mM EDTA) until the loading dye front has migrated the desired distance. The DNA gel was then imaged on a UV trans-illuminator (UVitec with Mitsubishi P91 printer).

2.3 Tissue Culture Techniques

2.3.1 Growth and maintenance of cell lines

LNCaP (Horoszewicz *et al.,* 1983) and PNT1a (Lang *et al.,* 2000) cells were maintained in RPMI 1640, [+] L-Glutamine (Gibco, Life technologies), supplemented with 10% (v/v) fetal bovine serum (FBS) (Gibco, Life technologies). PC3 (Kaighn *et al.,* 1979), Normal Adult Primary Human

Dermal Fibroblasts (HDF ATCC-PCS-201-012 a kind gift from Irene Canton) and Human DAG1 null fibroblasts (Riemersma *et al.,* 2015) were maintained in Dulbecco's Modified Eagle Medium (DMEM), + D-Glucose, +L-Glutamine, + pyruvate (Gibco, Life technologies), supplemented with 10% (v/v) FBS. HDF were also supplemented with 1% (v/v) penicillin/ streptomycin (Gibco, Life technologies). All cells were grown in an incubator (Galaxy S Biohit) at 37°C, 5% CO_2. Cells were passaged between 60-80% confluency as assessed on an inverted microscope (CETI) at 10 x magnification. Cells were passaged with 0.25 % (v/v) trypsin-EDTA (Sigma) and neutralised with media. Dissociated cells were centrifuged 100x g (11030 rotor, Sigma) for 3 minutes and resuspended in culture media before prior to plating at the required density for future experiments or further growth in plastic culture flasks (Greiner Bio-one).

2.3.2 POLY-L-LYSINE COATING OF DISHES AND COVERSLIPS

The tissue culture surface was covered aseptically with 0.1mg/ml poly-L- lysine (Sigma) in PBS. Surfaces were incubated in solution for 2 hours before washing twice with PBS followed by drying in the incubator.

2.3.3 CELL COUNTING USING A HAEMOCYTOMETER

10 µl of a single cell suspension in growth media was diluted 1:10 in 90 µl Trypan Blue solution 0.4% (Sigma, T8154). Cells were counted using a haemocytometer. The glass slide of the haemocytometer is laser etched with counting grids. The indentation creates a capillary space over the counting grids of 0.1mm. 10 µl of the cell suspension diluted in trypan blue was loaded to fill the capillary space of the haemocytometer and the cells counted according to the manufacturer's instructions. Briefly, the number of cells inside 8 x 1mm^2 squares of the chamber grid were counted using a 10x magnification on an inverted microscope (CETI). Non-viable cells that had taken up trypan blue were discounted. Each mm^2 contains 100 nl of liquid therefore to calculate the number of cells per ml average number of cells per mm^2 must be multiplied by 10^4. Viable cell number was calculated using the following formula:

$$\frac{Viable\ cells\ in\ 8\ \ mm^2\ squares}{8} \times Dilution\ Factor(\times 10^4\ ) = Total\ viable\ cells/ml$$

2.3.4 GROWTH CURVE OF LNCAP CELLS IN STANDARD CONDITIONS

Cells were trypsinised from a flask at 60-80% confluency and counted using a haemocytometer. Cells were then centrifuged and resuspended in growth medium to make a 1 x 10^6 cells/ml cell suspension which was then counted again to verify accurate cell numbers. The suspension was diluted in growth medium to produce a 1 x 10^4 cells/ml suspension. 1 ml

of the suspension was then added to each well of a 12 well plate that had been pre-coated with poly-l-lysine. Cells were counted every other day for 12 days using the CASY Model TT Cell counter and analyser (Innovatis). Media was changed in the remaining wells on days 2, 6 and 10.

To count the cells the media was removed from the 4 replicate wells into a 15ml falcon tube. The wells were washed with 0.5 ml PBS, which was also added to the tube. 0.5 ml trypsin-EDTA was added per well and incubated at 37°C until all the cells had detached. 0.5 ml of growth media was added to neutralise and the cell suspension added to the tube. The well was washed a final time with 0.5 ml sterile CASYton solution (Roche) and added to the collected cells. 1 ml of the 3ml cell suspension was made up to 10ml with CASYton solution in a CASYCup (Roche) and inverted gently several times to mix. Cells were counted using the 150 µM capillary, scale 0-40 µM, range 10- 34 µM with 3 cycles of 400 µl for each count and a dilution of 1: 10 as 1 ml of cell suspension was diluted in 9 ml CASYton. A background count of CASYton alone was calculated and subtracted from the cell count of each well. The cells/ ml value was multiplied by 3 to get a total cell number per well. Four independent growth curves were conducted.

2.3.5 NEON TRANSFECTION SYSTEM ELECTROPORATION OF LNCAP CELLS

Cells were electroporated using the Invitrogen Neon transfection System with the MPK 5000 electroporator. Cell numbers and transfection conditions, for both 100 µl and 10 µl kits, were optimised based upon the Neon transfection cell protocol and cell line data and are summarised in the table below.

Tip	Well	Cell Number	Amount of DNA (µg)	Solution R (µl)	Pulse Voltage (v)	Pulse Width (ms)	Pulse Number
10 µl	1 well/6 well	0.5 x 10^6	2.4	12	1200	20	2
100 µl	100 mm dish	3.6 x 10^6	3.6	120	1200	20	2

LNCaP cells were grown to the required density and then trypsinised as described above. Cells were washed once in PBS and then resuspended in PBS and counted using a haemocytometer. The necessary number of cells was centrifuged 500 x g for 3 minutes (11030 rotor, Sigma) and resuspended in the recommended amount of Solution R. The resuspended cells were combined with the amount of DNA shown in the table. The DNA and cell suspension was

loaded into the appropriate volume Neon pipette tip which was then docked in the pipette station containing 3ml E2 Solution. The cells were then microporated under the conditions detailed in the table. Electroporated cells were seeded onto culture dishes or coverslips that had been pre-coated with poly-l-lysine and contained pre-warmed growth medium. Cells were grown for a minimum of 24 hours prior to subsequent experiments.

2.3.6 CYCLOHEXIMIDE PULSE CHASE ASSAY OF ABDGFLAG, ABDGFLAGT788A AND ABDGFLAGT788D IN LNCAP

LNCaP cells were transfected with αβDGflag, αβDGflagT788A or αβDGflagT788D (Appendix B, Table B.1) and seeded into 100mm dishes as described above. Cells were grown for 24 hours. Cells were washed once with PBS and then incubated with growth medium containing either DMSO (control) or 100µg/ml cycloheximide (Sigma, C7698). The cells were incubated at 37°C, 5% CO_2 and harvested at 0, 6, 12 and 24 hours post cycloheximide treatment.

2.3.7 THYMIDINE BLOCK SYNCHRONISATION OF LNCAP FOR CELL CYCLE ANALYSIS

2.3.7.1 Thymidine block treatment of LNCaP cells optimisation

LNCaP cells were seeded at a density of 5 x 10^5 per 100mm dish, pre-coated with poly-l-lysine and allowed to adhere and grow for 48 hours. Cells were washed gently 2 times with PBS and incubated with RPMI 1640, 10% FBS supplemented with 2mM thymidine (Sigma, Cat no. T1895) or PBS control. Cells were returned to the incubator and over a time course of every 2 hours 18-32 hours post thymidine treatment one 100mm dish was fixed for flow cytometry and cell cycle profiling.

2.3.7.2 Double thymidine block synchronisation for cell cycle analysis of LNCaP cells

LNCaP cells were seeded at a density of 5 x 10^5 per 100mm dish, pre-coated with poly-l-lysine and grown for 48 hours. Cells were washed twice with PBS and incubated with RPMI 1640, 10% (v/v) FBS containing either 2mM thymidine or PBS control. Cells were incubated with 2mM thymidine for 32 hours and then washed carefully twice with PBS. Fresh growth medium was added to release cells from the block for 9 hours. The cells were then subject to a second 2mM thymidine block for a further 22 hours. Cells were washed twice with PBS and released into the cell cycle by the addition of fresh growth medium. The cells were harvested every 2 hours over a 14 hour time course post release (Adapted from Bootsma et al. 1964 and Bostock et al. 1971). One 100mm dish was fixed for flow cytometry analysis, One 100mm dish was harvested for whole cell lysate and four 100mm dishes were used for cell fractionation per time point.

2.3.8 NOCODAZOLE TREATMENT OF LNCAP CELLS

2.3.8.1 Nocodazole treatment of LNCaP cells optimisation

LNCaP cells were seeded at a density of 5 x 10^5 per 100mm dish and grown for 48 hours on poly-l-lysine pre-coated dishes. Following two PBS washes the cells were incubated with either 50 ng/ml, 100 ng/ml or 500 ng/ml Nocodazole (Sigma, Cat. No. M1404) or DMSO diluted in growth medium at 37°C, 5% CO_2. One dish per condition was then fixed for cell cycle analysis through flow cytometry at 12, 18, 24 and 30 hours after Nocodazole treatment.

2.3.8.2 Nocodazole induced mitotic arrest of LNCaP cells

LNCaP cells were seeded at a density of 5 x 10^5 per 100mm dish and grown for 48 hours on poly-l-lysine pre-coated dishes. Cells were washed twice with PBS and incubated with growth medium containing 100 ng/ml Nocodazole or DMSO for 30 hours at 37°C, 5% CO_2. Cells were then fixed or harvested for downstream applications. Adapted from Zieve et al. 1980.

2.3.9 FLOW CYTOMETRY ANALYSIS OF PROPIDIUM IODIDE STAINED MAMMALIAN CELLS

2.3.9.1 EtOH fixation of cells for flow cytometry

Media from the cells to be analysed were added to a falcon tube. The remaining cells were detached from the dish with tryspin-EDTA and added to the tube. Cells were centrifuged 500 x g for 3 minutes at room temperature and washed in 10 ml PBS. The cell number was calculated via a haematocytometer and 1.5 x 10^6 cells centrifuged as above. The PBS was aspirated leaving approximately 200 µl in which the cells were gently resuspended. Ice cold 70% (v/v) EtOH was added dropwise with gentle resuspension up to 1 ml. Following a 30 minute incubation on ice the cell suspension was centrifuged 500 x g for 7 minutes at 4°C (Sigma 1-15K, rotor 12132-H) and the supernatant aspirated, leaving 200 µl. The cells were subject to a second dropwise resuspension in ice cold 70% EtOH and incubated for a further 30 minutes on ice prior to freezing at -20°C for up to two weeks prior to staining and flow cytometric analysis.

2.3.9.2 Propidium Iodide (P.I.) staining of LNCaP cells

EtOH fixed cells stored at -20°C were incubated on ice for 5 minutes. Following centrifugation (Sigma 1-15K, rotor 12132-H) at 500 x g for 7 minutes at 4°C the cell pellets were washed twice by the dropwise addition of ice cold PBS to 1.5 ml. The cells were then resuspended in 1 ml of propidium iodide stain (20 µg/ml propidium iodide (Sigma, Cat. No, P4170), 200 µg/ml RNAse A (Sigma, Cat no. R6513) in PBS) for 30 minutes in the dark at room temperature. Cells were then centrifuged and the supernatant aspirated, leaving 600 µl remaining. The cells were

resuspended in the remaining stain, transferred to a FACStube for analysis on the flow cytometer (Adapted from Pozarowski et al. 2004).

2.3.9.3 Flow cytometry analysis of the cell cycle population of P.I stained LNCaP cells

Each sample was analysed on the CyAn ADP (Beckman Coulter) using Summit software with the assistance of Dr. Mark Jones, Andrews Lab. Cells were first gated for side scatter (size) and forward scatter (granularity) to exclude debris and the majority of apoptotic cells from the analysis. The subsequent population was gated for doublet discrimination. Cells were gated for pulse width against pulse area or length to discriminate between single cells in G2 or two G1 cells which are stuck together. These would have similar fluorescence but doublet cells are slightly larger, therefore taking longer to pass through the laser and can be excluded from the analysis. Finally, histograms of the single cell population were created, plotting cell count against FL3 area (P.I.) as a measure of fluorescence intensity. Cells in G1 have a 2N DNA content whilst cells which have replicated their DNA but not yet divided, ie those in G2 or M phases, have a 4N DNA content. Cells in S phase will have DNA content ranging between 2N and 4N. Data was analysed as above and final figures produced with FlowJo software.

2.3.10 FACS ANALYSIS OF AN ASYNCHRONOUS POPULATION OF MAMMALIAN CELLS FOR CELL CYCLE ANALYSIS

2.3.10.1 Cell Dissociation

Cells were grown in T175 flasks for at least 48 hours to 60% confluency. The growth medium was removed to a falcon tube and following two PBS washes, cells were incubated with PBS based enzyme-free cell dissociation buffer (Gibco, LifeTechnologies, 13151-014) until cells detached from the flask. Cells were collected in growth medium, combined with the washes and retained media and centrifuged at 500 x g for 3 minutes (11030 rotor, Sigma) ready for subsequent fixation or staining.

2.3.10.2 EtOH fixation and propidium iodide staining of an asynchronous population for FACS analysis.

Cell pellets were resuspended in 20 ml PBS and the cell density calculated using a hemocytometer. Cells were centrifuged at 500 x g for 3 minutes at room temperature and a minimum of 4 x 10^7 cells were resuspended dropwise in ice cold 70 % EtOH (v/v) to a final concentration of 1.5 x 10^6 cells/ml. Fixation and P.I. staining protocols were continued as described in sections 2.3.9.1. and 2.3.9.2 prior to FACS analysis by Dr. Mark Jones.

2.3.10.3 Hoechst 33342 (H33342) staining of an asynchronous population of live mammalian cells for FACS analysis

2.3.10.3.1 Dissociated Cells

Cell pellets from section 2.3.10.1 were resuspended in growth medium and counted using a hemocytometer. 2-5 x 10^7 cells were resuspended in pre-warmed growth medium containing 5 µg/ml H33342 (Sigma, Cat no. B2261) at a concentration of 5 x10^6 cells/ml. A control population of cells was incubated with dH_2O diluted in growth medium. Cells were mixed gently and incubated in the dark at 37°C for 30 minutes. Cells were transferred to FACS tubes. FACS implementation was conducted by Dr. Mark Jones on the Jazz (BD Life Science) FACS machine see section 2.3.10.4.

2.3.10.3.2 Adhered Cells

5 µg/ml H33342 in pre-warmed growth medium was added to cells whilst still adhered to the flask at approximately 60% confluency (5 ml/ T175) for 30 minutes at 37°C. Cells were detached from the flask as described in section 2.3.10.1, with the addition of 5 µg/ml H33342 to the dissociation buffer, and resuspended in growth medium supplemented with 5 µg/ml H33342 at a concentration of 5 x 10^6 cells/ ml prior to FACS analysis by Dr. Mark Jones see section 2.3.10.4.

2.3.10.4 FACS of asynchronous populations of mammalian cells for cell cycle analysis.

Cells were sorted on the Jazz (BD Life Science) MoFlo (Beckman Coulter) FACS machines by Dr. Mark Jones using BD FACS or Summit software respectively. Cells were gated to exclude debris, select single cells and display cell cycle phases based upon DNA content as described previously in section 2.3.9.3. When sorted on the MoFlo all three cell cycle phases were collected into PBS or growth medium simultaneously whilst on the Jazz, S and G_1 were collected first until 1- 2 x 10^6 viable cells had been collected for each phase and then S and G_2M cells collected for the remainder of the sample. Collected samples were centrifuged at 500 x g for 3 minutes at 4°C (Sigma 4-16KS, rotor 12269) and processed according to downstream applications.

2.4 ZEBRAFISH HUSBANDRY

2.4.1 HOME OFFICE REGULATION

All studies were carried out in accordance with Home Office requirements for the use of animals in scientific research. Embryos under 5 days post-fertilisation (d.p.f) were used under UK Home Office project license of Prof. Steve Winder, license number 40/3693.

2.4.2 MAINTENANCE OF ADULT ZEBRAFISH

Adult zebrafish were maintained in the UK Home Office approved Bateson centre aquaria at the University of Sheffield. The aquaria follow a 14:10 hour light: dark cycle and are maintained according to standard protocols (Nüsslein- Volhard and Dahm, 2002).

2.4.3 ZEBRAFISH STRAINS

Heterozygous Dystroglycan mutant ($dag1^{hu3072}$) zebrafish (Lin et al 2011, Gupta et al 2011) are kept as breeding stocks in the aquaria on a London Wildtype (LWT) background.

2.4.4 EMBRYO COLLECTION

A tray containing marbles with a filter grid bottom was inserted into a collection tray and placed securely into the tank containing adult heterozygous *DAG* zebrafish, ensuring that the fish can move into and around the tray. The trays were left in the tank overnight. The eggs were removed from the collection tray and washed with clean system water to remove debris. The eggs were transferred to 10cm petri dishes containing E3 media (5mM NaCl, 0.17mM KCl, 0.33mM $CaCl_2$, 0.33mM $MgSO_4$, 0.0001% methylene blue) with 40 eggs per dish and incubated at 28°C.

2.4.5 DETECTION OF MUSCLE PHENOTYPE VIA BIREFRINGENCE ASSAY

At 4 days post-fertilisation (d.p.f.) embryos in E3 media in petri dishes were incubated on ice to slow movement and then transferred to a glass dish. Embryos were viewed between two polarising filters on a dissecting microscope (Leica MZ FLIII). The polarising filters are rotated so that only the light refracting through the striated muscle was visible. The sibling embryos were then sorted into wt or mutant groups based upon the degree of disrupted muscle phenotype. Images were acquired using a Jenoptik ProgRes C4 camera attached to a Leica MS5 microscope with Prog Res Capture Pro software.

2.5 MICROSCOPY TECHNIQUES

2.5.1 IMMUNOFLUORESCENCE STAINING OF MAMMALIAN CELLS

Cells were seeded onto 13mm glass coverslips (VWR) pre-coated with poly-l-lysine at the required density and grown for a minimum of 24 hours. Prior to fixation the cells were washed three times with PBS. Cells were fixed with paraformaldehyde (PFA) except for when visualising microtubules or, when indicated, centrosomes in which case a methanol/ acetone

fixation was used. For PFA fixation cells were fixed for 10 minutes with 3.7% (v/v) PFA (Sigma) in PBS and permeabilised for 5 minutes with 0.1% triton X-100 in PBS. In the case of methanol/acetone fixation, cells were fixed for 10 minutes with methanol at -20°C followed by 1 minute of acetone at -20°C. Coverslips were then washed 3 times with PBS and inverted cell side down onto 20 µl blocking buffer (5% (v/v) FBS, 3% BSA (w/v) in PBS) on parafilm for 1 hour at room temperature in a humidified chamber. Coverslips were then transferred to 15 µl primary antibody diluted in blocking buffer and incubated for 1 hour as described above. The cells were then washed in PBS 3 times to remove any unbound or low affinity binding of the primary antibody. Coverslips were again inverted cell side down onto blocking buffer containing diluted, fluorescent conjugated secondary antibodies and incubated in the humidified chamber in the dark for 1 hour at room temperature. The coverslips were then washed gently three times in PBS to remove excess secondary antibody and allowed to dry. Coverslips were then mounted onto 5µl hydromount (National Diagnostics) containing 10 ng/ml DAPI (Sigma) as a nuclear counterstain and 2.5% of the antifade preservative 1,4-Diazabicyclo [2.2.2]octane (DABCO) (Sigma) on glass slides (Fisher, 0.8-1.0mm). Slides were stored in the dark at 4°C before viewing on a microscope.

2.5.2 BrdU incorporation and staining of mammalian cells for microscopy analysis

Cells were grown on 13mm glass coverslips pre-coated with poly-l-lysine for at least 48 hours. The growth media was then removed and replaced with 10µM BrdU (Sigma, Cat. No. M099488)) or H_2O control diluted in pre-warmed growth medium for 1 hour at 37°C, 5 % CO_2. For double immunofluorescence staining of BrdU alongside another antibody, the cells were fixed, blocked and stained first for the other antibody according to the immunofluorescence protocol in section 2.5.1. The following procedure was carried out in a humidified chamber, protected from the light. After the incubation with the secondary antibody the coverslips were washed three times in PBS and fixed for a second time in 3.7 % PFA (v/v) for 10 minutes at room temperature. The cells were then permeabilised and the DNA denatured by incubation in 4 N HCl, 0.1% triton x-100 in PBS for 10 minutes at room temperature. Following three PBS washes the cells were incubated with a primary antibody against BrdU diluted in blocking buffer for 1 hour at room temperature. Cells were then washed three times prior to incubation with an appropriate fluorescent conjugated secondary antibody against the Brdu primary antibody in blocking buffer. The coverslips were washed a further three times with PBS, allowed to dry and then mounted on glass slides in hydromount, 10 ng/ml DAPI, 2.5 % (w/v) DABCO and stored at 4°C in the dark until viewed on a microscope.

2.5.3 Whole mount Immunofluorescence staining of zebrafish embryos

Four d.p.f. sibling embryos, sorted by birefringence were euthanised by hypothermal shock. The embryos were then placed into 1.5ml Eppendorf tubes with five embryos per tube. The embryos were gently washed once with 1 ml PBS and then fixed in 1.5 ml 4% PFA in PBST (PBS, 0.2% (v/v) tween-20) on a slow rotator at 4°C overnight. All subsequent washes are 1ml unless stated otherwise. Following fixation the embryos were washed in PBST followed by dH_2O for 5 minutes each at room temperature with gentle rocking. The embryos were then incubated with acetone at -20°C for 15 minutes, followed by one 5 minute dH_2O wash and two 5 minute washes with PBST at room temperature. The embryos were then blocked in PBD (PBS, 0.2% (v/v) tween-20, 1% BSA (w/v) 0.01% DMSO (v/v)) supplemented with 2% FBS (v/v) for 30 minutes at room temperature with gentle rocking. The embryos were then submerged in 500 µl primary antibody diluted in PBD/FBS blocking buffer and incubated on a roller at 4°C overnight. The following day the embryos were washed for 30 minutes in PBD four times and then incubated in 1ml of secondary antibody diluted in PBD, 2% FBS overnight at 4°C. The embryos were then washed four times for 30 minutes in PBD at room temperature, followed by a further two 5 minute washes in PBST. The embryos were then positioned in the desired lateral orientation with thin forceps onto 1% (w/v) agarose combs in 35 mm dishes. The embryos were then sealed in position by the addition of a thin layer of 1.5% (w/v) low melting agarose. Once set the agarose was immersed in PBS and the dishes stored at 4°C in the dark prior to viewing on the confocal microscope.

2.5.4 Epifluorescence Microscopy

Slides were viewed using a Leica DMIRE2 inverted fluorescent microscope powered by a Leica CTRMIC controller. Leica narrow pass filters were used; A4; DAPI (excitation at 360 nm, emission at 400nm), L5; FITC/GFP/Alexa Fluor 488 (excitation at 480 nm, emission at 505 nm) and N2.1; Rhodamine/ Texas Red/ Alexa-Fluor 594 (excitation 515-560 nm, emission at 580 nm) Images were obtained with a Leica HCX PL 63x oil immersion objective lens and a Leica DC350F CCD camera. Images were acquired using the Leica Q-Fluoro software and analysed using Image J.

2.5.5 CONFOCAL MICROSCOPY

Confocal microscopy was carried out in the Wolfson Light Microscopy Facility, University of Sheffield.

2.5.5.1 Nikon A1 Confocal

Confocal images of mammalian cells were obtained using an inverted Nikon A1 confocal with a CFI Plan ApoChromat VC 60x oil (NA 1.4) objective. The immersion oil had a refractive index of 1.518 (Immersion oil Type-F, Olympus) Excitation sources: 405 nm, 457-514 argon laser, 561 nm sapphire laser, 642 nm diode laser. The detector collected emission bandwidths for each filter as follows; blue, DAPI; 425-475 nm, Green; AlexaFluor488/ FITC; 500-550nm, red; AlexaFluor594/ Texas Red; 570- 620nm. During image acquisition the pinhole was set at 1.0 Airy Units (A.U.) and the pixel size set at 512 x 512 or 1024 x 1024. Z stacks were collected bottom to top. Images were acquired using Nikon NIS Elements software V4.30 and were processed and analysed using Fiji (is just ImageJ) software.

2.5.5.2 Olympus FV1000 Confocal BX61 Upright

Confocal images of zebrafish embryos were acquired on and Olympus FV1000 Confocal BX61 Upright using a LUMPlan F1 60x (NA 0.9) water dipping lens. Excitation source 405 nm diode, 488 argon laser, 543 diode and 640nm diode. The emission filters had bandwidths of blue; DAPI; 425-475 nm, green; AlexaFluor488; 500-530nm, red; AlexaFluor594/ Texas Red; >560 nm. During image acquisition the pinhole was set to 1.0 A.U. and pixels 512 x512. Images were acquired using Olympus Fluoview FV-ASW software and processed using Image J.

2.5.6 FIJI PROCESSING OF MICROSCOPY IMAGES

Images were analysed using FIJI (Is Just Image J). Images from each channel were opened in greyscale as 16 bit images. Intensity and gamma levels were manually adjusted taking care not to add or subtract from visual data. Images were then scaled and cropped and saved as TIFF images. In the case of z stacks individual slices were also saved as Jpegs. False colour images were generated and converted to RGB colour. Images were saved in TIFF and Jpeg formats.

2.5.7 FIJI QUANTIFICATION OF CENTROSOME TO NUCLEUS DISTANCE

Images were opened in FIJI and the scale set. The straight line tool used to manually draw a line between the centrosome and the nucleus and the distance recorded and exported to Graphpad Prism 6.0

2.6 BIOCHEMISTRY TECHNIQUES

2.6.7 LYSATE PREPARATION FROM MAMMALIAN CELLS

Cells in petri dishes were washed twice with cold PBS on ice and then lysed with radio immunoprecipitation assay buffer (50mM Tris- HCl pH 7.5, 150 mM NaCl, 1 mM EGTA, 1 mM EDTA, 1% Triton X-100 (v/v), 0.5% Sodium Deoxycholate (w/v), 0.1% SDS (w/v)) or mild lysis buffer (50 mM Tris-HCl pH 7.4, 150 mM NaCl, 1 mM EDTA, 1% Triton X-100 (v/v) supplemented with the appropriate protease and phosphatase inhibitors (Table B.3) on ice for 15 minutes. Cell lysates were then harvested using a cell scraper and transferred to a 1.5ml Eppendorf tube. To shear the DNA, lysates were sonicated (Sanyo Soniprep 150) briefly three times for 10 seconds followed by 10 seconds of rest and then centrifuged at 18000 x g (Sigma 1-15K, rotor 12132-H) for 15 minutes at 4°C to pellet the cell debris. The resulting supernatant was transferred to a micro centrifuge tube and either used immediately or stored at -20°C (James et al. 2000)

2.6.8 LYSATE PREPARATION FROM ZEBRAFISH EMBRYOS

One euthanised 4 d.p.f. embryo was added to 20 µl RIPA buffer supplemented with protease and phosphatase inhibitors (Table B.3) in a 1.5 ml Eppendorf tube on ice. The embryo and RIPA buffer was then pipetted up and down 25 times to disrupt the tissue and then sonicated briefly 3 times for 10 seconds with a 10 second break in between each sonication (Sanyo Soniprep 150). The tubes were then centrifuged at 18000 x g (Sigma 1-15K, rotor 12132-H) for 15 minutes at 4°C. The resulting supernatant was removed to a fresh micro centrifuge tube and mixed with an equal volume of 2x laemelli sample buffer before boiling for 10 minutes at 100°C in a dry heat block. The lysates were then stored at -20°C for future use.

2.6.9 CELL FRACTIONATION AND NUCLEAR FRACTION PREPARATION FROM MAMMALIAN CELLS

Cells were washed twice with cold PBS on ice and incubated with the minimum volume of cold hypotonic Buffer I (0.32M Sucrose, 10mM Tris-HCl pH 8.0, 3mM calcium chloride, 2mM magnesium acetate, 0.1mM EDTA, 0.5% NP-40 (v/v), 1mM DTT) supplemented with protease and phosphatase inhibitors (Table B.3.) on ice for 15 minutes. The cells were collected using a cell scraper and disrupted further with 35 strokes in a cold glass Dounce homogeniser. The lysate was then centrifuged at 600 x g for 10 minutes at 4°C (Sigma 4-16KS, rotor 12269). The resulting pellet containing the nuclear fraction and the non- nuclear supernatant were

retained for further purification. The supernatant was centrifuged twice at 9300 x g for 10 minutes at 4°C (Sigma 4-16KS, rotor 12269) to remove nuclear contaminants and the final supernatant retained as the purified non-nuclear fraction. The pellet containing the nuclear fraction following the 600 x g centrifugation was resuspended in 400 µl Buffer I and an equal volume of buffer II (2M Sucrose, 10mM Tris-HCl ph 8.0, 5mM Magnesium Acetate, 0.1mM EDTA, 1mM DTT). This mixture was carefully overlaid onto an equal volume of a 1.8 M sucrose cushion in an ultracentrifuge tube and centrifuged at 21000 x g for 55 minutes at 4°C (Beckmann Coulter Optima™ MAX Ultracentrifuge, rotor MLA-80). The resulting pellet was resuspended in RIPA buffer or mild lysis buffer supplemented with protease and phosphatase inhibitors, sonicated (Sanyo Soniprep 150) three times for 10 seconds to shear the DNA and centrifuged at 18000 x g for 15 minutes at 4° (Sigma 1-15K, rotor 12132-H) and the supernatant retained as the nuclear fraction. The fractions were either used immediately or stored at -20°C for future use (Mathew et al. 2013).

2.6.10 Protein concentration determination via the MicroBCA™ assay

The protein concentration of lysates and fractionation samples was calculated using the MicroBCA™ protein assay kit (Thermo Scientific), according to the manufacturer's instructions. Briefly the protein sample was diluted 1:125 in RIPA buffer to a total volume of 500 µl and mixed with 500 µl working reagent (Reagents MA:MB:MC at a ratio of 25:24:1) along with a blank consisting of working reagent and RIPA buffer. Each sample was made in triplicate. The diluted protein samples were then incubated at 60°C for 1 hour, protected from light and then allowed to cool to room temperature. The absorbance of each sample at 562 nm was measured via a spectrophotometer (7315 model Jenway) in 1cm path length polystyrene cuvettes. The average reading per lysate was then used to calculate the protein concentration from a standard curve of BSA concentrations of 0- 200 µg/ ml.

2.6.11 Immunoprecipitation of FLAG- tagged proteins using anti-Flag M2-agarose affinity gel

Immunoprecipitation (IP) of flag-tagged proteins was carried out using Flag M2 resin (Sigma, Cat no. A2220) according to the manufacturers protocol. Briefly, the Flag M2 resin was thoroughly resuspended and 40 µl/IP was transferred to a clean tube. The resin was washed five times with 20 resin bed volumes of 1x TBS at 7000 x g for 30 seconds (Sigma 1-15K, rotor 12132-H). 200-400 µg of lysate was incubated with the resin and adjusted to a total volume of 1 ml with lysis buffer (50 mM Tris-HCl pH 7.4, 150 mM NaCl, 1 mM EDTA, 1% Triton X-100 (v/v)). The samples were then left at 4°C on a roller overnight. Following incubation the

samples were centrifuged at 7000 x g for 30 seconds at 4°C (Sigma 1-15K, rotor 12132-H) and the supernatant carefully removed using a narrow-end pipette tip. The resulting resin was washed three times with 500 µl cold 1x TBS. Samples were either boiled in 2x Laemelli sample buffer at this stage and stored at -20°C until use or the flag tagged protein was eluted. To elute the flag tagged protein the resin was incubated with 150 ng/ml of competing 3x flag peptide (Sigma, Cat. No. F4799) on a roller for 30 minutes at 4°C. The mixture was then centrifuged for 30 seconds at 7000 x g at 4°C (Sigma 1-15K, rotor 12132-H) and the supernatant containing the eluted protein was transferred to a new tube for immediate use or stored at -20°C.

2.6.12 SDS- Polyacrylamide Gel Electrophoresis (SDS-PAGE)

SDS-PAGE mini-gels (10 cm x 10 cm x 1 mm) were prepared individually using the Bio-rad casting system. The mini-gels consisted of a 10 or 12 % resolving gel with a 5% stacking gel (Table B.4.). The samples, having previously been boiled with Laemelli sample buffer, were run on the mini-gels in Bio-rad tanks filled with 1x SDS running buffer(200 mM Glycine, 25mM Tris, 0.01% SDS). Samples were run alongside a broad range molecular weight protein ladder (PageRuler Plus Prestained Protein ladder, Thermo Scientific, Cat no. 26619). Samples were separated at 100 V through the stacking gel and at 120- 150 V at fixed voltage through the resolving gel.

2.6.13 Coomassie Blue safe stain of SDS-PAGE gels

Following SDS electrophoresis, gels were rinsed briefly in dH_2O. Gels were then immersed in Coomassie Blue Safe Stain (60-80mg Coomassie brilliant blue G250, 3ml Concentrated HCl)and microwaved for 10 seconds before incubation at room temperature and gentle rocking for 1 hour. The coomassie stain was then discarded, the gel washed in dH_2O twice and then destained in dH_2O overnight. Gels were imaged using the Biorad Chemidoc XRS system with Image Lab software (Biorad).

2.6.14 Separation of protein lysates on Phos-TAG gels (Kinoshita *et al.* 2009)

Phos-Tag (Phos-Tag™ Acrylamide AAL-107, NARD) gels were prepared in the same way as the mini gels described above with the changes recommended in the manufacturer's protocol. Prior to the addition of the polymerising reagents APS and TEMED to the 10% resolving gel, the Phos-tag reagent and $MnCl_2$ were added at a molar ratio of 2:1 $MnCl_2$: Phostag. Gels with Phostag concentrations of 20 µM, 50 µM and 100 µM were used. The 5% stacking gel was prepared as above (Table B.4.). Phos-tag mini gels were run at 100 V through the stacking gel and 30mA through the resolving gel until the dye front had migrated the desired distance.

Prior to downstream electrotransfer and western blotting, the gels were removed from the glass cassettes and washed twice with 2 mM EDTA in transfer buffer for 10 minutes to chelate Mn_2 ions, which may interfere with the transfer, followed by two washes of 5 minutes in transfer buffer alone.

2.6.15 Electrotransfer

Proteins were electroblotted from SDS-PAGE mini gels to PVDF (Polyvinylidene fluoride) membranes (Immobilon- PSQ, 0.2 µM, Merck Millipore) using a mini Trans-Blot electrophoretic transfer cell (Biorad). The SDS-PAGE gel containing the electrophoresed proteins was immersed in Towbin transfer buffer (25 mM Tris, 192 mM Glycine, 20 % Methanol (v/v), 0.02% SDS (w/v)) along with the methanol activated PVDF, chromatography paper (Whatman) and fibre pads. Once all the components had been equilibrated in transfer buffer for 10 minutes they were assembled into the transblot cassettes and the chamber filled with Towbin transfer buffer as per the manufacturer's instructions. The membranes were blotted at a fixed voltage of 100 V for 75 minutes. Membranes were then removed from the transfer apparatus and immersed in TBST (50 mM Tris-HCl pH 7.4, 150 mM NaCl, 0.5% Tween 20 (v/v)).

2.6.16 Western Blotting

Electroblotted membranes were blocked in 5% (w/v) skimmed milk powder or 5% BSA in TBST for 1 hour at room temperature with gentle rocking. The membrane was then incubated with the primary antibody (Table B.5.) diluted to the required concentration in blocking buffer at 4°C overnight with gentle rocking. The membranes were then washed three times with TBST for 10 minutes followed by incubation with the appropriate secondary antibody (Table B.6.) in blocking buffer for 1 hour at room temperature. Excess unbound antibody was removed from the membranes with three further TBST washes of 10 minutes each. A chemiluminescent signal was generated by incubating the membranes with freshly mixed ECL solution (equal volumes of ECL I (100 mM Tris-HCl pH8.5, 25mM Luminol, 396µM p-Coumaric Acid) and ECL II (100 mM Tris-HCl pH8.5, 0.02% (v/v) H_2O_2) for 30 seconds. The membrane was then transferred to the Bio-rad Chemidoc XRS system and the chemiluminescent signal recorded over a time course of up to 45 minutes.

2.6.17 Membrane stripping

In instances when the membrane was to be re-probed the antibody were removed from membranes using a low pH mild stripping buffer (15g Glycine, 1g SDS, 1 ml Tween 20, pH 2.2). The membrane was incubated twice for 10 minutes each with mild stripping buffer at

room temperature, followed by two 10 minute PBS washes and two 5 minute TBST washes. The membrane was then ready to continue with the blocking and antibody incubation steps as described in section 2.6.10.

2.6.18 Peptide Arrays

Peptide arrays consisting of 15 residue oligomers, with a single step residue, covering the cytoplasmic domain of βDG were obtained from Intavis AG. The arrays were washed three times for 10 minutes with TBST and then blocked with 5% (w/v) skimmed milk powder in TBST for 1 hour at room temperature. The array was then incubated with primary antibody diluted in blocking buffer overnight at 4°C. The following day the array was washed three times in TBST for 10 minutes each to remove excess antibody and then incubated with the appropriate secondary antibody in blocking buffer for 1 hour at room temperature. The array was subject to three final 10 minute TBST washes before incubation with ECL solution for 30 seconds to generate a chemiluminescent signal which was the recorded on the Biorad Chemidoc XRS system.

2.6.19 Densitometry quantification of Western blot bands

Densitometry analysis of western blot bands was carried out using the Image Lab software (Biorad). Images with saturated pixels were excluded from analysis. Lanes were manually defined and the bands detected automatically. Using plots of intensity versus relative front the integrated area under the peak for each band was recorded (Volume intensity) and exported to GraphPad 6.0 for analysis.

The nuclear: non-nuclear ratio was calculated by dividing the intensity of the western blot bands, as detected by densitometric analysis, by the volume loaded for 20µg of each sample to determine the intensity/µl. The approximate total volume of the non-nuclear and nuclear fractions for each sample was 440µl and 110µl respectively. The nuclear fraction is therefore 4 times more concentrated than the non-nuclear fraction. The intensity/µl of the cytoplasmic fraction was multiplied by 4 to adjust for the fact that an absolute amount (20µg) rather than proportional amounts were loaded for the fractionation experiments. The nuclear: non-nuclear ratio was then calculated.

2.6.20 STATISTICAL ANALYSIS

Data was compiled and analysed in Microsoft excel and graphpad prism 6.0. The mean and standard error of the mean (S.E.M) are reported. Normality distribution was analysed via histogram and the D'Agostino and Pearson and Shapiro-Wilk normality tests. For correlation analysis the Spearman non-parametric test was used. Mann-Whitney U test was used in the analysis of the centrosome-nucleus distance.

Characterisation and validation of β-Dystroglycan antibodies

3.1 INTRODUCTION

3.1.1 DYSTROGLYCAN LOCALISATION AND EXPRESSION

DG expression is ubiquitous, and its expression and localisation has been well characterised in multiple tissues including skeletal muscle, heart, small intestine, kidney, skin, mammary gland, prostate and the central nervous system (Ibraghimov-Beskrovnaya et al 1993, Durbeej et al. 1995, Durbeej et al. 1998, Henry et al. 2001, Sgambato et al. 2006, Herzog et al. 2004, Mathew et al. 2013).

DG expression and localisation is also well studied in multiple research models used by the scientific community. For example, in zebrafish, DG and other components of the DGC localise to the vertical myosepta, the boundaries between somites to which the muscle fibres attach (Gupta et al. 2011, Lin et al. 2011) and in mice DG is located at the PM of cells with strong localisation at sites in contact with the basement membrane (Durbeej et al.1995, Williamson et al. 1997, Anderson et al. 2007). Multiple cell lines including myoblasts, fibroblasts and numerous cancer cell lines have also been used to study DG localisation, regulation and function (Gonzalez-Ramirez et al. 2008, Mathew et al. 2013, Mitchell et al. 2013, Sgambato et al. 2006, Sotgia et al. 2003, Thompson et al. 2010). DG expression levels are variable across different cell lines as is the extent of post-translational events such as glycosylation and proteolytic cleavage. (Mathew et al. 2013, Thompson et al. 2010, Mitchell et al. 2013, Losasso et al. 2000). In most cell lines, DG localises to the plasma membrane and is strong at the basal surface and cell-cell junctions, as well as at focal adhesions and filopodial and invadapodial protrusions, consistent with its role as an adhesion molecule. (Spence et al. 2004, Thompson et al. 2010). Importantly, in both tissue samples and cell lines, DG is also detected within the nucleus and intracellular vesicles (Lara-Chacon et al 2010, Mathew et al 2013, Leocadio et al 2016, Sotgia et al 2003). Characterising the localisation and expression of βDG provides important clues as to its regulation as well as the emerging functions of DG, distinct from its role at the PM.

3.1.3 DYSTROGLYCAN ANTIBODIES AS RESEARCH TOOLS

Key to many techniques investigating the modification, localisation and function of DG are antibodies. Western blots (WB), Immunoprecipitation, ELISAs, flow cytometry, immunohistochemistry (IHC) and many other techniques all require the use of antibodies. Antibodies can detect a specific protein, or even specific modified forms of a protein, and can provide a wealth of information on the target protein of interest.

3.1.5 DYSTROGLYCAN ANTIBODIES

3.1.5.1 α-Dystroglycan antibodies

The study of αDG is notoriously difficult due to the relative lack of antibodies that reliably detect αDG. This unreliability is largely due to the highly variable glycosylation of αDG. The most widely used αDG antibodies are the monoclonal antibodies IIH6 and VIA4-1, both of which recognise close, but distinct, epitopes on the fully glycosylated form of αDg (Ervasti et al, 1993, Durbeej et al 1993, Hara et al 2011, Humphrey et al 2015). Because of its ability to block laminin binding, the IIH6 epitope is proposed to be the glycosylated laminin binding site added by the glycosyltransferase LARGE, however this is not the case for VIA4-1 (Durbeej et al 1995, Hara et al 2011). IIH6 and VIA4-1 recognise smears of signal between 120-180 KDa depending on the tissue analysed via western blot (Holt et al 2000, Ervasti et al, 1993, Durbeej et al 1993). Both antibodies stain the sarcolemma in normal skeletal muscle when detected by IHC (Ervasti et al, 1993, Durbeej et al 1993, Humphrey et al 2015). IIH6 and VIA4-1 are widely used clinically because the hypoglycosylation typical in many dystroglycanopathies is detected by a loss of immunoreactivity by both antibodies (Brown et al 2004.). This loss of staining may also in part be due to loss of core αDG from the membrane (Brown et al 2004).

Antibodies that recognise the peptide backbone in the less highly glycosylated C-terminal domain of αDG are also being produced. For example, a polyclonal antibody produced by Kroger et al raised against amino acids 565-584 of the C-terminal of αDG stains the sarcolemma in skeletal muscle sections in IHC but works poorly on western blots (Herrmann et al 2000). This is also the case for DAG-6F4, a monoclonal antibody that recognises a seven amino acid epitope ($_{493}$PNQRPEL$_{499}$) in the C-terminal domain of αDG (Humphrey et al. 2015). This epitope is at the start of a predicted IgG-like domain near to the βDG binding site and is proposed to be in an extended conformation with little glycosylation (Humphrey et al. 2015). Why these antibodies are efficient in IHC but not in western blots, where the proteins have been extracted and denatured, remains unclear but is likely due to the difference in 3D conformation of the glycan side chains in each technique (Humphrey et al. 2015), again highlighting the difficulties in antibody technology imposed by high levels of glycosylation.

3.1.5.2 β-Dystroglycan antibodies

A larger number of reliable antibodies are available for the study of βDG, those used in this study are detailed in Table 3.1. Currently βDG antibodies are limited to detecting the very C-terminus of the cytoplasmic domain of βDG and as of yet no antibodies are available to the extra cellular or even juxtamembrane cytoplasmic domains. One of the best characterised anti-βDG antibodies is the mouse monoclonal MANDAG2 (MDG2) (Helliwell et al 1994). MDG2 was raised against an immunogen peptide of the last 15 amino acid residues in the C-terminus of βDG (Helliwell et al 1994). The epitope of MDG2 was further elucidated by functional epitope mapping studies by James *et al* and Pereboev *et al* using spot arrays and point mutations or random phage display libraries respectively (James et al 2000, Pereboev et al 2001). James *et al.* identified the crucial residues of the epitope to be PxYVP, which is within the seven residues SPPPYVP that Pereboev *et al.* concluded contained the epitope (James et al 2000, Pereboev et al 2001). James *et al* went on to show that MDG2 binding to the epitope was abolished by introduction of phosphorylation at Y892 (James et al 2000). In support of this specificity to the non-phosphorylated form of Y892, both groups showed that a substitution of Y892 to a phenylalanine, which is essentially used as a non-phosphorylatable control for the phospho-tyrosine residue, was tolerated by MDG2 but no other substitutions were (James et al 2000, Pereboev et al 2001). As previously mentioned, phosphorylation at Y892 has important functional implications for βDG interactions and localisation, therefore an antibody sensitive to phosphorylation at this site is a valuable tool.

Table 3.1. βDG antibodies used in this study. The antibodies are reported alongside their reported epitopes, species, class and source.

Antibody Name	Epitope/ Target	Species/ Class	Reference/ Source
MANDAG2 (MDG2)	βDG, carboxyl terminus, residues 881-895	Mouse IgG1 monoclonal	Thi Man and G. Morris (Pereboev et al. 2001)
1709	βDG, carboxyl terminus residues 881-895 phosphorylated at Y890 (mouse) /Y892 (human)	Rabbit IgG Polyclonal	In house (Ilsley et al. 2001)
JAF1	βDG, carboxyl terminus, 7 amino acid residues	Rabbit IgG Polyclonal	D. Mornet (Rivier et al. 1999)
βDG C-20	βDG, carboxyl terminus 20 residues	Goat IgG Polyclonal	Santa Cruz (sc-16165)

1709 is a rabbit polyclonal antibody that was raised against phospho-peptide KNMTPYRSPPPpYVPP (Ilsley et al 2001) found at the C-terminal of βDG. The epitope is very similar to that of MDG2 but crucially is specific for phosphorylation at Y892. Indeed, on peptide SPOT arrays 1709 does not detect the same peptide without phosphorylation at Y892 (Miller et

al. 2012). JAF1 is also a rabbit polyclonal antibody raised against a peptide containing 7 C-terminal amino acid residues of βDG (Rivier et al. 1999). C20 is a commercially available goat polyclonal antibody raised against the C-terminal 20 residues of βDG. Other commercially available antibodies include the mouse monoclonal 43DAG, which was raised against a peptide containing 15 C-terminal residues, much like MDG2, and also the rabbit polyclonal anti- βDG H-242 which targets residues 831-895 of βDG. All of the above have been shown to detect a 43KDa band corresponding to full length βDG via western blot and localise to the sarcolemma in skeletal muscle sections via IHC (James et al 2000, Ilsley et al 2001, Pereboev et al 2001, Rivier et al 1999, Lara-Chacon, 2010, Mathews et al 2013, Miller et al 2012). Given the number of βDG antibodies now available it was decided to compare the epitopes, localisation and the expression profiles detected by the antibodies MDG2, 1709, JAF1 and C20 , particularly in the prostate cancer cell lines to be used as the model systems in this body of research.

Given that the βDG antibodies have been raised against different antigens, they are likely to detect different epitopes (Pereboev et al. 2001, Ilsley et al. 2001, Rivier et al. 1999). The antibodies may therefore detect distinct populations of βDG, for example as a consequence of regulatory PTM contained within the epitopes, as is the case with 1709 and its detection of βDG phosphorylated at Y892 (Ilsley et al. 2001). The use of 1709 as a tool in the characterisation of βDG localisation is of particular interest for this body of research, as phosphorylation at Y892 has been implicated in the regulation of the nuclear localisation of βDG (Lara-Chacon et al. 2010). Whilst the antibodies MDG2, 1709, JAF1 and C20 have all been used, to varying extents, in the investigation of βDG localisation and expression in a number of model systems, there has been little direct comparison of the populations of βDG that these antibodies detect. A thorough comparison of βDG with the different antibodies in the prostate cell lines to be used as a model system in this project may provide further insight into the subcellular localisation of βDG in these cells as well as clues as to the regulation of βDG. It is of equal importance to validate each of the anti- βDG antibodies as specific tools in the detection of βDG.

3.1.6. THE IMPORTANCE OF ANTIBODY VALIDATION

Antibodies are routinely used in research for a number of techniques as well as clinically. In order to obtain reliable results, it is therefore important to validate antibodies to determine their specificity and reproducibility in the varying techniques in which they are used. An antibody that works efficiently at recognising the epitope in western blots, when the protein is denatured, may not recognise the epitope when the protein is in its native conformation in IHC. In addition, in techniques such as IHC a fixative may further complicate the issue by altering the presentation of the epitope (Bordeaux et al 2010). Moreover, antibodies must be

assessed for cross reactivity whereby an antibody may recognise an epitope in a protein other than the intended target. In the case of polyclonal serum antibodies additional IgG that recognise different antigens may also be present and therefore produce background signal which may confound interpretation of the results (Bordeaux et al 2010, Lipman et al 2005).

3.1.7 Chapter Aims

The aims of the research conducted in this chapter are:

- to validate the specificity of four βDG antibodies used in this study in different applications, namely immunoblotting and immunofluorescence microscopy.

- to characterise the expression and localisation of βDG, as detected by the different antibodies, in the model systems used in this body of work.

3.2 Results

3.2.1 Characterisation of carboxyl terminal epitopes of b-Dystroglycan antibodies by peptide Arrays

The different antibodies used in this study to detect βDG (Table 3.1) have been raised against different epitopes in the carboxyl terminus of βDG (Helliwell et al 1994, Ilsley et al 2001, Rivier et al 1999). In order to characterise and compare the differences in epitope at the most basic residue sequence level, the antibodies were used to immunoblot βDG peptide arrays obtained from Invatis AG (Fig 3.1A,B). Each array consists of the 110 amino acids of the cytoplasmic domain of βDG synthesised as 15 residue peptides, overlapping in 1 residue steps (Fig 3.1B), each repeated three times.

The monoclonal antibody, MDG2, was raised against a peptide covering the 15 carboxyl residues of βDG and therefore, unsurprisingly, detects the carboxyl terminal two spots with a consensus sequence of KNMTPYRSPPPYVP (Helliwell et al 1994) (Fig 3.1A). MDG2 does not, however, detect a peptide of the same sequence that has been modified to contain a phosphorylated tyrosine residue (Y892), KNMTPYRSPPPpYVPP (Spot E15). 1709, on the other hand, specifically detects only this phosphorylated peptide (Fig 3.1A). MDG2 and 1709 can therefore, in principle, be used to specifically detect non-phosphorylated and phosphorylated Y892 βDG respectively. MDG2 has been extensively analysed in the literature and the epitope has been further refined to PPYVP highlighted in red (Fig 3.1A) (James et al 2000, Pereboev et al 2001).

The JAF1 polyclonal antibody, a kind gift from D. Mornet, was raised against the 7 C-terminal amino acid residues of βDG (Rivier et al 1999). The JAF1 peptide array detects strong binding on 2 spots with a consensus sequence KNMTPYRSPPPYVP, confirming a short carboxyl terminus epitope which potentially overlaps with that of MDG2. JAF1 also detects a peptide modified to replace Y892 with a phenylalanine (Fig 3.1A). The peptide array results indicate that the JAF1 epitope includes Y892 and is sensitive to its phosphorylation status, detecting the non-phosphorylated form.

The commercial goat polyclonal antibody C20 detects far more spots on the peptide array, corresponding to the 16 peptides covering the final 30 residues at the carboxyl terminus of βDG. There is not a single consensus sequence contained within all of these spots, however, C20 is a polyclonal antibody and therefore likely to bind to multiple epitopes within the antigen. From the staining of the peptide array with C20 one could argue that there at least 2 epitopes within this stretch of residues. Residues PMEGKGSRP (Green residues, Fig 3.1A) are contained within the strongly stained spots D23-E5 whilst spots E13 and E14 are also strongly detected and may contain another epitope. C20 does not detect the phospho-Y892 peptide nor the Y to F peptide of spot E18. Given the larger stretch of peptides detected, there is the possibility that C20 recognises an epitope that is independent of the phosphorylation status of Y892. It is important to consider that the epitope(s) recognised by C20 may not be sequential, and may depend on 3D structural elements that are not represented in the 15 amino acid peptides.

The peptide arrays confirm that the four βDG antibodies have epitopes in the carboxyl terminus of βDG, however they are all subtly different with respect to the length and position of the epitope and on the effect of phosphorylation on antibody binding.

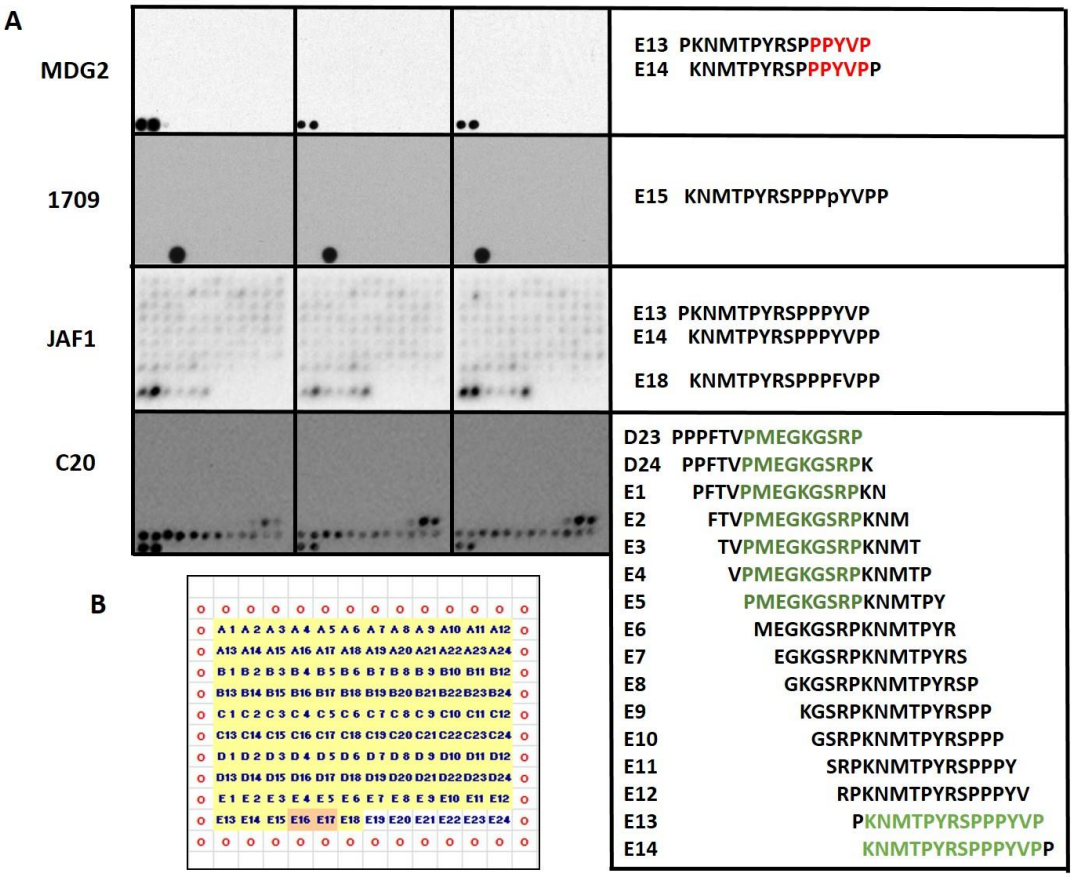

Figure 3.1. Peptide arrays of βDG immunoblotted with βDG antibodies. A. Peptide arrays covering the sequence of βDG in 15 residue length peptides were probed with MDG2, 1709, JAF1 and C20. The corresponding peptide position and sequence are detailed with validated epitopes highlighted in red. Two separate potential epitopes of C20 are highlighted in green. B. The layout of the peptide array.Each array contains 3 repeat units therefore each antibody is assessed in triplicate. MDG2 and 1709 peptide arrays conducted by C. Moore.

3.2.2 Characterisation of βDG antibodies via immunoblotting

Immunoblotting enables the detection of the levels and potential modification of specific proteins within a sample. Antibodies have varying degrees of robustness and specificity for every technique. Moreover, different epitope recognition, as is the case with the βDG antibodies used in this study, may result in the detection of different species or fragments of a protein by different antibodies. Total cell lysates from five different cells lines were immunoblotted with MDG2, 1709, JAF1 and C20 antibodies to assess the performance of the antibodies as well as the protein expression profiles of the lysates of the model systems to be used in this study (Figure 3.2).

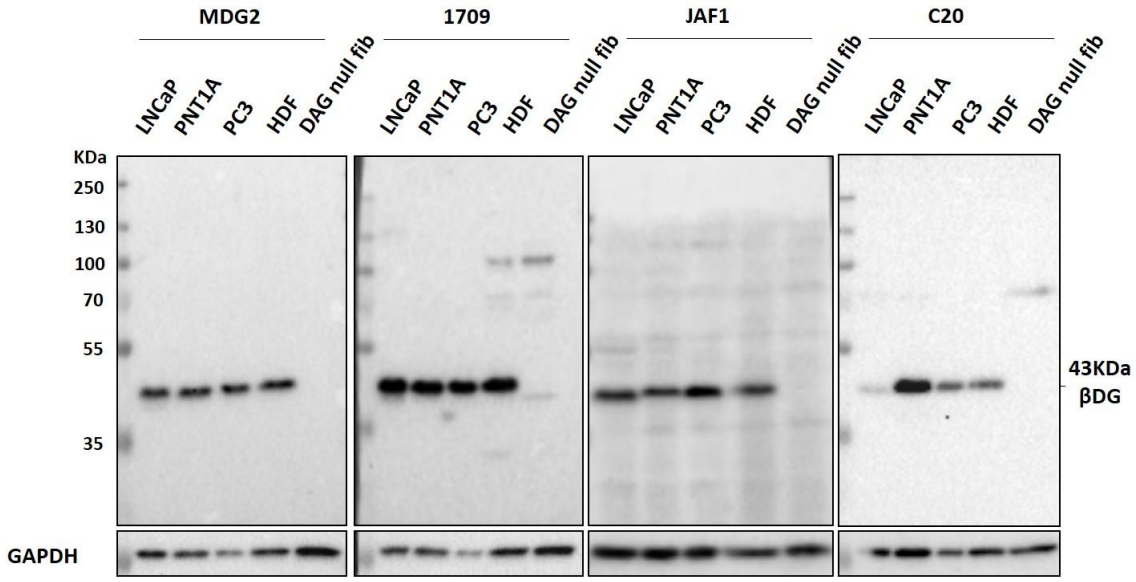

Figure 3.2. βDG antibodies immunoblot comparison and specificity on a range of total cell lysates. 20µg of lysates from 'normal' prostate cell line PNT1A, prostate cancer lines; LNCaP and PC3 and primary fibroblasts; control HDF and DAG null fibroblasts were immunoblotted with MDG2, 1709, JAF1 and C20. Full length, 43 KDa βDG is labelled. GAPDH was probed as a loading control.

The 'normal' immortalised prostate cell line, PNT1A, and the prostate cancer cell lines, LNCaP and PC3, all show strong detection of the 43 KDa band representing mature, full length βDG (Fig 3.2). The levels of full length βDG detected by 1709 and MDG in these three lysates appears to be similar whilst the levels detected by JAF1 and C20 appear to be more variable, with slightly lower levels detected in the LNCaP lysates (Fig 3.2). A strong 43 KDa band can also be detected in control primary human dermal fibroblast (HDF) cells by all four antibodies. Importantly, in the case of MDG2, 1709 and C20 the 43KDa band is not detected in a lysate obtained from primary human DAG null fibroblast cells (Fig 3.2). These cells have been isolated from a patient with Walker-Warburg Syndrome with a homozygous loss-of-function frameshift mutation, resulting in a premature stop codon in the N-terminal sequence encoding αDG and subsequently are absent for both full length α and βDG (Riemersma et al. 2015). As such this lysate can be used as a control for antibody specificity. JAF1, however, occasionally does detect a faint band at approximately 43 KDa (not shown) but the inconsistent appearance of this band suggests it may be an artefact of the experiment, whilst 1709 and C20 also detect some high molecular weight bands between 70-130 KDa in the DAG null lysates (Fig 3.2). There is therefore some non-specific binding by these antibodies.

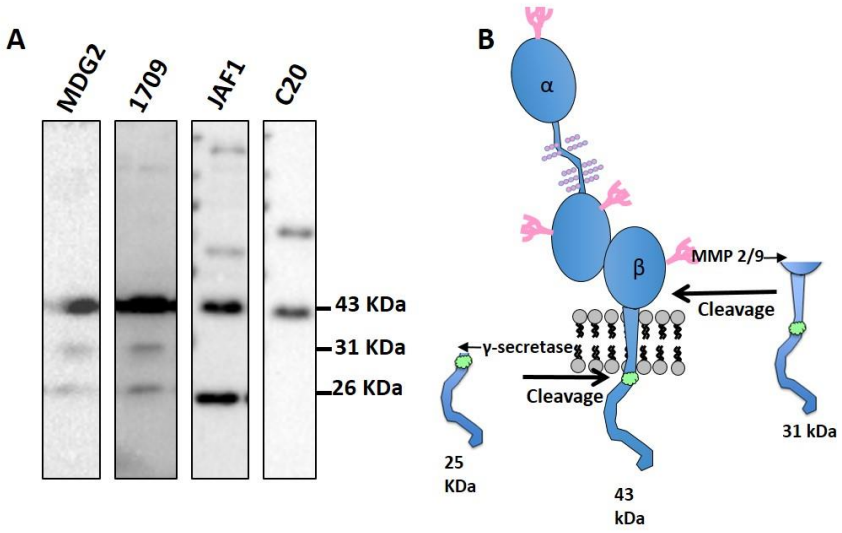

Figure 3.3. The detection of βDG fragments in LNCaP lysates via immunoblotting. A. Immunoblots with MDG2, 1709, JAF1 and C20 on total cell lysates of LNCaP grown at high density detect the full length 43 KDa band of βDG. In addition, MDG2, 1709 and JAF1 detect a 26KDa fragment of βDG, furthermore a 31 KDa band is also detected by MDG2 and 1709. B. A schematic diagram of full length 43 KDa βDG and the subsequent 31 KDa and 26 KDa βDG cytoplasmic fragments produced by proteases MMP2/9 and γ- secretase respectively (orange arrows). The nuclear localisation signal (NLS) is marked in green.

In addition to the full length 43 KDa protein, a 31 KDa protein fragment comprising the transmembrane and cytoplasmic domain and a 26 KDa cytoplasmic domain have been reported in the literature as a result of proteolytic cleavage (Figure 3.3 B) (Yamada et al, 2001, Zhong et al. 2006, Losasso et al 2000, Singh et al 2004, Cross et al 2008, Leocadio et al 2016). Both MDG2 and 1709 detect bands at 31 and 26 KDa when lysates collected from LNCaP grown at high density were immunoblotted (Figure 3.3 A). JAF1 detects the 26 KDa band strongly but does not consistently detect the 31 KDa band, whilst C20 does not robustly detect either fragment. Very occasionally a 17KDa fragment can be detected by 1709 and MDG2 (See Matthew et al 2013).

For the majority of this study MDG2 and 1709 are the main antibodies used for the reason that they robustly and specifically detect 43 KDa βDG, are sensitive to the cleavage fragments of βDG and give important information regarding the phosphorylation status of βDG at Y892.

3.2.3 Characterisation of Beta-Dystroglycan antibodies and Beta-Dystroglycan localisation via immunofluorescence microscopy in Prostate cell lines.

Immunofluorescence microscopy is a widely used technique in investigating the localisation of a specific protein. The different βDG antibodies available in this study were used to stain the

three different prostate cell lines that are the model systems used in this work, with the aim of characterising the localisation of βDG in these cell lines and determining if the different antibodies detect different localisation patterns of βDG as a consequence of their different epitopes.

3.2.3.1 βDG localisation and antibody characterisation via immunofluorescence microscopy in LNCaP cells

The lymph node derived, metastatic prostate cancer LNCaP cells were grown in 2D culture, immunostained and imaged via confocal microscopy. MDG2 staining shows a strong localisation of the non-phosphorylated Y892 form of βDG at the cell periphery and cell-cell-junctions (Figure 3.4A, arrows) and faintly in the cytoplasm. There is also staining at the nuclear envelope (Figure 3.4A, arrowheads). The Y892 phosphorylated form of βDG, as stained by 1709, also localises to the cell periphery and cell-cell junctions, albeit fainter than MDG2. 1709 displays a stronger cytoplasmic and nucleoplasmic localisation. JAF1 staining is reminiscent of MDG2, which is unsurprising given their similar epitopes, and stains the cell periphery, cell-cell junctions and cell protrusions. JAF1 also stains the nuclear envelope and faintly punctately in the nucleoplasm. C20 gives a distinctly different localisation pattern to the other βDG antibodies described above. C20 stains extremely faintly at the cell periphery and clearly detects βDG in nuclear structures that may be the nucleoli. βDG localisation in the nucleoli has previously been reported in C2C12 cells via colocalisation studies with nucleolar protein Nopp140 (Martinez-Vieyra et al. 2013). Control staining was carried out with the relevant secondary antibodies alone (Figure 3.4.B). Extremely faint, uniform background staining was detected with all the secondary antibodies, indicating that the staining patterns observed could be attributed to the primary antibodies.

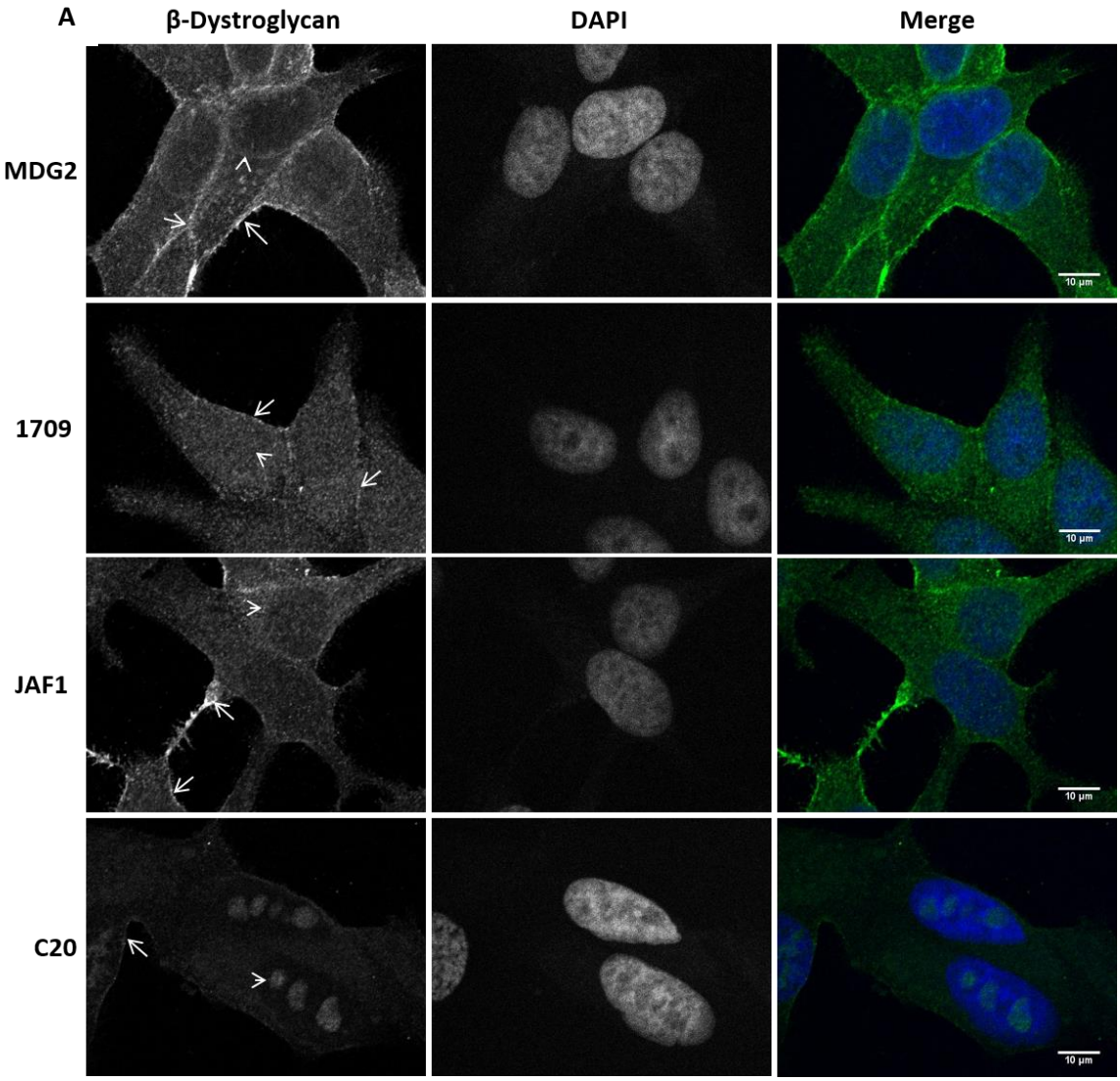

Figure 3.4.A βDG localisation as detected by different βDG antibodies via immunofluorescence in LNCaP cells. LNCaP cells were stained with MDG2, 1709, JAF1 and C20 (green) and the nuclei counterstained with DAPI (blue). All βDG antibodies detect βDG localisation at the plasma membrane and cell-cell interactions (arrows) and also in the nucleoplasm, nuclear membrane or, in the case of C20, nucleoli to varying degrees (arrow heads). Images are confocal slices of 0.28µm taken from the middle of the nucleus. Images were taken at 60x magnification. Scale bar 10 µm.

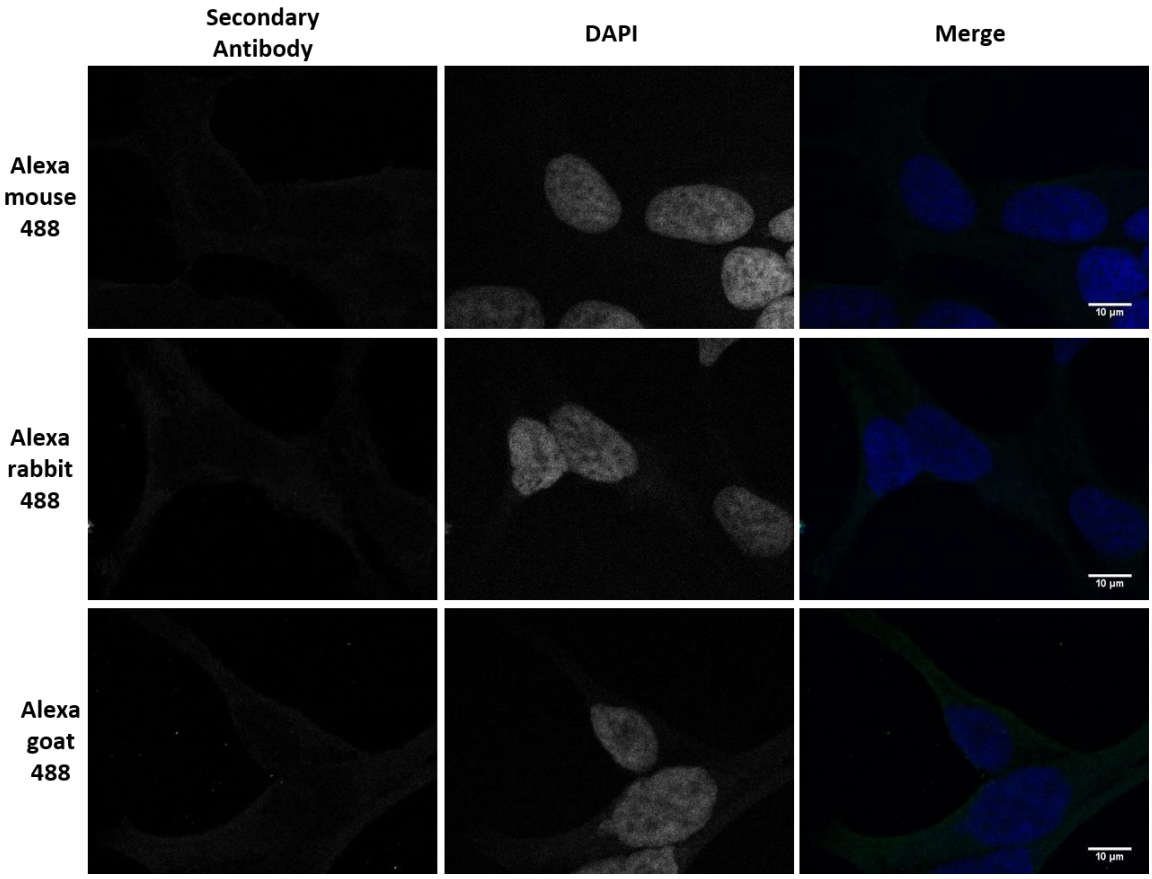

Figure 3.4. B. Secondary antibody control validation. LNCaP cells were processed and analysed as in Fig 3.4.A but lacking the primary antibody. Alexa rabbit 488, Alexa mouse 488 or Alexa goat 488 secondary antibodies (green). Nuclei were counterstained with DAPI. Images are confocal slices of 0.28µm taken from the middle of the nucleus. Images were taken at 60x magnification. Scale bar 10 µm.

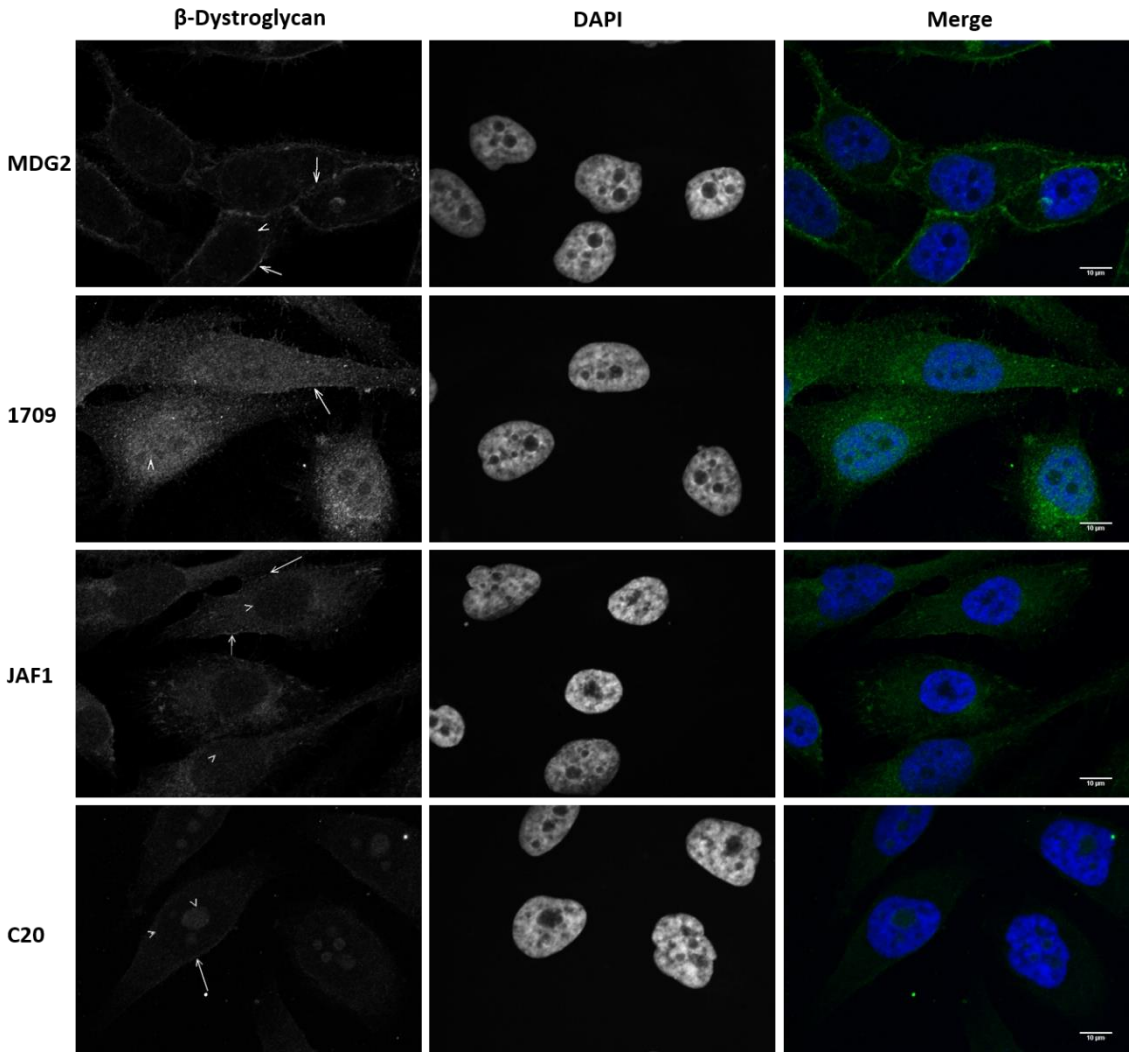

Figure 3.5 βDG localisation as detected by different βDG antibodies via immunofluorescence in PC3 cells. PC3 cells were stained with MDG2, 1709, JAF1 and C20 (green) and the nuclei counterstained with DAPI (blue). βDG can be seen at the plasma membrane (arrows), cytoplasm and in the nucleus (arrow heads). Images are confocal slices. Images were taken at 60x magnification. Scale bar 10 µm.

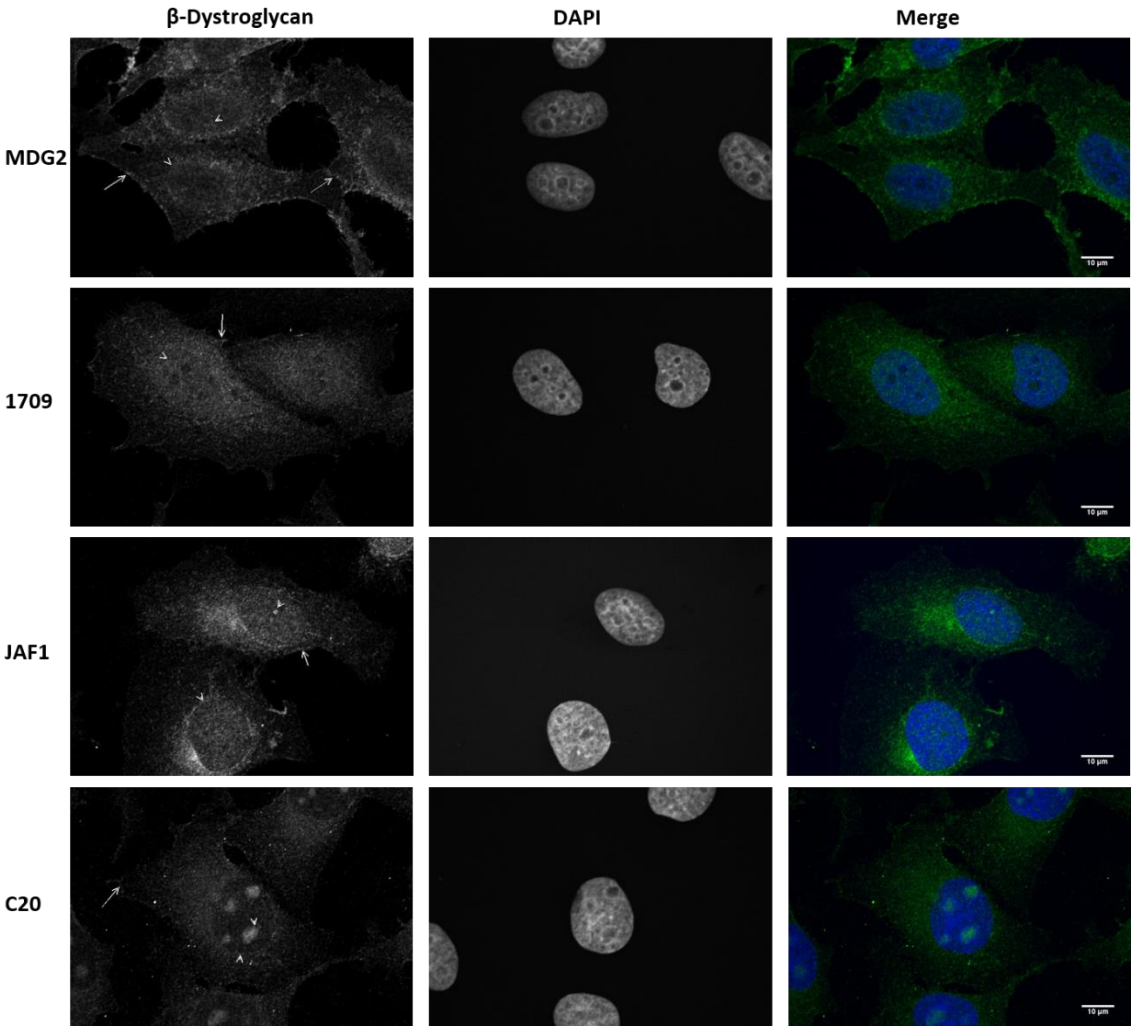

Figure 3.6. βDG localisation as detected by different βDG antibodies via immunofluorescence in PNT1A cells. PNT1A cells were stained with MDG2, 1709, JAF1 and C20 (green) and the nuclei counterstained with DAPI (blue). βDG can be seen at the plasma membrane (arrows), cytoplasm and in the nucleus (arrow heads). Images are confocal slices. Images were taken at 60x magnification. Scale bar 10 µm.

3.2.3.2 βDG localisation and antibody characterisation via immunofluorescence microscopy in PC3 cells

The prostate cancer cell line, PC3, displayed strong peripheral and cell-cell junction staining of βDG when immunostained with MDG2 (Figure 3.5, arrows), similar to the LNCaP cells, and faint localisation at the nuclear envelope (Figure 3.5, arrowheads). PC3 cells, however, had far fainter cytoplasmic staining of βDG when detected by MDG2 than LNCaP. 1709 detected faint peripheral localisation of pY892 βDG and a strong punctate cytoplasmic stain. 1709 also detects a diffuse nucleoplasmic localisation, which appears to be excluded from the nucleoli. JAF1 faintly stains the cell periphery as well as a very faint cytoplasmic and perinuclear localisation. There is also some very faint staining within the nucleus. C20 very faintly stains the cell periphery and detects localisation in the nucleoli.

3.2.3.3 βDG localisation and antibody characterisation via immunofluorescence microscopy in PNT1A cells

In the immortalised 'normal' prostate epithelium line, PNT1A, MDG2, again showed strong localisation of βDG at the cell periphery and cell-cell junctions as well as cell protrusions (Figure 3.6). MDG2 also detected faint staining at the nuclear envelope. However, MDG2 also displayed punctate cytoplasmic and perinuclear localisation along with some faint localisation within the nucleus. 1709 does not appear to uniformly stain the cell periphery but could be detected in cell protrusions and regions of the cell periphery. Once again, 1709 displayed punctate cytoplasmic and perinuclear staining as well as clear nucleoplasmic localisation. JAF1 staining at the cell periphery was weak and irregular however JAF1 detected a strong, punctate cytoplasmic and perinuclear stain. JAF1 also stained at the nuclear envelope and nucleoplasm as well as some punctate nuclear structures. C20 faintly detected βDG at cell protrusions and faintly in the cytoplasm, but its localisation was again strongest in the nucleoli structures.

When immunostained for βDG the prostate cell lines all had similar but subtly different localisation patterns, this may be a consequence of the different origins of derivation, disease status and subsequent processing of βDG of the cell lines. In all three cell lines βDG was to some extent localised to the cell periphery and cell junctions in accordance with its role as a cell adhesion molecule, and was also detected in the nucleus at the nuclear envelope, nucleoplasm and nucleoli. Furthermore, it is clear that the different antibodies raised to detect βDG in some instances have strikingly different localisation profiles within a cell type. This is due to the different epitopes recognising different subsets of βDG, be it a result of different PTM, for example phosphorylation at Y892 or additional unknown PTM, different fragments or epitope availability all of which may have a different fate or function and therefore different localisation within a cell.

3.2.4 βDG ANTIBODY LOCALISATION AND CHARACTERISATION IN HUMAN DERMAL FIBROBLASTS (HDF) AND DAG NULL FIBROBLASTS

To obtain a more comprehensive understanding of βDG localisation as detected by the different antibodies in a wider range of cell types, immunostaining was carried out on human primary fibroblast cells. Furthermore, DAG null fibroblasts, as previously described, have a mutation in the DAG1 gene, resulting in the absence of both α and βDG (Figure 3.1) and are therefore a good negative control to test the βDG antibodies on (Riemersma et al 2015).

HDF and DAG null fibroblasts were immunostained with βDG antibodies and imaged via confocal microscopy (Figure 3.7). Figure 3.7 shows that when the control HDF cells are stained with MDG2 membrane peripheral, punctate cytoplasmic, nuclear envelope and nucleoplasmic

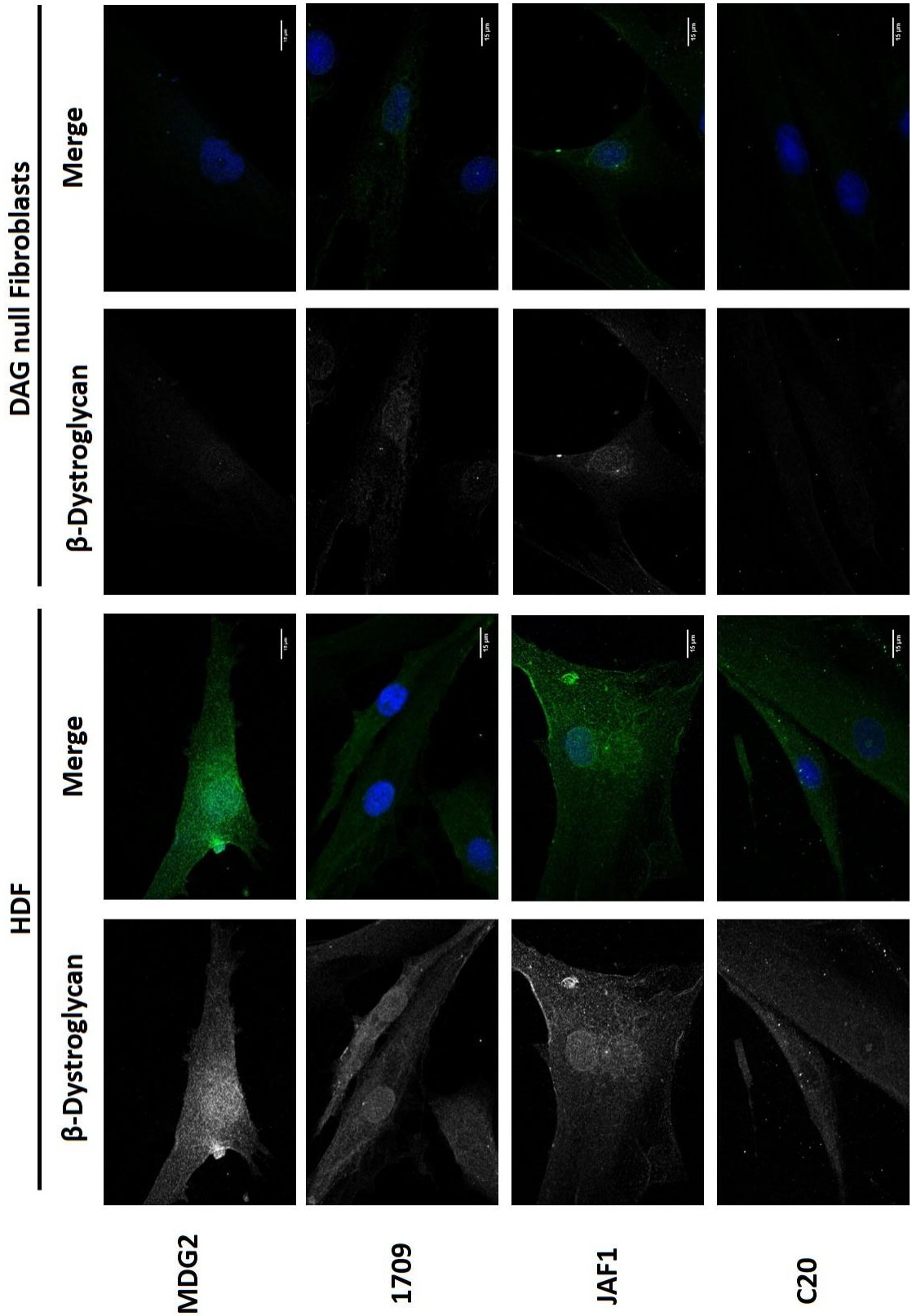

Figure 3.7. βDG antibody localisation and specificity comparison in HDF and DAG null fibroblasts via confocal immunofluorescence microscopy. HDF and DAG null fibroblasts were immunostained with MDG2, 1709, JAF1 and C20 (green) and the nuclei counterstained with DAPI (blue). βDG was detected at the plasma membrane by all 4 antibodies and to varying degrees in the nucleus at the nuclear envelope, the nucleoplasm and the nucleoli in the control HDF cells. MDG2 shows an almost complete lack of staining in DAG null fibroblasts whereas 1709, JAF1 and C20 show different extents of staining non-specific to βDG. Images are confocal slices. Magnification 60x. Scale bar is 15 µm.

localisation is detected. 1709 does not localise strongly to the periphery or cell-cell junctions, nor does JAF1, however both antibodies detect diffuse cytoplasmic staining and strong nucleoplasmic and nuclear envelope localisation (Figure 3.7). C20 staining is relatively weak in HDF cells, though there is faint, diffuse cytoplasmic staining and accumulation in the nucleoli. When stained and imaged in the same conditions, the DAG null fibroblasts give an indication of βDG antibody specificity. The majority of MDG2 staining is absent, with no staining at the periphery and a very faint signal detected in the nucleus (Fig 3.7). 1709 and JAF1, however, display a relatively strong signal, although it is reduced compared to the HDF cells (Fig 3.7). Cytoplasmic and nuclear staining can be detected by both antibodies in the DAG null cells. Very little non-specific fluorescence signal is detected by C20 in these conditions. These results show that MDG2 and C20 are largely reliable antibodies for use in immunofluorescence studies, whilst care must be taken if using 1709 and JAF1 antibodies when interpreting images, particularly the nuclear signal.

3.2.5 βDG ANTIBODY LOCALISATION AND CHARACTERISATION IN *DAG1* AND SIBLING ZEBRAFISH

Zebrafish have been used to study the regulation and function of DG. Importantly, for studies of DG, there is a mutant line, which has a point mutation in the DAG1 gene and subsequently reduced transcripts and a complete absence of DG protein (Lin et al 2011, Gupta et al 2011). For the purpose of this chapter the *DAG1* model also provides a second system in which to characterise βDG localisation and to test the specificity of the βDG antibodies.

4 d.p.f *DAG1* zebrafish embryos were sorted into DAG^{sib} ($DAG^{+/+}$ and $DAG^{+/-}$) or $DAG^{-/-}$ populations according to their muscle phenotype as assessed by birefringence assay. DAG^{sib} displayed smooth, bright muscle segments when viewed with polarised light whilst $DAG^{-/-}$ embryos had patchy, disrupted muscles (Figure 3.8.A). In order to confirm the accuracy of the phenotype characterisation by the birefringence assay and assess βDG antibody specificity, total lysates were obtained from the zebrafish embryos, run on SDS PAGE and immunoblotted with MDG2, 1709 and JAF1 (Figure 3.8.B).

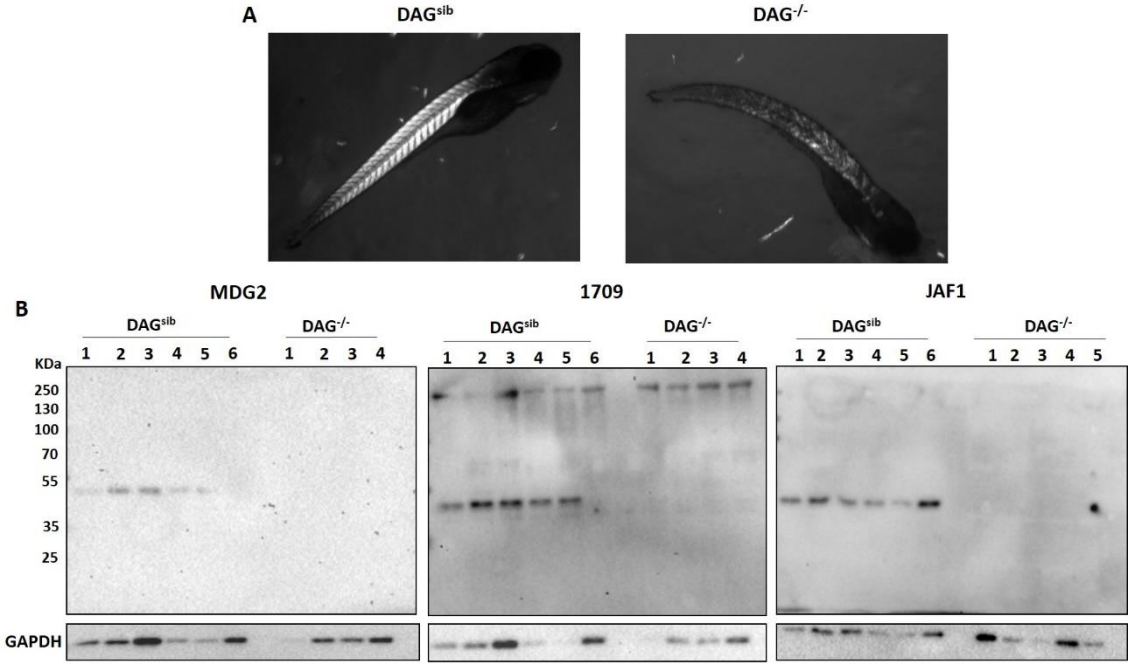

Figure 3.8. βDG immunoblotting antibody comparison and specificity in DAG$^{-/-}$ and DAG^{sib} zebrafish embryos. A. Representative images of DAG^{sib} and DAG$^{-/-}$ phenotypes as detected by birefringence assay clearly showing the disrupted muscle phenotype in the DAG$^{-/-}$ embryos. **B**. Total lysates obtained from single 4 d.p.f DAG^{sib} and DAG$^{-/-}$ zebrafish embryos were immunoblotted with MDG2, 1709 and JAF1. Full length βDG was detected in DAG^{sib} lysates but was absent from DAG$^{-/-}$ indicating antibody specificity. 1709 did detect some high molecular weight non-specific bands. GAPDH was used as a loading control.

All three antibodies detected bands corresponding to full length, 43 KDa βDG in the DAG^{sib} lysates, though the bands detected by MDG2 were very faint. The 43 KDa bands were absent in the DAG$^{-/-}$ lysates, indicating, firstly, that the birefringence assay was a robust technique to identify DAG$^{-/-}$ embryos, although to be certain genotype analysis would be required. Secondly it shows that all three antibodies are specifically detecting βDG at 43 KDa. 1709 detects bands at a range of molecular weights in both DAG^{sib} and DAG$^{-/-}$ lysates, indicating that 1709 can detect bands that are not specific to βDG and should thus be interpreted cautiously. None of the antibodies detected the smaller fragments of βDG, this could be because of the processing of βDG in these embryos or because the protein concentration obtained from the embryos was low and the assay is not sensitive enough to detect low concentrations of these fragments.

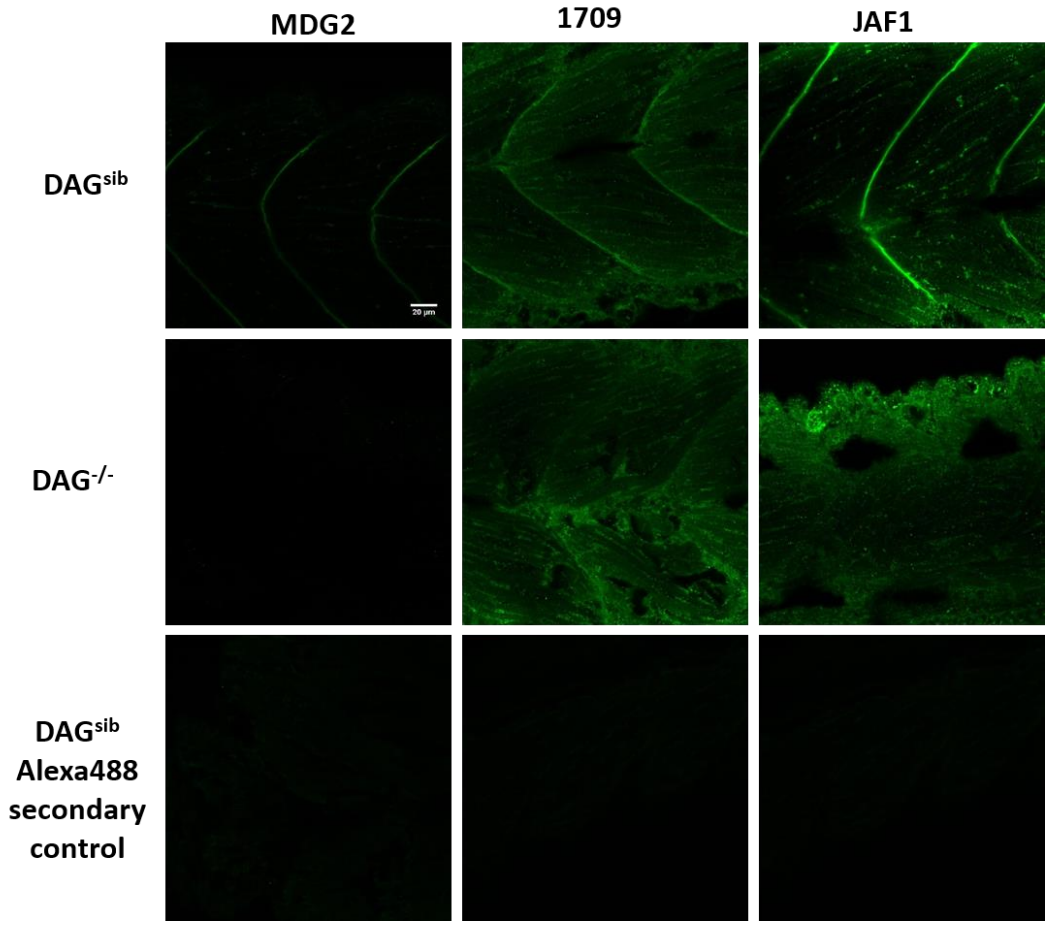

Figure 3.9.: βDG antibody immunofluorescence comparison and specificity in DAG$^{-/-}$ and DAG^{sib} zebrafish embryos. 4 d.p.f DAG$^{-/-}$ and DAG^{sib} zebrafish embryos were stained with MDG2, 1709 and JAF1 antibodies (green) and imaged via confocal microscopy. Secondary antibody controls for mouse and rabbit Alexa488 antibodies alone on DAG^{sib} embryos was included. All three βDG antibodies clearly stain the myosepta in the sibling embryos however 1709 and JAF1 also display staining non-specific to βDG in the DAG$^{-/-}$ embryos. Scale bar is 20µm.

DAG^{sib} and DAG$^{-/-}$ 4 d.p.f embryos were also subject to immunostaining and imaging via confocal microscopy (Figure 3.9). In the DAG^{sib} embryos MDG2 staining was predominantly in the myosepta with some faint, punctate staining within the somites, which may be the neuromuscular junctions (NMJ). 1709 and JAF1, however, detect punctate staining in the somites as well as a more diffuse stain in these segments. Both 1709 and JAF1 also localise strongly to the myosepta in the DAG^{sib} embryos. In DAG$^{-/-}$ embryos MDG2 does not stain the aforementioned structures and looks to be specific for βDG. In embryos immunostained with 1709 and JAF1, the staining is lost from the myosepta, indicating that this is true βDG localisation, however, the somites display clear punctate and diffuse staining that is therefore non-specific to βDG. A secondary antibody control confirms that the staining observed is a consequence of the primary antibodies (Figure 3.9). These results concur with the specificity conclusions drawn from the immunofluorescence analysis with the HDF and DAG null fibroblast cells.

3.3 DISCUSSION

3.3.1 CHARACTERISING AND COMPARING THE EPITOPES OF BDG ANTIBODIES

To date the antibodies available for the detection of βDG have epitopes in the C-terminal cytoplasmic domain of the protein, a region which is largely unstructured and contains close to 25% proline residues. The four antibodies recognising βDG used in this study; MDG2, 1709, JAF1 and C20 were all raised against peptide immunogens in the C-terminus of βDG (Helliwell et al 1994, Ilsley et al 2001, Rivier et al 1999). Although the peptide immunogens give some indication as to the epitope of the protein, epitope mapping can be used to refine and gain further specificity insight into the antibody epitope(s).

The peptide spot array for MDG2 identifies a consensus sequence of KNMTPYRSPPPYVP in which the epitope lies and concurs with the previously published functional epitope mapping studies by James *et al* and Pereboev *et al* (James et al 2000, Pereboev et al 2001). Pereboev *et al.* also proposed that P891 played an important role in epitope recognition by MDG2. The authors proposed that the high number of epitope residue matches in the chemically synthesised peptides used by James *et al.* could mask the contribution of residues that become slightly less important as more residues match, such as P891, whilst the random peptide library may be more sensitive to these residues (James et al 2000, Pereboev et al 2001). Regardless of P891 contribution, both reports and the array presented in this study agree on an overlapping consensus epitope of MDG2 containing PxYVP. The observation that MDG2 is sensitive only to the non-phosphorylated Y892 peptide and not the phospho-peptide included on the array again agrees with the previously published epitope mapping studies (James et al 2000, Pereboev et al 2001). Phosphorylation at Y892 is a key regulator of βDG and has been shown by multiple groups to be involved in DG localisation, degradation and interaction with binding partners (James et al 2000, Ilsley et al 2001, Sotgia et al 2001, Sotgia et al 2003, Yang et al 1995, Miller et al 2012, Lara-Chacon et al 2010, Mathew et al 2013)

The peptide spot arrays indicate that 1709 has an epitope that is very similar to that of MDG2 with the vital difference that it specifically recognises phosphorylated Y892. Point mutation studies have not been conducted to refine the epitope, however, support for 1709 specificity to the pY892 species is seen in its inability to recognise the Y892F peptide on the array and its loss of immunoreactivity for lysates run on western blots and in IHC sections from Y890F/Y890F mice, whilst MDG2 still detects βDG in these samples (Miller et al 2012). Thus MDG2 and 1709 are specific sensors for the phosphorylation status of Y892 in the C-terminal

tail of βDG and as such are valuable tools in the study of βDG and its fate given the key regulatory role of pY892.

The JAF1 epitope also appears to overlap with MDG2 and be sensitive to the phosphorylation status of Y892, recognising the non-phosphorylated form of βDG only. The C20 antibody likely detects multiple epitopes, as is expected for a polyclonal antibody and it is possible that at least one site does not include Y892 and is therefore independent of Y892 phosphorylation status, unlike the other antibodies presented above. Further refinement of JAF1 and C20 epitope to the specific vital residues would require further analysis such as systematic point mutations. There may also be other PTM within the epitopes that affect antibody binding which are not represented in these peptide arrays. For example, βDG is thought to contain at least one other phosphorylated tyrosine, of which there are multiple potential candidate residues within the C-terminal tail of βDG (James et al 2000, Moraz et al 2012).

The epitope of MDG2, 1709, JAF1 and potentially C20 overlap with the PPxY sequence which is a known recognition motif for WW domain protein binding as well as the binding motifs for SH2 and SH3 domain proteins (Pereboev et al 2001, James et al 2000, Yang et al 1995, Sotgia et al 2001) and is the site at which multiple interaction partners have been shown to bind to DG (Reviewed in Moore *et al.* 2010). The plethora of interactions at this site raises the question of 'epitope masking' whereby the antibody cannot access the epitope as it is blocked by another protein or structural element. 3D X-ray crystallography analysis of a βDG 15mer peptide, containing the PPxY motif, show the βDG peptide binding a surface made by one of the EF hands and the WW domain of dystrophin (Huang et al 2000, Pereboev et al 2001). In theory the PPxY and WW domains are interacting in this way at the sarcolemma, therefore there is some question as to how MDG2 and JAF1 still recognise this epitope in tissue sections. Explanations may be that the antibody still weakly recognises the epitope in complex, that the antibody displaces dystrophin in the IHC staining procedure or that not all the βDG at the sarcolemma is in complex via the epitope and is therefore available for antibody recognition (Pereboev et al 2001).Furthermore, the visualisation of βDG at certain adhesion structures such as focal adhesions has historically been difficult to detect because of molecular crowding and subsequent epitope masking at this site and can be improved using SDS antigen retrieval techniques (Moore et al 2010, Thompson et al. 2010). The competition between antibodies and interacting partners can be advantageous as demonstrated in the use of utrophin monoclonal antibodies that disrupted utrophin binding to βDG to determine the site of interaction between the two proteins (Morris et al 1999).

Peptide libraries and other forms of epitope mapping are useful in providing a basis of the core peptides involved in epitope recognition, however they are limited as they give no information

regarding how an antibody may interact with an epitope in the protein's 3D native conformation. An antibody's interaction with its antigen involves the shape, charge, hydrophilicity and hydrogen bonds of the available epitope side chains. Side chains that are available in the relatively linear peptide arrays may be buried in 3D structures or the antibody may recognise residues that are distant in the linear peptide sequence but spatially close in the 3D structure. Peptide arrays also do not account for the contributions of PTM unless specifically designed to do so. However, given the immunogen used, the peptide array data and the fact that the cytoplasmic domain of βDG is largely disordered, it can be proposed that at least MDG2, 1709 and JAF1 recognise linear epitopes in the βDG protein.

3.3.2 Beta-Dystroglycan antibody characterisation and validation in immunoblotting

In western blots proteins have been denatured from their native 3D conformation and separated by size via SDS PAGE. It may therefore seem logical that antibodies that recognise linear epitopes should work well for western blots, however this is not always the case, an example being the aforementioned α-DG antibody DAG-6F4 (Humphrey et al 2015). In the case of MDG2, 1709, JAF1 and C20, all of the antibodies detected a band at 43KDa in all of the lysates tested from cell lines LNCaP, PC3, PNT1A and HDF as well as those from the DAG^{sib} zebrafish embryos. The 43 KDa band represents the mature form of βDG and its mass reflects the high number of prolines within its cytoplasmic tail as well as PTM including N-glycosylation (Holt et al. 2000).The βDG antibodies used in this study have been widely reported in the literature as detecting the 43KDa band of βDG in blots across a range of species including human, mouse, zebrafish and different tissue and cell types including skeletal muscle, brain and prostate (Pereboev et al 2001, Rivier et al 1999, Lara- Chacon et al 2010, Miller et al 2012, Lipscomb et al 2016, Mathew et al 2013). More specifically MDG2 and 1709 have been shown in previous studies by the Winder group to detect full length βDG in the 'normal' immortalised prostate cell line PNT1A and the metastatic prostate cancer lines LNCaP and PC3 (Mitchell et al 2013, Mathew et al 2013, Leocadio et al 2016). The levels of DG expression in prostate cell lines are heterogeneous (Mathew et al 2013). The level of βDG was reported to be highest in LNCaP out of the prostate lines tested by Mathew et al (Mathew et al 2013) however the same cannot be concluded from figure 3.1, where the levels of βDG detected by JAF1 and C20 in the LNCaP lysate are low when compared to the other cell lines, though relatively strong when detected by MDG2 and 1709. βDG levels look largely similar across the cell lines when detected by MDG2 and 1709 and slightly more variable with JAF1 and C20. It is hard to dissect what this means for total βDG levels. These cell lines may truly have different ratios of species

detected by the different epitopes or may be detecting overlapping pools. Regardless, all four antibodies clearly detect full length βDG.

The βDG antibodies also detect the 31 and 26 KDa βDG fragments in LNCaP lysates to varying degrees. The 31 and 26 KDa fragments are produced by cleavage of the cytoplasmic domain by MMP2/9 and γ-secretase respectively and have been reported in previous studies by the Winder group and others in multiple cell lines including LNCaP (Yamada et al, 2001, Zhong et al. 2006, Losasso et al 2000, Mitchell et al 2013, Mathew et al 2013, Leocadio et al 2016). All of the epitopes are in the extreme C-terminal domain and are present in theory in both fragments, it is therefore unclear why C20 does not detect the fragments in this instance. It is possible that PTM within these fragments may disrupt C20 binding to the epitope or that C20 has a weak affinity for the antigen and the signal is reduced even further in the case of the low levels of the fragments. JAF1 and C20 were not extensively screened on lysates of different cell densities in other cell types and it cannot be ruled out that they would detect fragments there. 1709 has also been reported to detect a 17KDa fragment and can detect more and higher levels of fragments than MDG2 in the same sample, suggesting a potential role for Y892 phosphorylation in the fate or regulation of these fragments (Mathew et al 2013, Leocadio et al 2016). The functions of these fragments are as of yet unknown however their presence is increased upon increasing cell density and stimulation of the notch pathway (Mitchell et al 2013, Leocadio et al 2016). This could account for the variability of the presence of fragments in different experiments. Moreover, different cell lines appear to produce different levels of fragments, perhaps indicating different DG processing in these cell lines. Increased proteolytic cleavage of DG has been reported in carcinoma cells (Cross et al. 2008, Singh et al. 2001), therefore the different detection of c-terminal fragments in different cell lines might be a consequence of altered DG processing activity in the cancer cells. It is also interesting to consider that no antibodies are available to detect the remaining portions of βDG once the C-terminal has been cleaved so the fate of these N-terminal fragments remains unclear.

Importantly the validity of the antibodies in immunoblotting was tested in two different systems lacking the DG protein; the DAG null fibroblasts and the $DAG^{-/-}$ zebrafish embryos. It should be noted that the HDF line is not the best control for the DAG null fibroblasts as they are of different origins. Ideally the null fibroblasts re-expressing βDG or fibroblasts from the same origin in a healthy patient would be used as a control. HDF cells are, however, sufficient for the purpose of this analysis as a wildtype DG expressing fibroblast line. C20 and 1709 detected some high molecular weight bands in the null systems, thus indicating cross-reactivity with additional proteins. The cross-reactivity could be a consequence of recognition of the epitope in other proteins, indeed, proline stretches followed by a tyrosine are not uncommon.

A search of the epitope PPYVP in BLAST returns 30 proteins in humans that also contain this sequence in addition to DG (Altschul et al. 1990). It is important to note that PPYVP is the epitope for MDG2, as BLAST searches do not account for PTM, however it is possible that these proteins may also be phosphorylated at the tyrosine residue and thus represent the 1709 epitope. In addition, that MDG2 appears to specifically detect βDG (Fig 3.7, Fig 3.8) despite the potential presence of other proteins containing the relevant epitope, suggests that either a structural element is important in the recognition of the epitope, or that the alternative epitopes contain a modification or interaction that precludes detection by MDG2. In the case of polyclonal antibodies such as 1709, JAF1 and C20, additional IgG antibodies produced by the host may be present and therefore detect other proteins. This latter scenario could be resolved by affinity purification of the antibodies.

3.3.3 Beta- Dystroglycan localisation and antibody validation via immunofluorescence techniques

Whilst valuable information regarding expression levels and modifications can be learnt from immunoblotting, a further and complementary technique to investigate βDG localisation is immunofluorescence microscopy. Multiple groups have shown βDG to be localised to a range of cellular compartments including the cell periphery, NMJ, filopodia, nucleus and intracellular vesicles (Pereboev et al 2001, Spence et al. 2004, Thompson et al. 2010, Lara-Chacon et al 2010, Mathew et al 2013, Leocadio et al 2016, Sotgia et al 2003, Miller et al 2012) across a variety of tissues and species, consistent with a range of functions and fates of βDG, some known and others yet to be elucidated.

The four βDG antibodies were used to stain a selection of human cell lines and zebrafish tissue. Interestingly, not only did the cell lines display slightly different localisation of βDG when analysed with the same antibody but the antibodies detected different localisations of βDG within a cell line. The strong localisation of the non-phosphorylated Y892 species, as detected by MDG2, at the cell periphery fits with a current hypothesis in the literature that non-phospho Y892 βDG is able to interact with binding partners e.g. utrophin at the plasma membrane whilst disruption of these interactions leaves the cytoplasmic tail free for phosphorylation by src and subsequent internalisation and potential degradation (Sotgia et al 2003, Miller et al 2012, Lipscomb et al 2016) or translocation to the nucleus (Lara-Chacon et al 2010, Mathew et al 2013, Leocadio et al 2016). In line with this hypothesis, pY892 βDG as detected by 1709, is reduced at the cell periphery in all cells and is virtually non-existent in PNT1A cells and instead displays a more diffuse cytoplasmic and nuclear localisation.

JAF1 staining varies considerably between the cell types, resembling that of MDG2 at the periphery in LNCaP, is greatly reduced at the PM and cytoplasmic in PC3 cells and shows a stronger cytoplasmic and nuclear staining in PNT1A. The peptide epitope is similar to MDG2 and it may therefore be logical to expect more PM staining however it is difficult to tell how JAF1 is detecting the native conformation of the epitope. These results also raises questions about the differential processing of βDG at different stages of prostate cancer progression (Cross et al 2008, Henry et al 2001, Mitchell et al 2013, Mathew et al 2013, Leocadio et al 2013), as modelled to some extent by the included cell lines (Horoszewicz et al 1983, Mathew et al 2013).

C20 gives a strikingly different localisation pattern with very little at the plasma membrane and strong staining of structures within the nucleus that are likely nucleoli. βDG localisation at the nucleoli has previously been reported in C2C12 myoblasts by Martinez-Vieyra et al via confocal microscopy and was supported by the presence of Nopp140, a nucleoli marker in the fraction containing proteins immunoprecipitated by βDG (Martinez- Vieyra et al, 2013). Why C20 stains the nucleoli so strongly where the other antibodies do not is curious but could be due to a different population that is detected by a more N-terminal epitope or the localisation may be regulated by PTM within the C20 epitope. Furthermore, it is not possible to tell from immunofluorescence analysis which size species of βDG is present. Some species of βDG appear to have preferential locations, for example it has been shown that a tagged 26KDa fragment of βDG targets strongly to the nucleus (Mathew et al 2013). Alternative techniques such as biochemical fractionation and subsequent western blotting could help to resolve this.

All four antibodies show nuclear localisation of βDG, though to varying extents and at different nuclear structures. The detection of βDG in the nucleus raises questions as to its role and regulation there and shall be examined further throughout this thesis.

As with immunoblotting, it is important to verify antibody specificity for immunofluorescence microscopy. MDG2 and C20 look to be specific for βDG as they gave little to no staining in the DAG null systems that they were tested in, with a very faint nuclear presence detected by MDG2. 1709 and JAF1 perform poorly in the DAG null systems. In both systems the signal detected with 1709 and JAF1 is notably reduced or absent in areas of known βDG localisation such as the cell periphery and vertical myosepta however cytoplasmic and nuclear staining is still present in both DAG null fibroblasts and the $DAG^{-/-}$ zebrafish. Controls with secondary antibody alone indicate that the staining is a consequence of the primary antibody. These results suggest that although 1709 and JAF1 detect βDG, that is not the only protein that they detect. This background staining may be because of the antibodies binding to especially ‘sticky’ structures such as skin in the zebrafish embryos but may also be due to similar epitopes being

detected in proteins other than DG or the presence of other antibodies in the sera. Any immunofluorescence studies undertaken with 1709 and JAF1 should be interpreted with caution and validated with other techniques such as comparing staining patterns in DAG null systems or using a tagged protein. To improve and ensure the specificity of the antibodies they should be subject to affinity purification.

3.3.4 SUMMARY

1. The peptide epitopes of the βDG antibodies used in this study are located at the extreme C-terminal of βDG and are subtly distinct in location or PTM recognition.
2. The antibodies all detect full length 43 KDa βDG and variably detect the 31 and 26 KDa cytoplasmic fragments of βDG in a range of cell lines and tissues.
3. All four antibodies display different localisation patterns of the different populations of βDG within a cell line and variably detect βDG at the cell periphery, nucleus, cell protrusions, myosepta and intracellular vesicles.
4. According to the DG null systems used MDG2, 1709 and C20 can be used to specifically detect the 43 KDa band of βDG via immunoblotting although 1709, JAF1 and C20 can detect non-specific bands of higher molecular weight.
5. MDG2 and C20 appear to be specific for βDG in immunofluorescence studies whilst 1709 and JAF1 detect variable levels of non-specific staining.

Chapter 4: Nuclear β Dystroglycan and the role of phosphorylation at T788

4.1 Introduction

4.1.1 The function and mechanisms of translocation of nuclear βDG

The concept of βDG being solely an adhesion receptor at the plasma membrane with structural roles in the DGC no longer holds true, with the expanding knowledge of interacting partners and its localisation to subcellular compartments, such as the nucleus, all hinting at a multitude of complex functions (Oppizzi et al. 2008, Lara-Chacon et al 2010, Sotgia et al, 2001, Spence et al 2004, Moore and Winder 2010). The information regarding βDG in the nucleus is growing, however a great deal remains to be understood about the nuclear functions and mechanisms of regulation of βDG.

DG appears to be important for maintaining nuclear morphology and interacts with a number of structural nuclear proteins (Martinez-Vieyra et al, 2013). Regarding the mechanisms of nuclear translocation, it has been established that βDG is capable of undergoing rapid nucleocytoplasmic shuttling and contains a NLS located at the juxtamembrane region of its cytoplasmic domain (Lara-Chacon et al., 2010, Oppizzi et al., 2008). Furthermore, βDG was identified as interacting with importin a/b and Ran-GTP suggesting the classical nuclear import cycle across a nuclear pore as a likely method of nuclear translocation (Lara Chacon et al., 2010). However, little is known about the series of events and potential PTM that regulate βDG nuclear translocation and its retention and functions in the nucleus.

4.1.2. Phosphorylation of βDG

Phosphorylation is a particularly well studied and important modification of βDG. As has previously been mentioned, phosphorylation at Y892 (human) /Y890 (mouse) by src kinases is a key modulator of βDG regulating its interactions with binding partners and signalling molecules (Ilsley et al 2001, James et al. 2000, Yang et al. 1995). Phosphorylation at Y892 also promotes internalisation from the plasma membrane (Sotgia et al. 2001) and potentially subsequent degradation in a ubiquitin dependent manner (Miller et al. 2012).

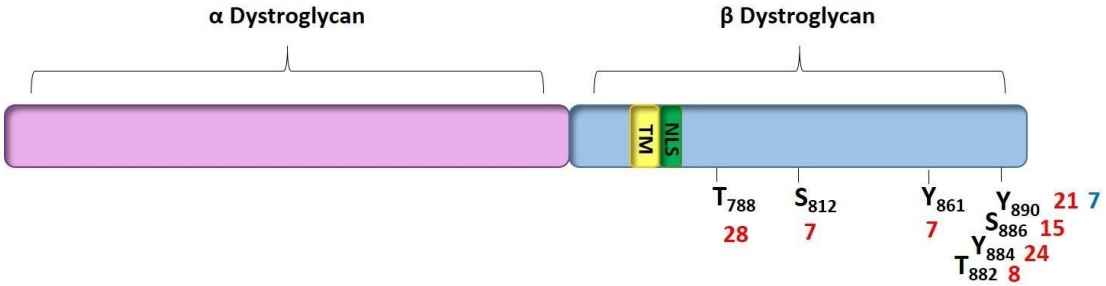

Figure 4.1. Schematic of α and β Dystroglycan with selected putative sites of phosphorylation in the cytoplasmic domain of βDG. The locations of the transmembrane (TM, yellow) domain and the nuclear localisation signal (NLS, green) of mouse βDG are indicated. Putative sites of tyrosine (Y), Threonine (T) and Serine (S) phosphorylation as reported on phosphosite plus are indicated in black. Only residues that have been reported in more than five independent reports have been included. Adjacent numbers in red indicate the number of reports in which phosphorylation at these residues have been detected through high throughput proteomic mass spectrometry. Adjacent numbers in blue are reports in which phosphorylation of a residue has been identified using site-specific methods (Hornbeck et al. 2014).

Phosphorylation at Y892 is the only site to have been confirmed to be phosphorylated by site specific methods, however there is evidence for the phosphorylation of βDG at other residues within its cytoplasmic tail, as previously described. Analysis of the sequence of βDG identifies multiple putative sites of phosphorylation not only at tyrosine, but also serine and threonine residues. Furthermore, according to PhosphoSite plus, a resource for the studies of protein modifications (Hornbeck et al. 2014), the phosphorylation of βDG has been identified in multiple reports in high through put mass spectrometry studies at Y, S and T residues (Fig 4.1). These putative sites of phosphorylation must be interpreted with caution as they have only been identified through non-targeted mass spectrometry and may therefore be false positives or not biologically significant however there is certainly enough evidence to warrant further investigation into the role of phosphorylation at these putative sites on the regulation of βDG.

4.1.3 The role of phosphorylation on the nuclear localisation of proteins.

Phosphorylation is known to regulate the nuclear transport of a number of proteins, though the method through which this is achieved can be complex. Phosphorylation is able to both enhance and inhibit nuclear import of different target proteins (Nardozzi et al. 2010). Phosphorylation can enhance nuclear localisation by a number of mechanisms for example phosphorylation may enhance the binding affinity (eg Epstein-Barr virus Nuclear antigen (EBNA)) (Kitamura et al. 2006) or recognition by importins (e.g. Hepatitis B virus (HBV)) (Rabe et al. 2003). Alternatively, phosphorylation can promote a conformational change that alters

the position of the NLS enhancing its docking to the nuclear pore complex (e.g. SV40) (Fontes et al. 2003) or exposing the NLS to the relevant importins (e.g. Signal transducers and activators of transcription (STATs)) (Meyer et al. 2002). Phosphorylation of some components of the nuclear translocation machinery inhibits nuclear import whilst phosphorylation within the NLS can also promote cytoplasmic retention of a protein, potentially by reducing its affinity for importins (eg parathyroid hormone related protein (PTHrP)) (Lam et al. 1999).

4.1.4 Phosphorylation and nuclear βDG

The phosphorylated Y892 form of βDG has been identified in the nucleus of multiple cell types (Mitchell et al. 2013, Mathew et al. 2013, Leocadio et al. 2016). It was initially proposed that tyrosine phosphorylation may play a role in nuclear translocation of βDG. However, as discussed in section 1.6.3, the role of phosphorylation on the regulation of nuclear βDG is complex. Peroxyvanadate treatment of C2C12 cells saw an increase in the nuclear level of βDG, however point mutation studies using a non-phosphorylatable form, Y892F (human), in C2C12 cells and the equivalent residue, Y890F, in a construct containing mouse DG in LNCaP cells do not suggest a role for this modification in nuclear localisation of full length βDG (Lara-Chacon et al. 2010, Leocadio 2014). pY892 βDG might regulate functions of βDG in the nucleus and interestingly it has been proposed that the level of pY892 βDG is slightly increased in the nucleus of prostate cancer tissues relative to normal tissue in immnunohistochemical stains (Mathew et al. 2013). The increase in nuclear level seen with peroxyvanadate may be accounted for by the phosphorylation of another residue within βDG or by influencing any number of proteins involved in nuclear transport or βDG interaction that may also be phosphorylated.

Given the potential role for additional phosphorylated residues in the nuclear translocation of βDG it was of great interest when, in a recent mass spectrometry study conducted in the Winder lab, the presence of a phosphorylated threonine peptide, at residue T790 in human which is equivalent to residue T788 in mouse DG, was identified in a nuclear fraction but not the non-nuclear fraction of LNCaP cells (Leocadio et al. 2014). Residue T790 (human) and T788 (mouse) have been identified as phosphorylated in 28 independent mass-spectrometry studies from a variety of tissues and cell types, reported on the curated modifications database Phosphositeplus, though it has not yet been confirmed by site-specific techniques (Fig 4.1) (Hornbeck et al. 2014). Originally Oppizzi et al. reported the NLS to be a bipartite sequence with a pair of lysines ^{793}KK^{794} 10 amino acids downstream of the NLS at ^{776}RKKRKGK^{782} and is conserved in multiple organisms. It has since been shown that residues 776-782 are necessary and sufficient for βDG nuclear targeting (Oppizzi et al. 2008, Lara-

Chacon et al. 2010). Interestingly T790 sits between these two sequences. We therefore hypothesised that βDG is phosphorylated at T790 and is important for its nuclear localisation or function. A construct containing mouse DG is used to study the effects of phosphorylation at this threonine residue of interest, which shall therefore henceforth be referred to as T788 in this thesis.

4.1.5 Chapter Aims

The aims of the research conducted in this chapter are:

- To investigate the effect of the loss of DG on nuclear morphology in Human primary DAG null fibroblasts.
- To characterise the subcellular localisation of endogenous βDG in prostate cell lines.
- To investigate the phosphorylation of βDG and a potential role for phosphorylation at T788 on the nuclear localisation of βDG and βDG regulation.

4.2 Results

4.2.1 Nuclear morphology is disrupted in DAG null primary fibroblasts

The availability of a fibroblast cell line isolated from a patient with Walker Warburg syndrome with a mutation resulting in the absence of α- and βDG protein (Riemersma et al. 2015) provides a useful tool in the study of DG function and was used to address the question of whether DG plays a role in nuclear morphology. Immunoblots of whole cell lysates (WCL) harvested from the DAG null fibroblasts and probed with antibodies against βDG (MDG2) and pY892 βDG (1709) confirmed the absence of βDG at the protein level in the DAG null fibroblasts whilst full length 43 KDa βDG is strongly expressed in the control HDF cells (Fig 4.2 Ai). In order to determine if complete loss of βDG from the cell affects the overall nuclear morphology HDF and DAG null fibroblasts were immunostained for lamin A/C and the nucleus counterstained with DAPI and viewed via immunofluorescence microscopy (Fig 4.2 A-I). Nuclei were classified as having a 'normal' morphology if the nucleus was a regular oval shape with a smooth and even lamin A/C distribution (Fig 4.2 A-C). 92.7% of the HDF control cells displayed a 'normal' nuclear morphology compared to only 36.8% of the DAG null fibroblasts. 63.2% of the DAG null fibroblasts were classified as having an abnormal nuclear morphology compared to just 7.3% abnormal nuclei in the HDF cells (Fig 4.2 J). The DAG null fibroblasts displayed a broad array of disrupted morphology including blebbing, displayed in 41.71% of cells (Fig 4.2 D, E, K), irregular shape, including what appeared to be a twisting of the nucleus, 21.33% (Fig 4.2 F, G, K), multiple nuclei,

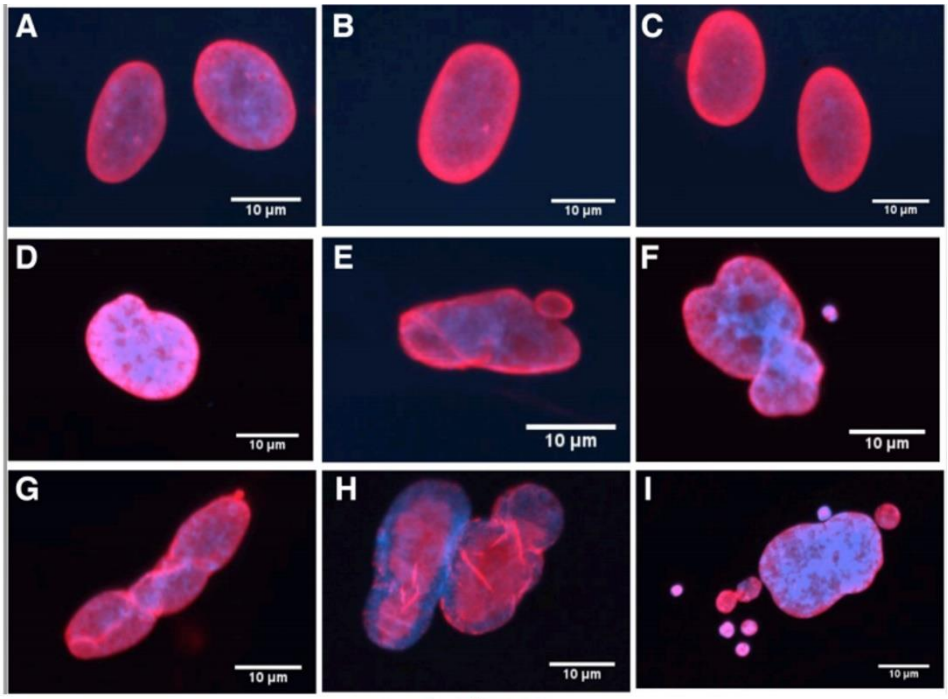

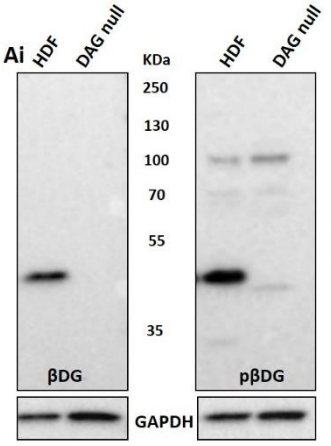

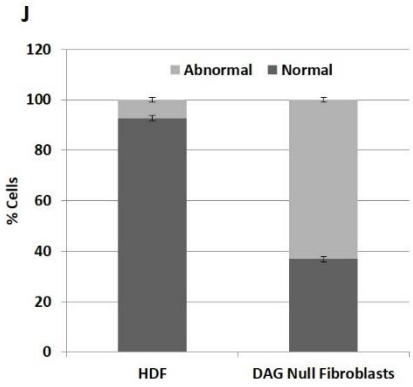

K

Morphology	% Cells	S.D.
Blebbed	41.71	19.59
Irregular Shape	21.33	9.22
Micronuclei	8.71	5.15
Multiple nuclei	4.35	2.57

Figure 4.2 Nuclear morphology is disrupted in DAG null fibroblasts. Ai) Immunoblot of HDF and DAG null fibroblast total cell lysates. Immunoblot with anti- βDG (MDG) (left) and pY892 βDG (1709) (right). GAPDH was used as a loading control. A-I) Immunofluorescent microscopy of HDF and DAG null fibroblast nuclei. Cells were stained for lamin A/C (red) and the nuclei counterstained with DAPI (blue). A-C) 'Normal' nuclei from HDF cells. D-I) 'Abnormal' nuclei from DAG null fibroblasts, representative images of blebbing (D, E), irregular shape (E, F, G), multiple nuclei (H) and micronuclei (I). Images were taken via widefield epifluorescent microscopy, magnification 60x, Scale bars 10µm. J) Quantification of mean percentage of 'normal' and 'abnormal' nuclear morphology of HDF and DAG null fibroblasts. Error bars ±SD. N=2, at least 100 cells per cell type/replicate. K) Classification of the types of aberrant nuclear morphology as a percentage of the total population of DAG null fibroblasts. Nuclei were classified as blebbed, irregular shape/ twisted/ micronuclei or multiple nuclei. N=2, at least 100 cells per cell type/replicate.

8.71% (Fig 4.2 H, K) and micronuclei 4.35% (Fig 4.2 I, K) Percentage quantifications of the classifications of aberrant nuclei of the DAG null fibroblasts is summarised in the Fig 4.2 K

The dramatic disruption of nuclear morphology upon the absence of α and β DG clearly suggests a role for βDG in maintaining correct nuclear morphology. However further investigation is required to determine the contribution of loss of the nuclear DG and subsequent effects on its nuclear interactions versus the loss of DG from the PM and elsewhere in the cell which will potentially result in signalling or cytoskeletal defects both of which are important to nuclear positioning and morphology.

4.2.2 Lamin localisation in DAG null Fibroblasts

The lamins are components of the nuclear lamina and play an important role in nuclear structure and transcriptional regulation (Prokocimer et al. 2009). It has previously been shown that cells with reduced levels of DG as a result of RNAi have mislocalised lamin B1 (Lara-Chacon et al. 2010). HDF and DAG null fibroblasts were immunostained with antibodies detecting lamin A/C or lamin B1 to investigate if these nuclear lamina components were also mislocalised in primary human fibroblasts absent for DG. Lamin B1 staining in the DAG null fibroblasts was slightly fainter and less uniform compared to the HDF control cells (Fig 4.3 A). Lamin B1 staining of HDF cells was not as uniform as expected within the nucleus and may be a consequence of the antibody. Lamin A/C staining does not appear to be different between the DAG null and control fibroblasts (Fig 4.3 B). Although further analysis such as western blot to detect the levels and more detailed confocal analysis is required, these results suggest that lamin B1 but not lamin A/C localisation is affected by the absence of DG.

4.2.3 Characterisation of nuclear bDG in prostate cell lines

DG has been shown to be localised to the PM and in the nucleus of prostate cells and is implicated in prostate cancer progression (Losasso 2000, Sgambato et al 2007, Mitchell et al. 2013, Mathew et al. 2013, Leocadio et al. 2016). Whilst DG has been studied in primary prostate tissue samples from patients, the expression, nuclear translocation and a number of PTM of βDG have been investigated in a number of prostate cell lines, particularly LNCaP, a widely used model of prostate cancer (Horoszewicz et al. 1983, Thalmann et al. 1994). LNCaP and other CaP lines and have provided valuable information as to how DG affects epithelial-mesenchymal transition, migration and metastasis and consequently how DG may play a role in the disease state but also contribute to the broader knowledge of how DG is modified and regulated (Losasso 2000, Sgambato et al 2007, Mitchell et al. 2013, Mathew et al. 2013, Leocadio et al. 2016).

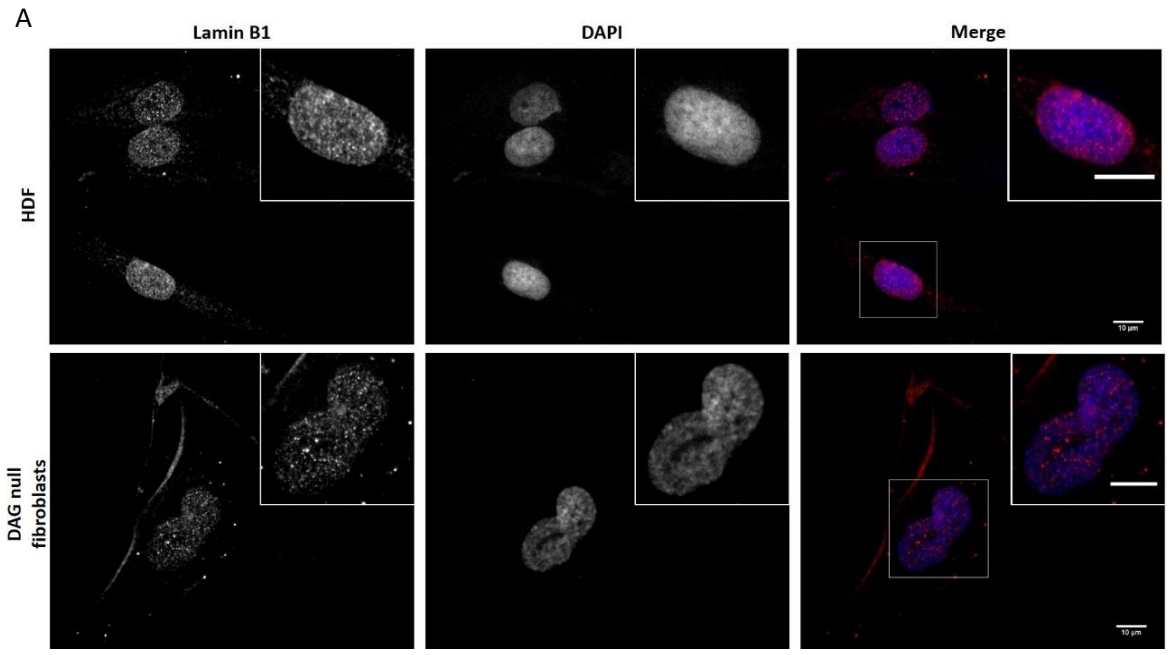

Figure 4.3: Lamin B1 and lamin A/C localisation in DAG null fibroblasts. HDF and DAG null fibroblasts were fixed and immunostained with lamin B1 (A) (above) or lamin A/C (B) (below) (red). Nuclei were counterstained with DAPI (blue). Inset are enlarged images of a representative nuclei (box, merge). Cells were imaged using widefield epifluorescence microscopy, 60x magnification, scale bar 10 µm

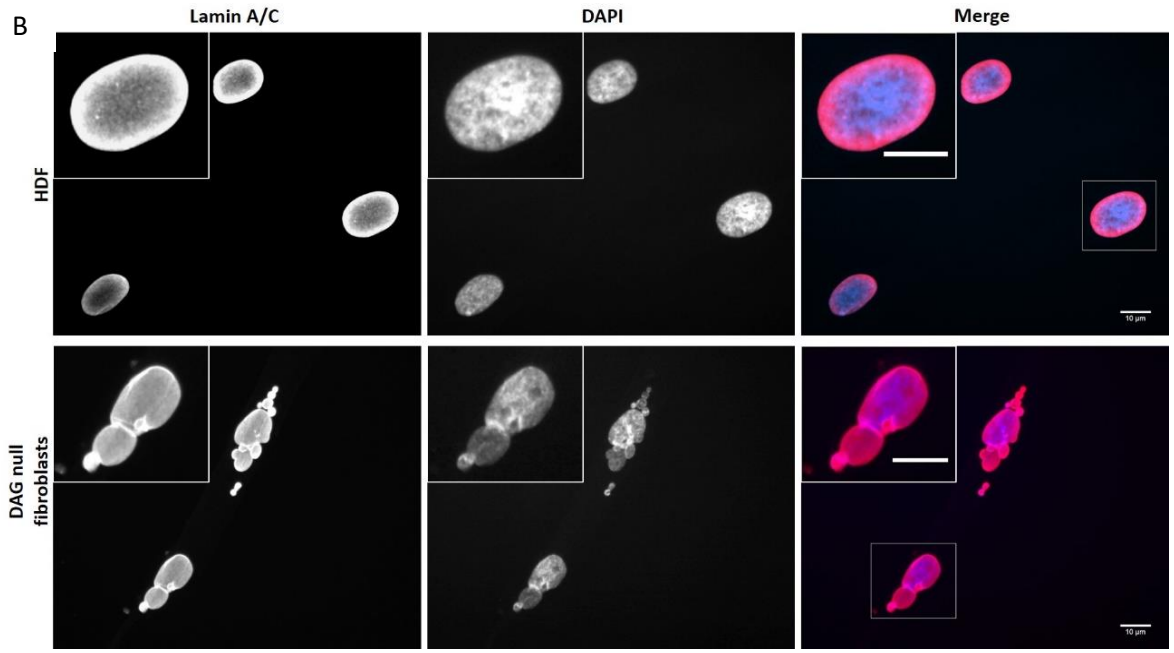

The nuclear localisation of βDG was characterised in the immortalised normal prostate epithelial cell line PNT1A and the metastatic prostate cancer cell lines PC3 and LNCaP. Whilst the focus of the research in this chapter is on nuclear βDG, further characterisation of βDG in these cell lines can be found in Chapter 3, sections 3.2.2 and 3.2.3. Biochemical fractionation and subsequent immunoblotting of PNT1A, LNCaP and PC3 cells detected full length 43 KDa βDG strongly in the non-nuclear fractions and more weakly in the nuclear fractions of all the cell lines (Fig 4.4). βDG was detected by antibodies against the non-phosphorylated and phosphorylated Y892 form of βDG. The level of nuclear βDG is variable and is strongest in the LNCaP cells. Whilst it is preferable to quantify the nuclear to non-nuclear ratio from the immunoblots this was not possible due to the detection of βDG bands in the non-nuclear fractions reaching saturation before the βDG in the nucleus is sufficiently detected. High molecular weight species of βDG at ~ 60 KDa and between 130-250 KDa can also be detected in the nuclear fraction with the pY892 βDG antibody (Fig 4.4). The high molecular weight species detected may be a modified form of βDG, for example, ubiquitination of βDG has been proposed (Miller et al. 2012, Leocadio 2014). Alternatively, the band between 130-250 KDa may represent an oligomerised form of βDG (Holt et al. 2000). As discussed in Chapter 3, mass spectrometry would be required to confirm these bands as βDG as 1709 can sometimes detect non-specific bands. The 31 and 26KDa fragments of βDG could occasionally be detected in both fractions but less in the nuclear fraction (Data not shown.) Although the markers of the non-nuclear and nuclear fractions are clean, to fully confirm the purity of the fraction and the nuclear localisation of βDG a marker of the ER, such as calnexin, should be included.

βDG localisation was also investigated via confocal immunofluorescence microscopy. Anti-βDG antibodies MDG2 and C20 were used as they give minimal background staining in immunofluorescence studies (Chapter 3). Confocal slices from the middle of the nucleus and MAX projections across the whole cell were used. MDG2 detects βDG faintly at the nuclear envelope in LNCaP, PC3 and PNT1A cells (Fig 4.5 White arrowhead). A diffuse nucleoplasmic as well as some brighter foci are detected within the nucleus. The nucleoplasmic stain is slightly stronger in the PNT1A cells compared to the LNCaP and PC3 cells (Fig 4.5 White arrowhead). βDG is also detected strongly at the PM, cell-cell junctions, cell protrusions and in the case of PC3 and some LNCaP cells in a perinuclear structure that is potentially the endoplasmic reticulum or golgi. C20 detects a distinctly different localisation of βDG in the nucleus. Whilst a faint nuclear envelope stain could sometimes be detected, C20 predominantly localised to the nucleoli in all three cell lines (Fig 4.6).

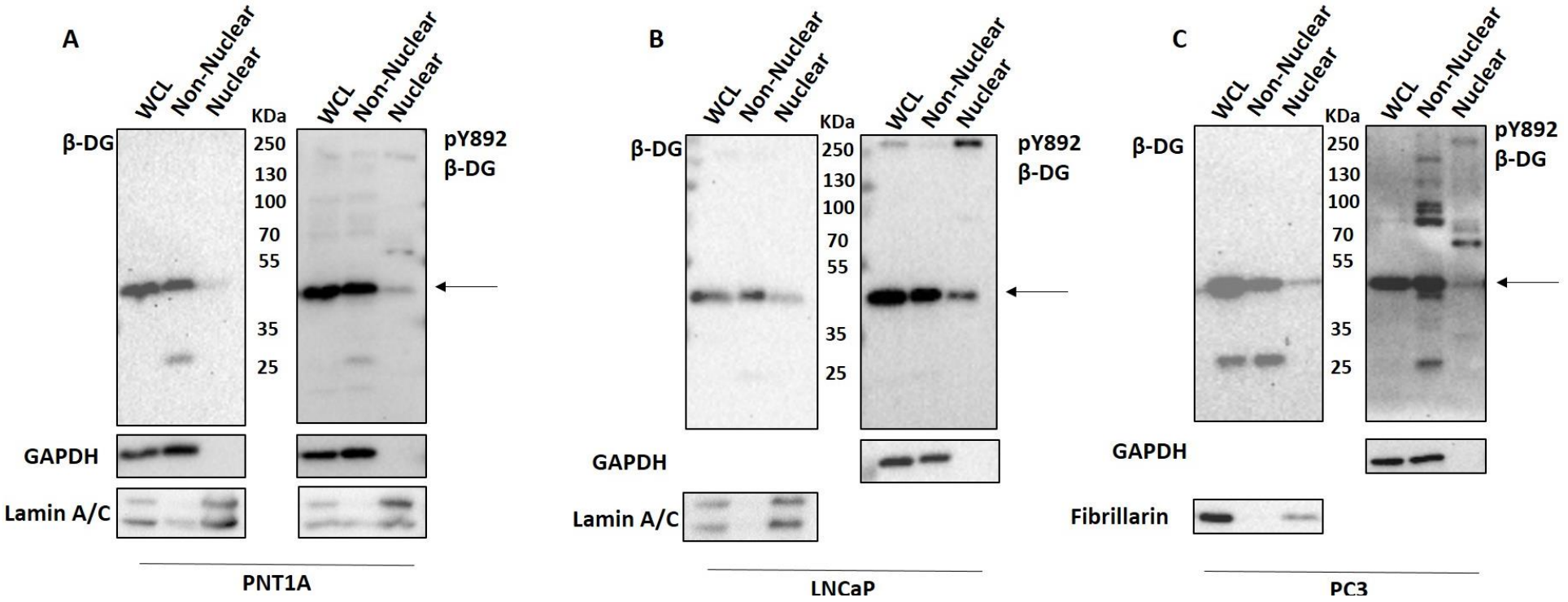

Figure 4.4 βDG is detected in the nucleus of prostate cell lines via immunoblotting. A) PNT1A, B) LNCaP and C) PC3 cells were harvested for whole cell lysate (WCL) or subject to biochemical fractions to separate non-nuclear and nuclear fractions. Samples were then immunoblotted for βDG (MDG2) and pY892 βDG (1709). Arrows indicate full length 43 kDa βDG. GAPDH and lamin A/C or fibrillarin were used as purity markers and loading controls of the non-nuclear and nuclear fractions respectively.

To further characterise the localisation of βDG at the nuclear envelope, LNCaP cells were coimmunostained for βDG (MDG2) and lamin B1. Confocal microscopy analysis shows that βDG and lamin B1 colocalise at the nuclear envelope (Fig 4.7 A). Moreover, in the orthogonal view of a cross-section of the nucleus, βDG colocalises with lamin B1 at the nuclear envelope at the top and along the depth of the nucleus (Fig 4.7 B). Interestingly βDG was often detected strongly on top of the nucleus in patches.

Combined these results agree with the growing number of reports showing that DG is found in the nucleus of prostate cell lines, both non-cancer and cancer derived. Moreover, βDG is found at multiple nuclear structures. The fact that the two antibodies detect different localisation and therefore potentially separate populations of βDG is interesting and could mean that PTM, differentially detected by the antibodies, could affect the nuclear localisation of βDG. Finally, these results indicate that LNCaP, PC3 and PNT1A can be used as model systems to investigate the regulation and role of βDG within the nucleus.

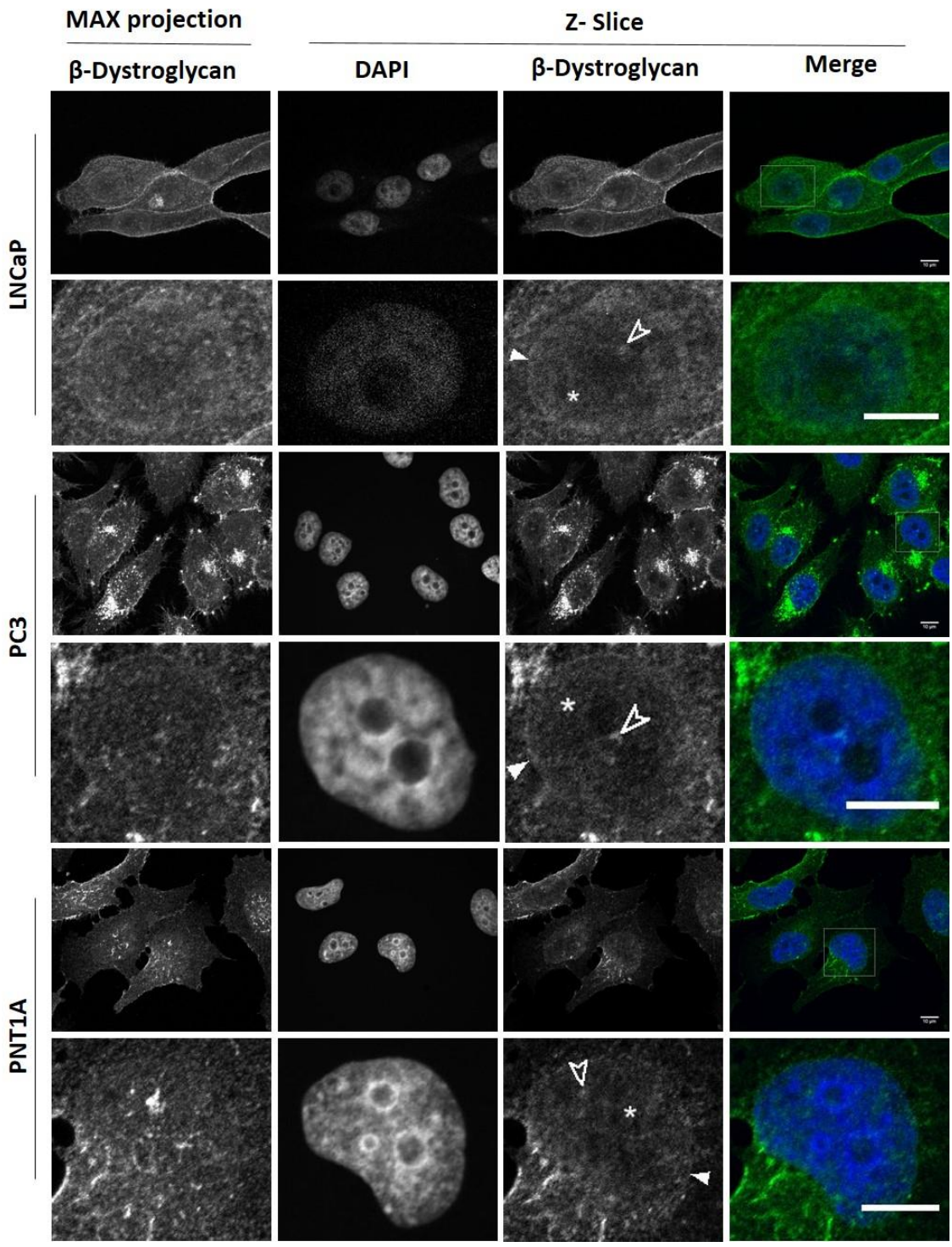

Figure 4.5: Confocal immunofluorescence microscopy localisation of βDG in prostate cell lines using anti-βDG antibody MDG2. LNCaP, PC3 and PNT1A cells were fixed and stained for βDG (MDG2) (Green) and the nuclei counterstained with DAPI (Blue). Representative images of a maximum projection of βDG staining and Z slices from the middle of the nucleus are presented. Enlarged images of the nucleus indicated in the merged image with a box. In the nucleus βDG is detected at the nuclear envelope (filled white arrowhead), nucleoplasm (*) and as strong foci (empty white arrow heads). Images were taken at 63x magnification. Scale bar 10µm.

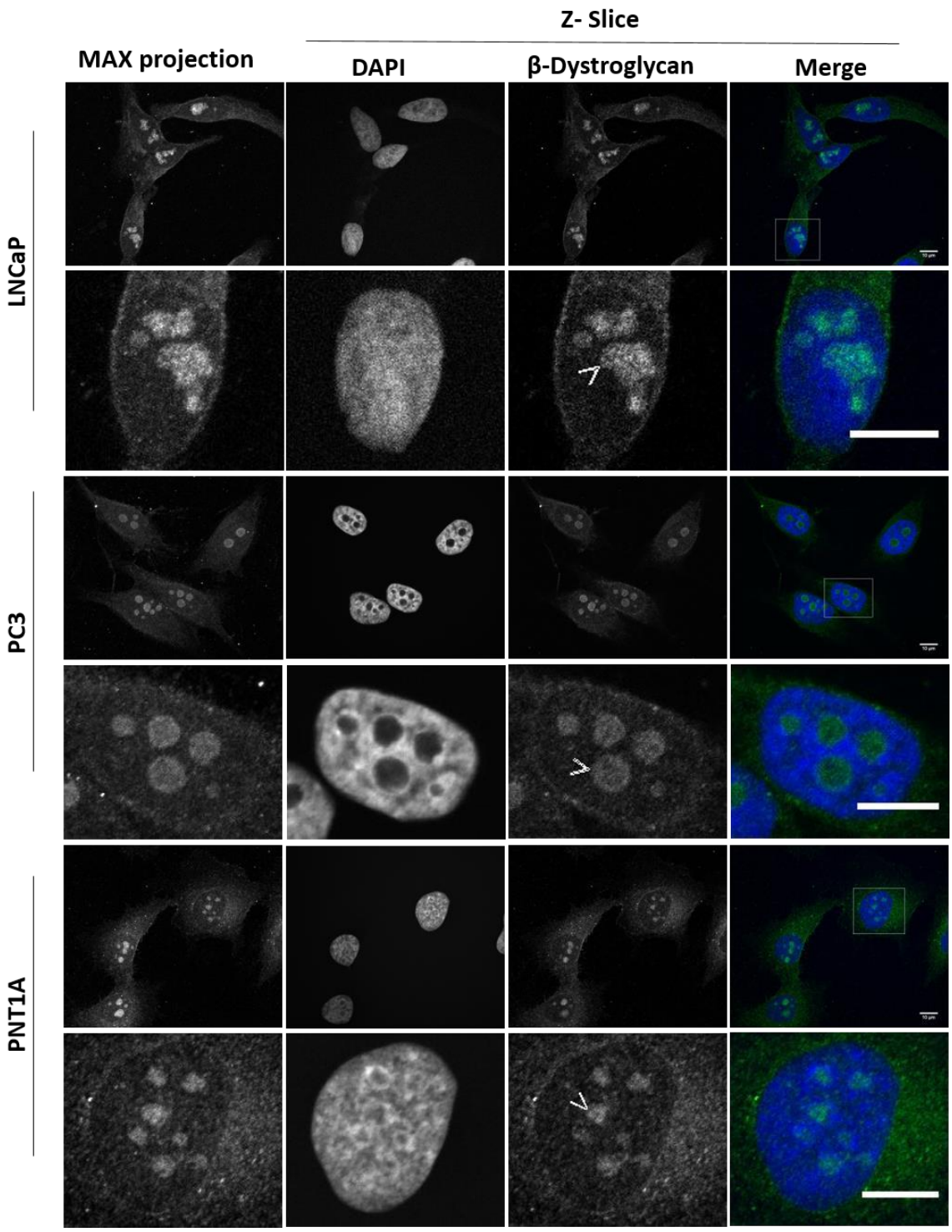

Figure 4.6: Confocal immunofluorescence microscopy localisation of βDG in prostate cell lines using antiβDG antibody C20. LNCaP, PC3 and PNT1A cells were fixed and stained for βDG (C20) (Green) and the nuclei counterstained with DAPI (Blue). Representative images of a maximum projection of βDG staining and Z slices from the middle of the nucleus are presented. Enlarged images of the nucleus indicated in the merged image with a box. In the nucleus βDG is detected faintly at the nuclear envelope and nucleoplasm and strongly in subnuclear compartments, likely the nucleoli (white arrow heads). Images were taken at 63x magnification. Scale bar 10µm.

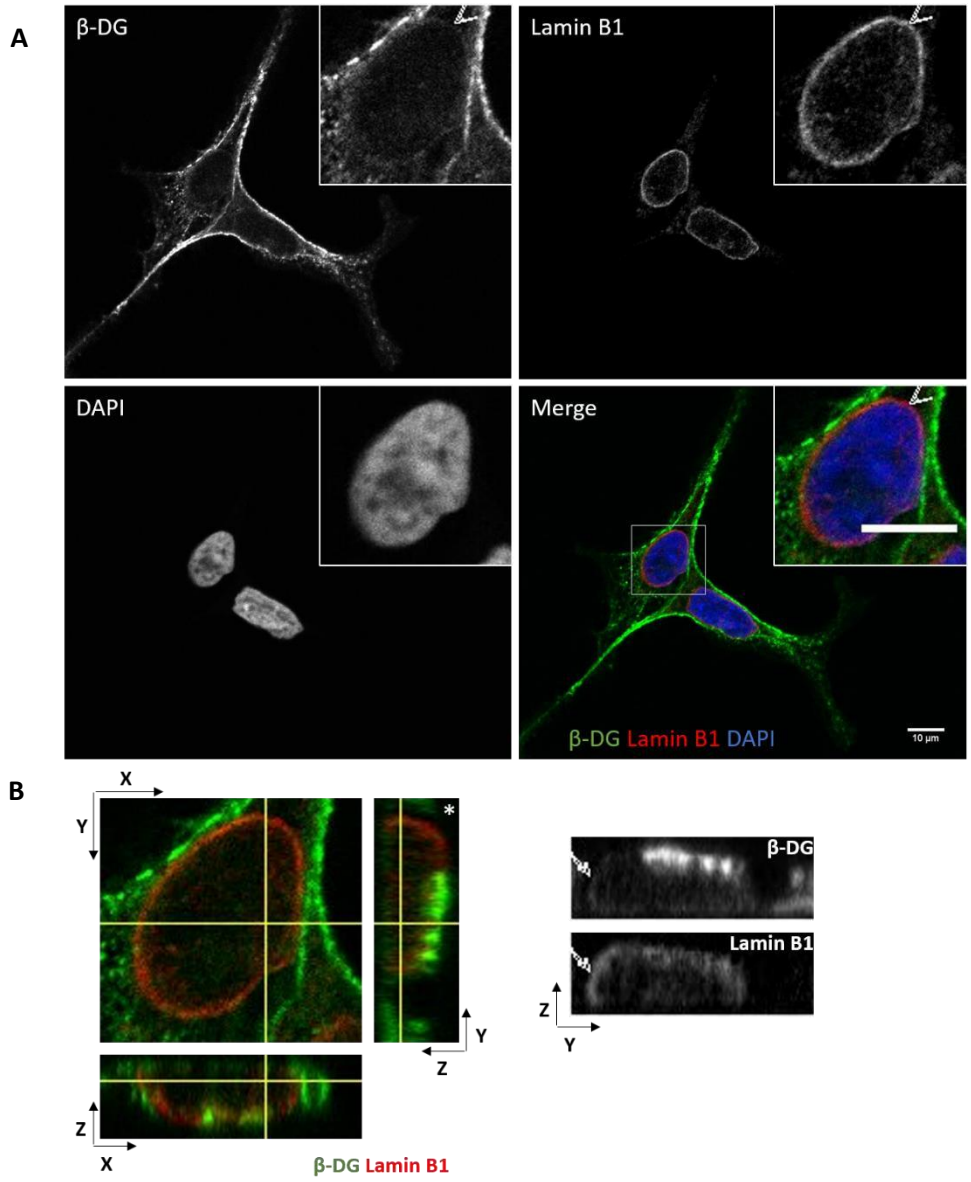

Figure 4.7. βDG and lamin B1 colocalise at the nuclear envelope in LNCaP cells. LNCaP cells were fixed and stained for βDG (MDG2) (green) and Lamin B1 (red). Nuclei were counterstained with DAPI (blue). Colocalisation of βDG and lamin B1 can be seen in Z-slices from the middle of the nucleus (A) and in orthogonal views of the stacked images (B). Images were taken at 63x magnification. Scale bar= 10µm.

4.2.4 FLAG TAGGED ALPHA-BETA DYSTROGLYCAN CAN BE DETECTED IN THE NUCLEUS OF LNCAP CELLS

In the study of a protein it is often useful to incorporate a tag. Among other uses, tags enable the purification and detection of a protein of interest. Previously in the Winder lab an internal flag tag has been incorporated into mouse full length αβDG (Leocadio 2014, Leocadio et al. 2016) because of concern that a C-terminal tag affects phosphorylation at Y892. A flag tag is a hydrophilic peptide consisting of eight residues, DYKDDDDK. The flag tag was inserted at residue 803 (Fig 4.8 A) (Leocadio et al. 2016), a site within the cytoplasmic domain of βDG, with few sites of interaction as predicted by ELM and C-terminal to the NLS (green box, Fig 4.8 A) (Gould et al. 2010). Sequence alignment also shows that the sequence of βDG at this site already contains a number of residues required for a flag tag and therefore required few changes to the original sequence of βDg (red box, Fig 4.8A).

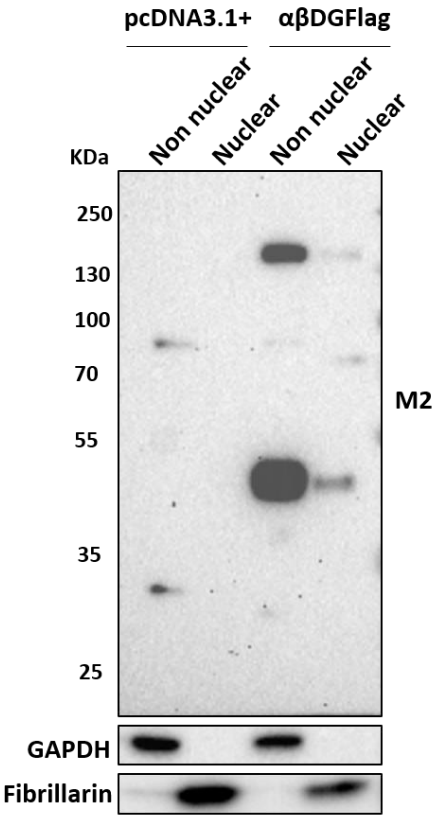

Figure 4.8. αβDGflag is detected in the nucleus of LNCaP cells. A) Sequence alignment of the original sequence of βDG and the sequence of αβDGflag. The flag tag (red residues) was inserted C-terminal to the NLS (green box and residues) of βDG in the cytoplasmic domain. Residues that were retained from the original sequence are denoted with an *. B) LNCaP cells transiently transfected with the control empty plasmid, PcDNA3.1+ or αβDGflag and grown for 24 hours. Cells were subject to biochemical fractionation and immunoblotted for anti-flag M2. GAPDH and Fibrillarin were used as purity/loading controls for the non-nuclear and nuclear fractions respectively.

αβDG flag expression in LNCaP cells has been characterised in detail elsewhere (Leocadio, 2014) and in section 4.2.9 below. LNCaP cells were transiently transfected with a plasmid containing αβDGflag, grown for 24 hours and then subject to biochemical fractionation. Importantly, whilst the majority of βDG is in the non-nuclear fraction, a full length band of βDG can be seen in the nuclear fraction when detected with M2 anti-flag antibody (Fig 4.8 B). Faint higher molecular weight bands can also be detected at 60-70 KDa and ~160 KDa in the nuclear fractions as was also detected by 1709 (Fig 4.4). As previously mentioned these high molecular weight species may be as a consequence of other post-translational modifications. It is also important to consider that the M2 antibody has previously been reported to detect native proteins in mammalian cells in addition to the exogenous FLAG tag (Schafer et al. 1995). The detection of native proteins may account for the bands detected in the lysates from the pcDNA3.1+ transfected cells, including a band at ~90 KDa, which can also be seen in the αβDGflag transfected lysate.

4.2.5 Investigating the phosphorylation of beta-dystroglycan

Phosphorylation at residues additional to Y892 may also regulate the localisation and function of βDG. To investigate the phosphorylated species of βDG, WCL from αβDGflag transfected LNCaP cells was run on a phostag gel and immunoblotted for M2 flag, βDG (MDG2) and pY892 βDG (1709). Phostag gels contain an acrylamide accessory which specifically binds to divalent phosphate groups via its two metal ions (Mn^{2+}) and thus retards the movement of the protein through the gel in SDS-PAGE (Kinoshita et al. 2005).

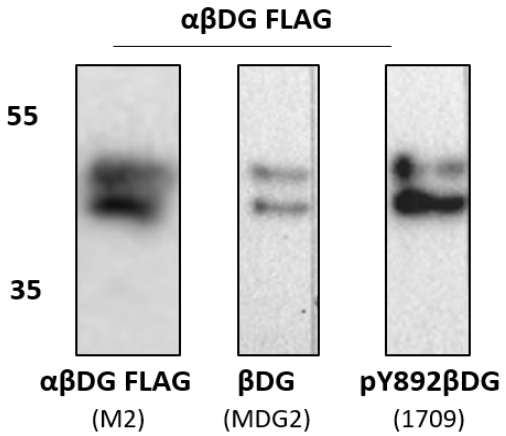

Figure 4.9. Full length αβDGflag resolves into two bands on a phostag gel. Total cell lysate was harvested from LNCaP cells transiently transfected with αβDGflag and grown for 24 hours. Lysate was run on a 20 µM phostag, 10% acrylamide gel and immunoblotted for flag (M2 antibody), βDG (MDG2 antibody) or pY892 βDG (1709 antibody). Two distinctly resolved bands were detected by each antibody.

The presence of two bands detected by each of the antibodies suggests the presence of phosphorylated species of βDG (Fig 4.9) 1709 and MDG2 are reporters of the phosphorylated and non-phosphorylated Y892 forms of βDG respectively (See Chapter 3) (Pereboev et al. 2001, Ilsley et al 2001, James et al. 2000), therefore the fact that both of

these antibodies detects two distinct bands suggests that βDG is also being phosphorylated at a site distinct from Y892. However, Fig 4.9 should be interpreted with caution as it does not include the necessary controls to confirm that the two bands are a result of phosphorylation. In order to confirm that the shift in band migration is due to phosphorylation the lysates should be treated with phosphatases to remove the phosphorylation and thus only one band should be detected on the phostag blot. Additionally, to determine that the two bands are not an artefact of the flag tagged protein, a control of non-transfected cells should have been included.

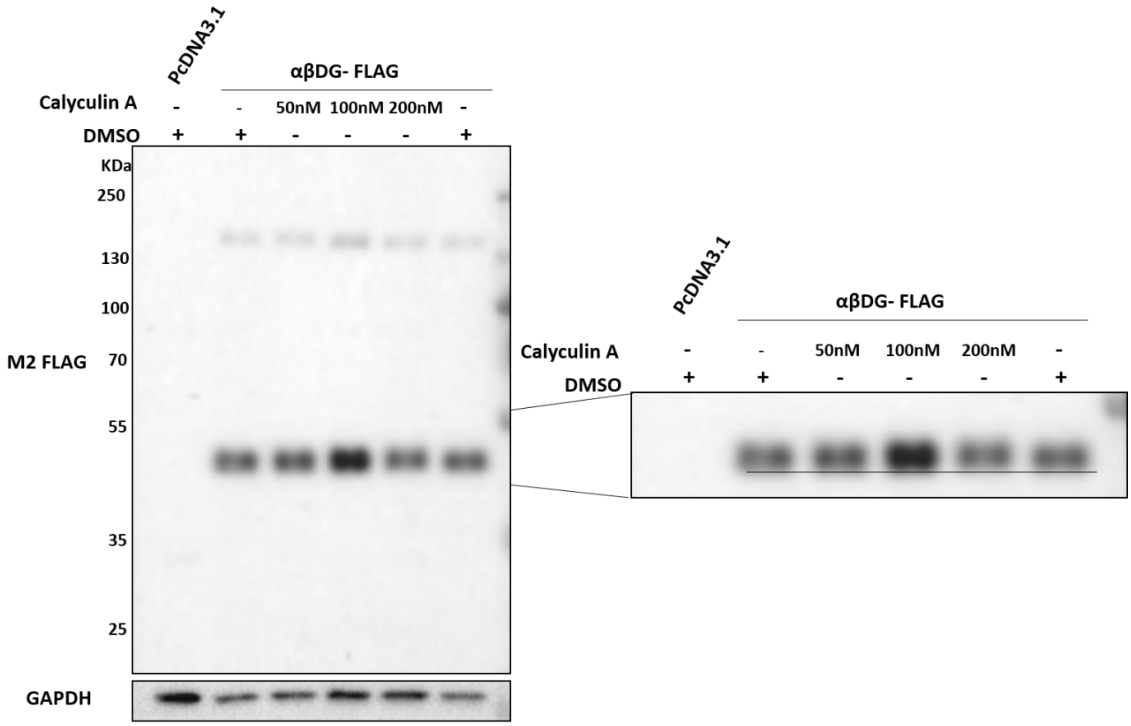

Figure 4.10. Calyculin A treatment of αβDGflag LNCaP cells. LNCaP cells transiently transfected with αβDGflag were grown for 24 hours and then incubated with either DMSO or Calyculin A at a final concentration of 50, 100 or 200nM Calyculin A for 20 minutes. Total cell lysates were then collected and immunoblotted for anti-flag M2. Empty vector PcDNA3.1 treated with DMSO was included as an antibody specificity control. Enlarged version with a straight line drawn for migration comparison. GAPDH was included as a loading control.

An alternative method to determine if a protein is phosphorylated is by treating with phosphatases or phosphatase inhibitors. When treated with increasing concentrations of Calyculin A, an inhibitor of serine/threonine phosphatases very little, if any, change was seen in the migration of full length βDG flag, as detected by M2 anti-flag, relative to the DMSO treated control (Fig 4.10). Whilst Fig 4.10 does not support the presence of phosphorylation of βDG at serine and threonine residues, it does not rule it out. It is possible that the small migration shift (~80 Da) caused by an altered phosphorylation state

of one or two residues would be too small to detect on a 12.5% acrylamide gel. If this experiment were to be repeated a detection method with increased sensitivity such as Phostag gels, should be used. It is also important to note that it not possible to determine from this experiment whether any detected mobility shift in a protein is direct phosphorylation at a serine or threonine residue or if the broad Calyculin A treatment is affecting an upstream signalling pathway that in turn modulates the phosphorylation at a Y, S or T residue.

4.2.6 Generation of alpha-beta DG flag T788A and T788D LNCaP transgenic lines

Multiple studies have shown that Y892 is not crucial for the nuclear localisation of βDG (Lara-Chacon et al. 2010, Leocadio 2014). Other sites of phosphorylation within βDG may regulate the nuclear localisation of βDG. In order to investigate the effect of phosphorylation at T788 on the localisation of βDG, site directed mutagenesis was used to substitute the threonine to an alanine or an aspartate to represent a non-phosphorylatable and phospho-mimetic form of T788 respectively (Fig 4.11). Alanine and Aspartate were chosen due to their relatively similar size and side chain structure to threonine, with aspartate containing the negatively charged side chain to mimic the negative phosphate group of phosphorylated threonine. The introduction of the mutations was confirmed by DNA sequencing (Appendix Fig B.1) and the plasmids purified for transfection into LNCaP cells.

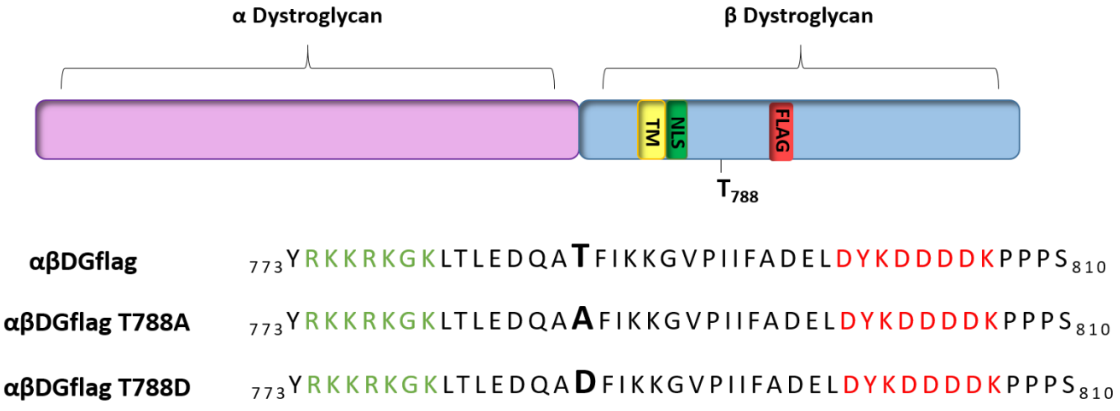

Figure 4.11. Schematic of mouse αβDGflag and the generation of a non-phosphorylatable and phospho-mimetic T788 flag tagged αβDG. Site directed mutagenesis of threonine 788 of mouse βDG to an alanine non-phosphorylatable (T788A) and an aspartate phospho-mimetic (T788D) form. Residue 788 is highlighted in bold. The transmembrane domain (TM) is depicted in yellow, Nuclear Localisation Signal (NLS) in green and the flag tag in red.

4.2.7 CHARACTERISATION OF ABDGFLAGT788A AND ADDGFLAGT788D LNCAP TRANSGENIC CELLS

The plasmids encoding αβDGflag, αβDGflagT788A and αβDGflagT788D were electroporated into LNCaP cells and grown for 48 hours. Immunoblot analysis with anti-flag M2 antibody detected a 43 KDa band representing full length βDG in all three of the flag transfected cell populations but not in the empty vector control (Fig 4.12 A). This demonstrates the specificity of the antibody and that recombinant protein at the right size is being expressed. Moreover, when WCL from LNCaP transiently transfected with wt, T788A and T788D αβDGflag was subject to immunoprecipitation with anti-flag M2 resin and immunoblotted with a rabbit anti-flag (rflag) antibody or with 1709 (pY892 βDG) a band at 43 KDa was detected in the flag construct transfected cells but not in the resin only or empty vector control lanes (Fig 4.12 B, C). The detection of both the T788A and T788D mutants of βDG by 1709 demonstrates that βDG can be phosphorylated at Y890 (mouse) regardless of the phosphorylation status of T788. To further verify the flag tagged recombinant protein being detected is βDG, immunoprecipitation with βDG antibodies followed by probing with anti-flag antibodies could be conducted. 1709 also detected the high molecular weight band between 130-250 KDa in all three of the flag construct expressing lysates (Fig 4.12 C). The 26 KDa and 32 KDa fragments of βDG were inconsistently detected in lysates from LNCaP cells expressing the αβDGflag wt, T788A and T788D constructs (Data not shown).

In order to investigate the phosphorylation of the mutated βDG constructs, the WCL of αβDGflag, αβDGflagT788A and αβDGflagT788D were run on a 20μM phostag gel and probed with anti-flag M2 (Fig 4.12 D). All three lysates still displayed two distinct bands between 35-55 KDa, however, as discussed for Fig 4.9, this experiment lacks the necessary controls to investigate if the separation of the bands is due to phosphorylation and should therefore be interpreted with caution. There is very little difference in the migration of the αβDGflagT788A, αβDGflagT788D and αβDGflag bands, nor is there a difference in the number of βDG bands present, suggesting that there has not been a change in the number of phosphorylation modifications on the constructs. However, it is not possible to conclude that this indicates that there has not been a change in the phosphorylation status of residue T788 in αβDGflag as compensatory phosphorylation events may have occurred in the two mutant constructs, which would prevent a shift on the Phostag gel. Further site specific analysis such as mass spectrometry and phospho site specific antibodies could be used to investigate phosphorylation at residue T788.

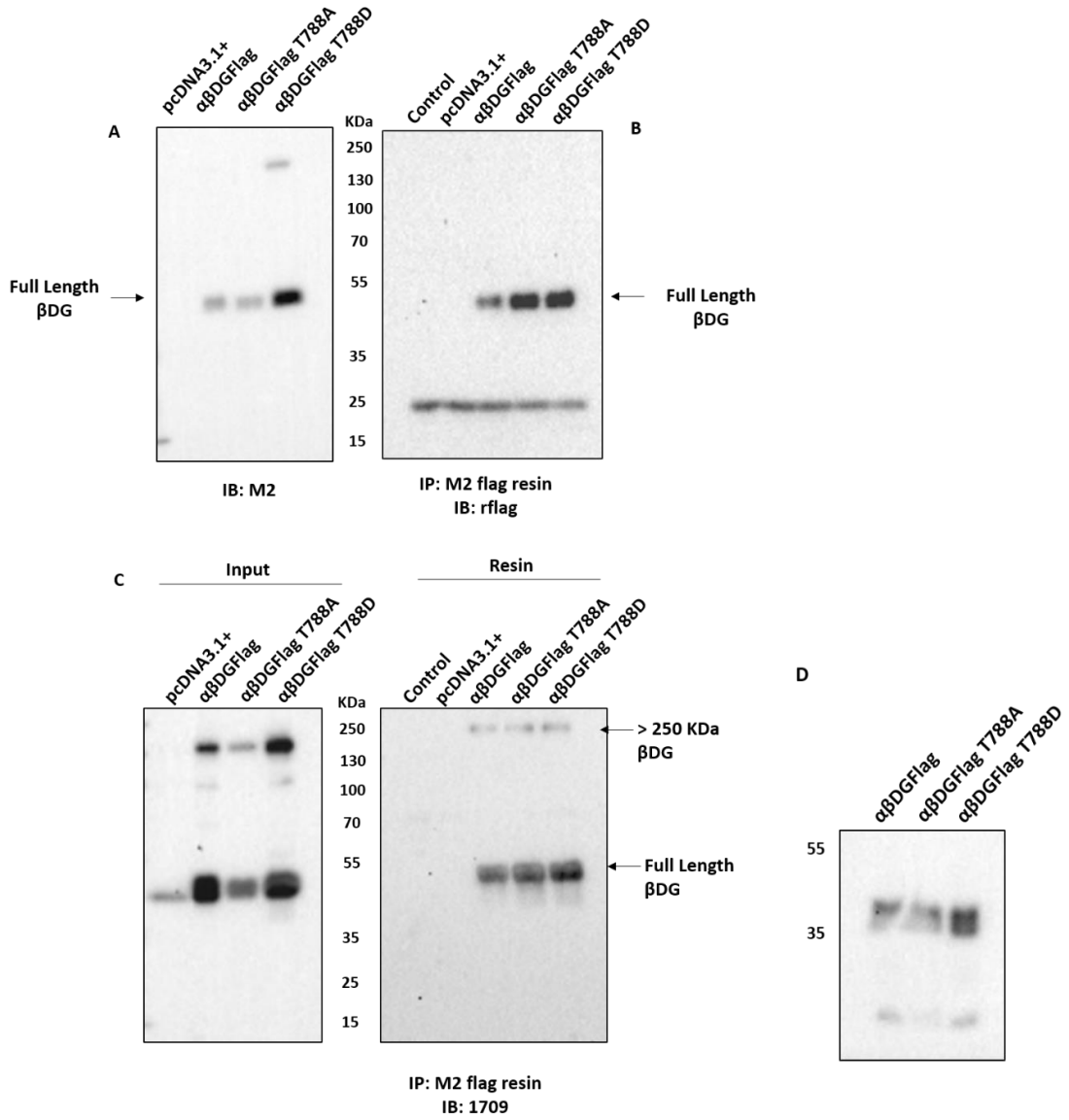

Figure 4.12. Characterisation of αβDGflag, αβDGflagT788A and αβDGflagT788D. LNCaP cells were transfected with pcDNA3.1+, αβDGflag, αβDGflagT788A or αβDGflagT788D and grown for 48 hours. Total cell lysates were harvested and immunoprecipitated with anti-flag M2 resin. A no lysate control was included in the immunoprecipitations. Total cell lysate (A), or M2 affinity resin with immunoprecipitated proteins (B) or both (C) were immunoblotted for M2 flag (A), rabbit flag (rflag) (B) or pY892 βDG (1709) (C). Full length and high molecular weight species of βDG are indicated with arrows. D. Total cell lysates of αβDGflag, αβDGflagT788A and αβDGflagT788D were run on a 20µm phostag gel and resolve as two distinct bands.

Confocal immunofluorescence microscopy analysis showed that αβDGflag, as detected by anti-flag M2, in LNCaP cells localised strongly to the plasma membrane and displayed punctate staining within the cytoplasm and very weakly in the nucleus (Fig 4.13). The αβDGflagT788A and αβDGflagT788D mutants also localise to the plasma membrane, cytoplasm and weakly to the nucleus. There is nucleoplasmic and brighter foci staining in the nucleus. These results suggest that, contrary to the mass spectrometry data, phosphorylation at T788 occurs not only in the nucleus of cells and it cannot be said from this data that it affects the nuclear localisation of βDG. None of the constructs demonstrate the same strong localisation to the nucleoli as detected by the C20 antibody (Fig 4.6) and is more reminiscent of MDG2 staining. All three flag constructs also colocalise with 1709 detection of pY892 βDG at the PM and within the cytoplasm of the cell (Fig 4.14) All three constructs, when detected with anti-flag M2, also contained populations that do not colocalise with 1709 and are therefore not phosphorylated at Y892 (Fig 4.14). It is important to remember that 1709 also detects proteins other than βDG in immunofluorescence studies (chapter 3). Given that these are transient transfections, not stable cell lines, the expression of the recombinant protein was variable and it is difficult to detect what might be subtle changes in βDG localisation. Whilst quantification of nuclear: cytoplasmic ratio of immunofluorescence images can be used to study the nuclear trafficking of proteins, in the case of βDG technical issues arise due to the fact that no one area within the cytoplasm, nucleus or confocal slice is representative to obtain an accurate average N:C ratio for a cell, for example due to strong staining at the PM and basal surfaces of the cell as well as variable staining of intracellular structures such as the golgi, vesicles and sub-nuclear structures. Whilst quantification of nuclear to non-nuclear ratios of βDG via immunofluorescence has been reported in the literature (Lara-Chacon et al. 2013) how the above concerns were resolved is unclear.

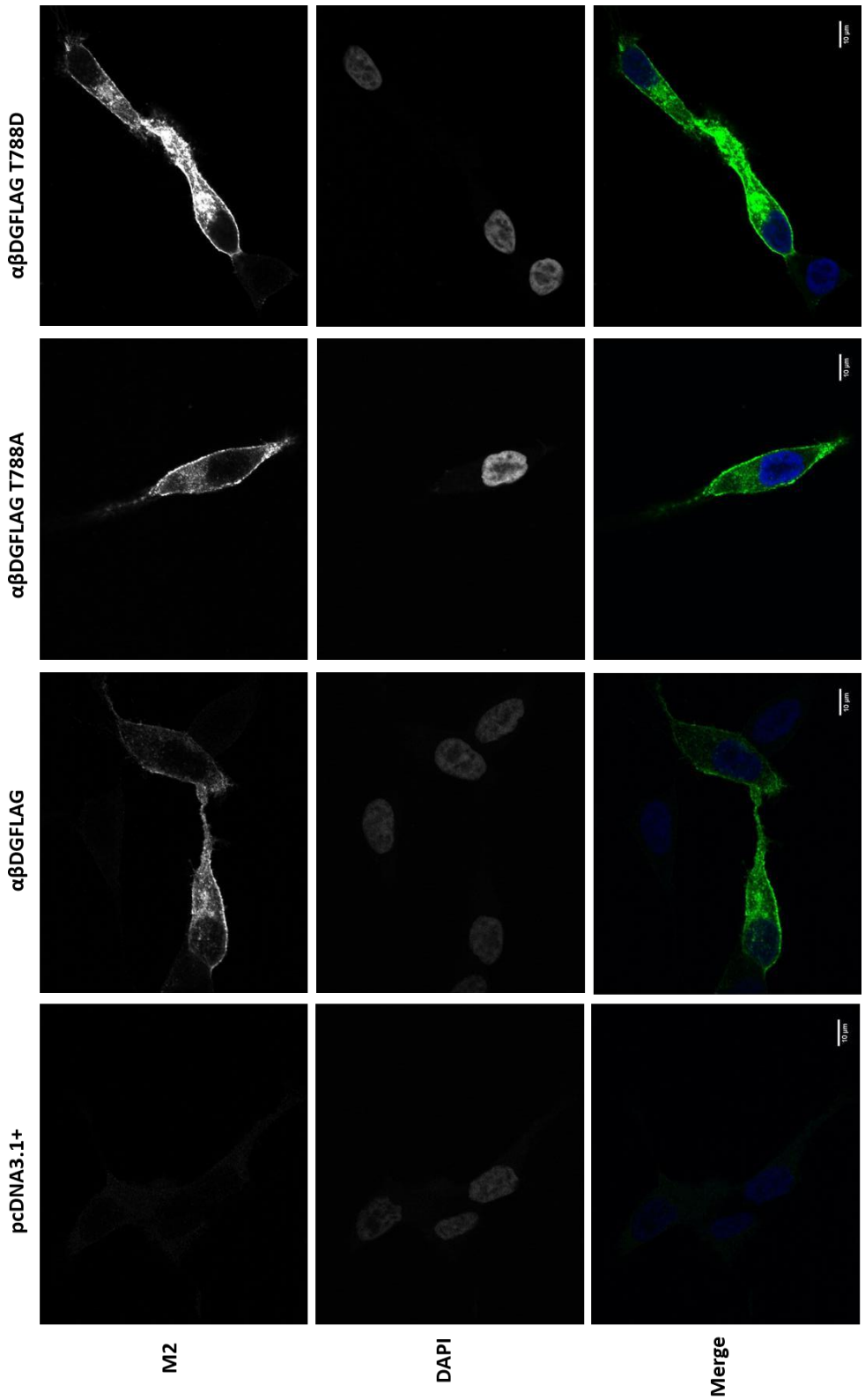

Figure 4.13. Characterisation of αβDGflag, αβDGflagT788A and αβDGflagT788D via immunofluorescence confocal microscopy. LNCaP cells were transfected with pcDNA3.1(+), αβDGflag, αβDGflagT788A or αβDGflagT788D and grown for 24 hours. Cells were fixed and immunostained with anti-flag M2 antibody (green) and the nuclei counterstained with DAPI (blue). All three flag constructs localise strongly at the plasma membrane, cytoplasm and very faintly in the nucleus. Exogenous protein occasionally accumulated in internal structures, presumably the golgi or ER. Images are Z slices taken from the middle of the nucleus. Images were taken at 60x magnification. Scale bar 10µm.

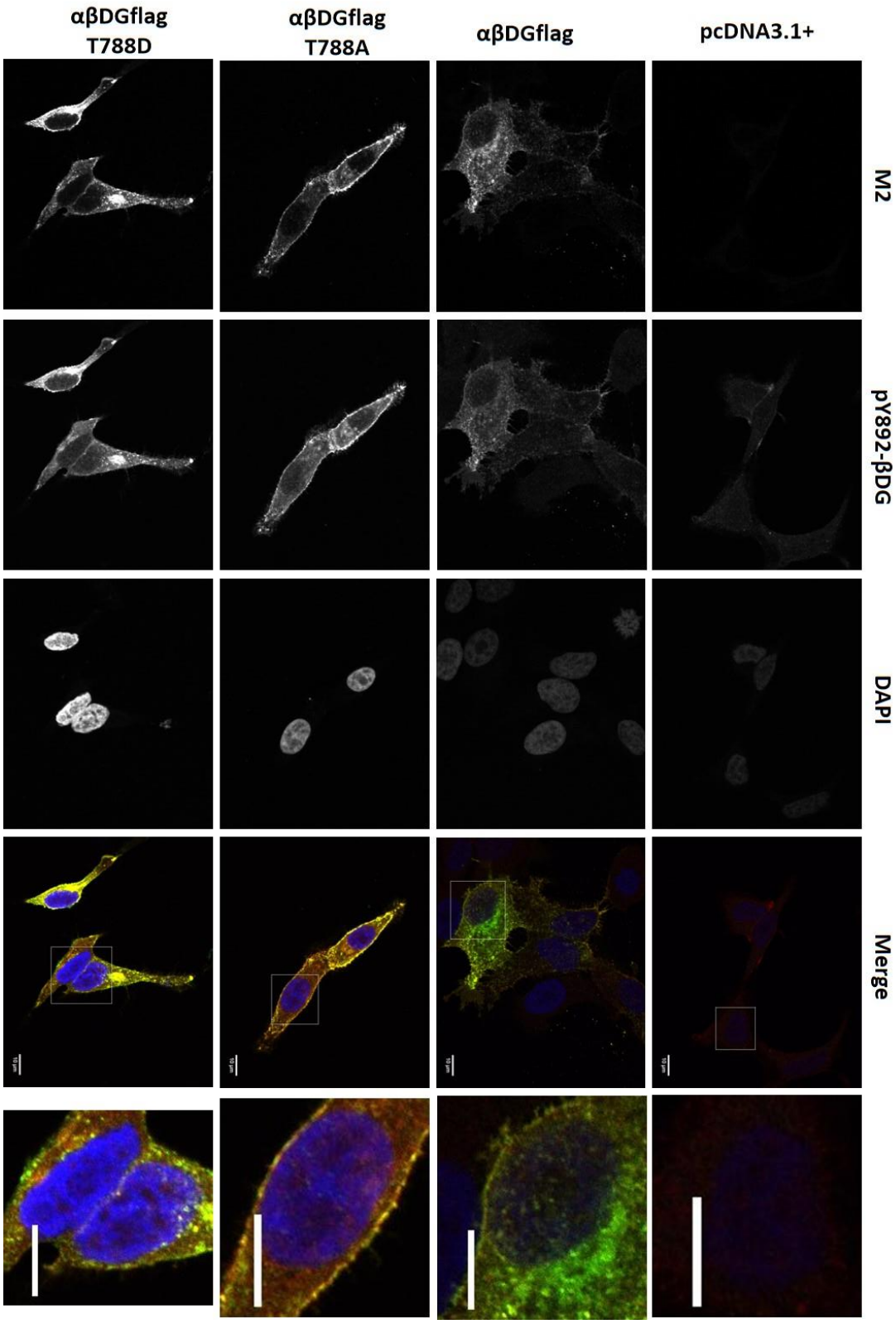

Figure 4.14 αβDGflag, αβDGflagT788A, αβDGflagT788D colocalisation with pY892 βDG. LNCaP cells were transfected with pcDNA3.1(+), αβDGflag, αβDGflagT788A or αβDGflagT788D and grown for 24 hours. Cells were fixed and immunostained with anti-flag M2 antibody (green), pY892 βDG (red) and the nuclei counterstained with DAPI (blue). A population of all 3 flag constructs colocalises with pY892 βDG at the plasma membrane, cytoplasm and the nucleus. Enlarged images of a nucleus (box, merge). Images are Z slices taken from the middle of the nucleus. Images were taken at 60x magnification. Scale bar 10µm.

Consequently, as an alternative method to investigate αβDGflag, αβDGflagT788A and αβDGflagT788D localisation, LNCaP cells were subject to biochemical fractionation 24 hours after transfection and immunoblotted with anti-flag M2 (Fig 4.15). All three forms of flag recombinant protein could be detected in the nuclear fraction at 43 KDa, though it was strongest detected in the non-nuclear fractions. The band between 130-250 KDa could be detected variably in the nuclear and strongly in the non-nuclear fractions. The 31 and 26 KDa fragments of βDG were only detected in the nonnuclear fractions (Fig 4.15). The loading of non-nuclear and nuclear sample is 20ug of the total protein, rather than proportional which would better suit the quantification of a nuclear: non-nuclear ratio. However quantification of the nuclear: non-nuclear ratio has been attempted taking into account the volumes of each sample loaded on the SDS-PAGE gels as well as the approximate total volumes of the nuclear and non-nuclear fractions. It should be noted that this quantification comes with a number of caveats, for example the total volumes of the cytoplasmic and nuclear fractionation are approximate due to potential loss of sample in the fractionation process, such as sonication. Nonetheless the quantification provides an indication as to the levels of FLAG-tagged βDG in the nucleus relative to the rest of the cell and therefore if this is altered by the phospho-null or phospho mimetic mutation at T788. Whilst the average of the four repeats indicates a marginally higher nuclear: non-nuclear ratio in both the αβDGflag T788A (0.29± 0.12) and αβDGflag T788D (0.27± 0.05) transfected cells compared to wt αβDGflag (0.22± 0.08) it is important to note that there is considerable variability in the nuclear: non-nuclear ratio in each of the individual replicates. Statistical significance cannot be tested as the number of replicates (4) is not enough to provide power in the non-parametric test to be used given the non-normal distribution of the data. To ensure that the nuclear fraction is not contaminated, future fractionation experiments should contain a marker of the ER such as calnexin. It is also important to take into account potential differences in the transfection efficiency and protein stability of each construct on the quantification of nuclear: non-nuclear ratio (see section 4.2.10).

Together these results do not demonstrate a clear role for phosphorylation of T788 in the nuclear localisation of βDG. Both the non-phosphorylatable and phospho mimetic versions of αβDGflag at T788 could be found at the plasma membrane, cytoplasm and nucleus at variable levels. This does not exclude the possibility, however, that phosphorylation at T788 is important for a nuclear function of βDG that has not been investigated in the time frame of this project. It is also important to note that an aspartate mutation does not have the same structure and properties as true phosphorylation and may therefore not be sufficient to accurately mimic the biological roles of the post-translational modification.

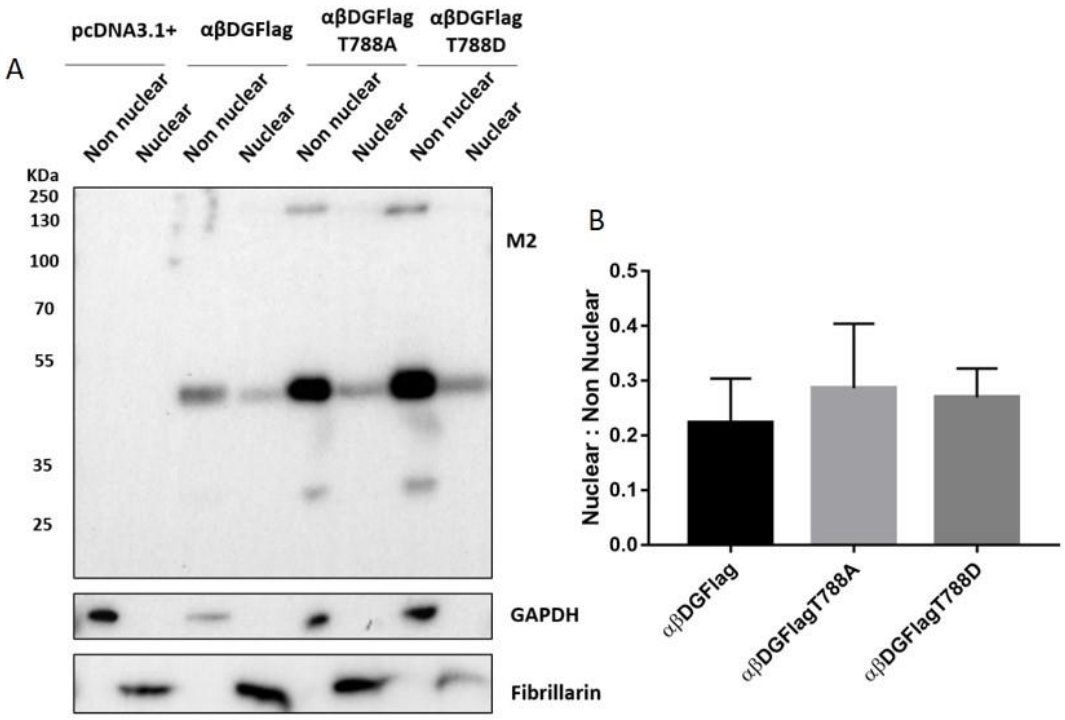

Figure 4.15. αβDGflag, αβDGflagT788A and αβDGflagT788D are all detected in the nucleus of LNCaP cells. A) LNCaP cells were transfected with pcDNA3.1+, αβDGflag, αβDGflagT788A or αβDGflagT788D and grown for 24 hours prior to biochemical fractionation. Non-nuclear and nuclear fractions were immunoblotted with anti-flag M2 antibody. Full length 43KDa βDG can be seen in the nuclear fraction of each sample. GAPDH and Fibrillarin were included as loading controls of the non-nuclear and nuclear fractions respectively. B) Quantification of the mean nuclear: non-nuclear ratios of full length 43KDa βDG of αβDGflag, αβDGflagT788A or αβDGflagT788D samples. The intensity of the bands was detected by densitometric analysis and divided by the volume of sample loaded. The intensity of the non-nuclear sample was adjusted to take in to account the 4:1 ratio of the total volumes of the non-nuclear and nuclear samples. The nuclear: non-nuclear ratio was then calculated. Error bars represent S.E.M. N=4.

4.2.8 THE STABILITY OF RECOMBINANT ABDGFLAG, ABDGFLAGT788A AND ABDGFLAGT788D

Whilst characterising the αβDGflag recombinant proteins it was observed that the turnover of αβDGflag was very rapid. The protein level at 48 hours post transfection, as quantified from immunoblots, was approximately a fifth of the level that was expressed at 24 hours post transfection and almost gone by 96 hours post transfection (Fig 4.16). Although transfection levels vary, this trend in rapidly reducing levels of protein expression was seen through a variety of immunoblot and immunofluorescence experiments (Data not shown). The

αβDGflagT788D mutant however appeared to be expressed at a higher level at these later time points. These experiments were all conducted in cells transiently transfected with the flag tagged βDG constructs, and although the differing levels of protein could be a consequence of differing transfection efficiency or protein expression, an alternative hypothesis is that phosphorylation, or at least the phosphomimetic mutation at T788 confers stability to βDG protein.

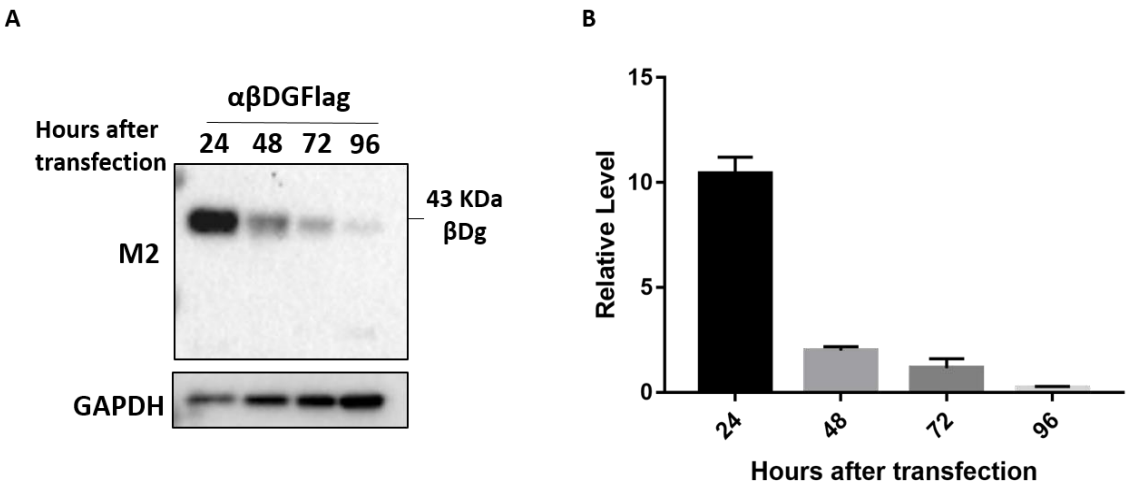

Figure 4.16. Expression profile of αβDGflag over a timecourse. LNCaP cells were transfected with αβDGflag and total cell lysates harvested at 24, 48, 72 and 96 hours post-transfection. (A) Lysates were immunoblotted for M2 flag. Full length, 43KDa βDG is indicated. GAPDH was included as a loading control. (B) Quantification of the level of 43 KDa βDG relative to GAPDH by densitometric analysis. N=3. Error bars = S.D.

To investigate this hypothesis LNCaP cells were transfected with αβDGflag, αβDGflagT788A or αβDGflagT788D, grown for 24 hours and then treated with cycloheximide (CHX), an inhibitor of translation elongation, to prevent protein synthesis. WCL were then collected at 0, 6, 12 and 24 hours post cycloheximide treatment and subject to immunoblot and detection by anti-flag M2 (Fig 4.17 A). The level of full-length βDG was normalised to the actin control and calculated as a percentage of the level of normalised βDG at 0hr of cycloheximide treatment (24 hours post transfection) (Fig 4.17 B-C). Whilst the αβDGflagT788A protein level was similar to that of αβDGflag across the time course, the phospho mimetic T788D mutant showed a trend of increased stability, though the levels were more variable (Fig 4.17 B-C). Pairwise comparisons of the levels of each flag construct 24 hours post CHX treatment by the non-parametric Mann-Whitney U test did not detect a statistically significant difference. The band between 130-250 KDa also rapidly reduced in all three flag tagged recombinant proteins after 6 hours of cycloheximide treatment suggesting

that it is rapidly processed or degraded. These data could be affected by potentially variable transfection efficiency between the wells, further experiments in cell lines stably expressing the constructs would validate if the stability of βDG can be regulated by T788 phosphorylation.

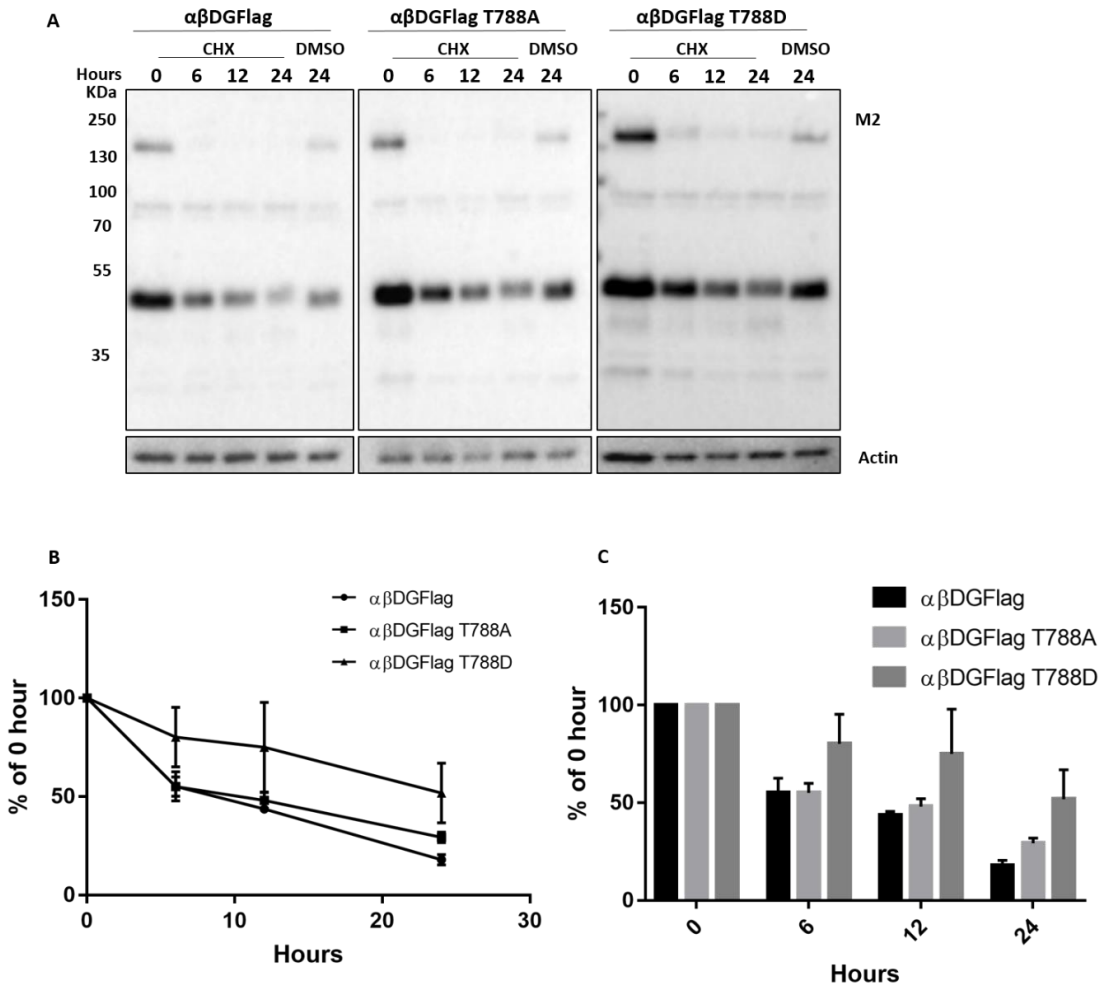

Figure 4.17. Cycloheximide pulse chase analysis of αβDGflag, αβDGflagT788A and αβDGflagT788D stability.

LNCaP cells were transfected with αβDGflag, αβDGflagT788A and αβDGflagT788D and grown for 24 hours. At 24 hours post-transfection cells were treated with 100µg/ml cycloheximide (CHX) or a DMSO control. Lysates were collected at 0, 6, 12 and 24 hours after treatment of CHX. The DMSO treated sample was collected at 24 hours post treatment. (A) Lysates were immunoblotted for M2 flag. Actin was included as a loading control. The level of 43KDa βDG was normalised to the actin loading control and then the expression calculated as a percentage of the expression at 0 hours of CHX treatment. Quantification displayed as a (B) a line chart and (C) a bar chart N=3. Error bars= S.E.M.

4.3 DISCUSSION

4.3.1 NUCLEAR MORPHOLOGY IS DISRUPTED IN DAG NULL PRIMARY FIBROBLASTS

The roles of DG in the nucleus are not fully understood, however dystroglycan has been reported to play a role in maintaining nuclear architecture and organisation (Lara-Chacon et al. 2013). The DAG null fibroblasts obtained from a patient with Walker-Warburg syndrome (Riemersma et al. 2015) were used to assess nuclear morphology in the absence of α and βDG.

The absence of βDG in the patient cells has been confirmed in this study via immunoblot with two separate anti- βDG antibodies (Fig 4.2Ai). The absence of alternative splice variants was confirmed via reverse transcription PCR of the DAG null fibroblast mRNA in the initial characterisation of the cells, moreover, lack of functional α- and βDG in the DAG null fibroblasts was confirmed via western blot and by lack of signal detected in a laminin overlay (Riemersma et al. 2015). It should be noted that re-expression of DG in the DAG null fibroblasts would be a more suitable control as the cells would then be known to be of the same origin and ages as opposed to non-isogenic HDF cells.

Immunofluorescence analysis and subsequent quantification of 'abnormal' nuclear morphology of HDF control fibroblasts and DAG null fibroblasts and showed that dramatically more DAG null fibroblasts displayed a disrupted nuclear morphology compared to the control cells (Fig 4.2 A-K). The aberrant nuclear morphology in the DAG null fibroblasts was diverse, with nuclei showing irregular shapes, blebbing, twisting, micronuclei and multiple nuclei (Fig 4.2 A-K). This is consistent with the hypothesis that DG is important for maintaining nuclear morphology and supports a previous report in which RNAi partial knockdown of DG in C2C12 myoblast cells resulted in a six-fold increase in aberrant nuclear morphology, with aberrant nuclei being irregular blebbed shape or 2-fold larger or smaller (Lara-Chacon et al. 2010).

The complex functions of βDG are facilitated in part by its inclusion in multiprotein complexes and its interaction with a plethora of protein binding partners (Moore et al. 2010). It has previously been demonstrated by electron microscopy that βDG localises to the inner nuclear membrane whilst immunoprecipitation and pull down assays show that βDG associates with structural components of the nuclear envelope such as emerin, lamin A/C and lamin B1 (Lara-Chacon et al. 2013). The colocalisation of βDG with lamin B1 in LNCaP cells is consistent with this (Fig 4.17). Moreover, in C2C12 cells depleted for βDG by RNAi the localisation of lamin B1 and emerin but not lamin A/C to the nuclear envelope was disrupted and their stability was reduced (Martinez- Vieyra et al. 2013). In support of this lamin B1 but not lamin A/C staining looks to be slightly reduced and disrupted in DAG null fibroblasts (Fig 4.3). Martinez-Vieyra et

al have proposed a model in which βDG targets emerin to the nuclear envelope whereby it interacts with lamin B1 promoting their stability and also associating with lamin A/C. Interestingly, C2C12 cells depleted for α-dystrobrevin, which also interacts with lamin B1, resulted in a reduction of other DAPC components in the nucleus and 45% of the nuclei displayed an irregular morphology, including blebbing (Aguilar et al. 2015). Nuclear blebs are protrusions from the nuclear surface that are rich in A type lamins and are regions in which the fibres of the lamin meshwork display a greater degree of separation (Prokocimer et al. 2009, Funkhouser et al. 2013). When B-type lamins are depleted, the lamins begin to segregate from one another and form an uneven network and subsequent blebbing of the nuclear envelope (Funkhouser et al. 2013). It is therefore possible that βDG contributes to the maintenance of the nuclear morphology through its interactions with the nuclear lamina, potentially as part of a nuclear DAPC. Future work elucidating the composition of a nuclear DAPC and its interactions with the nuclear lamina warrants further investigation.

A small number of DAG null cells had multiple nuclei or micronuclei (Fig 4.2 H, I). Multiple nuclei can arise from issues with segregation of the two daughter cells following cell division. Micronuclei are formed as a consequence of improper segregation of chromosomes during mitosis with a segment or whole chromosome remaining separate from the other chromosomes and is eventually encased in its own nuclear envelope during telophase, separate from the main nucleus (Luzhna et al. 2013). DG depletion delays cell cycle progression (Sgambato et al. 2006, Higginson et al. 2008, Villarreal-Silva et al. 2010) and also plays a mechanical role in the contractile ring and tethering the plasma membrane to the cytoskeleton during cytokinesis. (Higginson et al., 2008). Nuclear morphology defects were not reported during the study of cytokinesis in the DG knockdown cells (Higginson et al., 2008), however, given the interaction of DG with a number of its structural components it would be interesting to investigate if βDG affects nuclear membrane assembly following mitosis in more detail, for example through microscopy of live cells in mitosis.

There is preliminary evidence that βDG can interact with SUN1, a component of the LINC complex in the inner nuclear membrane (personal communication M. Laredo and S. Winder). Sun proteins in the inner nuclear membrane bind to emerin and A-type lamins, but not B-type lamins (Haque et al. 2006). When lamin A/C is depleted SUN1 remains localised to the nuclear envelope with a few nuclei displaying disrupted localisation at the nuclear poles, therefore suggesting the presence of other factors anchoring SUN1 in the INM (Haque et al. 2010). The LINC complex has important roles in regulating nuclear shape and position (Razafsky et al. 2009). An interesting line for future work is to investigate an interaction between βDG and

SUN proteins, which are components of two key mechanical and structural complexes and the implications for this on the structure of the nucleus.

The importance of lamins and components of the LINC complex in nuclear morphology are clear when looking at diseases that affect the nuclear envelope. Laminopathies are a large group of diseases caused by mutations in lamins, which can deplete the amount of lamin or perturb their interactions with binding partners such as SUN1 and Emerin and result in aberrant nuclei. Laminopathy patients display a large array of clinical symptoms including muscular dystrophy and neuropathy (Worman, 2012). Further examples of diseases caused by mutations in NE proteins include Hutchinson-Gilford progeria syndrome (HGPS) (Chen et al. 2014) and Emery-Dreifuss muscular dystrophy (EDMD) (Holt et al. 2003), where loss of lamin A/C or emerin cause abnormalities in the nuclear envelope and nuclear morphology. Given the apparent emerging roles of DG in nuclear architecture and the fact that DG is a component of the DAPC, a complex in which mutations often result in muscular dystrophies, it would be interesting to investigate nuclear DG in the context of laminopathies and other muscular dystrophies. Indeed, it is important to consider that the DAG null fibroblasts came from a patient with Walker-Warburg syndrome and if the apparent nuclear defects may have contributed to the disease symptoms.

From this analysis it is not possible to separate the roles of DG at the plasma membrane or cytoplasm from DG in the nucleus on the nuclear phenotype. Therefore, it must be considered that lack of DG at the plasma membrane could contribute to the aberrant nuclear morphology as a consequence of disrupted signalling pathways or cytoskeletal interactions. Both actin and microtubules can affect nuclear morphology, furthermore both are important in cell polarity and migration and subsequently nuclear positioning (Martins et al. 2012). In DG knockdown cells there are no reported gross changes in the cytoskeletal organisation, although when overexpressed it can bundle F-actin (Chen et al. 2003). To test the role of non-nuclear βDG on nuclear morphology via the cytoskeleton, βDG knockdown cells could be treated with cytoskeletal disruptors such as cytochalasin or nocodazole to see if the nuclear morphology is altered. Alternatively, βDG with a functional or mutated NLS could be re-expressed in DAG null cells to assess if either restores the nuclear phenotype.

4.3.2 CHARACTERISATION OF THE NUCLEAR LOCALISATION OF ENDOGENOUS βDG IN PROSTATE CELL LINES

The localisation of βDG to the nucleus in normal and cancerous prostate tissue and cell lines has been reported in multiple studies (Mitchell et al. 2013, Mathew et al. 2013, Leocadio et al. 2016). Here we show that βDG is in the nucleus of multiple prostate cell lines; the immortalised normal prostate epithelia line PNT1a and the metastatic prostate cancer lines LNCaP and PC3 by biochemical fractionation (Fig 4.4) and immunofluorescence microscopy (Fig 4.5, Fig 4.6), in agreement with the previously published literature.

The localisation of DG in prostate epithelia is well characterised. In benign prostate epithelia there is strong localisation of βDG at the intercellular junctions between luminal cells, basal cells and at the site of basal cell attachment to the basement junction (Sgambato et al, 2007, Mitchell et al 2013, Mathew et al. 2013). In prostate tumour cells α and βDG levels are reduced at the plasma membrane in correlation with disease progression but is re-expressed at metastatic sites (Mitchell et al, 2013, Sgambato et al, 2007, Sgambato et al 2003). As previously discussed, there is an increasing body of work investigating the mechanisms of βDG regulation in normal and prostate tissue which have identified a plethora of PTM contribution to the regulation of βDG and how these processes may be aberrant in epithelial cancers including hypoglycosylation, phosphorylation and proteolytic cleavage (Sgambato et al. 2007, Sgambato et al. 2010, Mitchell et al 2013, Mathew et al. 2013, Leocadio et al. 2016, Bao et al 2010).

The profile of both phosphorylated and non-phosphorylated Y892 βDG was examined in LNCaP, PC3 and PNT1A cells following biochemical fractionation (Fig 4.4). Full length βDG, both phosphorylated and non-phosphorylated, was found in the nuclear and non-nuclear fractions of the cell lines investigated. In addition to full length βDG, high molecular weight species at 60 and 130-250 KDa of the Y892 phosphorylated form of βDG were sometimes detected in the nucleus as well as fragments of βDG and pY892 βDG at 31 and 26KDa, all of which have been previously reported in the literature (Losasso et al. 2008, Mitchell et al. 2013, Mathew et al. 2013, Leocadio et al. 2016).

The higher molecular weight species indicate the presence of post-translational modifications on βDG, one candidate for which is ubiquitination. As previously discussed mass spectrometry analysis (Lee et al. 2011), MG132 treatment and pull down by a high- affinity specific ubiquitin binding resin, MultiDsk (Leocadio, 2014, Miller et al. 2012) have all provided evidence for DG ubiquitination. The presence of these high mw species in the nucleus, although needing further verification as ubiquitinated species, may suggest that following its roles within the

nucleus, βDG could be ubiquitinated and degraded by the nuclear ubiquitin proteasome or be ubiquitinated and exported to be degraded in the cytoplasmic proteasome. This hypothesis could be tested using nuclear import and export inhibitors combined with Multidsk and inhibitors of the proteasome such as MG132.

The presence, production and role of the cleavage fragments of βDG in the plasma membrane, nucleus and in prostate cancer progression have been addressed in multiple studies from the Winder lab and others (Singh et al. 2004, Lossasso et al. 2008, Sgambato et al. 2003, Yamada et al. 2001, Mitchell et al. 2013, Mathew et al. 2013, Leocadio et al. 2016). Increased proteolytic cleavage of both α and βDG has been reported in correlation with loss of DG from the PM as is seen in epithelial carcinoma progression (Lossasso et al. 2008). Increased cell density results in an increase in proteolytic cleavage and nuclear targeting of βDG, particularly the 26 KDa fragment, moreover, a recent study shows that this is a consequence of γ-secretase and furin cleavage, which may be mediated in a notch dependent manner (Mitchell et al. 2013, Leocadio et al. 2016). Future work could aim at investigating a functional role of fragments of βDG in the nucleus. As has previously been mentioned the targeting of a cytoplasmic fragment of βDG to the nucleus saw the differential regulation of a small number of genes in a microarray, hinting at a potential signalling function (Mathew et al. 2013).

The localisation of βDG to the nucleus in PNT1A, LNCaP and PC3 cells was also corroborated by immunofluorescence microscopy. βDG was detected in the nucleus using two different antibodies and the three cell lines showed very similar localisation profiles, at the nucleoplasm, nuclear envelope, nucleoli and distinct nuclear foci, although the levels at these sites, particularly the nucleoplasm, was variable across the cell lines (Fig 4.5, Fig 4.6). The localisation profiles of the two antibodies, MANDAG2 (Fig 4.5) and C20 (Fig 4.6) were surprisingly different, with C20 strongly localising to the nucleoli. This could potentially be explained by the fact that the antibodies detect different epitopes within βDG and therefore may encompass different PTM which may regulate specific nuclear localisation or the epitopes may be blocked by binding partners at different sites within the nucleus. The epitopes have been discussed in more detail in Chapter 3.

βDG colocalisation with lamin A/C at the nuclear envelope in LNCaP cells has also been demonstrated. These results are in agreement with multiple reports in the literature detailing βDG nuclear localisation in several nuclear compartments and its association with protein markers of these compartments (Martinez- Vieyra et al. 2013, Fuentes- Mera et al. 2006, Mathew et al. 2013, Leocadio et al. 2016). Roles for βDG, and its interactions, at the nuclear envelope have been discussed previously (Section 4.3.1) however a role for βDG in thenucleolus is less well studied. The nucleolus is the site of rRNA transcription, processing and ribosome

assembly (Raska et al. 2006). Interestingly, recent mass spectrometry analysis of proteins immunoprecipitated with βDG from biochemically fractionated LNCaP cells detected a number of proteins involved in ribosomal processes including CRM1 a nuclear export factor and u3RN, a small nuclear RNA, (Leocadio 2014). Although validation is required to confirm these interactions, it could hint at a functional role for βDG in the nucleolus as well as the splicing speckles and cajal bodies, where it has also been detected (Martinez-Vieyra et al. 2013).

It is known that lamin A/C and B1 can be found in the nucleolus and are important in maintaining its structure and function (Martin et al. 2009). It is also known that βDG associates with nuclear lamins and that nucleolar structure is disrupted upon DG knockdown in C2C12 cells (Martinez-Vieyra et al. 2013), therefore βDG localisation in the nucleoli may contribute to the structure of these subnuclear compartments via components of the nuclear lamina. Interestingly α-dystrobrevin has also been identified in the nucleolus and when α-dystrobrevin is downregulated there are changes in the nuclear structure as well as a reduction in the levels of a number of nucleolar proteins including fibrillarin and Nopp140 (Hernandez-Ibarra et al. 2015). It would therefore be interesting to assess if the roles of α-dystrobrevin and βDG in the nucleolus are as part of a nuclear DAPC. In order to further elucidate the precise localisation of βDG in the nucleus of these cell lines, co-localisation analysis of protein markers of different nuclear structures and βDG could be conducted alongside immunoprecipitation and pull down assays as has been conducted in other cell lines (Hernandez-Ibarra et al. 2015, Martinez- Vieyra et al. 2013).

The results above also show that LNCaP, PC3 and PNT1A cells can all be used as models to investigate the nuclear regulation and functions of βDG.

4.3.3 FLAG TAGGED ALPHA-BETA DYSTROGLYCAN CAN BE DETECTED IN THE NUCLEUS OF LNCAP CELLS

The addition of a tag can aid in the study of a specific protein, however, it also has its caveats with a major concern being that the position or size of a tag may affect the conformation, PTM or interaction sites of a protein thus disrupting its normal cellular function. The expression of recombinant tagged βDG is no exception. Firstly, the functional processing of βDG is complex, with the production of α and βDG from a single propeptide, meaning that recombinant expression is best when both α and βDG are encoded for (Ibraghimov-Beskrovnaya et al. 1993, Holt et al. 2000). Secondly, the cytoplasmic tail of βDG is proteolytically cleaved and the position of the tag therefore needs to be carefully considered (Yamada et al. 2001, Singh et al. 2004, Leocadio et al. 2016). Thirdly the cytoplasmic tail is the site of multiple protein interactions and functional PTM which a tag could potentially disrupt (Moore et al. 2010, Ilsley et al. 2001, James

et al. 2000 Yang et al 1993). Whilst βDG has been expressed with multiple tags including His, myc and GFP tags with success it has recently been shown that tags at the C-terminus of βDG can affect either the phosphorylation at Y892 or the ability to detect the Y892 phosphorylated form of the protein (Leocadio 2014). A flag tag was therefore inserted at a region of no known or putative interactions at residue 803, downstream of the NLS (Fig 4.8 A), and has been characterised previously by D. Leocadio (Leocadio, 2014). Importantly for this study full length 43 KDa αβDGflag as well as some high molecular weight species at ~60 and between 130-250KDa, can be found in the nucleus when transfected into LNCaP cells, as corroborated by Fig 4.8 B. Low levels of αβDGflag can also be seen in the nucleoplasm, nuclear envelope and nuclear foci via confocal microscopy. Thus αβDGflag can be used to investigate the functions and regulation of βDG and its nuclear localisation.

4.3.4 INVESTIGATING THE PHOSPHORYLATION OF BDG

Phosphorylation is one of the most abundant PTM in the modification of the proteome and the reversible nature of the modification often leads to it being referred to as a 'molecular switch', regulating a diverse array of cellular processes. There was no significant retardation in the migration of βDGflag via SDS PAGE when cells were treated with Calyculin A (Fig 4.10), whilst this result does not support the reported phosphorylation of βDG at serine and threonine residues identified by mass spectrometry studies (Hornbeck et al. 2014) it is unlikely that the resolution of the SDS-PAGE gel is sensitive enough to detect changes in migration caused by the altered phosphorylation status of a small number of residues. Furthermore a positive control of a protein known to be substrates of serine/ threonine phosphatases would verify the activity of the Calyculin A. Shifts in migration of βDG have been reported following treatment with both Calyculin A and peroxyvanadate together (Leocadio 2014). The identification of two separately migrating bands of βDG between 35-55 KDa when run on a phostag gel could indicate phosphorylated species of βDG, although additional controls are required to support this hypothesis (fig 4.9). Moreover, whilst phosphorylation at Y892 will be represented within these bands, as shown by the detection of both bands with pY892 specific 1709 antibody, their detection with MDG2, the epitope of which precludes pY892 (James et al. 2000, Ilsley et al. 2001), suggests the presence of additional sites of phosphorylation of βDG. There is compelling evidence for the phosphorylation of additional tyrosine residues to Y892 in the cytoplasmic domain of βDG, particularly the evidence presented by Moraz et al. that tyrosine phosphorylation but not the Src dependent phosphorylation of Y892 are important for Lassa virus internalisation (Ilsley et al 2001, James et al. 2000, Moraz et al 2012). Phosphorylation at serine and threonine residues of βDG is less well studied, reciprocal immunoprecipitations for

βDG and phospho-serine/ phospho threonine and the use of phospho-site specific antibodies would determine if there is further support for phosphorylation at these residues.
The mapping and validation of sites of phosphorylation of βDG will provide further insight into the regulation and functions of βDG and whether these modifications contribute to the localisation, stability, signalling scaffold and protein interaction capabilities of βDG.

4.3.5 CHARACTERISATION OF THE EFFECT OF PHOSPHO-NULL AND PHOSPHO- MIMETIC MUTATIONS AT T788 ON THE LOCALISATION OF BDG

To test the hypothesis that phosphorylation at T788 plays a role in the nuclear localisation of βDG phospho null (T788A) and phosphomimetic (T788D) mutations were introduced into αβDGflag (Fig 4.11).

The αβDGflag, αβDGflagT788A and αβDGflagT788D all expressed as a band at 43 kDa as well as occasional detection of high MW bands at 130- >250 kDa and the 31 and 26 kDa fragments, see discussion in previous sections (Fig 4.12 A). After IP for flag proteins the same bands were detected with an antibody against βDG and rflag (Fig 4.12 B, C). As to the question of the localisation of βDG when mutated at residue T788, it is clear from both biochemical fractionation (Fig 4.15) and confocal immunofluorescence microscopy (Fig 4.13, Fig 4.14) that the T788D mutant does not target βDG specifically to the nucleus, but is localised strongly at the PM and cytoplasm also. However, it remains possible that phosphorylation at T788 acts dominantly and target βDG to the nucleus in a way that T788D is not able to mimic. Given the localisation of αβDGflagT788D, it is possible to hypothesise that phosphorylation at T788 may also have a role outside of the nuclear functions of βDG, however this would require investigation through further functional analysis. All three αβDGflag constructs have very similar localisations and can be detected only faintly in the nucleus. Quantification of the biochemical fractionation suggests that the levels of αβDGflag, αβDGflagT788A and αβDGflagT788D in the nucleus relative to the rest of the cell is variable and there appears to be no effect on the nuclear localisation of βDG in response to the phospho null and mimetic mutations at T788. Further in depth confocal analysis alongside markers of subnuclear compartments may be useful to assess for any subtle changes to localisation at these sites.

Although there does not appear to be an overriding role in nuclear localisation for phosphorylation at T788, that is not to say that is does not have another functional or regulatory role. T788 lies within a stretch of the cytoplasmic domain of βDG that is rich in functional binding. In this region there are binding motifs for importin, ezrin and MAPK proteins ERK and Mek (Oppizzi et al 2008, Lara-Chacon et al 2010, Spence et al. 2004, Batchelor et al. 2007, Moore et al 2010, Vasquez-Limeta et al. 2014). Whilst pT788 is not

directly within these sites it is interesting to note that in ELM pT788 is identified as a putative binding site, although non-canonical, for Forkhead- associated (FHA) domain containing proteins, with another at canonical site at T782. FHA domain proteins have diverse cellular functions such as signal transduction and can be found at the PM and in the nucleus where they have roles in cell-cycle checkpoint regulation and DNA repair (Weiling et al. 2013). Although it is purely speculation it is interesting to consider that pT788 regulates interaction with a binding partner, further work would be required to identify if T788 truly is a site of protein interaction.

The migration shift of both T788A and T788D mutants on a phostag gel is minimal and does not support a change in the number of phosphorylated species of βDG, however nor it does not rule out compensatory phosphorylation events within βDG (Fig 4.12 D). No evidence has been presented to confirm the presence of phosphorylation of βDG at T788, nor how accurately the A and D mutants would serve as functional forms of the non-phosphorylated and phosphorylated forms of this site respectively. *In silico* analysis using the NetPhosK 1.0 server suggests Protein Kinase C (PKC) as a putative kinase responsible for phosphorylation at this site, though the surrounding sequence also resembles a non-canonical binding site for Polo-like kinase 1 (Plk1) (Kettenbach et al. 2013). *In vitro* radiolabelling assays could be conducted to determine if βDG is a substrate of these kinases.

4.3.6 THE STABILITY OF RECOMBINANT PROTEINS ABDGFLAG, ABDGFLAGT788A AND ABDGFLAGT788D

It was observed that αβDGflag expression reduced rapidly after transfection (Fig 4.16) whilst αβDGflagT788D seemed to persist for longer. The apparent consistency with which this was observed led to the hypothesis that the T788D mutation was conferring stability to the protein. In CHX chase assays, in which protein synthesis is inhibited, the turnover of αβDGflag and αβDGflagT788A were similar whilst αβDGflagT788D, though more variable showed a trend of being more stable (Fig 4.17). The half-life of cell surface βDG expressed in HC11 murine mammary epithelial cells was calculated to be approximately 12 hours (Sgambato et al. 2006). Although not a direct comparison of half-life, at 12 hours following CHX treatment αβDGflag and αβDGflagT788A are at 43.69 %±1.909 and 48.06 %±3.951 , which is close to the 50 % level as would be predicted from the previous reports, whilst αβDGflagT788D is at 75.08± 22.82% of the relative protein level at 0 hours (Fig 4.17 B, C). There are concerns that CHX treatment confers cellular stress and may perturb components of the degradation pathway and therefore other measures of protein stability are required.

It is interesting, however to hypothesise that T788 is part of a phosphodegron motif, particularly as it is in close proximity to multiple lysine residues, one of which, K806, is a

putative site of ubiquitination (Lee et al. 2011). Further experiments such as the treatment with proteasome inhibitor MG132 and identification of ubiquitinated species of αβDGflag, αβDGflagT788A and αβDGflagT788D should be investigated to determine if there is a differential turnover rate between the mutant forms of βDG.

The rapid loss of the 130-250 kDa band detected by the flag antibody following CHX treatment is interesting and may be that this protein species is being rapidly degraded or proteolytically cleaved into smaller fragments.

4.3.7 SUMMARY

1. Nuclear morphology is severely aberrant in a DAG null fibroblast cell line.
2. βDG is in the nucleus of PNT1A, LNCaP and PC3 cells and is localised at the subnuclear level at the nuclear envelope, nucleoli and nucleoplasm.
3. βDG is phosphorylated.
4. Phospho null and phospho mimetic mutations at T788 do not affect nuclear localisation of βDG and both mutants are found localised at the plasma membrane, cytoplasm and nucleus.
5. There may be a role of phosphorylation at T788 in the stability of βDG.

Chapter 5: The cell cycle and nuclear dystroglycan

5.1 INTRODUCTION

5.1.1 THE CELL CYCLE

The cell cycle is a complex series of sequential events that results in the duplication of genetic material and division of a cell. The progression of a cell through the division cycle is fundamentally interlinked with a vast array of cellular processes including differentiation, migration and adhesion (Walker et al. 2005, Shen et al. 2001, Lovisa et al. 2015, Giancotti 1997, Pugacheva et al. 2006). The correct coordination of these events alongside regulated cell death is required for normal development and adult homeostasis (Budirahardja et al. 2009, Caldon et al. 2010, Frisch et al. 1994). When the cell cycle process is disrupted it results in the aberrant proliferation of cells and is responsible for numerous human diseases, including cancer (Sherr. 1996, Stoker et al 1968, Malumbres et al. 2009).

5.1.1.1 The phases of the cell cycle

The phases of the eukaryotic cell cycle are well defined, discrete events. Cells spend the majority of their life cycle in interphase which consists of GAP phase 0 (G_0), GAP phase 1 (G_1), Synthesis (S) and GAP phase 2 (G_2). During G1 the cell grows in size, synthesises proteins and RNA and duplicates cellular organelles in preparation for the division of the cell. During G_1 a cell can make the decision to exit the cell cycle and exist in a quiescent state in G_0, which may be as a consequence of terminal differentiation or if the conditions are not favourable to cell division. In S phase the DNA is duplicated, resulting in replicates of 2 sister chromatids of each chromosome. G_2 follows S phase and is a further period of growth. Following interphase the cell enters into mitosis (M phase), with the replicated chromosomes being divided into two identical nuclei. Mitosis can further be divided into distinct phases, namely prophase, prometaphase, metaphase, anaphase and telophase and finally cytokinesis; the division of the cytoplasm and the separation of the two daughter cells (Fig 5.1) (Duronio et al. 013, Budirahardja et al. 2009, Malumbres et al. 2009).

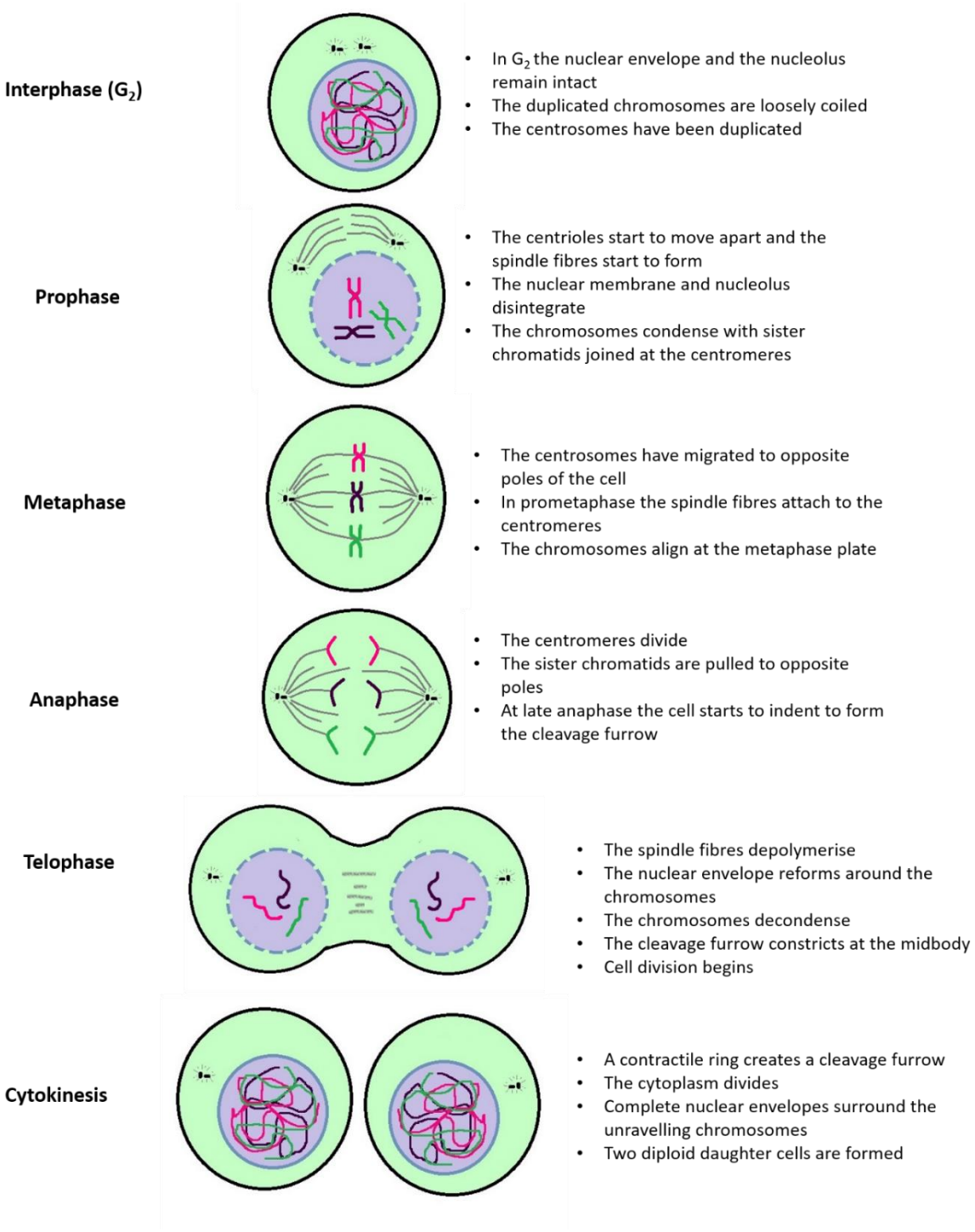

Figure 5.1. Schematic of the phases of mitosis in mammalian cells

5.1.1.2 Regulation of the cell cycle

The cell cycle proceeds through tightly regulated checkpoints, the purpose of which is to monitor if conditions are conducive to cellular proliferation and to prevent propagation of damaged or an incorrect amount of DNA (Budirahardja et al. 2009, Malumbres et al. 2009). There are three key checkpoints in the cell cycle. A G1 checkpoint, known as the restriction point in mammalian cells, in which cells assess nutrients, cell size, DNA damage and growth factors, if these conditions are favourable it is at this restriction point that a cell will commit to the cell cycle (Malumbres et al. 2009, Duronio et al. 2013). There is also a G2 checkpoint in which the cell again verifies cell size and the accuracy of DNA replication and a spindle assembly checkpoint in mitosis to verify spindle attachment to the chromosomes which is crucial for correct chromosome segregation (Malumbres et al. 2009, Mussachio et al. 2007).

The basic cell cycle machinery driving unidirectional progression of the cell cycle are the heterodimeric complexes of cyclins and cyclin dependent kinases (CDKs) (Nurse et al. 1976). Cyclins are the regulatory subunit whilst CDKs are catalytic. The levels of the specific cyclins peak at specific stages of the cell cycle, only when bound to its cyclin regulator can the constitutively expressed CDKs phosphorylate target proteins to coordinate entry into the next phase of the cell cycle. Cyclin dependent kinase inhibitors (CDKIs) are a further subset of cell cycle regulatory proteins which inhibit the activity of the cyclin-CDK complexes (Duronio et al. 2013, Sherr et al. 1999). Crucially the cell must be able to sense the surrounding environment and respond appropriately to the external cues with regards to its decision to enter the proliferative cycle. This requires the convergence and integration of signals from multiple mitogenic signalling pathways, cytokines, Notch and Wnt signalling and signalling from ECM receptors all of which can ultimately regulate the cell cycle machinery (Duronio et al. 2013., Nelson et al. 2002, Moreno-Layseca et al. 2014, Zhang et al. 2002, Torii et al. 2006)

5.1.2 The cell cycle and Adhesion receptors

During the cell cycle cells undergo vast changes in shape, size, metabolism and signal transduction (Duronio et al 2013, Budirahardja et al. 2009, Malumbres et al. 2009, Walker et al. 2005). Inevitably timely progression of the cell cycle requires the tightly controlled but dynamic regulation of numerous proteins (Balk et al. 2008, Moir et al. 2000, Dabauvalle et al. 1999, Caldon et al. 2010). The interdependence of the cell cycle and adhesion proteins is a well-studied process (Pugacheva et al. 2006, Walker et al. 2005.). It is known that the attachment of cells to adjoining cells or their substrate modulates the progression of cells through the cell cycle (Nelson et al. 2002, Frisch et al. 2001) and concurrently the transition of cells into certain phases, is matched by distinct alterations in the adhesion properties of these cells (Pugacheva et al. 2006). During mitosis the majority of focal adhesions are disassembled,

and the actin skeleton is reorganised, whilst in adherent cells, during cytokinesis, the correct localisation of adhesion receptors at the PM is necessary for reattachment (Yamakita et al. 1999, Walker et al. 2005, Kunda et al. 2009, Pugacheva et al. 2006). Additionally, a number of adhesion receptors have been implicated in the signalling pathways required for G1-S transition (Giancotti et al. 1997, Tetsu et al. 1999, Hamaratoglu et al. 2006).

The integrin family of adhesion receptors are a prime example of the interplay between ECM adhesion receptors and the cell cycle. Integrins bind to components of the ECM and recruit binding partners such as FAK, talin and even growth factor receptors such as PDGFR or EGFR (Pugacheva et al. 2006, Nobes et al. 1995, Walker et al.2005, Moro et al. 1998). Integrins mediate cell cycle progression by triggering signalling cascades such as the mitogenic Ras-raf-MEK-ERK cascade as well as by modulating the signalling of growth factor receptors, ultimately contributing to regulation of the cell cycle machinery, particularly the transcription and stabilisation of cyclin D and therefore G1 to S phase cell cycle progression (Moro et al. 1998, Chambard et al. 2007, Moreno-Layseca et al. 2014, Torii et al. 2006).

The cadherin family of proteins involved in adherens junctions also demonstrate a role in proliferation. Cadherins can inhibit proliferation via lateral contact inhibiton by sequestering intracellular binding partners such as β-catenin in the classical cadherin pathway (Pugacheva et al. 2006). In response to signals such as the wnt pathway or when adherens junctions are disassembled, β-catenin is released from the membrane bound complex (Masckauchan et al. 2005, George et al. 2004). The cytoplasmic β-catenin can then translocate to the nucleus whereby it interacts with members of the T-cell factor (TCF) family of transcription factors to initiate transcription of a number of target genes, including those involved in proliferation such as cyclin D1 (Tetsu et al. 1999). Interestingly a number of cell surface receptors themselves have demonstrated a cell cycle dependent nuclear translocation or to perform specific functions. Although not adhesion receptors, some of the best characterised examples are EGFR and FGFR, both of which have been detected transiently in the nucleus during G1 (Planque 2006, Lo et al. 2005, Schausberger et al. 2003).

Given the overlap between the cell cycle and adhesion, it is not surprising that certain proteins can contribute to, and are regulated by, both of these processes. Importantly, the relationship between cell attachment and proliferation is implicated in cancer biology and many adhesion proteins are aberrantly regulated in cancer. In these cases both the lack of adhesion and disrupted regulation of signalling pathways can contribute to the cancer phenotype. Therefore, it is important to understand the complex interaction between adhesion receptors and proliferation.

5.1.3 NUCLEAR MORPHOLOGY AND THE CELL CYCLE

Whilst the cell undergoes vast morphological changes during the cell cycle, so too does the nucleus (Foisner 2003, Tsai et al. 2014). In mammalian cells during interphase the nucleus maintains an intact nuclear envelope that functions to partition and regulate the exchange of proteins, mRNA and DNA between the cytoplasm and nucleus. In interphase the nucleoli are present as dense structures (Hernandez-Verdun 2011). During interphase the nuclear membrane and the nuclear lamina are relatively stable. There is, however, still a dynamic regulation of components for example in G1 there is an increase of Lamin A in the nucleoplasm before incorporation into the growing nuclear lamina (Moir et al. 2000a, Moir et al. 2000b).

The most dramatic changes to the nuclear morphology, however, occur at the onset and conclusion of mitosis. In vertebrates open mitosis requires the breakdown of the nuclear envelope (Foisner 2003). In this process the nuclear lamina depolymerises, the nuclear membrane fragments and the nuclear pore complexes are disassembled. A key regulator of nuclear lamina depolymerisation is the phosphorylation of the lamins and lamina proteins by mitotic kinases such as Cdk1 and PKC (Moir et al. 2000a, Nikolakaki et al. 1997, Ottaviano et al. 1985). Phosphorylation promotes disassembly of the lamins and dissociation of lamina proteins from the chromatin (Foisner et al. 1993). Microtubules are believed to play a role in the fragmentation of the nuclear envelope, creating a tension that pulls the nuclear membrane apart (Gonczy 2002, Salina et al. 2002, Beaudouin et al. 2002). During mitosis A type lamins are released into the cytoplasm and diffuse whereas B type lamins remain associated with membrane fragments and potentially with the lamin B receptors (LBR) via their C-terminal farnesyl modification (Foisner 2003, Meier et al.1994, Ye et al. 1994). The membrane fragments merge into the ER with a few studies suggesting that the nuclear membrane can be incorporated into vesicles with differing populations accommodating membrane fragments from different origins (Dabauvalle et al. 1999, Ellenberg et al. 1997, Yang et al. 1997, Maison et al. 1993). Similarly, the nucleolus is disassembled in early prophase prior to NEBD (Hernandez-Verdun 2011). Components of the ribosomal machinery around which the nucleolus is formed are phosphorylated by mitotic kinases promoting their release (Negi et al. 2006). A number of proteins normally associated with the nucleolus form a perichromosomal matrix during mitosis, hinting at some form of remaining association (Gautier et al. 1992).

During the formation of the new daughter cells the nuclear envelope must be reformed around the divided chromosomes. This requires the targeting of the nuclear envelope components to the surface of the chromosomes and the fusion of the membranes. It has been shown that the reformation of the nuclear envelope is a tightly regulated, sequential process requiring a complex array of interactions between the chromatin and nuclear envelope

components (Foisner 2003). For example, it has been shown that as early as late anaphase, LEM domain containing lamina binding proteins such as lamina associated polypeptide 2 (LAP2), and emerin accumulate around the chromatin whereby they can bind to the chromosomal protein barrier-to-autointegration factor (BAF) (Haraguchi et al. 2001, Dabauvalle et al. 1999, Lee et al. 2001, Manilal et al. 1998, Foisner 2003) LBR can also associate with chromatin binding proteins and bind to the DNA itself, thus targeting components of the nuclear envelope to the chromatin (Ye et al. 1994). A hierarchical recruitment of other NE components then follows with components of the nuclear pore complex, then B type lamins followed by A type lamins being assembled into the nuclear envelope (Bodoor et al. 1999, Haraguchi et al. 2000). The early stages of nuclear envelope assembly are often regulated by dephosphorylation events (Thompson et al. 1997), whilst the later events of membrane fusion have been shown to require Ran GTPase activity (Hetzer et al. 2000). The nucleoli start to reform in telophase and require the coordinated recruitment and activation of rDNA transcription and RNA processing complexes around which the dense nucleoli structures form (Hernandez- Verdun 2011, Tsai et al. 2014).

5.2 DAPC COMPONENTS AND THE CELL CYCLE

The interplay of components of the DAPC and the cell cycle has been studied by multiple groups. It has been shown that depletion of Dp71 in PC12 cells caused a delay in cell proliferation, with flow cytometric analysis identifying a subtle delay at the G_0/G_1 transition (Villarreal-Silva et al. 2011). Furthermore, during cytokinesis Dp71 was found to localise to the midbody and cleavage furrow where it colocalised with lamin B1 and βDG (Villarreal-Silva et al. 2011). Additionally, β-dystrobrevin depletion in C2C12 myoblasts perturbed cell cycle progression with an increased number of cells in G_0/G_1 and reduced cells in S phase relative to the controls (Aguilar et al. 2015). Furthermore, there was a decrease in cells actively synthesising DNA, as detected by BrdU analysis, in the β-dystrobrevin knockdown cells (Aguilar et al. 2015).

5.3 DYSTROGLYCAN AND THE CELL CYCLE

5.3.1 Dystroglycan and proliferation

There are multiple studies linking the cell cycle to dystroglycan expression and localisation. An initial study by Hosokawa et al. demonstrated that overexpression of full length βDG reduced the growth rate of bovine aortic endothelial cells (BAE), whilst expression of a cytoplasmic fragment of βDG increased proliferation, an early hint at a complex relationship between the cell cycle and βDG (Hosokawa et al. 2001). The study went on to further show that βDG levels increased in proliferating cells compared to quiescent cells and that this level fluctuated in

synchronised cells, increasing as the cells entered S phase and then decreasing (Hosokawa et al. 2001). A dynamic regulation of βDG in the cell cycle was further supported by Sgambato et al. working on murine mammary HC11 cells. The authors demonstrated that in synchronised cells the level of DG at both mRNA and protein levels fluctuated in a cell cycle dependent manner, again peaking at S phase (Sgambato et al. 2006). Interestingly, whilst βDG peaked at S phase, the levels of αDG appeared to decrease progressively after release into the cell cycle, thus suggesting differential regulation of the two subunits, and indicating that regulation is occurring at the post-transcriptional and post-translational level (Sgambato et al. 2006). The reduction in levels of αDG upon growth stimulation has also been seen when rat thyroid cells were stimulated by thyrotropin (TSH) (Collins et al. 2001). In the case of the HC11 cells, reduction of βDG via RNAi resulted in a slower rate of proliferation with an increased number of cells in S phase and accordingly there was increased levels of cyclin D and E and a reduction of CDKI p27Kip in these cells (Sgambato et al. 2006).

Multiple other groups have also reported altered proliferation rates upon modulating the levels of βDG. In swiss 3T3 cells reduced levels of DG resulted in lower proliferation rates, further analysis demonstrated that these cells had a delayed entry into S phase where they then persisted longer, also demonstrating a delayed transition into G2M (Higginson et al. 2008). Mitchell et al. demonstrated a complex relationship between DG levels and proliferation rate, in prostate cancer cell line PC3 both RNAi depletion and overexpression of βDG resulted in similarly reduced proliferation rates, proliferation was also reduced in DU145 prostate cancer line upon RNAi KD of DG (Mitchell, 2010, thesis). In the case of LNCaP cells overexpression of DG reduced proliferation whilst knockdown increased proliferation by approximately 25%.

5.3.2 Dystroglycan modulation of cell cycle signalling cascades

The ways in which DG could exert its influence on the cell cycle are not well understood however, one route is through its signal transduction properties. DG acts as a scaffold for MAPK signalling cascade molecules MEK and ERK, modulating their spatial and temporal activity (Spence et al. 2004). In Swiss 3T3 cells in which DG was depleted by RNAi and the cell cycle disrupted, there was also a 50% reduction in the levels of ERK. Similarly, a reduction in the phospho-ERK and phospho Mek was detected in HC11 cells depleted for DG via RNAi (Higginson et al. 2008, Sgambato et al. 2006). The Ras-MEK-ERK MAPK signalling cascade is a well characterised regulator of cellular proliferation (Chambard et al. 2007, Zhang et al.2002) and it is therefore tempting to speculate that DG may in part affect the cell cycle through its modulation of ERK signalling pathways.

Additionally, levels of PTEN were decreased whilst Akt and phospho-Akt levels were increased in DG depleted HC11 cells (Sgambato et al. 2006). PTEN is a phosphatase agonist of PI3K activity and can induce arrest in G1 via its inhibition of the Akt pathway (Ramaswamy et al. 1999, Radu et al. 2003). The DGC and βDG have previously been shown to modulate the PI3K/Akt signalling pathway when inhibited from binding to laminin (Langenbach et al. 2002, Yongmin et al. 2009). Activated Akt has been implicated in the inhibition of CDKI p27kip1 as well as promoting translation and nuclear localisation of cyclin D1 (Duronio et al. 2013). Thus demonstrating another pathway linking DG and the cell cycle.

The contribution of DG to signalling cascades is likely to be complex to dissect given its ability to modulate multiple pathways directly as well as indirectly through other DGC components and even more so given the high levels of cross-talk between the signalling pathways. For example, integrins also modulate the Ras-MEK-ERK signalling cascade and it has been shown that DG can act as a suppressor of laminin mediated integrin α6β1 activation of the ERK signalling pathway (Ferletta et al. 2003).

5.3.3 A role for Dystroglycan in cytokinesis

βDG has been reported to localised to the midbody and cleavage furrow during cytokinesis in a number of cell lines including swiss 3T3, Ref52 and Hela cells, colocalising with the contractile F-actin ring in dividing cells (Higginson et al. 2008). DG and ezrin are known interacting partners and were found to colocalise at the midbody and cleavage furrow (Batchelor et al. 2007, Higginson et al. 2008). Ezrin and other ERM family members have been shown to organise the actin cytoskeleton and recruit other transmembrane adhesion receptors, such as CD43, to the midbody during cytokinesis (Fehon et al. 2010, Solinet et al. 2013, Yonemura et al. 1998, Yonemura et al. 1993). When the cytoplasmic ezrin binding site of βDG was deleted the localisation at the midbody at later stages of cytokinesis was reduced (Higginson et al. 2008). In the DG knockdown cells there was, however, no disruption to the actin, microtubule or intermediate filament cytoskeletons and no observed cytokinetic defects, demonstrating that low levels of DG do not prevent cytokinesis (Higginson et al. 2008). Interestingly, ERK signalling has also been reported to be important for midbody abscission (Kasahara et al. 2007), thus it is tempting to speculate that βDG could contribute mechanically and via its signalling capabilities to midbody function in cytokinesis.

In the small number of studies in which the localisation of βDG in mitosis has been addressed, the focus has been largely of the dominant pool of βDG at the plasma membrane, as described above. However, given the emerging role of a small population of βDG at the nuclear envelope and its interactions with components of the nuclear lamina it would be interesting to try to address the localisation and dynamics of this population of βDG during mitosis.

5.3.4 A role for the cell cycle in the nuclear accumulation of βDG?

In a number of studies it has been reported that the level of nuclear βDG is variable within an asynchronous population (Mitchell et al. 2013, Mathew et al. 2013, Leocadio et al. 2016, Martinez-Vieyra et al. 2013). As previously mentioned, in a recent study in the Winder lab it was observed that stimulation of the androgen sensitive prostate cancer cell line, LNCaP, with the androgen dihydrotestosterone (DHT) stimulated a strong nuclear accumulation of βDG and that this nuclear accumulation fluctuated in a time dependent manner after androgen stimulation (Mathew et al. 2013, Mathew 2011 Thesis). Roles for AR regulation of βDG have previously been reported. Sgambato and colleagues observed that primary tumour samples from prostate cancer patients treated with the anti-androgen flutamide demonstrated reduced levels of α- and βDG at the cell surface (Sgambato et al. 2007). Studies in LNCaP cells showed that upon androgen stimulation both DG mRNA and βDG protein levels increased in a dose and time dependent manner indicating that androgens were regulating DG at a transcriptional level (Sgambato et al. 2007). The effect of androgens could be explained by the finding that, the DAG1 gene contains an Androgen Responsive Element (ARE) in its promoter region (Sgambato et al. 2007, Mathew et al. 2013).

When a ligand binds to the androgen receptor (AR) the receptors dimerise to form AR homodimers. The homodimers are then phosphorylated, after which the ARs translocate to the nucleus, binding to AREs of target genes promoting their transactivation (Balk et al. 2008, Koryakina et al. 2015). It has been shown that the AR can act as shuttle to transport proteins into the nucleus as is the case with β-catenin (Mulholland et al. 2002). It is tempting to propose a similar hypothesis regarding AR shuttling of βDG to the nucleus, however, rigorous investigation did not detect an interaction between the AR and βDG (Mathew et al. 2013).

LNCaP cells are androgen responsive and are stimulated to proliferate upon DHT treatment (Horoszewicz et al. 1983, Murthy et al. 2013). There is a large amount of cross talk between the AR signalling axis and the cell cycle pathways, with AR both contributing to and being modulated by the cell cycle. $p21^{cip}$,a cyclin is a direct target of the AR and is transcriptionally upregulated upon AR activation. Cyclin D expression is increased upon AR stimulation through increased translation through the mTOR pathway as well as through promoting the activity of mitogenic signal transduction pathways such as MAPK. (Koryakina et al. 2015, Balk et al. 2007). The androgen studies required the serum starvation and consequently synchronisation of the LNCaP cells at G_0/G_1 and are subsequently released into the cell cycle upon DHT treatment (Mathew et al. 2013). Fluctuation of nuclear βDG levels was also observed when serum starved and synchronised LNCaP cells were released into the cell cycle via addition of serum (Mathew 2011. Thesis). Importantly, βDG can be found in the nucleus at varying levels in cell lines that

do not express AR such as the AR negative prostate cancer PC3 cells, C2C12 myoblasts and Hela cells (Mitchel et al. 2013, Martinez- Vieyra et al. 2013, Lara- Chacon et al. 2010). Thus whilst AR and βDG association in complexes along with other proteins and a role for this in the nuclear translocation of βDG cannot be excluded, it is interesting to hypothesise that the fluctuating levels of βDG in the nucleus were a consequence of the mitogenic effects of the androgen and the progression of the cells through the cell cycle, rather than a direct response to the androgen pathway itself.

Given the high level of interdependence between βDG expression and localisation with the cell cycle and the observation of fluctuating level of nuclear βDG in synchronised proliferating cells we therefore hypothesised that there is a cell cycle dependent nuclear translocation of βDG.

5.1.4 Chapter Aims

The aims of the research conducted in this chapter are:

- To investigate the levels and localisation of β-dystroglycan at different stages of cell cycle progression in prostate cell lines.
- To investigate if the level of β-dystroglycan in the nucleus is regulated in a cell cycle dependent manner.
- -To investigate the localisation of βDG in mitotic LNCaP cells.

5.2 Results

5.2.1 Proliferation of LNCaP cells

The level of βDG in the nucleus of LNCaP cells in an asynchronous population is variable (Mitchell et al. 2013, Leocadio et al. 2016). Furthermore, a time dependent fluctuation in the nuclear levels of βDG could be detected upon the stimulation of synchronised cells with androgen or serum (Mathew et al. 2013). Given these observations, LNCaP cells were chosen as the main model in which to test the hypothesis of a cell cycle dependent regulation of nuclear βDG in this project. Growth curves of LNCaP cells in standard growth conditions of RPMI media supplemented with 10% FBS were conducted to determine the proliferation profile and rate of LNCaP cells. LNCaP cells were seeded at a density of 2.5 $x10^3$ cells/ cm^2 in 12 well plates. The cell number per well was calculated every two days for 12 days with an average of 4 wells taken per time point (Fig 5.2). 2.5 $x10^3$ cells/ cm^2 is a low density of cells and in these conditions the lag phase of growth is relatively long with a slow increase in growth up to 6 days after seeding (Fig 5.2). Cells reach exponential growth between 8 and 10 days (Fig

5.2) when seeded in these conditions and the doubling time during this phase was calculated to be 33.62 hours, which is within the 32-34 hour doubling time of LNCaP cells reported in the literature (Van Steenbrugge et al. 1991, Cunningham et al. 2015).

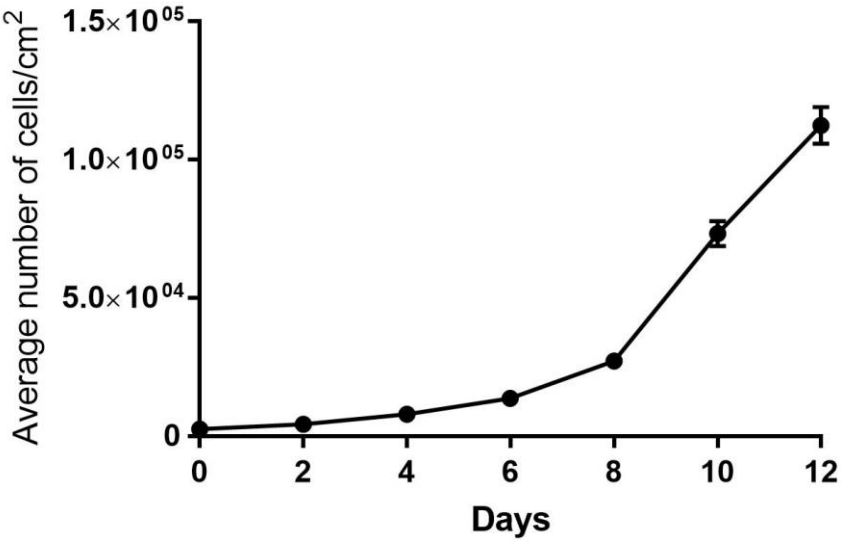

Figure 5.2. LNCaP growth curve. LNCaP cells were seeded at a density of 2.5 x 10^3 cells per cm^2 in a 12 well plate and grown in RPMI, 10% FBS for 12 days. The number of cells per well were counted every 2 days using the automated CasyCounter and the number of cells per cm^2 calculated. In each experiment the number of cells from 4 wells was counted at each time point and an average calculated. The graph depicts the averages of 4 independent experiments. Error bars are S.E.M.

5.2.2 THE LEVEL OF B-DYSTROGLYCAN FLUCTUATES IN A CELL CYCLE DEPENDENT MANNER IN THYMIDINE SYNCHRONISED LNCAP CELLS

A useful tool in the study of cell cycle events is the synchronisation of cell populations, enabling the clarification and enrichment of specific cell cycle stages. Preliminary studies with serum starvation resulted in poor synchronisation and slow progression of the LNCaP cells back into the cell cycle (Data not shown) therefore synchronisation of LNCaP cells with a double thymidine block was implemented. Thymidine is a pyrimidine nucleoside, high concentrations of which disrupt the deoxynucleotide metabolism pathway and DNA replication, thus arresting the cells at the G1/S phase border in the cell cycle (Bootsma et al. 1964). Thymidine synchronisation of cells is well studied and is useful in the study of S phase events (Bostock et al. 1971, Thomas et al. 1975), an additional reason it was chosen for this study given previous reports of increased levels of βDG in S phase (Sgambato et al. 2008, Hosokawa et al.2001)

.

5.2.2.1 Double thymidine block and synchronisation of LNCaP cells.

LNCaP cells were treated with 2mM thymidine for 18 to 32 hours to investigate the effect of thymidine treatment on LNCaP cell cycle distribution and determine the optimal length of treatment for subsequent synchronisation experiments. In asynchronous populations of LNCaP cells the majority of the cells exist in G1/G0 phase (~75- 80%), with small populations in S Phase (9.3-13.2%) and ~ 10% in G2M. Upon treatment with thymidine there was an increase in the population of cells in S phase, which increased with longer thymidine treatment (Appendix C, Fig C.1). At 32 hours of thymidine treatment 33.4% of the cells were in S phase, 60.9 % in G1 and 5.8% in G2M. It would be expected that upon thymidine treatment cells would arrest at G1/S transition, with the cells in S phase at the time of treatment arresting in S phase. It can be seen, however, in the longer treatments of thymidine that there is an increase in the number of cells progressing further into S phase, suggesting a 'leakiness' of the synchronisation at the G1/S phase transition as has previously been described by Bostock et al. (Bostock et al. 1971).

Double thymidine blocks are often used to achieve a greater synchrony of a population of cells. LNCaP cells were blocked first with thymidine for 32 hours. 32 hours was chosen because it resulted in a high number of cells in G1 and S phase and because this is the proposed length of LNCaP doubling time, therefore, during the treatment, the majority of the cells should have passed through the cell cycle to reach the G1/S transition at which the thymidine block acts. The cells were then washed and incubated with fresh media. A release period of 9 hours was chosen as this should be sufficient for the cells to progress out of S phase before a second 2mM thymidine treatment of 22 hours to enable the cells to move through G2 and M into G1 to arrest at the G1/S boundary (Murthy et al.2013). Cells were then released into the cell cycle and populations collected every 2 hours for 14 hours. (Fig 5.3A). The cell cycle distribution and progression of the LNCaP populations following release was monitored via propidium iodide staining and flow cytometry analysis (Fig 5.3.B.C and Appendix C, Fig C.2) and immunoblots for the phase specific cyclins. The intensity of the bands was determined by densitometry analysis and normalised to the GAPDH loading control. In order to combine the replicates, for each independent experiment each normalised intensity value was then calculated relative to the highest normalised intensity in the time course. Cyclin A1 was not quantified because of the weakness of the bands relative to the background.

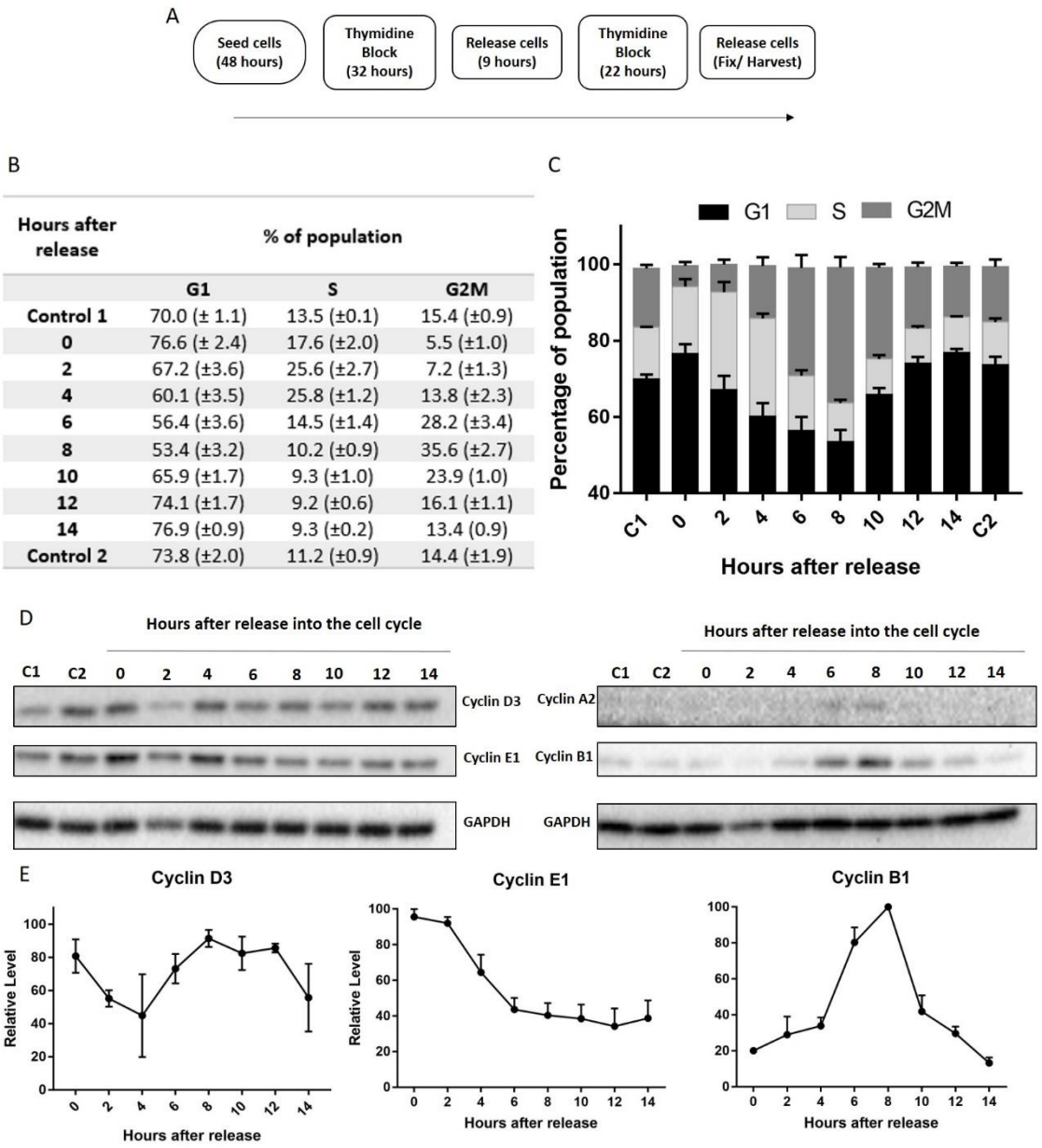

Hours after release	% of population		
	G1	S	G2M
Control 1	70.0 (± 1.1)	13.5 (±0.1)	15.4 (±0.9)
0	76.6 (± 2.4)	17.6 (±2.0)	5.5 (±1.0)
2	67.2 (±3.6)	25.6 (±2.7)	7.2 (±1.3)
4	60.1 (±3.5)	25.8 (±1.2)	13.8 (±2.3)
6	56.4 (±3.6)	14.5 (±1.4)	28.2 (±3.4)
8	53.4 (±3.2)	10.2 (±0.9)	35.6 (±2.7)
10	65.9 (±1.7)	9.3 (±1.0)	23.9 (1.0)
12	74.1 (±1.7)	9.2 (±0.6)	16.1 (±1.1)
14	76.9 (±0.9)	9.3 (±0.2)	13.4 (0.9)
Control 2	73.8 (±2.0)	11.2 (±0.9)	14.4 (±1.9)

Figure 5.3. Double thymidine block synchronisation of LNCaP cells and cell cycle progression. A) Cells were grown for 48 hours and then treated with 2mM Thymidine for 32 hours. Cells were released by addition of fresh media for 9 hours and then blocked for a further 22 hours with 2mM Thymidine. Cells were released into the cell cycle via the addition of fresh media and collected every two hours over 14 hours. Control 1 and control 2 were PBS control treatments at 0 hr and 14 hours respectively. The collected cells were harvested for lysate collection or ethanol fixed, stained with propidium iodide and analysed for cell cycle distribution via flow cytometry. B , C)The average number of cells at each phase of the cell cycle at each time point. N=4. D) Representative image of immunoblots of total cell lysates collected from double thymidine block synchronised LNCaP cells at each time point and immunoblotted for cyclins D3, E1, A2 and B1 and a GAPDH loading control. E) Quantification of cyclin immunoblot levels. The intensity of the bands was determined via densitometric analysis and was normalised to GAPDH. Each time point was then found relative to the level of the highest expression in each experiment. Mean values and S.E.M are displayed. Cyclin E1 and B1 N=4. Cyclin D3 and A2 N=3.

There was a tighter accumulation of cells at the G1/S transition at 0 hours than seen with the single treatments. The LNCaP cells had the highest population of cells in S phase (~25%) at 2 to 4hours post release which tallied with cyclin E1 expression (marker of G1-S transition), which was present in all of the samples, but was strongest at 0 to 4 hours (Fig 5.3). Cells peaked at G2M at 6- 8 hours post release, with 28.2-35.6 % in G2M population with cyclin A (late S through M) and cyclin B1 (M) detected at 6-10 hour and 6-8 hours respectively before moving back into G1 (~76%) at 12 hours (Fig 5.3). Cyclin D1 expression was variable throughout which can be expected given the high levels of G1 population see throughout the time course.

Although the results were relatively reproducible it must be noted that at each time point the majority of the cells were in G1 phase, which does not fall below 50% (Fig 5.3). Therefore, when interpreting results of the double thymidine synchronisation, it must be remembered that it is a mixed population of cell cycle phases, with what appears to be the synchronised progression of a sub-population of the cells through the cell cycle. Further optimisation of timing or different synchronisation techniques such as Isoleucine or nocodazole block, would likely enhance the synchronisation of the cell cycle enrichment of specific cell cycle phases.

5.2.2.1 βDG protein levels fluctuate in double thymidine synchronised LNCaP cells.

There is a complex relationship between dystroglycan and the cell cycle, including a role for the cell cycle in the expression of DG (Sgambato et al. 2008, Hosokawa et al. 2001). In order to determine if the βDG protein level varied as LNCaP cells progressed through the cell cycle after release from the thymidine block total cell lysates were collected at each time point and immunoblotted for both βDG and pY892 βDG. There is a strong expression of full length βDG and pY892 βDG across all of the time points collected with a slight, variable increase at 2 to 6 hours (Fig 5.4). There did not appear to be any clear changes in the faint high and low molecular weight species of βDG or pY892 βDG detected. When the levels of 43 KDa βDG and pY892 βDG were quantified as described above for the cyclins and the mean calculated, it showed an increase at 4 hours post release, correlating to a time point at which the amount of cells in S phase was at its highest at 25.8%±1.2 (Fig 5.4, Fig 5.3). The relative level of βDG and pY892 βDG following densitometric quantification at each time point is variable and for each independent replicate the highest expression level did not always correlate with the highest S phase containing time point (Fig 5.4, Appendix C.3). Given the variability between the independent replicates this experiment does not provide conclusive support for an increased level of βDG at S phase in LNCaP cells. The GAPDH levels are also variable within and between the individual replicate experiments and may be a contributing factor to the trend observed in the quantified relative levels of βDG and pY892 βDG (see discussion 5.3.1).

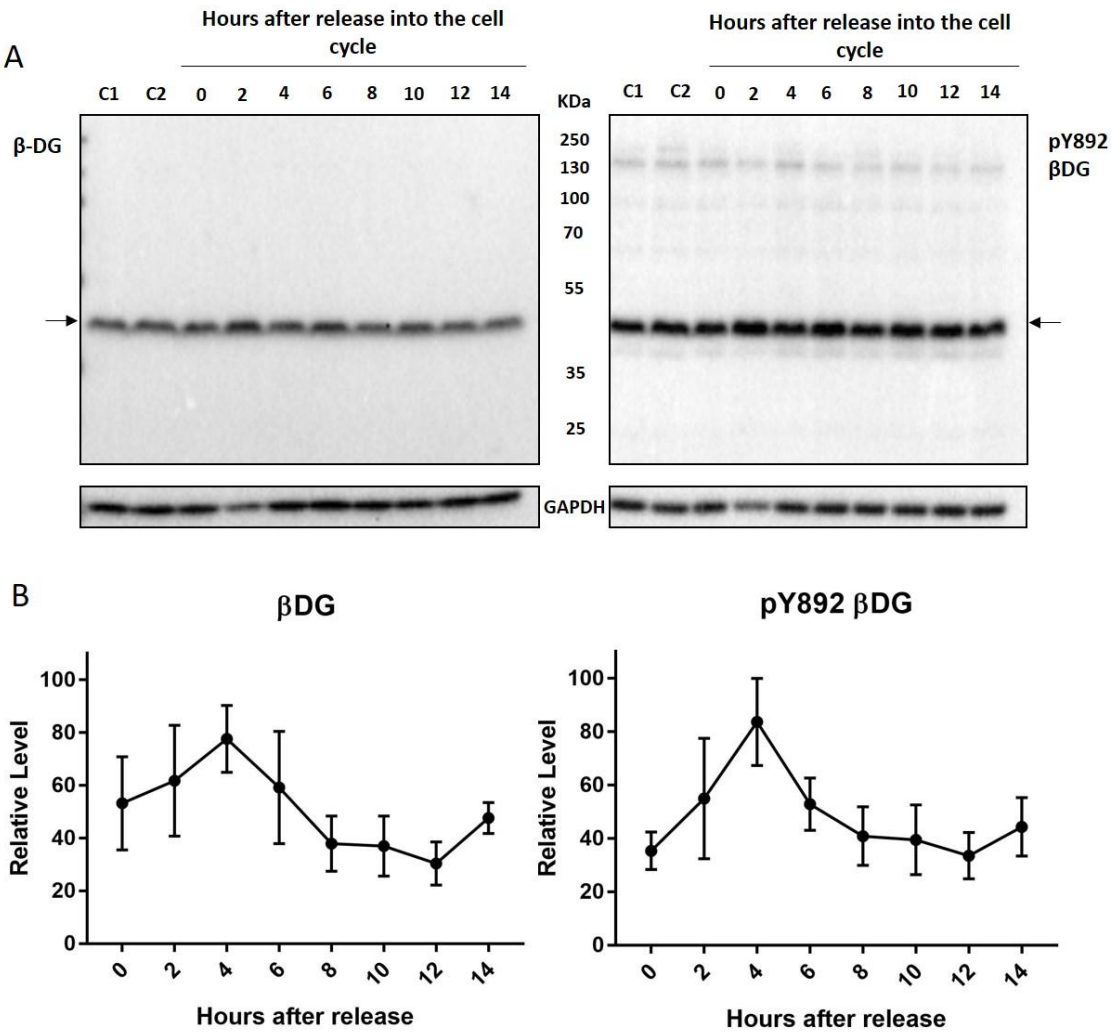

Figure 5.4. βDG and pY892 βDG levels in total cell lysates from thymidine synchronised LNCaP cells. A) Immunoblot of total cell lysates collected from double thymidine block synchronised LNCaP cells at each time point and immunoblotted for βDG and pY892 βDG and a GAPDH loading control. Arrows indicate full length 43 KDa βDG. B) Quantification of 43 KDa βDG and pY892 βDG immunoblot levels. The intensity of the bands was determined via densitometric analysis and was normalised to GAPDH. Each time point was then found relative to the level of the highest expression in each experiment. Mean values and S.E.M are displayed. N=4.

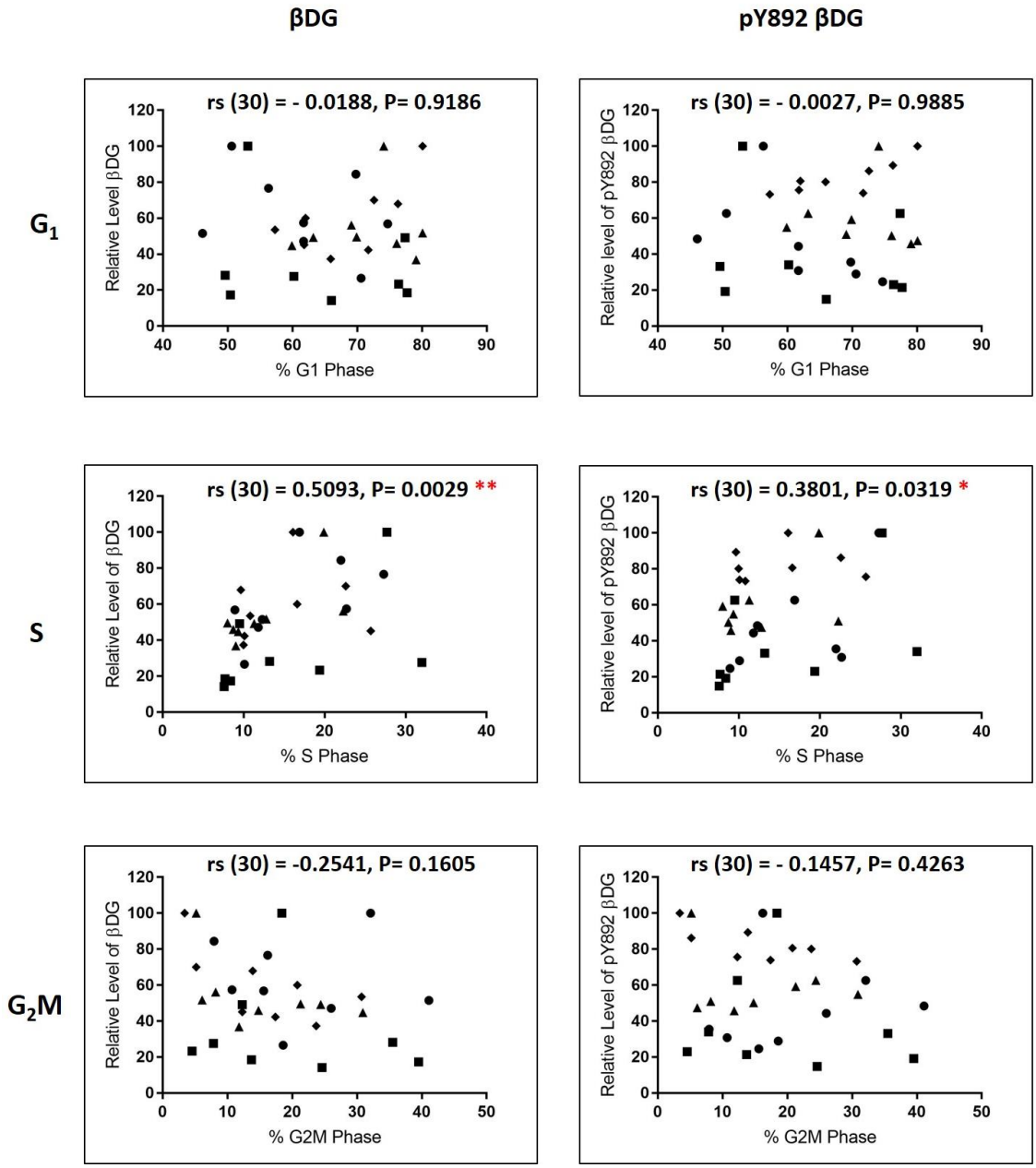

Figure 5.5. βDG and pY892 βDG levels relative to cell cycle phase percentages. The relative level of βDG (left) and pY892 βDG (right)as determined via immunoblot were plotted against the percentage of cells in G_1 (top), S (middle) or G_2M (bottom) as determined by flow cytometry at each time point. Data from each replicate are represented by a different shape. Correlation and statistics were calculated via Spearman non-parametric test. N=4. * in red denotes statistical significance, P< 0.05.

To assess the relationship between βDG level and the cell cycle phases in further detail, the relative level of full length βDG and pY892 βDG was plotted against the percentage of cells in each of the cell cycle phases at that time point for each individual experiment (Fig 5.5). The scatter plots all show relatively dispersed data. Spearmans correlation test was used to determine if there was a correlation between the level of βDG and the percentage of cells in a specific phase of the cell cycle. A non-parametric test was used as not all of the data sets were normally distributed, as determined by two different normality tests and frequency distribution histograms (not shown). The rs value provides a measure of the degree of correlation with 1 being a strong, positive correlation and -1 being a strong, negative correlation. Weak, positive correlations were found to be statistically significant in S phase for both βDG and pY892 βDG. In G1 and G2M analyses the correlations were very weak and not statistically significant (Fig 5.5). Although this analysis must be interpreted carefully, as the protein level is a combination of the entire population of cells and has been normalised to GAPDH, it hints at an increased level of βDG within cells with higher S phase populations, this is supported by the previous reports in the literature in which βDG is increased at both the DNA and protein level in S phase in HC11 and BAE cells (Sgambato et al. 2008, Hosokawa et al. 2001). If time permitted it would be important to repeat the western blot experiments with populations better synchronised or enriched for the specific cell cycle phases in LNCaP and other cell lines to see if the changes in βDG expression level could be verified further. Furthermore, it would have been interesting to assess the levels of mRNA to determine if the cell cycle dependent regulation was occurring at the transcriptional level.

5.2.3 THE LEVEL OF NUCLEAR B DYSTROGLYCAN IN CELL CYCLE PROGRESSING CELLS FOLLOWING THYMIDINE SYNCHRONISATION.

In order to determine if the level of βDG in the nucleus varied as the LNCaP cells progressed through the cell cycle the LNCaP cells were synchronised with a double thymidine block as described above and subject to biochemical fractionation to obtain non-nuclear and nuclear fractions at each time point. The cell cycle distribution was determined at each time point via fixation and propidium iodide staining of the populations, followed by flow cytometry analysis (Fig 5.6). The non-nuclear and nuclear fractions were immunoblotted for βDG and pY892 βDG (Fig 5.7, Fig 5.9). GAPDH and lamin A/C were included as markers of the purity of the fractionation for the non-nuclear and nuclear fractions respectively and showed clean fractionation. It should be noted that in the G2M populations, whilst G2 nuclei are likely to be fractionated cleanly, there is not an intact nucleus to separate in mitotic cells. Further characterisation of βDG in mitotic cells can be found in section 5.2.7.

A

Hours after release	% of population		
	G1	S	G2M
Control 1	72.3 (± 1.6)	12.3 (± 0)	14.7 (± 0.6)
0	78.6 (±0.3)	15.9 (± 1.3)	7.5 (± 1.2)
2	70.1 (± 1.5)	22.5 (± 0.8)	5.7 (± 1.6)
4	60.3(± 0.3)	23.4 (± 3.9)	11.1(± 3.6)
6	59.34(± 0.2)	10.6 (±3.1)	22.7 (± 2.2)
8	59.7 (± 2.6)	8.7 (± 1.1)	30.4 (± 1.6)
10	72.2 (± 1.3)	8.5(± 1.2)	25.1 (± 0.5)
12	80.8 (±0)	6.8 (± 1.5)	15.5 (± 1)
14	83.5 (± 0.5)	5.6 (± 0.7)	11.2 (± 0.9)
Control 2	76.6	9.9	14.0

B

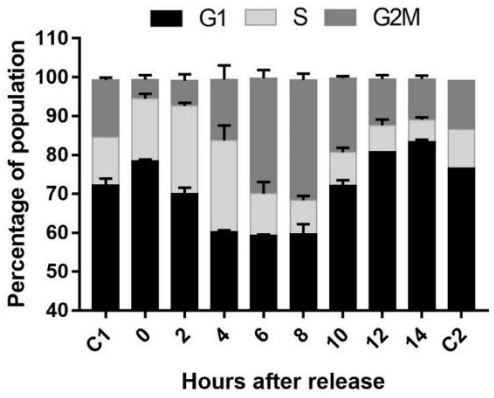

Figure 5.6 Double thymidine block synchronisation of LNCaP cells and cell cycle progression for fractionation experiments. Cells were synchronised via double thymidine block as previously described, The collected cells were harvested for fractionation or ethanol fixed, stained with propidium iodide and analysed for cell cycle distribution via flow cytometry.A, B)The average number of cells at each phase of the cell cycle at each time point. N=2.

Full length 43 KDa βDG in the non-nuclear fraction was slightly higher at 0 to 6 hours post release before decreasing variably between the two repeats (Fig 5.7, Appendix C.4). In the nuclear fractions the level of full length βDG was more variable both within and between replicates (Fig 5.7, Appendix C.4). Whilst the expression of βDG was consistently high at 4 hours and reduced at 0 and 14 hours, the remaining time points demonstrated significant variability. The increase in the level of βDG again overlapped with the time points of the highest levels in S phase at 22.5-23.4% at 2-4 hours post release (Fig 5.7, Fig 5.6). The intensity of the full length βDG was determined by densitometry analysis and normalised to GAPDH or the top band of the lamin A/C for the non nuclear and nuclear fractions respectively and then found relative to the highest intensity in that experiment (Fig 5.7 B, C). Normalising to lamin A/C is not an ideal loading control as lamins are regulated in a cell cycle dependent manner with regards to their phosphorylation and distribution (Moir et al. 2000). The effect of the cell cycle on the level of lamin total expression is less clear and thus this quantification should be interpreted critically as a means to normalise the expression for loading. However, it was attempted to load the same amount of nuclear extracts and quantification without normalisation and normalising to nucleolin, which also is dynamically regulated in the cell cycle, shows the same trend (Data not shown). To gain more confidence in the observation of a potential increased nuclear level of βDG at time points correlating with higher levels of S phase cells more repeats are needed unfortunately, despite repeated attempts, only two replicates were conducted due to insufficient synchronisation of LNCaP populations or contaminated fractionation.

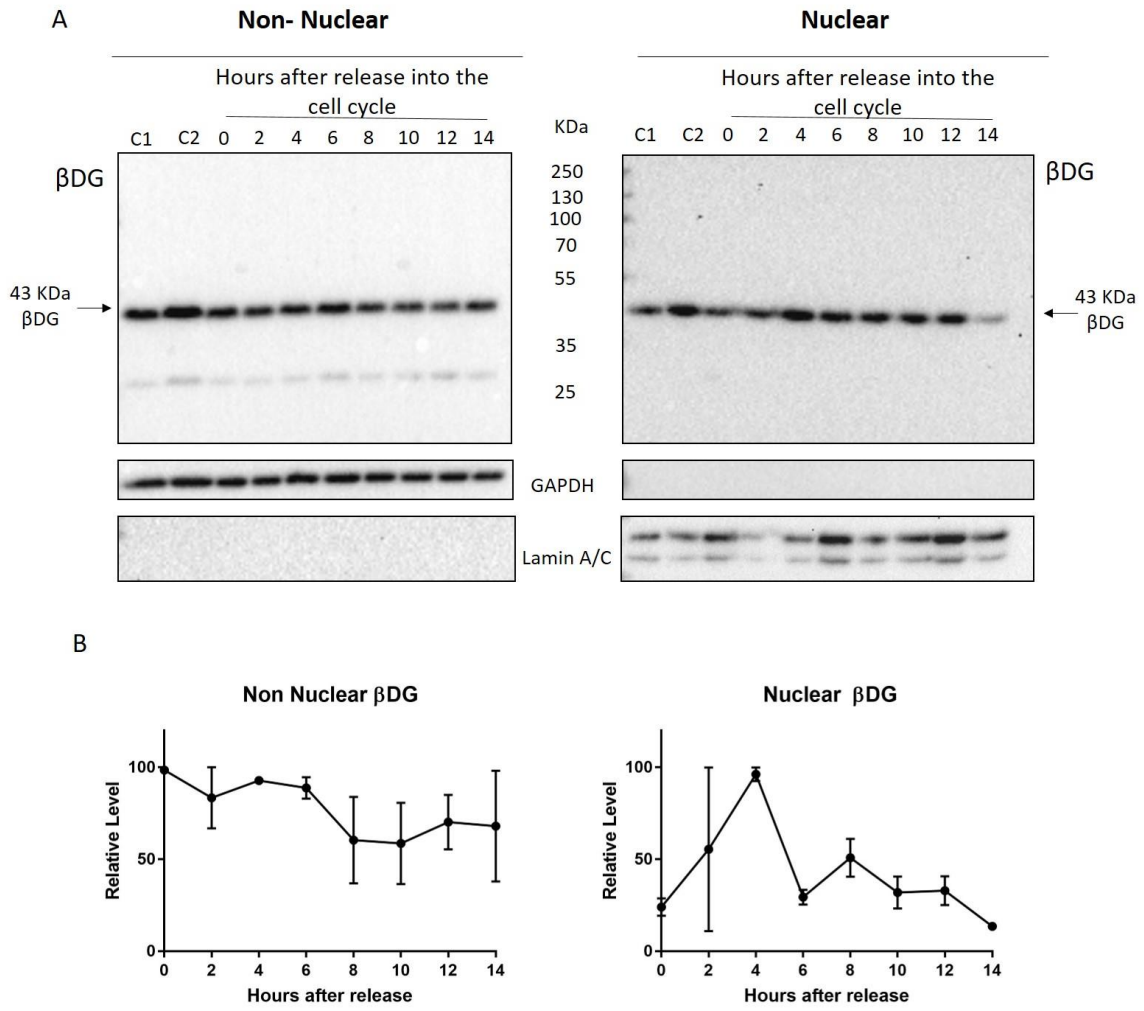

Figure 5.7. βDG levels in non- nuclear and nuclear fractions of thymidine synchronised LNCaP cells. A) Immunoblot of non-nuclear (left) and nuclear (right) lysates collected from double thymidine block synchronised LNCaP cells at each time point and immunoblotted for βDG. GAPDH and Lamin A/C were included as purity markers of the fractionation and loading controls of the non-nuclear and nuclear fractions respectively. Arrows indicate the full length 43 KDa βDG. B) Quantification of 43 KDa βDG in the non-nuclear and nuclear fractions. The intensity of the bands was determined via densitometric analysis and was normalised to the loading control. Each time point was then found relative to the level of the highest expression in each experiment. Mean values and S.E.M are displayed. N=2

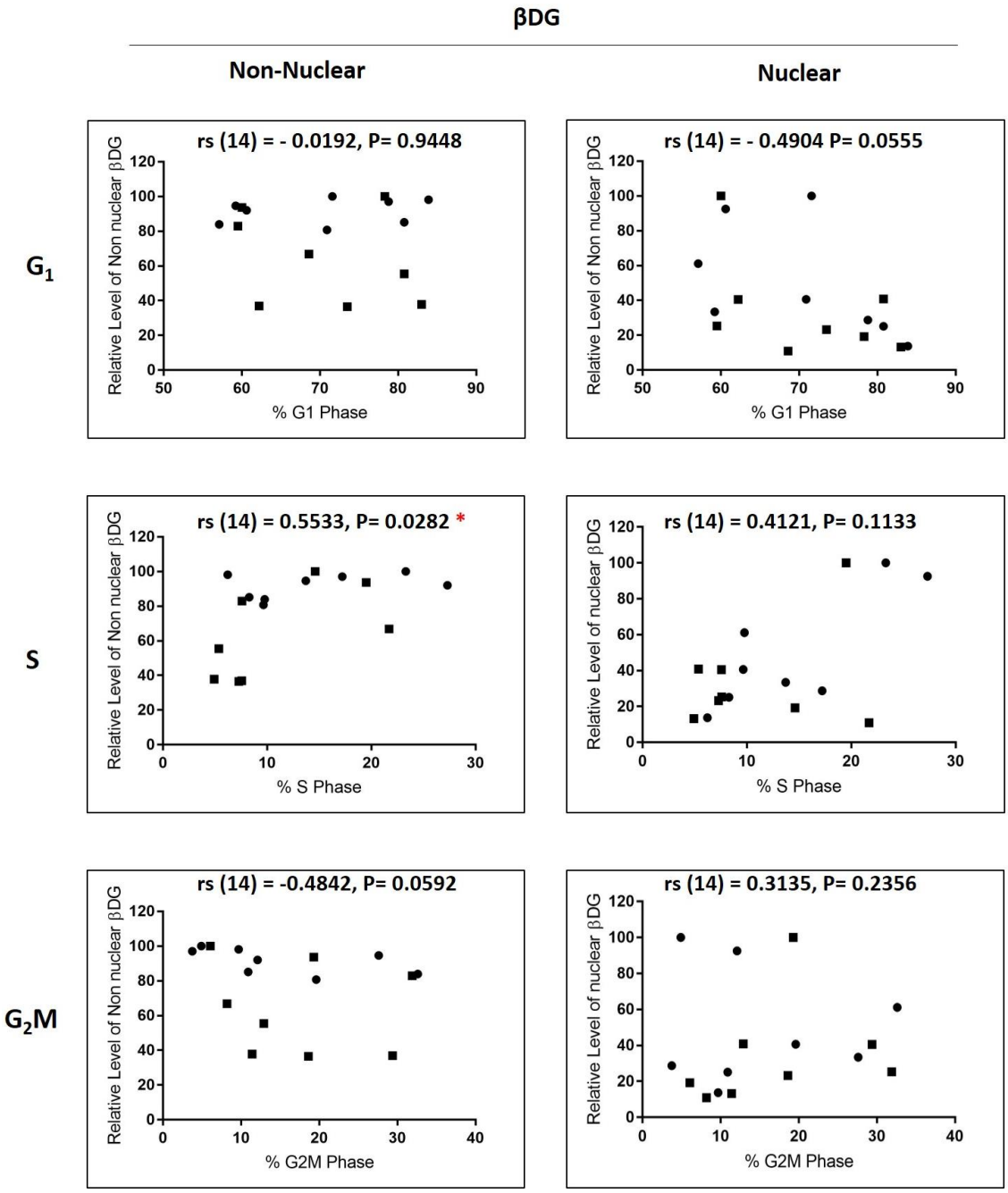

Figure 5.8. βDG levels in non-nuclear and nuclear fractions relative to cell cycle phase percentages. The relative level of βDG in non-nuclear (left) and nuclear (right) fractions as determined via immunoblot were plotted against the percentage of cells in G_1 (top), S (middle) or G_2M (bottom) as determined by flow cytometry at each time point. Data from each replicate are represented by a different shape. Correlation and statistics were calculated via Spearman non-parametric test. N=2. * in red denotes statistical significance, $P< 0.05$.

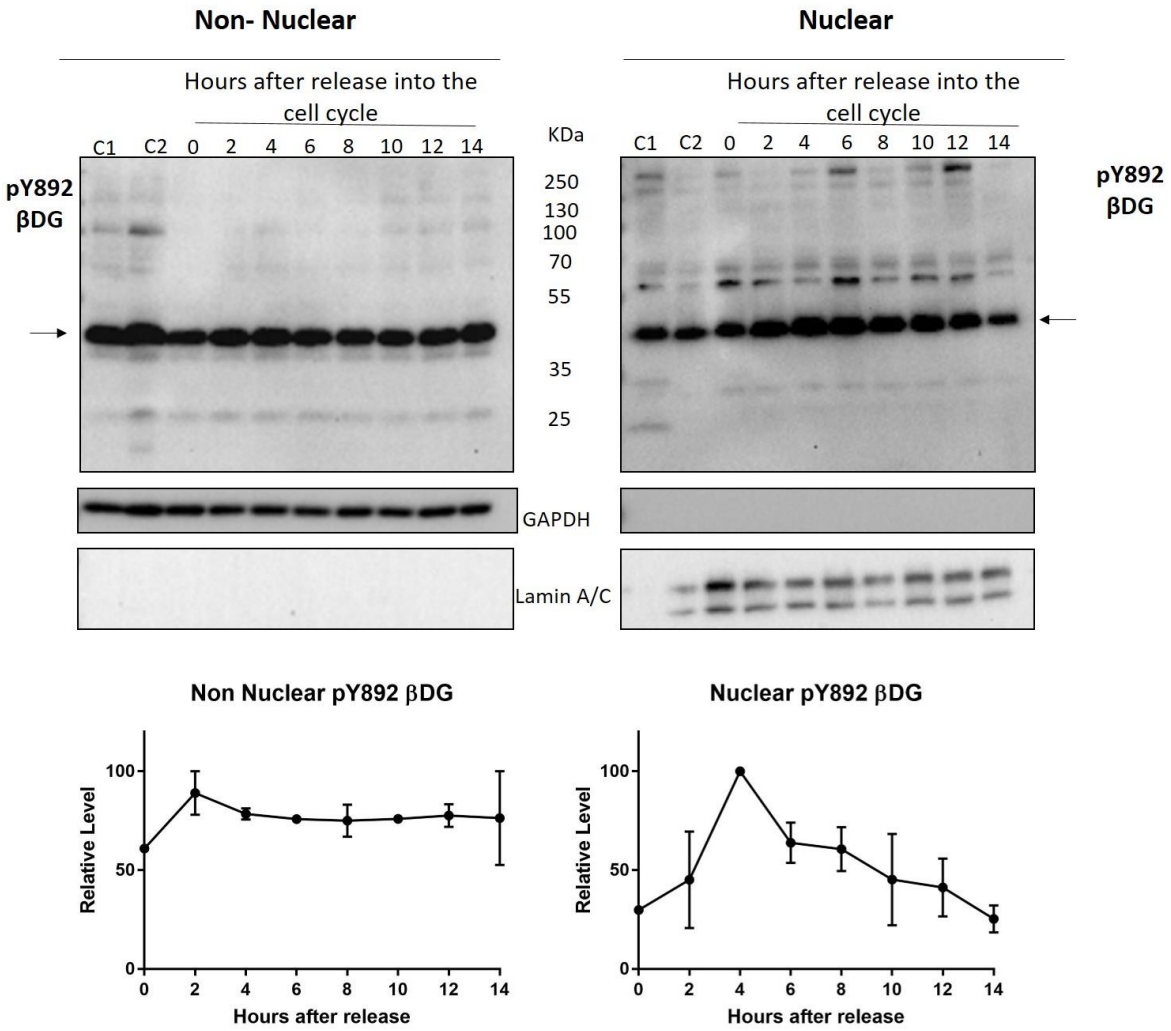

Figure 5.9. pY892 βDG levels in non- nuclear and nuclear fractions of thymidine synchronised LNCaP cells. A) Representative image of immunoblots of non-nuclear (left) and nuclear (right) lysates collected from double thymidine block synchronised LNCaP cells at each time point and immunoblotted for pY892 βDG. GAPDH and Lamin A/C were included as purity markers of the fractionation and loading controls of the non-nuclear and nuclear fractions respectively. Arrows indicate the full length 43 KDa pY892 βDG. B) Quantification of 43 KDa βDG in the non-nuclear and nuclear fractions. The intensity of the bands was determined via densitometric analysis and was normalised to the loading control. Each time point was then found relative to the level of the highest expression in each experiment. Mean values and S.E.M are displayed. N=2

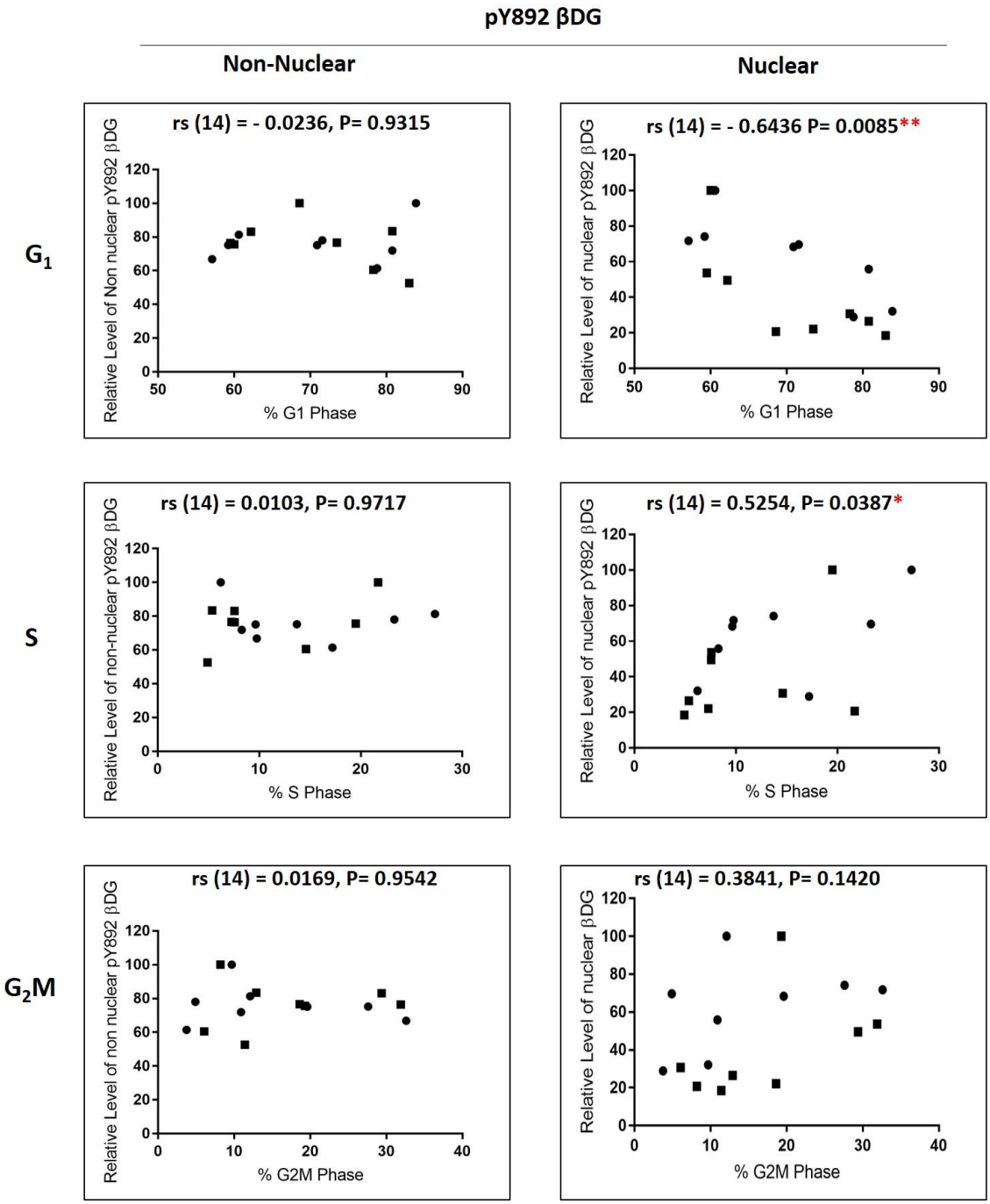

Figure 5.10. pY892 βDG levels in non-nuclear and nuclear fractions relative to cell cycle phase percentages. The relative level of pY892 βDG in non-nuclear (left) and nuclear (right) fractions as determined via immunoblot were plotted against the percentage of cells in G_1 (top), S (middle) or G_2M (bottom) as determined by flow cytometry at each time point. Data from each replicate are represented by a different shape. Correlation and statistics were calculated via Spearman non-parametric test. N=2. * in red denotes statistical significance, P< 0.05.

To get a more detailed analysis of the relationship between the level of βDG and the cell cycle, scatter plots for each time point detailing the percentage of cells in a specific phase and the level of βDG were plotted (Fig 5.8). Only the relative level of non-nuclear βDG in S phase showed a statistically significant weak, positive correlation as determined by spearmans parametric correlation analysis (Fig 5.8). Although there is no statistically significant correlation in the nuclear S phase levels of βDG, it is interesting to note that the samples with the highest levels of βDG were also the samples that had the highest levels of S phase cells. Again further replicates with increased enrichment of S phase cells as well as quantification relative to additional loading controls would be required to further test a hypothesis of increased nuclear βDG in S phase cells.

In the case of pY892 βDG, via immunoblot and quantification, the levels of full length pY892 βDG do not vary greatly over the time course in the non-nuclear fractions (Fig 5.9). The expression increases slightly after the initial release into the cell cycle but then decreases slightly and remains relatively constant. In the nuclear fractions there is a greater increase after entry into the cell cycle, with an increase at 4 hours then reducing for the remaining time points, although, once again there is variability between the replicates (Fig 5.9 A). The quantification must be treated critically due to the normalisation against lamin AC and GAPDH. The mean nuclear level of pY892 βDG peaks at phase when there is the highest proportion of cells in S phase. If the increase was due to number of cells in S phase alone, however, you would expect to see a larger increase at 2 hours compared to 6 hours as the percentage of cells in S phase at 2 hours is 22% compared to 10% at 6 hours (Fig 5.6). It may be that there is a more specific timing or event that sees an increased level of nuclear βDG in the cell cycle. In the scatter plots of pY892 βDG intensity against cell cycle phase percentage the correlations were again relatively weak (Fig 5.10). Interestingly, in the nuclear fractions there was a weak, statistically significant positive correlation of pY892 βDG relative to the number of cells in S phase, but also a stronger, statistically significant negative correlation between pY892 βDG and populations with a larger percentage of cells in G1 phase (Fig 5.10). Although further experiments with clearer populations of specific cell cycle phases is needed it appears that the pY892 βDG has more of a cell cycle dependence on its nuclear level rather that the non-phosphorylated or non-nuclear form.

From the immunoblot it is interesting to note that there is the presence of additional high molecular weight bands in the nuclear fraction that are not present or reduced in the non-nuclear fractions. Furthermore, the levels of some of these bands are clearly increased at different time points. For example, a band at approximately 60 KDa is particularly high at 0 hours and 6 hours post release, whilst the high molecular weight band >250KDa is increased at

6 and 12 hours (Fig 5.9). It would be interesting to use mass spectrometry to determine if these bands are post-translationally modified species of βDG and if these occur in a cell cycle dependent manner that contributes to βDG fate or function.

Although there are a number of caveats to these thymidine synchronised experiments, they do hint at a fluctuating level of βDG as the cells progress through the cell cycle. There is an indication that dystroglycan levels are increased in correlation with higher number of cells in S phase and that this may also be the case for nuclear βDG, particularly the pY892 phosphorylated form, which also seems to have an inverse relationship with populations of cells with higher proportions of G1 cells.

5.2.4 NUCLEAR BDG LEVELS IN BRDU POSITIVE LNCAP CELLS ARE NOT INCREASED

Because of the variability seen with in the thymidine experiments it was important to investigate the nuclear level of βDG in the cell cycle using different methods. An alternative method to investigate if the nuclear level of βDG was increased in S phase cells is via immunofluorescence intensity analysis. An asynchronous population of LNCaP cells was incubated with BrdU for 1 hour and then immunostained for BrdU and βDG (Fig 5.11.A). BrdU is a synthetic nucleoside that is incorporated into the DNA during DNA replication, thus subsequent immunodetection of BrdU positive cells enables identification of cells in S phase. Image J was used to make masks of the nuclei of images taken on an epifluorescence microscope. The intensity of βDG within the nucleus was normalised to the area and scored as a BrdU positive (S phase) or BrdU negative (non-S phase) nuclei. Quantification showed a broader spread of the intensity of βDG in BrdU negative cells relative to the positive cells (Fig 5.11.B). The mean of the BrdU negative cells was found relative to the BrdU positive cells for each replicate. There was no difference in the means of the two populations (Fig 5.11.C). This agrees with the thymidine treated LNCaP fractionation data in which no statistically significant correlation was detected between βDG and the percentage of cells in S phase. Unfortunately, 1709, the antibody that detects pY892 βDG, has been shown to detect the nucleus non-specifically when used for immunofluorescent studies (Section 3.2.4) and therefore could not be used accurately in the BrdU assay. The experiment should be repeated with antibodies that can detect the total population of βDG or tagged versions of βDG to account for the Y892 phosphorylated population. The BrdU immunofluorescence analysis was conducted on images taken from an epifluorescence microscope thus is also taking into account βDG expressed at the plasma membrane or cytoplasm that are included in the region of interest. Conversely it is taking into account the total nuclear region which confocal slices would not.

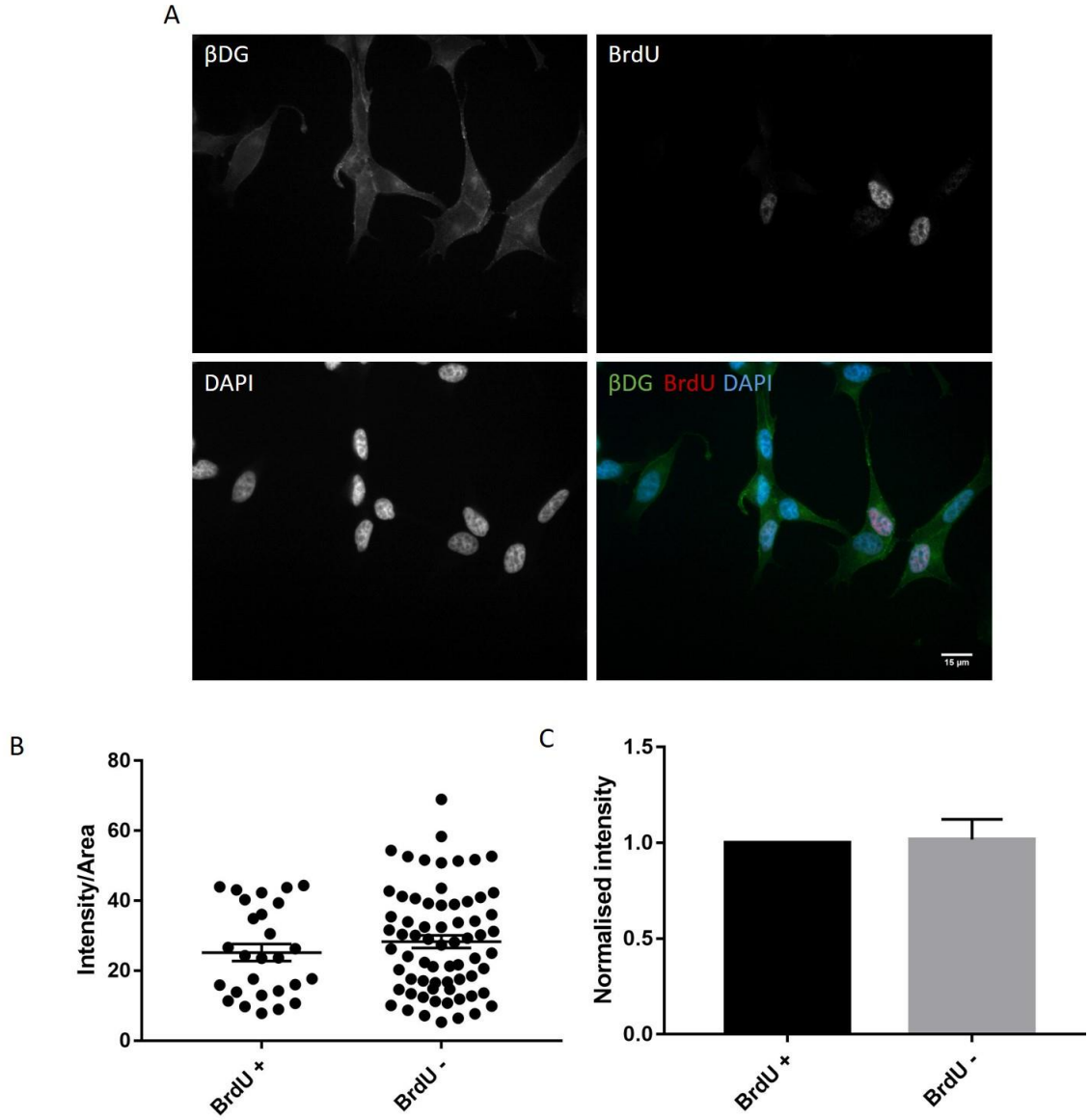

Figure 5.11 Nuclear βDG levels in BrdU positive LNCaP cells A) LNCaP cells were grown for 48 hours before being incubated with 10 µM BrdU for 1 hour at 37°C. Cells were immunostained for βDG (green) and BrdU (red). Nuclei were counterstained with dapi (blue). Images taken on an epifluorescence microscope, 63 x magnification. Scale bar 15µm. Fiji was used to create masks of the nuclei and the fluorescence intensity of βDG in the nuclei was measured. Intensity was normalised to the area of the nuclei. B) Representative graph from one replicate experiment of the fluorescence intensity of βDG normalised to the area of the nucleus in BrdU positive and BrdU negative LNCaP cells. Mean and S.E.M are depicted. C) The means of the fluorescence intensity of βDG normalised to the area of the nuclei in BrdU negative cells were found relative to that of BrdU positive cells. Error bars S.E.M. N=2, ≥80 cells per replicate.

5.2.5 βDG LOCALISATION IN THE NUCLEUS OF BRDU POSITIVE LNCAP CELLS

Although there was no detected change in the levels of βDG between the BrdU positive and BrdU negative cells, it was decided to characterise the localisation of βDG in S phase cells that were participating in DNA replication. LNCaP cells were incubated with BrdU and immunostained as described above and then imaged via confocal microscopy (Fig 5.12). BrdU was detected in specific foci in the nucleus at sites of DNA replication. βDG was detected strongly at the plasma membrane as expected and also at the nuclear envelope as previously described (Chapter 3). βDG was also detected as a faint nucleoplasmic stain with some stronger nuclear foci. The strongest foci did not appear to colocalise with the bright BrdU staining and were localised at sites likely to be the nucleoli as determined by the nuclear morphology in the DAPI staining. There was however a small degree of colocalisation of the BrdU with some of the weaker βDG foci (Fig 5.12). The localisation of βDG at the nuclear envelope and in the nucleoli did not appear to be increased in the BrdU positive cells compared to the BrdU negative cells although this was not quantified. It has been reported that the HCl treatment used in the immunofluorescence process to enable the antibody access to the BrdU might distort the localisation detected (Tang et al. 2007) and the analysis should be confirmed with 5-ethynyl-2'-deoxyuridine (EdU) incorporation, a modified thymidine analogue which does not require HCl treatment (Buck et al. 2008).

5.2.6 ANALYSIS OF βDG EXPRESSION AT DIFFERENT CELL CYCLE PHASES FROM AN ASYNCHRONOUS POPULATION

When synchronised with the double thymidine block, the LNCaP cells provided enriched populations of the different phases of the cell cycle, however, the proportions of S phase and G2M populations of cells were still low. Furthermore, whilst synchronisation is a useful tool, it can be argued that the addition of agents such as thymidine or nocodazole have broader effects on cell behaviour than just cell cycle synchronisation. Therefore, asynchronous, exponentially growing populations of LNCaP cells were stained with DNA dyes Hoechst 33342 (H33342) or propidium iodide prior to FACS analysis into G1, S and G2M populations for downstream processing.

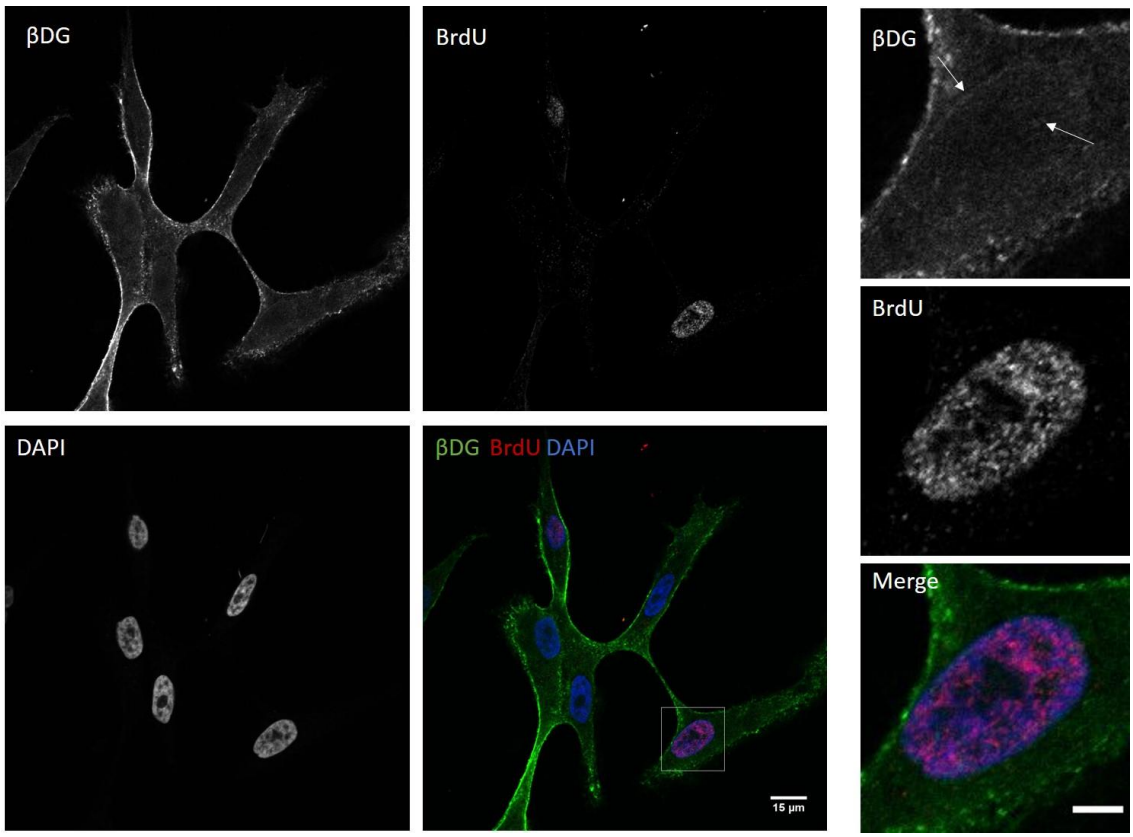

Figure 5.12. Confocal immunofluorescence of βDG in BrdU positive LNCaP cells. LNCaP cells were grown for 48 hours and incubated with BrdU as previously described. Cells were fixed and immunostained for βDG (green) and BrdU (red). Nuclei were counterstained in DAPI (blue). Images were obtained on Nikon A1 confocal. Slices from the middle of the nuclei are presented. Enlarged images of a BrdU positive nuclei (box in merged image) are shown in the panel on the right. White arrows indicated βDG at the nuclear envelope and internal nuclear foci. Scale bar 15µm and 5µm in enlarged image.

5.2.6.1 Optimisation of FACS sorting of asynchronous populations of prostate cells for cell cycle analysis

During the course of the project multiple attempts at optimising the conditions of the FACS analysis of asynchronous populations of cells were conducted.

As a receptor at the plasma membrane, the extracellular domain of βDG is exposed to external enzymes. Cells are commonly detached using trypsin-EDTA. Trypsin is a serine protease which cleaves peptide chains C-terminal to lysine or arginine residues, except when either is followed by a proline (Olsen et al. 2004). Analysis of the peptide sequence of βDG highlights multiple potential sites of trypsin cleavage within the external domain of βDG (Appendix C, Fig C.3). Indeed, lysates obtained from cells detached by trypsin incubation and immunoblotted for βDG or pY892 βDG showed a dramatic reduction in the level of full length 43 KDa βDG and an increase in the 35 KDa band. Cells detached with two different enzyme free dissociation

buffers retain the majority of the protein as 43 KDa βDG though there is a small increase in bands at 26 KDa (Appendix , Fig C.5). Subsequent FACS analysis used the Gibco enzyme free dissociation buffer so as not to cleave βDG prior to analysis.

Initial attempts at FACS sorting of LNCaP cells in which the LNCaP cells were detached with enzyme free dissociation media, stained with H33342 for 30 minutes prior to sorting and collected in PBS resulted in low yields of cells returned with a large number of cells were dying in the process of detaching and sorting the cells. Consequently, sufficient lysate extraction from the resultant populations was inconsistent (data not shown). Increasing the number of cells in the FACS experiment did not increase the yield.

It has previously been shown that reduced cell-matrix interactions in epithelial and endothelial cells can result in apoptosis in a process known as anoikis (Frisch et al. 1994, Frisch et al. 2001). It was hypothesised that the prolonged detachment of the cells necessary in the sort process was causing the cells to undergo apoptosis. In an attempt to reduce the time of detachment, cells were stained with H33342 prior to detachment with enzyme free dissociation buffer and sent immediately for sorting. In addition, the length of H33342 stain (25 minutes to 1 hour), the temperature (room temperature, ice or 37°C) and length of detachment (3- 15 minutes) and the collection temperature of the FACS sort (room temperature, ice or 37°C) were all varied in an attempt to improve accuracy and yield but showed little improvement or inconsistency in yield of cell number or lysate quality. As well as LNCaP cells, the prostate cell lines PC3 and PNT1A were also investigated. However, in all of the above cases the majority of cells still underwent apoptosis during the detachment or FACS sorting process with low yields of cells and inconsistent lysate quality. Live cell analysis was initially used as fixation can affect the quality of the protein extracted and fixation prior to FACS can alter the wavelengths and detection of dyes, however, the specificity of the phases in the live cell sorts was inconsistent, potentially as a consequence of poor H33342 staining or of a drifting population during and after sorting.

To attempt to reduce the apoptosis of the cells and to maintain the cells in their respective cell cycle phases, cells were fixed in EtOH and stained with propidium iodide prior to FACS sorting. Once again the return yields were very low. The cells are likely undergoing apoptosis during cell detachment or fixation and may be damaged during the sort process. Fixatives such as EtOH and PFA can cause difficulties for subsequent protein extraction causing protein precipitation and cross-linking respectively and EtOH fixation has been reported to result in the leaking of cytoplasmic proteins (Pollice et al. 1992). However, immunoblots following EtOH fixation of unsorted populations showed strong detection of βDG indicating a problem with

low cell yield rather than protein extraction. Further experiments combining PFA fixation with EtOH or MeOH permeabilisation may result in increased cell yield.

5.2.6.2 βDG and pY892 βDG protein expression in specific cell cycle phases from a FACS sorted asynchronous population

Although cell return yields remained low and inconsistent, it was possible to assess the levels of βDG and pY892 βDG via immunoblots in the populations of the cell cycle phases that were obtained. In the majority of cases there was little variation in the levels of βDG and pY892 βDG in the asynchronous, G1, S and G2M populations. This was the case for the LNCaP, PC3 and PNT1a cell lines tested. Figure 5.13 is an example blot from cells that were stained with H33342 for 30 minutes at 37°C whilst adhered and then sorted. The yield of G2M population in LNCaP cells was also very low and provided very low lysate concentration. Markers of different cell cycle phases for G1 (cyclin D3) S/G2 (cyclin A) and mitosis (Cyclin B1 and phospho histone H3) were included to assess the accuracy of the sorted populations (Fig 5.13). The specificity of the phases in the sorted populations was low, a recurring problem in the FACS sorts, it is therefore difficult to draw robust conclusions, however, there is no clear difference in the levels of βDG or pY892 βDG at any stage of the cell cycle.

5.2.6.3 pY892 βDG expression level in non-nuclear and nuclear fractions of cell cycle sorted populations of LNCaP cells.

When the cell yields were sufficiently high following the FACS sort the resultant populations were subject to biochemical fractionation in order to determine if there was a difference nuclear βDG in the different cell cycle phases. There was no apparent increase in the nuclear levels of full length pY892 βDG (Fig 5.14) in the nuclear fractions in asynchronous, G1 or S phase populations (Fig 5.14). Similarly, the non-nuclear levels of full length pY892 βDG did not seem to vary between the populations. It was apparent from the immunoblots that the expression profiles between the non-nuclear and nuclear fractions were strikingly different (Fig 5.14), as has been reported widely in the literature and elsewhere in this thesis (Chapter 4). The lower molecular weight 35 and 26 KDa bands could be detected in the non-nuclear but not the nuclear fractions (Fig 5.14). There were also high molecular weight bands that were present or at different strengths in the non-nuclear and nuclear fractions. The expression of these high and low molecular weight species do not appear to alter between the cell cycle phases, with the exception of the presence of some higher molecular weight species in the asynchronous nuclear fractions but not the specific cell cycle phase populations (Fig 5.14). The potential post-translational modifications resulting in the high molecular weight species and their significance have been discussed elsewhere in this thesis (Chapter 4). Further validation

of the specificity of the cell cycle stages in each population, for example by cyclin expression, is required before strong conclusions can be drawn regarding the levels of βDG in each of the phases. Furthermore, staining for βDG was weak and inconsistent in the fractionation experiments (Data not shown) and requires further optimisation.

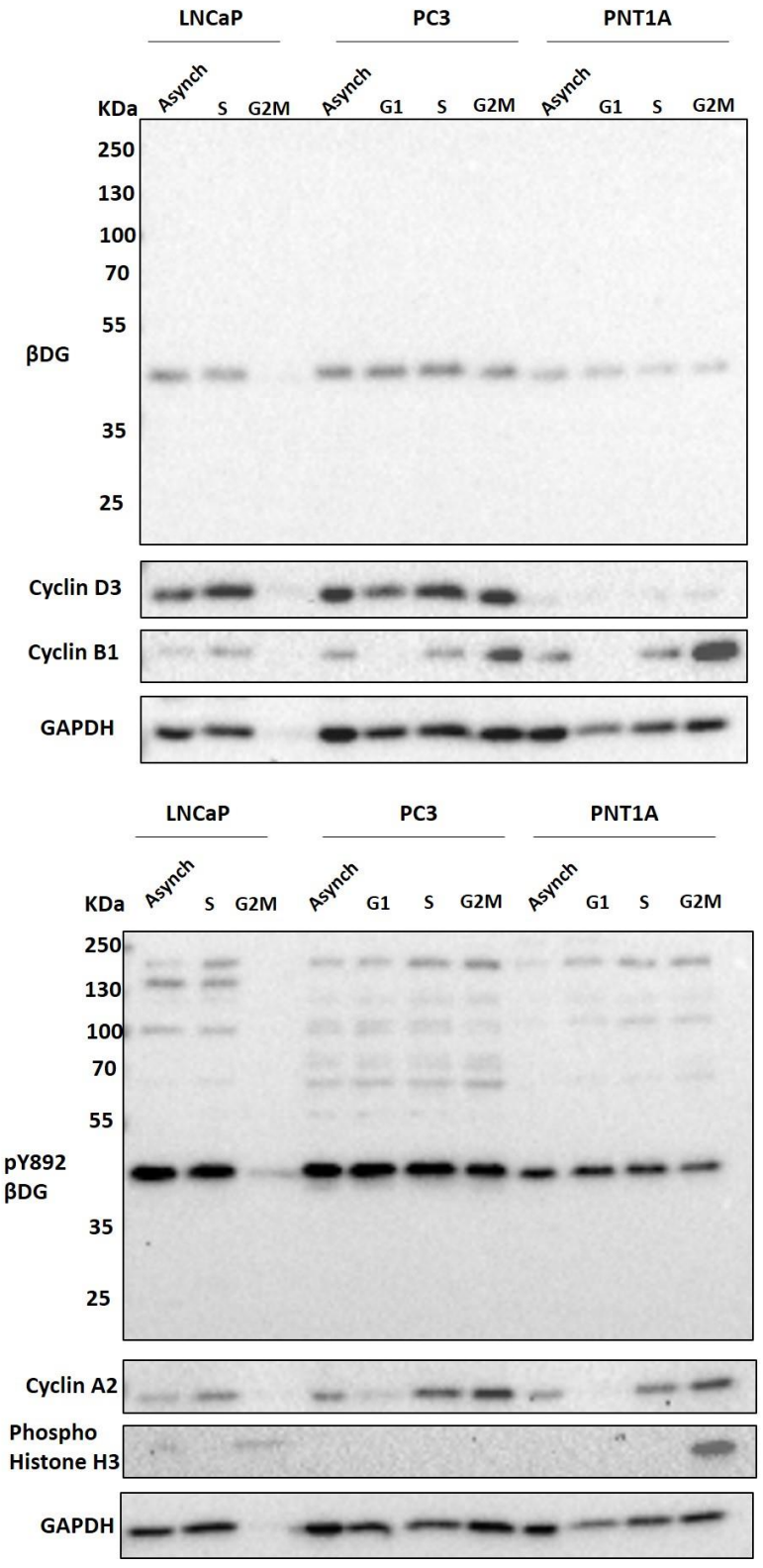

Figure 5.13 βDG and pY892 βDG levels at different cell cycle phases in FACS sorted asynchronous populations of prostate cell lines. Adhered LNCaP, PC3 and PNT1A cells were incubated with 5µg/ml H33342 for 40 minutes at 37°C. Cells were then detached with Gibco enzyme free dissociation buffer and sorted into G1, S and G2M populations on the BD Jazz FACS machine. A portion of the cells was not sorted and maintained as an asynchronous population. Total cell lysates were extracted from the resultant populations. Protein lysates were separated via SDS-PAGE and immunoblotted. Membranes were immunoblotted for βDG (top) and pY892 βDG (bottom) as well as cell cycle markers Cyclin D3, Cyclin B1, Cyclin A2 and phospho-histone H3. GAPDH was probed as a loading control.

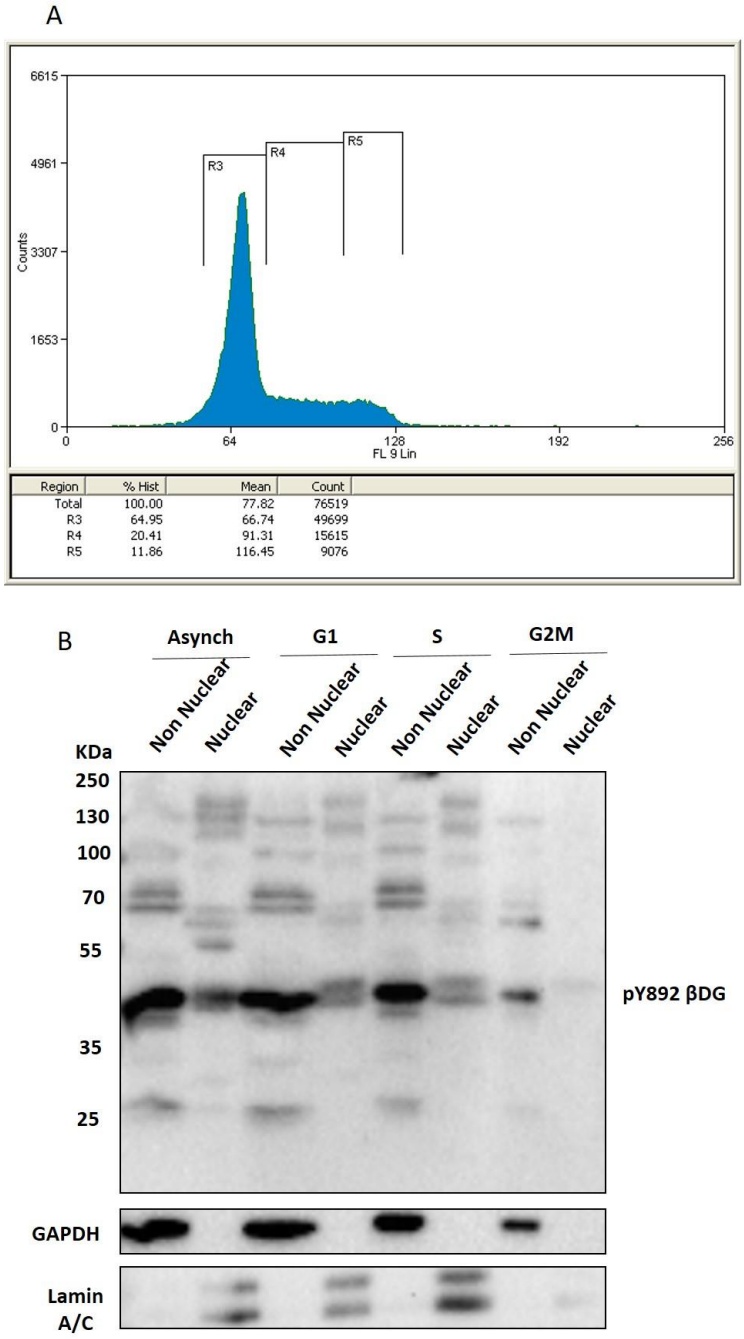

Figure 5.14. pY892 βDG levels in non-nuclear and nuclear fractions at different phases of the cell cycle. LNCaP cells were detached from the culture vessel using enzyme free dissociation buffer and incubated with 5µg/ml H33342 for 30 minutes. A) DNA histogram of H33342 stained LNCaP cells obtained from MoFlow FACS machine. Cells were sorted into G1 (R3 gate), S (R4 gate) and G2M (R5 gate) populations and an unsorted, asynchronous population was retained. B) Resultant populations underwent biochemical fractionation to obtain a non-nuclear and nuclear fraction. Fractions were run on an SDS-PAGE gel and immunoblotted for pY892 βDG. GAPDH and Lamin AC were included as loading controls and purity markers for the non-nuclear and nuclear fractions respectively.

5.2.7 βDG AND pY892 βDG PROTEIN LEVELS AND LOCALISATION IN MITOTIC LNCaP CELLS.

The division of the cell through mitosis sees dramatic rearrangements in cellular architecture, with the detachment of cells from their extracellular environment, rounding up of the cells, condensation of the DNA and breakdown of the nuclear envelope (Foisner 2003, Moir et al. 2000a, Pugacheva et al. 2006, Kunda et al. 2009). The localisation of many proteins during mitosis, particularly those within the nucleus or those actively involved in the division process is also radically different from interphase cells (Foisner 2003, Hernandez-Verdun 2011). Post-translational modifications, particularly phosphorylation events are often key regulators of the changes in cellular architecture or protein localisation (Nikolakaki et al. 1997, Ottaviano et al. 1985). Given the roles for βDG at both the plasma membrane and the nuclear envelope we decided to investigate the levels of βDG in mitotic enriched versus asynchronous populations of LNCaP cells.

5.2.7.1 Nocodazole induced G2M arrest of LNCaP cells

In order to arrest cells in mitosis, cells were treated with nocodazole. Nocodazole binds to β-tubulin, inhibiting di-sulphide bridge formation thus disrupting microtubule polymerisation. Disrupting microtubule polymerisation causes cells to arrest in G2/M due to defects in mitotic spindle formation (De Brabander et al. 1976, Jordan et al. 1992). The optimal concentration to arrest LNCaP cells in G2/M was determined by treating cells with a range of Nocodazole concentrations (50-500ng/ml) over a range of times (12, 18, 24 and 30 hours). Cells were then fixed in EtOH, stained with P.I. and the cell cycle profile determined by flow cytometry (Appendix C, Table C.1). Treatment of LNCaP cells for 30 hours with 100ng/ml nocodazole was optimal, resulting in ~72% of the cells in G2M compared to ~ 20% G2M cells in a population of cells treated with DMSO for the same length of time (Fig 5.15 A).

5.2.7.2 βDG and pY892 βDG levels in Nocodazole G2M arrested mitotic cells

To investigate if the expression levels or profiles of βDG are altered in mitotic cells LNCaP cells were treated with 100ng/ml Nocodazole for 30 hours and then the total cell lysates collected and subject to immunoblot for βDG or pY892βDG to cover the total population of βDG (Fig 5.15 B). Phospho-histone H3 was included as a marker of mitotic cells and shows a dramatic increase upon Nocodazole synchronisation of the cells. Although the immunoblots hinted at small differences between the levels of βDG and pY892βDG in the two populations, densitometric quantification of 43KD βDG (MDG) and pY892βDG (1709) did not detect a

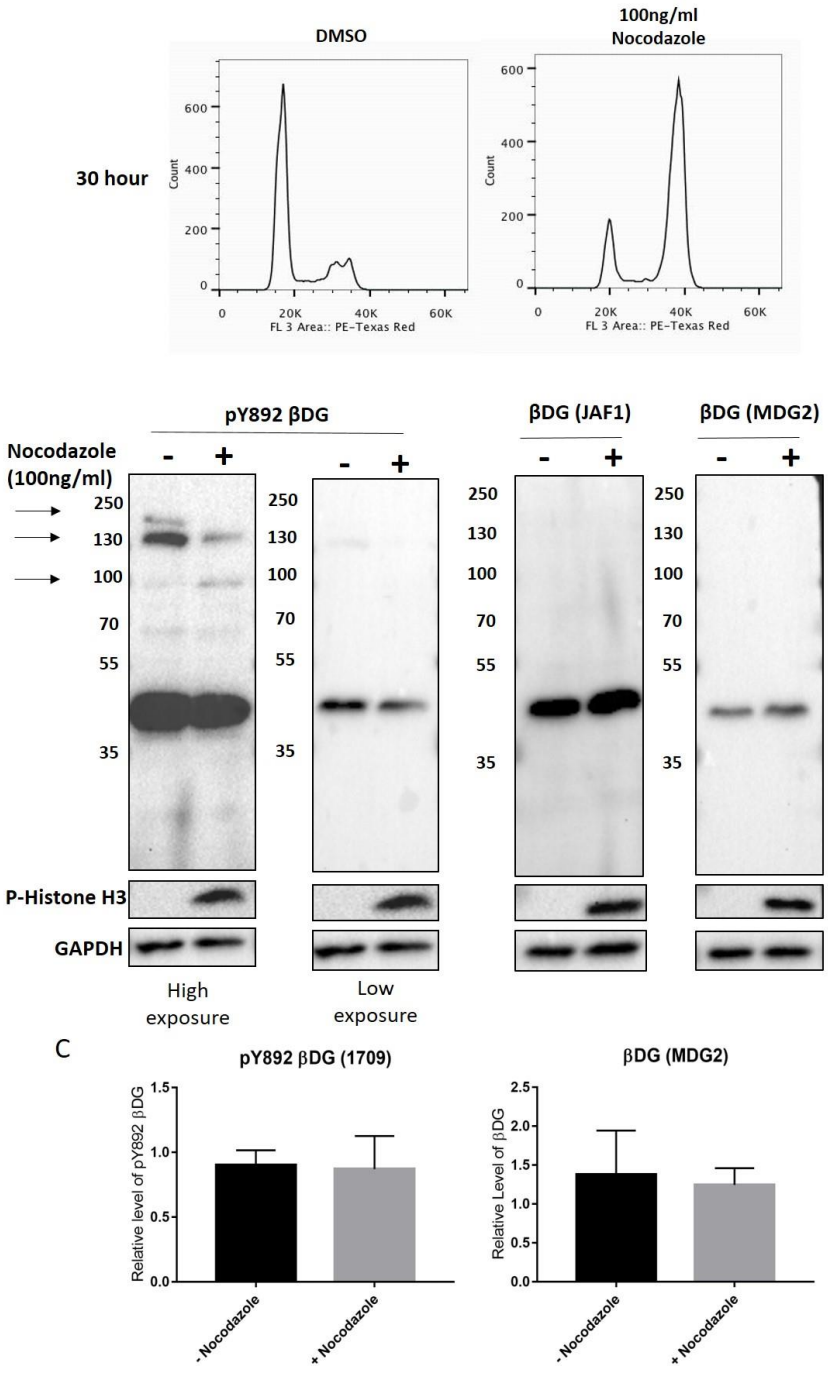

Figure 5.15 βDG and pY892 protein levels in Nocodazole induced mitotic cells. A) DNA histograms from flow cytometry analysis of propidium iodide stained, EtOH fixed LNCaP cells that had previously been treated with 100ng/ml Nocodazole or DMSO for 30 hours. B.) LNCaP cells were treated with DMSO (-) or 100ng/ml Nocodazole (+) for 30 hours. Total cell lysates were collected, run on SDS PAGE and immunoblotted. Membranes were probed for pY892 βDG, βDG with the JAF1 antibody and βDG with the MDG2 antibody. Arrows indicate bands at high molecular weight species that differ in expression between Nocodazole treated or untreated lysates. P-histone H3 (phospho histone H3) was included as a marker of mitotic cells. GAPDH was included as a loading control. C.) Quantification of 43 KDa βDG (MDG2) and pY892 βDG (1709) of DMSO and Nocodazole treated LNCaP cells. The intensity of the bands was determined via densitometric analysis and was normalised to GAPDH. Mean values and S.E.M are displayed. N=3

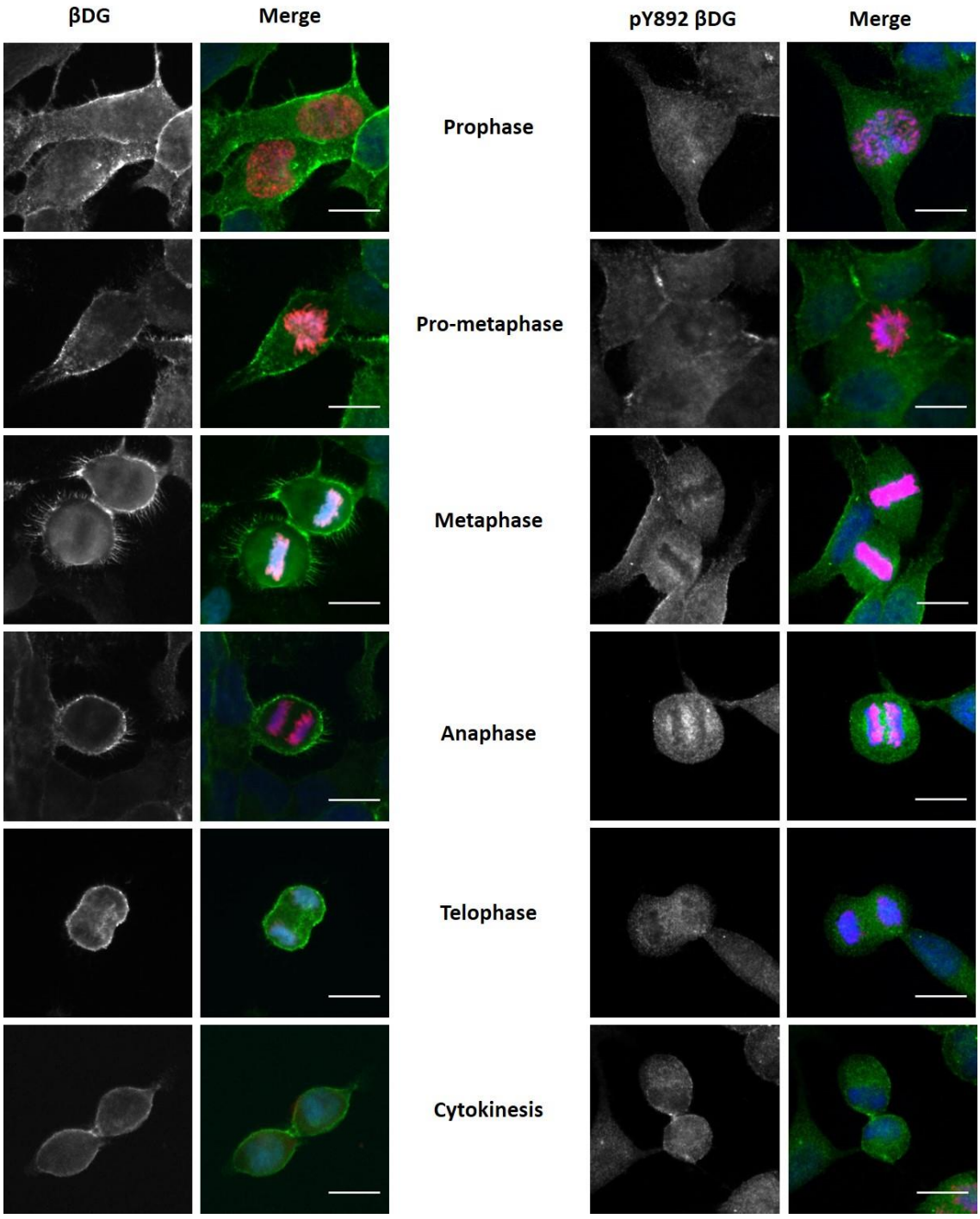

Figure 5.16 Localisation of βDG and pY892βDG in mitotic LNCaP cells. LNCaP cells were grown for at least 48 hours and then fixed for immunofluorescence analysis. Cells were immunostained for βDG (left, green) or pY892 βDG (right, green) as well as the mitosis marker phospho-histone H3 (red). DNA was counterstained with DAPI (blue). Images were obtained on an epifluorescence microscope at 63x magnification. Representative images of cells in the different phases of mitosis; prophase, pro-metaphase, metaphase, anaphase, telophase and cytokinesis, are presented. Scale bar 15 µm.

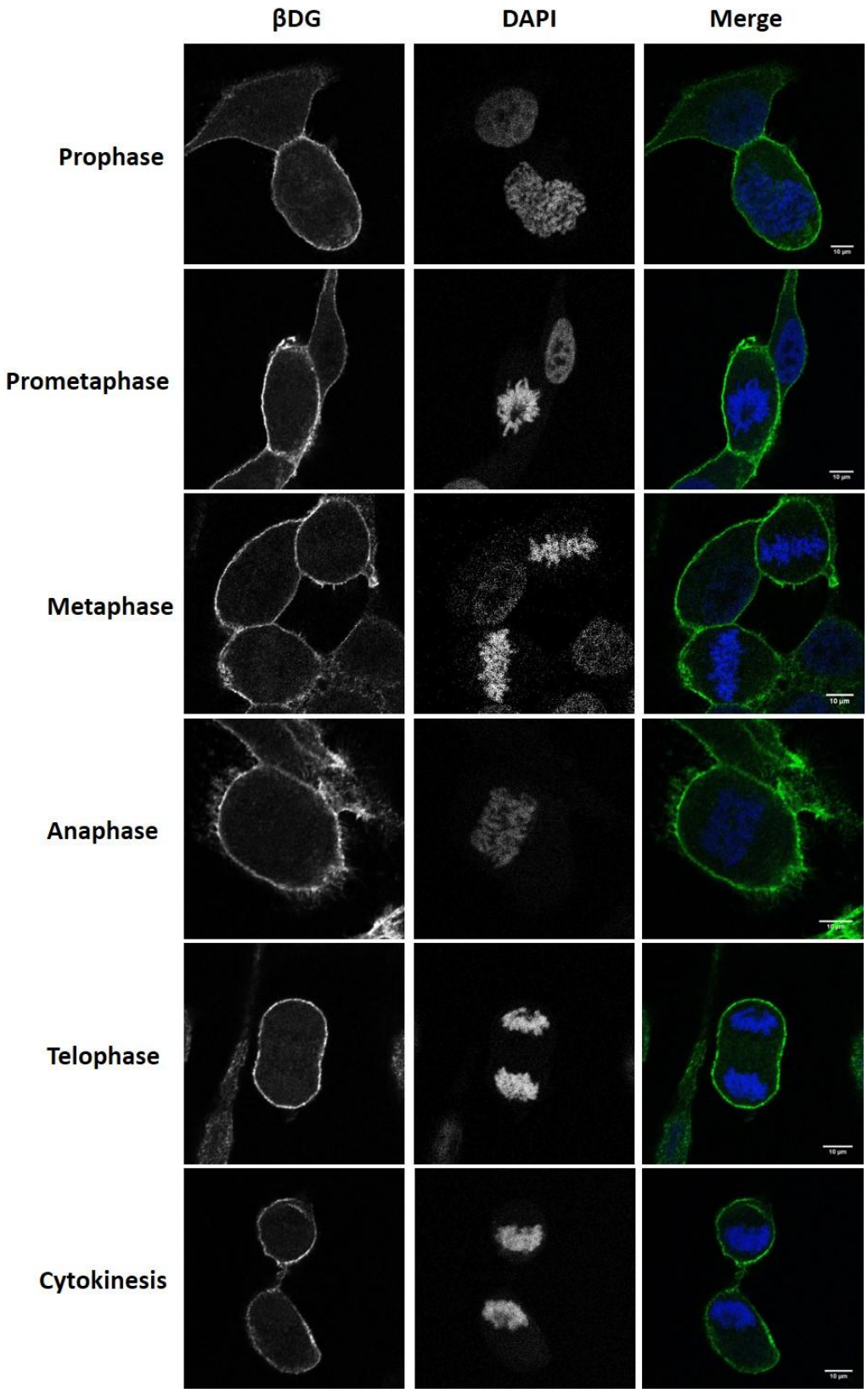

Figure 5.17. Confocal microscopy analysis of βDG localisation in mitotic LNCaP cells. LNCaP cells were grown for 48 hours then fixed for immunofluorescence analysis. Cells were immunostained with βDG (green) and the DNA counterstained with DAPI (blue). Representative confocal slice images of cells at each stage of mitosis. Images taken at 60x magnification, scale bar 10µm.

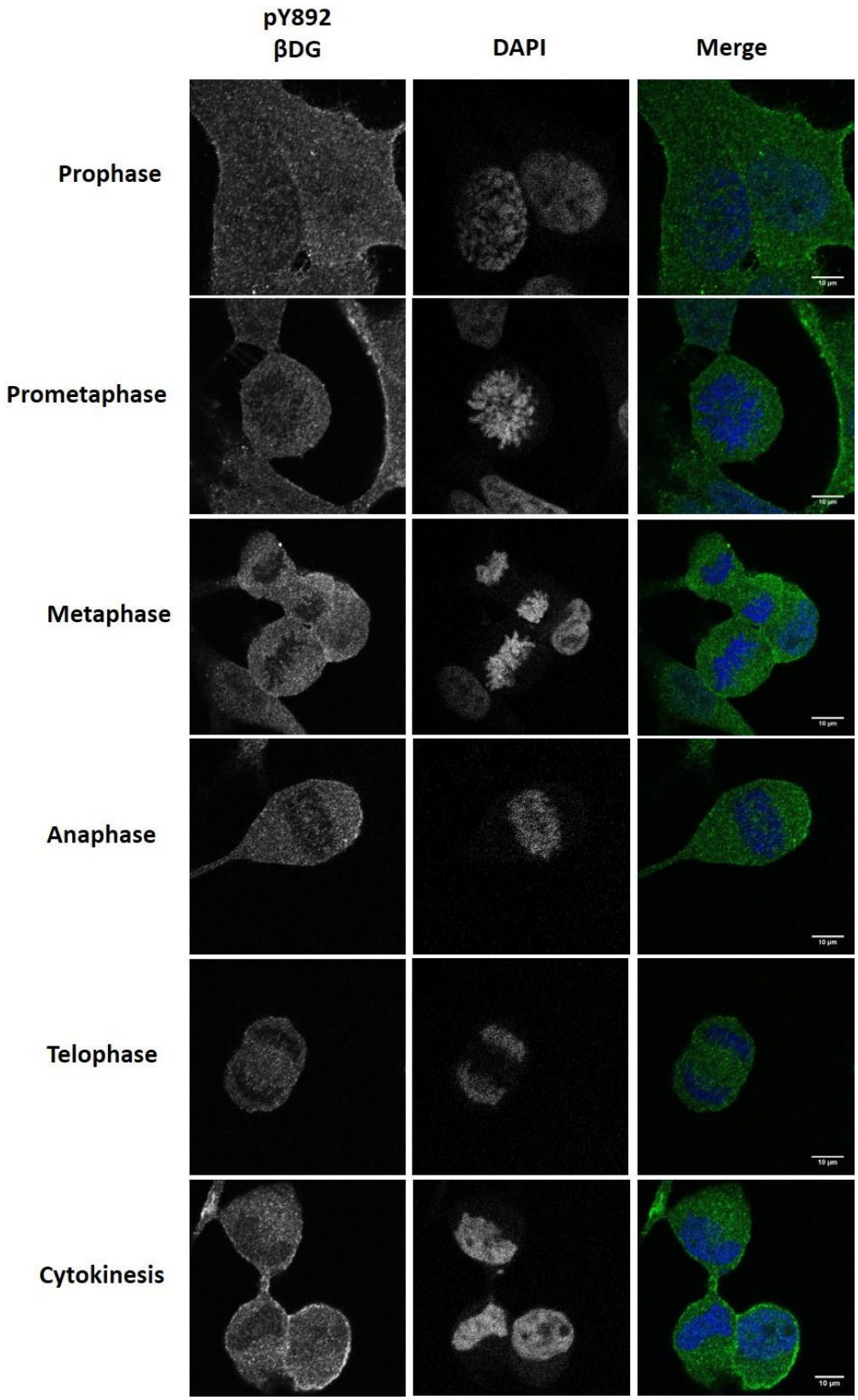

Figure 5.18. Confocal microscopy analysis of pY892 βDG localisation in mitotic LNCaP cells. LNCaP cells were grown for 48 hours then fixed for immunofluorescence analysis. Cells were immunostained with anti pY892 βDG (green) and the DNA counterstained with DAPI (blue). Representative confocal slice images of cells at each stage of mitosis. Images taken at 60x magnification, scale bar 10µm.

significant difference in the expression levels between the cells treated with nocodazole or DMSO (Fig 5.15 C). Only one repeat using JAF1 was available and therefore was not quantified. Upon increasing the exposure, high molecular weight species of pY892 βDG could be identified in control and mitosis enriched fractions (Fig 5.15 B). The level of a 130 KDa band was greatly reduced in the nocodazole treated population whilst a band at 100 KDa was slightly increased. There was also the presence of an additional band between 130-250 KDa in the control population (Fig 5.15 B). It would be interesting to determine the post-translational modifications responsible for these bands by mass spectrometry and to further investigate if these modifications can be regulated in a cell cycle dependent manner and if these modified forms of βDG have a cell cycle specific role. For example, it would be of interest to determine if βDG is phosphorylated by a mitotic or phase specific kinases which may in turn affect other PTM, including pY892 or ubiquitination.

5.2.7.3 Localisation of βDG and pY892 βDG in mitotic LNCaP cells.

To investigate the localisation of βDG during mitosis, LNCaP cells were fixed and immunostained for βDG prior to viewing via both epifluorescence and confocal microscopy (Fig 5.16, Fig 5.17). As has previously been reported, βDG localised very strongly at the plasma membrane during mitosis and can be seen in the cell protrusions and neighbouring cells (Higginson et al. 2008) (Fig 5.16, Fig 5.17). The strong βDG localisation at the cell periphery colocalises with the actin cortex formed in mitotic cells, as seen in figure 5.19 in confocal analysis of LNCaP cells co-immunostained with βDG and a fluorescently labelled phalloidin, which binds to F-actin filaments. During telophase βDG starts to accumulate at the site of formation of the cleavage furrow and localises strongly where the furrow will start to form on the apical surface of the cell and can be best seen in the orthogonal view in figure 5.19. During cytokinesis βDG localises strongly to the midbody where there is an accumulation of actin prior to abscission and the formation of the two daughter cells. The localisation at the periphery, mid body and cleavage furrow have all been described previously in the literature and can be linked to the role of βDG at the plasma membrane where it can interact with the cytoskeleton (Higginson et al. 2008).

βDG also localises to the nuclear envelope, nuclear speckles and nucleoplasm in interphase cells (Martinez-Vieyra et al, 2013, Mathew et al. 2013), however the localisation of this pool of βDG is less clear in mitotic cells. During mitosis the fate of nuclear envelope and nuclear proteins is varied being resorbed into the ER or dispersed in the cytoplasm (Foisner 2003). Analysis of confocal slices of mitotic LNCaP cells shows very faint cytoplasmic distribution of βDG in the cytoplasm of mitotic cells.

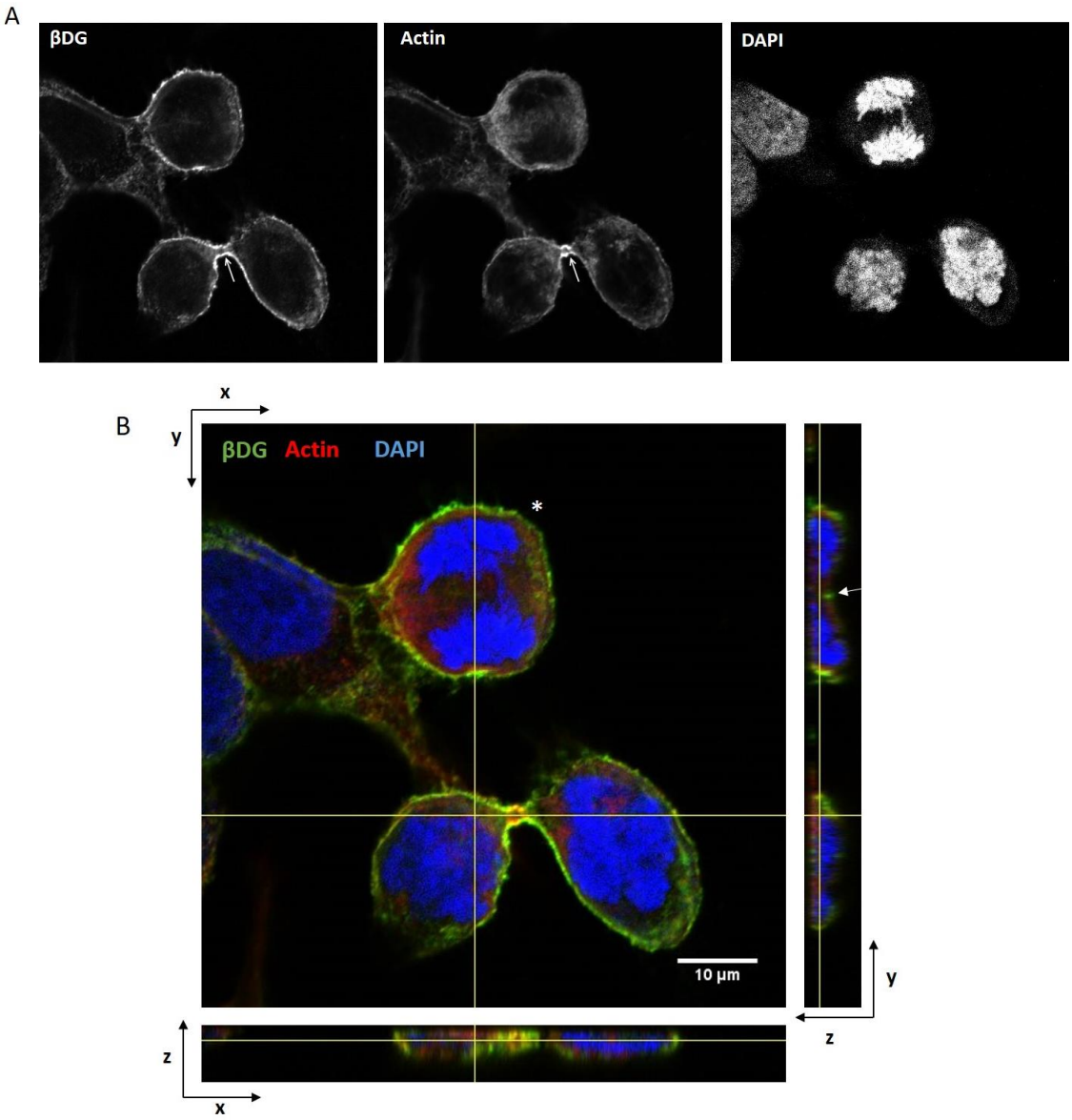

Figure 5.19 βDG and actin colocalisation in mitotic LNCaP cells. A) Representative images of confocal slices of LNCaP cells fixed and immunostained for βDG and actin (phalloidin). Arrow indicates strong localisation of βDG and actin at the midbody in a cell in late telophase/ cytokinesis. B) Merged image of mitotic LNCaP cells immunostained for βDG (green), Actin (red) and DNA (blue). Orthogonal slices along xz and yz axis are shown. White arrow in yz panel indicated βDG localisation to the top of the cleavage furrow in the late anaphase cell (white * in xy view). Xy images are confocal slices, images taken at 60x magnification, scale bar 10µm.

Co-staining of βDG with calnexin, a marker of the ER, in mitotic cells did not show a strong colocalisation (Fig 5.20). The level of βDG at the nuclear membrane is low and therefore it may be difficult to detect once the nuclear envelope has been disassembled. To further investigate the fate of βDG in mitotic cells it would be interesting to co-stain with proteins with which it colocalises in the nucleus, such as lamin A/C or B and emerin to see if they remain associated.

During the immunofluorescence analysis of mitotic cells the LNCaP cells were also stained with 1709, the antibody that detects the pY892 species of βDG (James et al. 2000) (Fig 5.17). pY892 βDG accumulated around the condensed DNA in mitotic cells, particularly during metaphase and anaphase (Fig 5.17). The strong accumulation of pY892 βDG around the condensed DNA was not detected in confocal analysis of 1709 stained LNCaP cells although occasionally a small increase in the diffuse perichromosomal staining of metaphase, anaphase and telophase LNCaP cells could be detected (Fig 5.18). It is not surprising that the accumulation is harder to detect in confocal slices, as these represent thin section of the cell compared to the sum stain observed through the total cell in the epifluoresence images. A number of proteins involved in adhesion processes, such as merlin and samp1, colocalise with mitotic spindles in mitosis, stabilising the microtubules (Solinet et al. 2013, Buch et al. 2009). 1709 detection of pY892 βDG did not colocalise strongly with the mitotic spindles themselves, as detected by co-localisation analysis with α-tubulin although a diffuse perichromosomal detection of pY892 βDG did overlap with the site of the mitotic spindle in the metaphase cells (Fig 5.21). Strikingly 1709 strongly detected the microtubule organising centre (Fig 5.21, arrows) and is discussed in detail in Chapter 6.

It was subsequently shown that 1709 exhibited non- βDG specific staining in immunofluorescence protocols however it is unclear if this localisation at the condensed chromatin is a true result or an artefact. Nuclear envelope proteins start to associate with the chromosomes as early as anaphase to initiate the reformation of the nuclear envelope after mitosis (Gautier et al. 1992, Haraguchi et al. 2001, Ye et al. 1994). Staining of mitotic DG null cells, or cells treated with anti-DG RNAi, with 1709 or the use of an affinity purified 1709 would be important in determining if the staining is artefactual. Alternatively, the localisation of a tagged version of βDG in mitosis could be investigated.

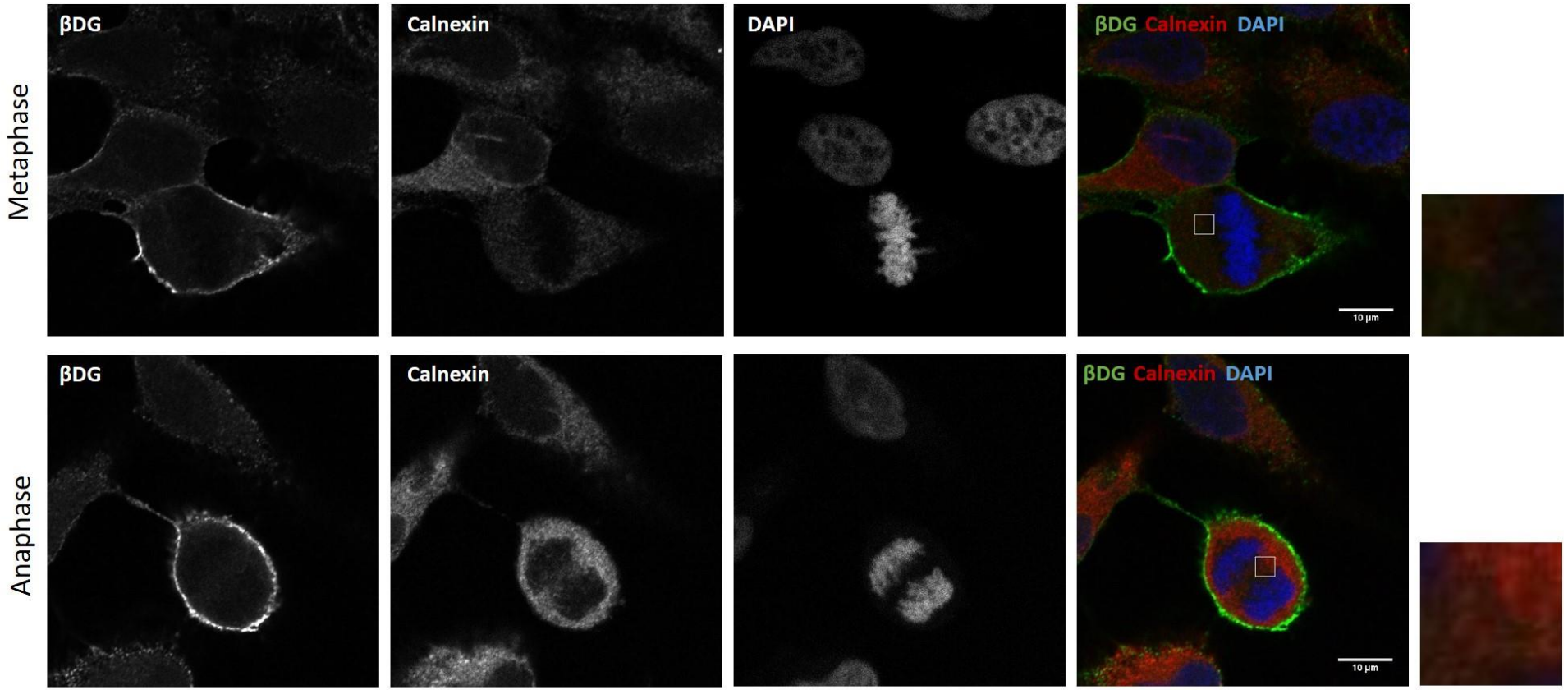

Figure 5.20 βDG and calnexin localisation in mitotic LNCaP cells. Representative images of confocal slices of LNCaP cells in metaphase (top) and anaphase (bottom). Cells were co-immunostained for βDG (green) and the ER marker calnexin (red). DNA was counterstained with DAPI (blue). Enlarged images of the white boxes indicated in the merge are shown on the right. Images taken at 60x magnification, scale bar 10µm.

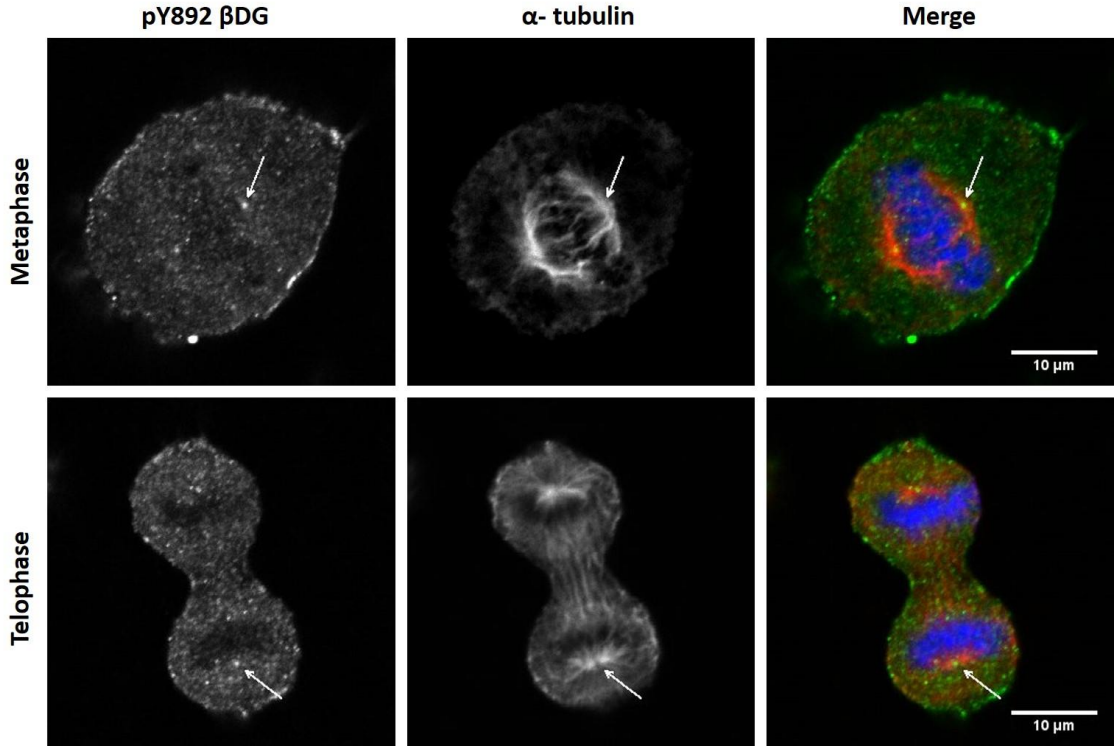

Figure 5.21. pY892 βDG does not colocalise with the mitotic spindles in mitotic LNCaP cells. LNCaP cells were fixed and co-immunostained for pY892 βDG (1709, Green) and α-tubulin (red). DNA was counterstained with DAPI. Cells in metaphase (top) and Telophase (bottom) are shown. Arrows indicate site of MTOC. Images are confocal slices taken at 60x magnification. Scale bar 10µm.

5.2.8 EXPRESSION OF ABDGFLAG REDUCES PROLIFERATION OF LNCAP CELLS

Immunoblot studies indicated that pY892 βDG may undergo greater nuclear fluctuations than βDG. Unfortunately, the 1709 antibody exhibits non-specific staining when used for immunofluorescence analysis (Chapter 3). A flag-tagged version of βDG, αβDGflag, can be detected in the nucleus as well as at the plasma membrane and detects both pY892 βDG and βDG (Section 4.2.9). Therefore, LNCaP cells were transiently transfect with αβDGflag for immunofluorescence analysis of cells at specific phases of the cell cycle. Very few αβDGflag expressing mitotic cells or cells in S phase as detected by BrdU (not shown) could be detected.

Manipulating the levels of βDG in a cell has been shown to alter the proliferation rates and cell cycle progression of a variety of cells (Sgambato et al. 2006, Hosokawa et al. 2001, Higginson et al. 2008, Mitchell et al. 2013). The proliferation of LNCaP cells transfected with αβDGflag was investigated by co-immunostaining for flag-tagged βDG and ki67, a marker of proliferation. In the non-transfected cells the number of ki67 positive and negative cells was

each about half of the population (Fig 5.22). In the case of the aβDGflag transfected cells, of which there were considerably fewer, only 15.2% of the population was ki67 positive. A DG-GFP construct and a GFP control construct was also included in the analysis to determine if the result was a consequence of the transfection process or increased DG levels. Again for both constructs, the non-transfected cells were split with approximately half of the population as either ki67 positive or negative. Both GFP and DG-GFP transfected cells had a reduced number of proliferating cells at 34.6% and 35.64% respectively, this suggests that it is the transfection process that is resulting in reduced proliferation (Fig 5.22). Having said that, the proliferation of the αβDGflag cells is about half that of the DG-GFP and GFP cells, which could be a consequence of the high levels of αβDGflag expressed. Mitchell et al. previously demonstrated a reduced rate of proliferation in LNCaP cells overexpressing βDG (Mitchell et al. 2013).

In confocal immunofluorescence analysis of αβDGflag in ki67 positive cells, βDG was detected accumulation at distinct foci within the nucleus however there was very little colocalisation with the ki67 positive structures (Fig 5.22 B). There is also a faint nucleoplasmic and nuclear envelope stain. The localisation of βDG within the nucleus did not appear to differ between Ki67 positive and negative cells. It is difficult to quantify the levels of βDG in the nucleus with the αβDGflag transfected cells due to the variable levels of expression in the transiently transfected population. Stably expressing cell lines may give a clearer indication on if there is a quantifiable change in the levels of βDG in the nucleus of proliferating cells.

5.2.9 ABDGFLAG LOCALISATION IN NOCODAZOLE ARRESTED MITOTIC LNCAP CELLS.

In order to assess if the perichromosomal accumulation of pY892 βDG detected by 1709 antibody in mitotic cells is a true localisation αβDGflag immunofluorescence studies were conducted. To enrich for mitotic cells, LNCaP cells were transfected with αβDGflag and grown for 24 hours prior to 18 hours treatment with 100ng/ml nocodazole. The treatment time was chosen as a balance between LNCaP recovery time after transfection, sufficient length of nocodazole treatment for mitotic arrest and to retain good expression level of αβDGflag, which has been shown to degrade rapidly (Section 4.3.6). Cells were then fixed and immunostained with anti-flag and viewed via confocal microscopy (Fig 5.23). Very few mitotic cells were observed and non-quantified observations indicated high levels of apoptosis. This may be because the combination of transfection and nocodazole treatment was too stressful for the cells or because increased levels of βDG make the cells sensitive to nocodazole treatment. Nocodazole disrupts microtubules and inherently causes an ‘abnormal’ mitosis, which may affect the localisation of βDG (De Brabander et al. 1976, Jordan et al. 1992). Nonetheless βDG localisation once again was strong at the periphery of the cells. The cytoplasmic stain was more punctate than observed with MDG2 staining. Whilst there was no

strong stain around the condensed DNA in the nocodazole treated cells (Fig 5.23), it is important to note that these cells are not in the mitotic phases (metaphase, anaphase and telophase) where the accumulation of endogenous protein was previously detected by anti-pY892 βDG antibody(Fig 5.16). Unfortunately, likely due to the low number of transfected cells and the time course of the experiment, only LNCaP cells in prophase and prometaphase were detected.

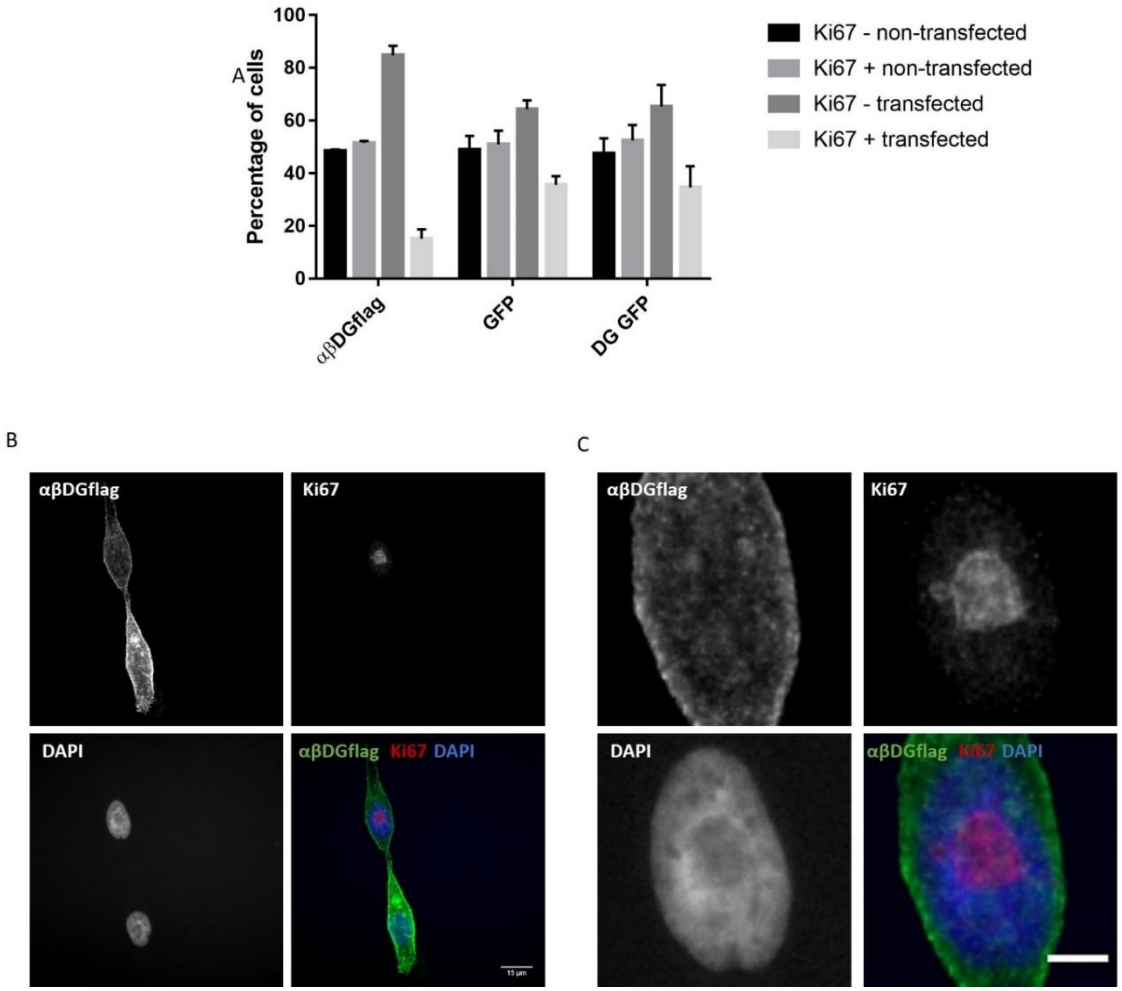

Figure 5.22 Proliferation and βDG localisation in βDG overexpression LNCaP cells. A) Proliferation of DG transfected LNCaP cells. LNCaP cells were transfected with αβDGflag, GFP or DG-GFP and grown for 48 hours. Cells were then immunostained for proliferation marker ki67 and αβflag in the case of the flag tagged DG construct. Images were obtained via epifluorescence microscopy. Cells were then quantified as transfected or non-transfected and within these populations as Ki67 positive (+) or Ki67 negative (-). The percentage of ki67 + or – cells was then calculated for the transfected and non-transfected populations. N=2, ≥ 300 cells per construct, Error bars SEM. B) Localisation of αβDGflag in Ki67 positive cells. LNCaP cells transfected with αβDGflag for 48 hours were fixed and immunostained for αβDGflag (green) and ki67 (red) nuclei were counterstained with DAPI (blue). Images are confocal slices taken at 60x magnification. Scale bar 15 µm. C) Enlarged image of ki67 nuclei from B). Scale bar 5µm.

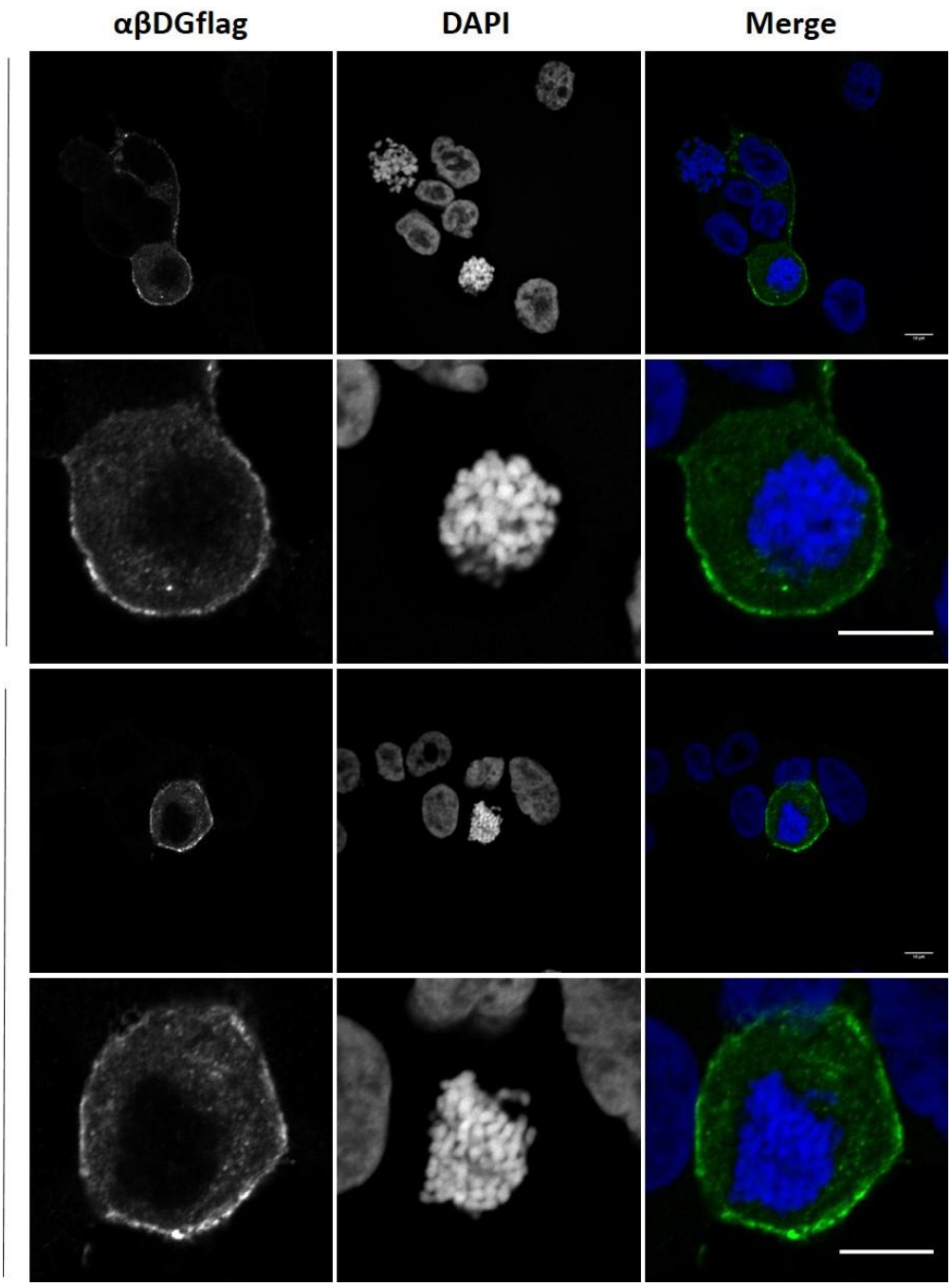

Figure 5.23. αβDGflag localisation in Nocodazole induced mitotic LNCaP cells. LNCaP cells were transfected with αβDGflag and grown for 24 hours. Cells were then treated with 100ng/ml Nocodazole for 18 hours. Cells were fixed and immunostained for αβDGflag (M2 flag, green). DNA was counterstained with DAPI (blue). Two representative images are shown with enlarged images of the 'mitotic' αβDGflag transfected cells. Images taken at 60x magnification. Scale bars, 10µm.

5.3 DISCUSSION

Different stages of the cell cycle see vast changes in cell morphology, interaction with the extracellular environment, DNA replication, signal transduction pathways and growth (Walker et al. 2005, Pugacheva et al. 2006 Budirahardja et al. 2009, Caldon et al. 2010, Frisch et al. 1994). Accordingly, the levels, localisation and activity of proteins involved in these processes is often regulated in a cell cycle dependent manner (Pugacheva et al. 2006, Dabauvalle et al. 1999, Balk et al. 2008, Muranen et al. 2005). A complex relationship between βDG and the cell cycle has long been reported but is by no means fully understood (Sgambato et al. 2006, Hosokawa et al. 2001, Higginson et al. 2008). It has been shown that modulating the levels of βDG can increase or decrease the rate of proliferation (Sgambato et al. 2006, Hosokawa et al. 2001, Higginson et al. 2008, Mitchell et al. 2013). An increased level of βDG has been reported in proliferating cells, furthermore, the levels of βDG mRNA and protein have been shown to be regulated in a cell cycle dependent manner in different cell lines, increasing in S phase (Sgambato et al. 2006, Hosokawa et al. 2001). Interestingly, there is a differential expression of βDG in the nuclei of cells in an asynchronous population of proliferating cells (Mitchell et al. 2013, Mathew et al. 2013, Leocadio et al. 2016, Martinez-Vieyra et al. 2013). Moreover, in growth arrested LNCaP cells stimulated into proliferation either by addition of androgen or serum there was a time dependent fluctuation in the nuclear levels of βDG (Mathew et al. 2013, Mathew 2011 Thesis). We therefore hypothesised that there was a cell cycle dependent regulation of the nuclear localisation of βDG.

5.3.1 A POTENTIAL FLUCTUATION IN THE TOTAL LEVELS AND NUCLEAR ACCUMULATION OF BDG AND PY892 IN A CELL CYCLE DEPENDENT MANNER

In this work we demonstrate mild fluctuation in the levels of full length βDG and pY892 βDG total cell lysates as well as in non-nuclear and nuclear lysates following the thymidine synchronisation and release of LNCaP cells into the cell cycle (Fig 5.4, Fig 5.7, Fig 5.9). Furthermore, following quantification of immunoblots, a weak, positive correlation was found between the levels of full length βDG and pY892 βDG within populations of cells with higher percentages of S phase cells (Fig 5.5) in support of the previously reported observations of increased levels of βDG in S phase cells in the literature (Sgambato et al. 2008). Interestingly, this correlation extended to the levels of pY892 βDG within the nucleus of S phase cells, though not the non-phosphorylated Y892 species of nuclear βDG. It is important to note that there is a report that GAPDH levels may be regulated in a cell cycle dependent manner in normal human cells, with slightly reduced levels in S phase (Mansur et al. 1993). It is therefore

possible that the GAPDH normalised data may over report the increased levels of βDG in S phase. It would therefore be important to repeat these experiments with an alternative loading control, such as the total protein loaded onto the gel to verify the potential fluctuation of the levels of βDG. Furthermore, the potential S phase dependent changes on the levels and localisation of βDG and pY892 βDG were not supported in analysis of lysates from cell cycle phase populations sorted by FACS analysis of an asynchronous population, in which the levels of both phosphorylated and non-phosphorylated species of βDG stayed relatively constant (Fig 5.14, Fig 5.13).

As previously discussed a problem encountered throughout this analysis was obtaining LNCaP populations sufficiently enriched for specific phases of the cell cycle (Fig 5.3, Fig 5.13), thus making it difficult to draw strong conclusions regarding the levels of βDG and potentially masking subtle changes in βDG distribution.

LNCaP cells have a relatively long doubling time of 32-34 hours and a long lag phase whilst they recover and adhere to the substrata following seeding. Whilst the LNCaP cells were grown for the 48 hours normally required to exit lag phase (Van Steenbrugge et al. 1991, Cunningham et al. 2015), it is possible that the LNCaP cells are not at exponential growth at the time of treatment, thus maintaining a sub population in G0 that are not synchronised by the thymidine block. Timing is crucial for tight synchronisation of cells (Bostock et al. 1971). Although a double thymidine block appeared to tighten the synchronisation, the synchronised subpopulation remained relatively small (Fig 5.6). Following thymidine block, cells are not arrested completely at the G1/S phase border, rather the rate of DNA synthesis slows and the length of S phase increases (Bostock et al. 1971, Thomas et al. 1975). The long doubling time of LNCaP complicates the timings of thymidine treatment as it must be long enough for the majority of cells to reach the G1/S restriction site but not too long for cells to progress out of S phase. Alternative methods of synchronisation of cells such as isoleucine blocks or Nocodazole blocks in mitosis are also available (De Brabander et al. 1976, Cifuentes et al. 2003). It would also be beneficial to use different cell lines with higher rates of proliferation, such as PC3 or PNT1A, to assess the levels of βDG in a synchronised population of cells.

In the case of the FACS sorted asynchronous cells the main problem was a low yield of return of cells as previously discussed. In an asynchronous population of LNCaP cells approximately 75% are in G1/G0, therefore there is already a low collection of S phase and G2M populations (Fig 5.3). In the case of unfixed samples, the cells may have undergone anoikis (Frisch et al. 1994, Frisch et al. 2001). The specificity of the live cell sorts was poor despite varying the conditions of treatment with H33342 (Fig 5.13) potentially as a consequence of the wavelength detection or cell populations drifting after sorting. It is likely that the length of the sort and the

forces applied during the process to cells that are already delicate following detachment or fixation causes further damage or apoptosis (Pollice et al. 1992). There are cell cycle reporter constructs, such as Fluorescent-ubiquitin based cell cycle indicators (FUCCI) that fluorescently report different phases of the cell cycle in live cells (Sakaue-Sawano et al. 2008). The fucci construct could be used as an alternative to the DNA ploidy based FACS sorting and may result in improved phase specificity.

In immunofluorescence analysis an increase of βDG in the nucleus of S phase cells, BrdU positive LNCaP cells was not detected (Fig 5.11). This correlated with the results from the thymidine synchronisation data that βDG levels in the nucleus fluctuated very little. Affinity purification of 1709 or analysis with a tagged construct of βDG will be important in analysing the nuclear levels of βDG in the future. Transfection of LNCaP with a flag tagged version of βDG resulted in reduced proliferation, thus very low numbers of S phase cells, and inconclusive results for BrdU analysis. The co-transfection of a fluorescently tagged βDG along with a cell cycle reporter such as fucci is an attractive option to look at the fluorescent levels of βDG in the nucleus in real-time, provided the issue of where to place the tag could be resolved.

Although no definitive conclusion can be reached from the analyses in this chapter regarding a cell cycle dependent regulation of nuclear βDG that does not mean it can be excluded. There may be a fluctuation within a tight time frame that is missed in these experiments because of the time points or sensitivity of the experiments. A number of proteins undergo sudden fluctuations in nuclear localisation. Merlin, a protein that is structurally related to the ERM proteins, accumulated in the nucleus in early G1 in a manner that was dependent of cell attachment but was exported from the nucleus in late G1 (Muranen et al. 2005).

The levels of pY892 βDG in the nucleus are more variable than the non-phosphorylated form (Fig 5.9, Fig 5.10). It would be interesting to determine if a cell cycle specific nuclear localisation or role requires phosphorylation at this residue. Mutating pY892 did not prevent the nuclear localisation of βDG in LNCaP or HeLa cells (Lara-Chacon et al. 2010, Leocadio 2015, Thesis), however these studies were in asynchronous populations, thus any cell cycle subtleties may have been masked. Phosphorylation at Y892 modulates the interaction of βDG with binding partners of its cytoplasmic domain (Ilsley et al 2001, James et al. 2000, Yang et al. 1995) and this may also be the case in the nucleus, with potential cell cycle dependent roles. An important question is if the increased nuclear pool of βDG has been internalised from the plasma membrane or is a separate population of βDG. A number of cell surface proteins, such as the growth factor receptors FGFR and EGFR, are internalised from the plasma membrane and subsequently translocate to the nucleus (Planque 2006, Lo et al. 2005, Schausberger et al. 2003). Phosphorylation at Y892 occurs in an adhesion dependent manner and promotes the

internalisation of βDG (James et al. 2000, Sotgia et al. 2003, Miller et al. 2012). It is therefore possible that the increased pY892 form in the nucleus is a consequence of its internalisation from the membrane rather than its cell cycle dependent nuclear targeting per se, though either or both of these processes could still be occurring in a cell cycle dependent manner or to facilitate cell cycle dependent nuclear functions. Biotinylation studies suggest that at least a pool of βDG is internalised from the PM (Vasquez-Limeta et al. 2014). It would be interesting to perform a pulse chase biotinylation study in cell cycle phase specific conditions to determine if internalisation and nuclear accumulation of βDG from the PM is altered between the phases.

Alternatively, there may be additional phosphorylation or other post-translational modification events that could regulate βDG in a cell cycle manner independently of, or in tandem with, phosphorylation at Y892. Indeed, in the nuclear fractions, higher molecular weight species of βDG were detected with an antibody recognising pY892 βDG and the levels of these species varied in the thymidine treated synchronised cells but not the FACS sorted populations (Fig 5.9). Interestingly, ELM analysis identifies two potential sites of phosphorylation by CDKs within the cytoplasmic tail of βDG at residues T850 and T884 (Gould et al. 2010). CDKs are proline directed kinases with a consensus sequence of xx[S/T]Px[K/R] (Songyang et al. 1994). Whilst there are no reported incidences of βDG phosphorylation at T850, multiple studies have identified phosphorylation at T884, as reported by phosphosite plus (Hornbeck et al. 2014). Furthermore, there are two identified consensus sequence sites for recognition by cyclin proteins within βDG (Gould et al. 2010). Binding of cyclins at these sites increases the interaction of a substrate with cyclin-CDK complexes thus facilitating their phosphorylation. The potential for βDG interaction with or modulation by key components of the cell cycle regulatory machinery is interesting and the introduction of mutations at these sites might highlight a cell cycle dependent role or regulation of βDG.

βDG can be seen at the nuclear envelope, nuclear foci and nucleoplasm of cells across different phases in an asynchronous population (Fig 5.11) (Martinez-Vieyra et al. 2013, Lara-Chacon et al. 2010, Mathew et al. 2013, Mitchell et al. 2013, Oppizzi et al. 2008). One could hypothesise from these observations that there is a basal level of βDG in the nucleus fulfilling a role that is not cell cycle phase dependent, for example, the proposed structural function of βDG at the NE, whereby βDG plays a role in maintaining nuclear morphology (Martinez-Vieyra et al. 2013). A role for βDG at a specific phase of the cell cycle may not necessitate a detectable change in the level of the protein in the nucleus or there may then be an influx of βDG to perform an as yet unidentified specific role at a certain phase of the cell cycle. Correlation analysis of the levels of βDG in the nucleus of thymidine synchronised cells hinted

at a potential increase with a higher population of cells in S phase, although this was not confirmed in FACS sorted populations or immunofluorescence quantification in BrdU cells. Increased levels of βDG at S phase of HC11 and BAE cells have previously been reported (Sgambato et al. 2006, Hosokawa et al. 2001). Furthermore, cells in which the DG level has been reduced by RNAi have displayed delays in entering or exiting S phase (Sgambato et al. 2008, Higginson et al. 2008). It is therefore interesting to speculate at a role for βDG in the nucleus of S phase cells or S phase progression.

As previously discussed, dystroglycan has been reported to modulate the activity of ERK in both a spatial and temporal manner. ERK has vital roles in G1 to S phase progression of the cell cycle (Chambard et al. 2007, Torii et al. 2006). Importantly a biphasic activity of ERK is required for cell cycle progression with an initial brief period of activity being sufficient to stimulate the expression of early genes such as c-fos, however a longer, sustained activity of ERK is necessary for the stabilisation and activity of the gene products and only in these conditions can cells progress through G1 phase of the cell cycle (Torii et al. 2006, Murphy et al. 2004). It is interesting to hypothesise, therefore that βDG could act as a scaffold to modulate ERK localisation or activity in the nucleus which may ultimately have a role on cell cycle progression. It would be particularly interesting to study the nuclear localisation of βDG and ERK in parallel throughout the progression of synchronised cells.

βDG may play an active role in the nucleus during S phase and this may not necessarily require an increase in its protein level. In a mass spectrometry study of proteins identified from an IP with αβflag in the nuclear fractions of LNCaP cells proteins involved in DNA replication were identified. Namely these were proteins of the mini-chromosome maintenance (mcm) complex; mcm2, 4, 5 and 7 (Leocadio, 2014). The mcm complex consists of 6 related helicase proteins and is important for initiation and elongation of DNA replication. The mcm genes are transcribed during late M and G1 phase whereby they are translocated to the nucleus and loaded onto origins of replication (Lei 2005). Here we show that βDG does not colocalise to active sites of DNA synthesis, as detected by BrdU labelling, supporting the observation previously published in C2C12 cells (Martinez-Vieyra et al. 2013). However, it has been reported that whilst a subset of mcm complex travels along the DNA with the replication fork, the majority of mcm proteins are not found colocalised with sites of DNA synthesis but as speckles within the nucleus where they modulate chromosome dynamics (Forsburg 2004, Krude et al. 1996). βDG may therefore interact with mcm proteins at these sites, though the putative interaction requires further colocalisation and binding studies.

Interactions between βDG and LINC complex components have been proposed (M. Laredo and S. Winder). MEFs from *SUN1-/- SUN2-/-* mice displayed an early cell cycle arrest in S phase

and an increased number of apoptotic cells compared to controls (Lei et al. 2012). The arrest in S phase was attributed to disrupted DNA damage response in these cells through interaction with DNA-dependent protein kinase (DNAPK) and ultimately through an ATM mediated response (Lei et al. 2012). Cells in which βDG has been reduced displayed an accumulation of cells in S phase and high levels of apoptosis (Sgambato et al. 2006, Higginson et al. 2008). In the mass spectrometry study D. Leocadio also identified DNAPK to be pulled down in IP with βDG (D. Leocadio, 2014). The interaction remains to be validated and could be direct or indirect through complexes potentially involving SUN proteins.

βDG may also have more passive roles in interphase and S phase in its role in the structure of the NE. Lamins and their interacting proteins LAPs can interact with the chromatin and whilst there is a structural element to this there may also be a regulatory role (Cai et al. 2001, Spann et al. 1997, Foisner 2003). Correct lamin organisation is required for DNA synthesis during S phase with arguments for both indirect or direct roles (Moir et al. 2000a, Spann et al. 1997). Those in support of an indirect role suggest that the lamina provide support to the nuclear envelope thus allowing for efficient accumulation of replication factors in the nucleus and thus DNA synthesis (Walter et al. 1998). However, there is strong evidence in support of a direct role based partly upon the observation of colocalisation of lamin B at nucleoplasmic foci with markers of DNA replication such as PCNA (Spann et al. 1997). Furthermore, expression of dominant negative lamin helped to identify a specific role in the elongation phase of DNA replication for organised lamins (Moir et al. 2000c). Whilst βDG does not localise to regions of active elongation it does help to regulate lamin organisation. Thus delays in S phase in DG RNAi cells may, in part, be attributed to disruption of lamins within the nucleus.

When studying proliferation in LNCaP cells it would be remiss to not discuss the role of the androgen receptor. During normal tissue development and homeostasis the androgen receptor plays an important role in driving epithelial cell proliferation (Balk et al. 2008, Koryakina et al. 2015). In prostate cancer, during the process of transformation the proliferation of cells through the AR pathway become autonomous (Balk et al. 2008, Yuan et al. 2006). LNCaP cells contain functionally active AR and respond to DHT treatment (Horoszewicz et al. 1983). A prerequisite of AR action is its translocation to the nucleus whereby it can bind to ARE in target genes or interact with co-activators or repressors (Balk et al. 2008). There are a number of potential ways in which the AR could influence the nuclear accumulation of βDG

As previously mentioned, androgen stimulation results in increased levels of cyclin D and cell cycle progression (Koryakina et al. 2015). Given the presence of putative cyclin interaction and CDK consensus sequences in βDG it would be interesting to investigate if cyclin D-CDK4/6

complexes can interact with and regulate βDG and potentially its nuclear localisation. To further dissect the roles of the AR and the cell cycle the nuclear translocation of βDG in synchronised or cell cycle phase sorted populations of cells negative for the AR should be tested. The later was attempted with H33342 FACS sorts of PC3 cells, however the results were inconclusive.

It is known that androgen treatment results in an increase in βDG at both the transcriptional and protein level. There is also a degree of cross-talk between the AR and pathways known to regulate βDG. In a study in mouse prostate epithelium when both c-src and AR levels were enhanced there was strong activation of the src kinase signalling pathway and enhanced AR activity (Cai et al. 2011). Src is the kinase responsible for phosphorylation at Y892 and as previously discussed there is a greater fluctuation in the nuclear levels of this species of βDG. It is possible to speculate c-src activity further modulated by AR activity in androgen responsive cell lines could contribute to the nuclear translocation of βDG to the nucleus. Additionally, stimulation of AR activity in LNCaP cells also sees induction of ezrin phosphorylation at residues T567 and Y353 by PKC and src kinases respectively (Chuan et al. 2006). Interestingly overexpression of a T567D phosphomimetic active form of ezrin resulted in an increased nuclear translocation of βDG (Vasquez-Limeta et al. 2014). This ezrin mediated translocation of βDG to the nucleus appeared to require F-actin and moreover was only a means of nuclear translocation for cytoplasmic, not membrane associated βDG (Vasquez-Limeta et al. 2014). It is therefore possible that the androgen activity, which varies throughout the cell cycle, could influence the nuclear translocation of a pool of βDG in an ezrin dependent manner.

Although no interaction between βDG and the AR was detected in a previous study it is still possible that they could enter the nucleus as part of a complex (Mathew et al. 2013). The nuclear translocation of both βDG and the AR to the nucleus occurs in a manner dependent on importin and Ran pathways (Lara-Chacon et al. 2010, Kaku et al. 2008). RanBPM is an AR coactivator and interestingly RanBPM has been identified as an interacting partner of βDG in a yeast-two hybrid screen (Winder lab, unpublished observations). It is therefore possible that βDG could form a complex with RanBPM and the AR and be shuttled to the nucleus in an AR dependent manner though interaction studies would be required to test this.

5.3.2 Dystroglycan localises to the cell periphery and midbody in mitotic LNCaP cells

During mitosis a large number of proteins see vast changes in their regulation and localisation. This is particularly the case for cell adhesion molecules as the cell contacts with the substrate are minimal during mitosis as the cell rounds up (Pugacheva et al. 2006, Kunda et al. 2009), and for components of the nuclear envelope which must break up and reform in a timely manner to allow for cell division (Fosnier 2003). βDG is a protein that has functions at both of these localisations thus we were interested in its localisation throughout mitosis, which may hint at the fate and potential additional cell cycle roles for this multifunctional protein.

In LNCaP cells arrested in mitosis by nocodazole treatment there was very little change the non-phosphorylated or pY892 forms of βDG (Fig 5.15). There were small changes in the levels of some of the higher molecular weight species of βDG between nocodazole treated and untreated samples as detected by this antibody. The modification and functions of these high molecular weight species of βDG are unknown.

βDG has multiple sites of phosphorylation with as yet unassigned roles. βDG has putative CDK phosphorylation sites that may regulate βDG in a cell cycle dependent manner (Gould et al. 2010). Phosphorylation by mitotic kinases is the principle means behind the control of a number of mitotic processes (Ottaviano et al. 1985, Moir et al. 2000a, Nikolakaki et al. 1997, Goss et al. 1994). As previously described, lamin phosphorylation in NEBD has been extensively studied (Ottaviano et al. 1985). Similarly, phosphatase activity is required for reassembly of the nuclear lamina with protein phosphatase 1 important for B-type lamin reassembly (Thompson et al. 1997). Emerin is reported to be phosphorylated at 26 sites during mitosis by multiple kinases, furthermore aberrant cell cycle dependent phosphorylation of emerin and altered subcellular localisation has been implicated in patients with EDMD (Berk et al. 2013). Yet another potential NE binding partner of βDG to display mitotic phosphorylation events is SUN1. Phosphorylation events catalysed by Cdk1 and Plk1 are important for reducing the interactions of SUN1 with lamin A/C, emerin and short isoforms of nesprin2 (Patel et al. 2014). It would therefore be interesting to test if mutations to the putative βDG CDK sites affects NEBD or reformation or DG localisation to the reformed nuclear envelope. Similarly, it could be important to see it different mitotic phosphorylation events of βDG's nuclear binding partners affects their interaction.

Separate from its roles at the nuclear membrane, βDG at the plasma membrane is known to play a role in cytokinesis and has been fairly extensively characterised (Higginson et al. 2008). As seen here and reported elsewhere in multiple cell lines, βDG localises strongly to the cell

periphery throughout mitosis (Fig 5.16, Fig 5.17). During late anaphase and telophase βDG localises at the site of the forming cleavage furrow and during cytokinesis localises strongly at the midbody, colocalising with the actin contractile ring (Fig 5.20). βDG has been shown to colocalise with ezrin at the cleavage furrow and midbody (Higginson et al. 2008). At the midbody βDG may play a role in tethering the plasma membrane to the actin contractile ring and either directly via βDG interaction with F-actin or through an indirect interaction with ezrin through a dbl/ezrin complex (Batchelor et al. 2007, Higginson et al. 2008). During mitosis ERM proteins, such as ezrin, help to facilitate cell rounding through the organisation and stiffness of the actin cortex. Thus βDG may be contributing to this process through its interactions with ezrin. The localisation of Dp71, another component of the DAPC has also been identified at the midbody during cytokinesis and when depleted results in reduction of βDG immunoreactivity at the midbody (Villarreal-Silva et al. 2011), hinting that the DAPC is important in this function. It is important to note however that cells which were depleted for βDG did not display detectable cytokinetic defects. DG null fibroblasts display abnormally shaped nuclei, however it is not known if this is due to cytokinetic defects in βDG or mislocalisation of components of the nuclear lamina

In mitotic cells βDG displayed a faint cytoplasmic stain and appeared to be excluded from the chromosome regions however the pY892 form of βDG accumulated around the condensed chromosome particularly through metaphase to telophase and may overlap with the site of the mitotic spindle (Fig 5.16, Fig 5.18, Fig 5.21). This accumulation remains to be verified as 1709 specificity is questionable, and attempts to assess the localisation of αβDGflag in mitotic cells was hampered by low numbers despite Nocodazole treatment (Fig 5.22, Fig 5.23). In the few mitotic cells there did not appear to be an accumulation of βDG around the condensed DNA however further investigation is warranted. Additionally, Nocodazole disrupts microtubules and therefore may disrupt any localisation to the mitotic spindles anyway (De Brabander et al. 1976). A number of cell membrane or cell adhesion molecules, such as Merlin, have been seen to associate with the mitotic spindles or kinetochores during mitosis.

During mitosis the components of the nuclear envelope are dissociated and undergo various fates. Fragments of the nuclear membrane and proteins that remain attached have been reported to be resorbed into the ER (Meier et al.1994, Dabauvalle et al. 1999, Ellenberg et al. 1997, Yang et al. 1997, Maison et al. 1993). Colocalisation with ER marker calnexin in mitotic LNCaP cells did not display a clear localisation. Other NE proteins such as lamin A/C are dispersed into the cytoplasm during interphase which may be the case with βDG. A number of NE proteins, including SUN1, LAP2β and lamin B1 have been shown to colocalise to the spindle poles in the early stages of mitosis (Haque et al. 2006, Beaudouin et al. 2002). The movement

towards the poles is in a microtubule dependent manner and is consistent with the NE proteins remaining attached to the nuclear membrane fragments after the NE is pulled apart forcibly by microtubules (Beaudouin et al. 2002). The reformation of the nuclear membrane around the chromosomes is a tightly regulated processes (Haraguchi et al. 2001). As early as late anaphase nuclear envelope proteins are recruited to the surface of condensed chromosomes (Gautier et al. 1992). In many cases this is facilitated through BAF which interacts with proteins such as Emerin and LAP2 through their LEM domains (Lee et al. 2001). Given the interaction of βDG with components of the nuclear envelope and the disruption in their organisation upon βDG depletion, it would be interesting to monitor the assembly of the nuclear envelope in βDG depleted cells following mitosis to see if there are any delays or abnormalities and could be done via live imaging of these cells.

Additionally, a proposed interaction between βDG and MAD2L2 has been identified in a yeast 2 hybrid screen (S. Winder, Personal communication). MAD2L2 is an adaptor protein involved in the spindle assembly checkpoint acting as an inhibitor or the anaphase promoting complex and preventing metaphase to anaphase transition until the chromosomes are aligned along the metaphase plate. MAD2L2 localises on the spindle during mitosis. Therefore, it would be interesting to investigate a potential MAD2L2- βDG complex at the mitotic spindle through interaction studies such as IPs and proximity ligation.

5.3.3 SUMMARY

1. Although highly variable, small fluctuations in the levels of βDG and pY892 βDG can be detected as synchronised LNCaP cells progress through the cell cycle upon release from thymidine block.
2. There is a weak positive correlation between the quantified level of full length pY892 βDG and the percentage of LNCaP cells in S phase in synchronised cells however this is not seen in FACS sorted populations or via immunofluorescence in BrdU S phase populations.
3. βDG does not localise to foci of DNA replication in BrdU positive cells.
4. βDG colocalises to the cell periphery, midbody and cleavage furrow in mitotic LNCaP cells and does not localise with the ER in the cytoplasm.
5. pY892 βDG may localise to the perichromosomal region of LNCaP cells in metaphase, anaphase and telophase.

Chapter 6: Analysis of β-Dystroglycan localisation at the centrosome

6.1 Introduction

6.1.1 The centrosome: function, structure and biogenesis

First described by Boveri in the early 20th century (Boveri, 1914), the centrosome is a small organelle located near to the nucleus with an essential function as a microtubule organising centre (MTOC) (Luders *et al.* 2007). As a MTOC the centrosome plays important roles in organising the polarity and orientation of microtubules in interphase cells, whilst in dividing cells, a duplicated pair of centrosomes act as the poles of the mitotic spindle, nucleating the growth of the microtubules and controlling assembly of the mitotic spindle (Reviewed in Azimzadeh et al. 2007, Luders *et al.* 2007). Consequently, the centrosome influences cell shape, polarity and migration as well as cell division and chromosome segregation (Chang et al, 2013, Obino et al. 2015). In addition to its structural roles the centrosome may also act as a signalling scaffold and, although there is no definitive evidence, it is thought to contribute to cell cycle progression and DNA damage response (Arquint et al. 2014, Terrin et al 2012, Barr et al. 2010.). Moreover, perturbation of centrosome structure and function has been implicated in carcinogenesis and chromosome instability (Boveri, 1914, D' Assoro, et al. 2002, Ganem et al. 2009). Given the important functions of the centrosome there is a great deal of interest in understanding the mechanisms that govern its function and regulation.

The centrosome consists of two perpendicular cylindrical centrioles, each centriole consisting of nine microtubule triplets (Fig 6.1A) (Paintrand et al. 1992, Gonczy. 2012, Nigg et al. 2011). Of the two centrioles, the older centriole, known as the mature, or mother, centriole also has subdistal and distal appendages required for its functions (Fig 6.1B) (Piel et. al. 2000). The centriole pair is embedded within the pericentriolar material (PCM), an electron dense cloud of many proteins which are important for the integrity and function of the centrosome (Fig 6.1.B). Extensive work has been undertaken to elucidate the identity, organisation and functions of the plethora of proteins constituting the PCM (Andersen et al. 2003, Lawo et al. 2012), an important example being gamma tubulin (Oakley 1990, Moudjou et al. 1996). γ-

tubulin is recruited to the PCM and forms the γ-tubulin ring complex (γ-TURC), mediating microtubule nucleation and capping (Oakley 1990, Weise et al., 2000, Moritz, et al. 1995, Teixido-Travesa et al. 2012) but is also associated with the centrioles themselves (Fuller et al. 1995, Moudjou et al., 1996).

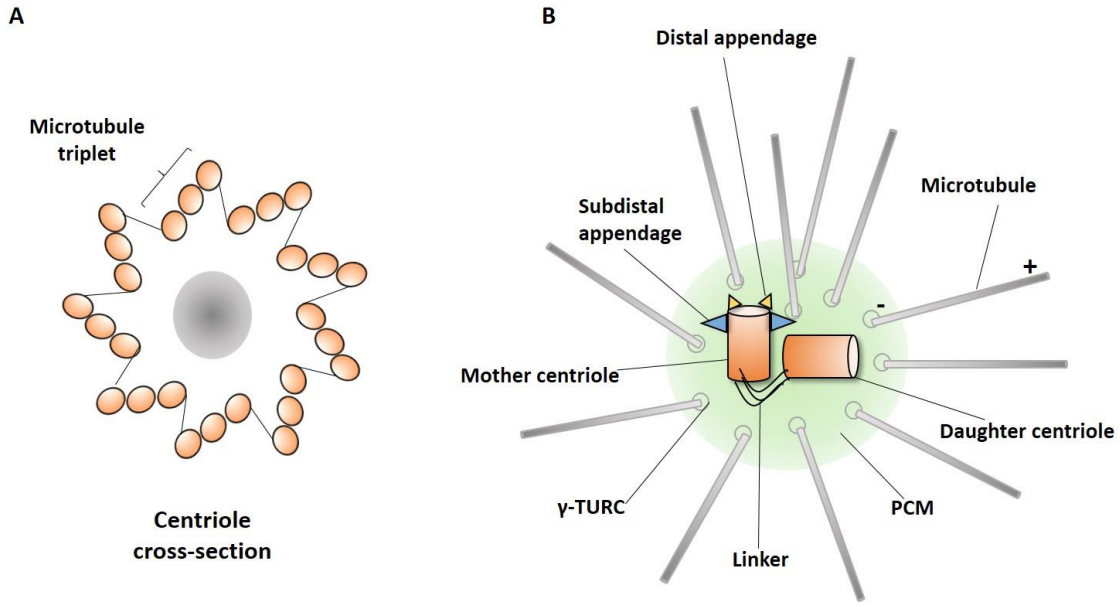

Figure 6.1: Centrosome structure and organisation. A. Schematic diagram of a cross-section view of a centriole, consisting of 9 microtubule triplets in a 'cartwheel' organisation. B. Schematic diagram of a centrosome in G1. A centriole pair consisting of a mother and daughter centriole tethered at their proximal ends by linker proteins. The mother centriole has both distal and subdistal appendages/ The centriole pair is embedded within the pericentriolar material (PCM), simplified here as a green circle. Microtubules nucleate from γ-TURC complexes recruited to the PCM.

The number of centrosomes and their position in a cell must be tightly regulated and largely depends on the cell cycle (Nigg, et al. 2011). Normally, in cycling cells, the centrosome is duplicated once per cell cycle in a manner closely synchronised with cell cycle progression (Tsou et al. 2006). Briefly, the centrosome duplication cycle starts at the G_1-S transition (Robbins et al. 1968). In G_1 the existing mother and daughter centriole are tethered at their proximal ends. At the G_1-S transition a new daughter centriole (procentriole) begins to form at one site on the lateral side of each existing (mother) centriole (Robbins et al. 1968). The procentriole is connected to the mother centriole by a linker. The procentrioles elongate throughout S and G_2. Then in M phase the tether between the two mother centrioles is released and the new centriole pairs disengage. The two newly formed centrosomes form the poles of the mitotic spindle whereupon each is segregated into the new daughter cells (Reviewed in Nigg et al. 2011). Importantly, in quiescent (G_0) cells the mother centriole can migrate to the cell surface whereby it associates with the plasma membrane and forms the

basal body from which the axoneme extends to form the primary cilium (Sorokin. 1962, Nigg, et al., 2011).

It is crucial that every centriole duplicates just once per cell cycle and that each pre-existing centriole forms just one new, adjacent centriole (Tsou et al. 2006). If there is multiple replication of centrioles there will be centrosome amplification (Ganem et al. 2009). Centrosome amplification was defined by D'Assoro et al. as centrosomes that are larger than normal, a cell with more than four centrioles or with more than two centrosomes present (D'Assoro et al., 2002). Centrosome amplification results in the formation of multipolar spindles and subsequent chromosome missegregation (Ganem et al. 2009). Boveri observed the formation of multipolar spindles in tumour cells with chromosome amplification and hypothesised the resultant chromosome missegregation contributed to the chromosome instability seen in malignant tumours (Boveri. 1914), a process now commonly reported to contribute to the disease phenotype in cancer cells (Ro et al. 2004).

6.1.2 Attachment of the centrosome to the nuclear envelope

In most metazoan cells the centrosome is positioned very close to the nucleus. There has long been the hypothesis that a physical tether connects the centrosome to the nuclear envelope, a hypothesis that was seemingly supported by the observation that the centrosome remained closely associated with the nucleus after disruption physically, after gentle homogenisation, or biochemically, after disruption of the nuclear membrane with triton-x-100 (Nadezhdina et al. 1979.).

The positioning of the centrosome close to the nucleus could be important for a number of reasons such as maintaining a close location to the chromosomes for the formation of mitotic spindle following nuclear envelope breakdown (Burakov et al. 2013). Moreover, it is known that centrosome position relative to the nucleus is important for cell polarity and migration (Luxton et al. 2011). For example, in migrating myoblasts it has been shown that the centrosome was positioned between the nucleus and the leading edge of the cell, as a consequence of active rearwards movement of the nucleus in an actomyosin dependent mechanism (Gomes et al. 2005). In the case of cell polarisation, the repositioning of the centrosome and the consequent reorganisation of the microtubule network allows the asymmetrical positioning of cellular organelles. For example, there is F-actin mediated retrograde transport of the nucleus and subsequent centrosome repositioning in polarised fibroblasts (Chang et al. 2013). In addition to the role of F- actin, the microtubule network and the microtubule motors, dynein and kinesin, regulate centrosome position. It is thought that

dynein brings the nucleus towards the centrosome, moving along microtubules towards the minus end at the centrosome (Burakov et al. 2003).

Once the centrosome is juxtaposed at the nuclear envelope the mechanisms by which the two organelles are tethered are not fully understood. In recent years, however, a number of proteins have been identified which play a role in the centrosome association to the nucleus. An early example came from *Caenorhabditis elegans* (*C. elegans*) in which ZYG-12, a KASH domain containing protein, was found to localise at the nuclear envelope and centrosome (Malone et al. 2003). ZYG-12 was proposed to anchor the centrosome to the nucleus by associating with itself on these two organelles whilst being anchored to the nuclear envelope via LINC complex component SUN-1 (Malone et al. 2003, Minn et al. 2009). This mechanism is true up until early embryogenesis however later does not appear to be the sole mechanism of nucleus-centrosome coupling (Zhou et al. 2009). In neuronal cells deletion of Hook3, the mammalian homolog of ZYG-12, led to disrupted assembly of proteins at the centrosome and attachment of microtubules to the centrosome (Ge et al. 2010). The connection between ZYG-12 and the centrosome itself remains unclear although it is known that Hook3 interacts with the PCM protein PCM-1 (Ge et al. 2010).

Since the *C. elegans* study there have been a number of reports implicating components of the LINC complex and its interacting proteins with the nuclear- MTOC attachment. The LINC complex is an important facilitator of interaction between the nucleoskeleton and the cytoskeleton (Reviewed in Razafsky et al. 2009). The cellular processes in which the LINC complex has roles is steadily expanding, with roles in cellular rigidity (Lombardi et al. 2011, Stewart-Hutchinson 2008), nuclear shape (Luke et al. 2008), nuclear movement, which is facilitated through the interaction of the LINC complex actin cables known as TAN lines (Luxton et al. 2010) and centrosome attachment to the NE (Malone et al. 2003), though there is still much to be explored in the mechanisms through which these are achieved.

In yeast *Schizosaccharomyces pombe (S. pombe)* it was found that microtubules were physically interacting with the nucleus, and the heterochomatin within, through a SUN- KASH complex of Kms2 in the outer nuclear membrane and Sad1 and Ima1 in the inner nuclear membrane (King et al. 2008). When Ima1 was disrupted or depleted the site of attachment of the MTOC to the nuclear membrane was disrupted (King et al. 2008). The mammalian homolog of Ima is Samp1. Samp1 can localise to the inner nuclear membrane where it interacts with component of the LINC complex SUN2 and lamins A/C (Borrego-Pinto et.al. 2012). Interestingly, Samp1 has also been detected at the spindle matrix and polar region of the

mitotic spindles during mitosis (Buch et al. 2009). Depletion of Samp1 led to an increased centrosome to nuclear envelope distance (Buch et al. 2009).

It has been shown that the nuclear envelope protein emerin couples the centrosome to the nucleus (Salpingidou et al., 2007). Emerin is predominantly thought of as an INM protein however it has been demonstrated that a pool of emerin is also found localised at the ONM. Salpingdiou *et al.* have demonstrated that an ONM pool of emerin can interact with β-tubulin and mediate the attachment of the centrosome to the NE (Salpingidou et al., 2007). Further support for the role of emerin in maintaining the connection between the centrosome and the nucleus can be seen in mice models of EDMD and fibroblasts from patients with x-EDMD, both lacking emerin protein, in which the distance between the centrosome and the nucleus was also increased (Hale et. al. 2008, Salpingidou et al., 2007). It was also found that centrosome to nucleus distance was increased in cells in which A-type lamins were deficient or reduced, such as is the case in laminopathies (Hale et. al. 2008). Emerin localisation is regulated by lamin A and the increased distance was attributed to mislocalisation or loss of emerin from the nuclear envelope in these cells (Hale et. al. 2008). Interestingly the multifunctional structural protein 4.1R was shown to immunoprecipitate with emerin and lamin A/C and furthermore when 4.1R was depleted both these proteins were mislocalised (Meyer et al. 2010). In these cells the centrosome to nucleus distance was also increased, again likely due to the disrupted localisation of emerin (Meyer et al. 2010).

It has also been shown that when nesprin 3, a KASH domain protein, is depleted in endothelial cells, centrosome polarisation and nucleus-centrosome distance is increased (Morgan et al. 2011). Nesprin 3 is smaller than the Nesprin 1 and 2 isoforms and contains a plectin binding domain rather than an actin binding domain at its N-terminus (Razafsky et al. 2009). Interestingly it has also been shown that BRCA2 interacts with plectin and mediates centrosome localisation (Niwa et al. 2009). Morgan et al therefore hypothesised that nesprin 3 mediates centrosome positioning through this plectin mediated interaction with the intermediate filaments (Morgan et al. 2011).

Centrosome coupling to the nucleus has also been shown to be regulated by Sun1 and Sun2 in complex with syne-2 in mice (Zhang et al. 2009). Knockouts of the aforementioned components resulted in large increases in nucleus- centrosome distance (Zhang et al. 2009). The connection between syne-2 and the centrosome is mediated through interactions with the microtubule motors dynein and kinesin (Zhang et al. 2009). Dynein and kinesin are thought to be important in the movement of the nucleus along the microtubules towards or away from the centrosome respectively (Razafsky et al. 2009, Zhang et al. 2009, Meyerzon et al. 2009). It

is, therefore, difficult to dissect a direct role of tethering from the disruption of the dynein/kinesin role in positioning in the SUN or Syne knock out animals and there may be as yet undiscovered connections between the LINC complex and the centrosome.

In addition to interactions with the microtubule network, the LINC complex is also well known to interact with the actin cytoskeleton (Zhang et al. 2002, Razafsky et al. 2009), and a role of actin in centrosome positioning is by no means new (Shay et al. 1974). A recent paper indicates a role for F-actin filaments nucleating from the centrosome in connecting the centrosome to the nucleus (Obino et al. 2015). It was hypothesised that Arp 2/3 dependent nucleation led to a network of F-actin filaments emanating from the centrosome that were bound by nesprin, holding the centrosome at the nucleus in lymphocytes (Obino et al. 2015). When Arp 2/3 was depleted at the centrosome during lymphocyte activation, resulting in reduced F-actin at the centrosome or when a dominant- negative form of nesprin unable to bind actin was expressed the centrosome was able to move further from the nucleus (Obino et al. 2015).

Thus there is an emerging web of complex interactions of nuclear proteins and cytoskeletal components involved in the tethering of the centrosome to the nuclear envelope.

6.1.3 DG AND THE CENTROSOME

There is little published work available regarding a role for dystroglycan at the centrosomes however in C2C12 cells in which DG had been reduced by RNAi the distance of the centrosomes from the nucleus was increased and there was also a significant increase in the number of cells with amplified (3-6) centrosomes (Martinez- Vieyra et al. 2013). Furthermore, DG has been shown to affect the localisation of nuclear envelope protein, emerin and potentially interact with components of the LINC complex, all of which modulate centrosome position, as described above (Martinez- Vieyra et al. 2013). Interestingly, in immunofluorescence studies conducted as part of this thesis pY892 βDG was observed to localise at the spindle poles in mitotic cells (Fig 5.20) and also displays a bright punctate stain in interphase cells (Data not shown, S. Winder personal communication). It was therefore decided to investigate βDG localisation and function at the centrosome.

6.1.4 CHAPTER AIMS

The aims of the research conducted in this chapter are:

-to investigate the localisation of βDG at the centrosomes.

-to investigate if centrosome duplication and positioning is disrupted in DAG null cells.

6.2 RESULTS

6.2.1 IMMUNOFLUORESCENCE ANALYSIS OF PY892 BDG LOCALISATION AT THE CENTROSOME

Whilst analysing the localisation of βDG in interphase it was observed that the antibody 1709, which recognises pY892, often displayed a bright punctate stain at one or two locations in the cell (Fig 6.2, arrows). The bright punctate stain was strongest in cells fixed via MeOH/ acetone fixation as used when observing microtubules (Chapter 5, Fig 5.20). Interestingly in mitotic cells there was a strong localisation of 1709 antibody signal at the mitotic spindle at a location where the MTOC would be expected to be (Chapter 5, Figure 5.20). These observations warranted further investigation into βDG localisation at the centrosome.

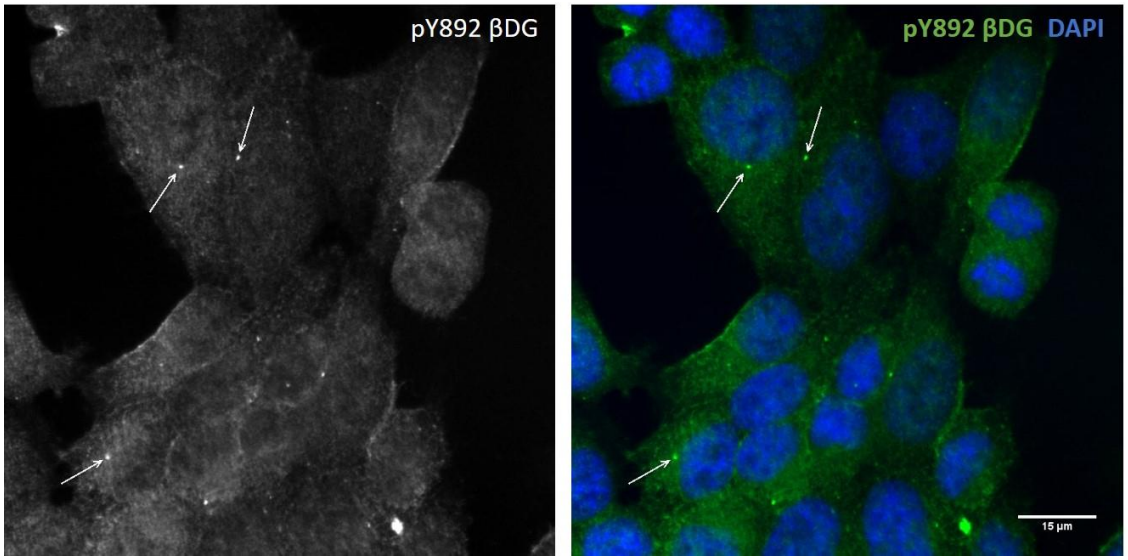

Figure 6.2 Punctate localisation of pY892 βDG in LNCaP cells. LNCaP cells were fixed with 3.7% PFA and stained for pY892 βDG with the 1709 antibody (green) nuclei were counterstained with DAPI (blue). Images were obtained via epifluorescence microscopy. Arrows indicate bright punctate structure detected by 1709. Scale bar 15µm.

6.2.2 ANTI B-DG ANTIBODIES 1709 AND JAF1 LOCALISE AT THE CENTROSOME IN INTERPHASE AND MITOTIC CELLS.

It was decided to investigate if βDG was localising to the centrosomes and to see if this was also the case for βDG that was not phosphorylated at pY892. LNCaP cells were fixed with MeOH/ Acetone and stained with one of three βDG antibodies, MDG2 and JAF1, the epitopes of which are non-phosphorylated βDG at Y892, or 1709, which detects the pY892 form of βDG. The cells were co-stained with γ-tubulin, a marker of the centrosome. MDG2 did not co-localise with γ-tubulin in either interphase of mitotic cells (Fig 6.3). 1709 and JAF1, however, both co-localised with the centrosome marker in both interphase and mitotic cells (Fig 6.3). This suggests that both phosphorylated and non-phosphorylated Y892 βDG may localise to the centrosome. The fact that JAF1 but not MDG2 localised at the centrosome despite having overlapping and very similar epitopes may be due to JAF1 recognising slightly different epitope that may be independent of Y892. 1709 and JAF1 localised to the centrosome at all stages of mitosis (not shown) but was particularly strong in metaphase cells (Fig 6.3). The colocalisation of 1709 and JAF1 but not MDG2 with γ-tubulin was also observed in PNT1A and PC3 cells (data not shown).

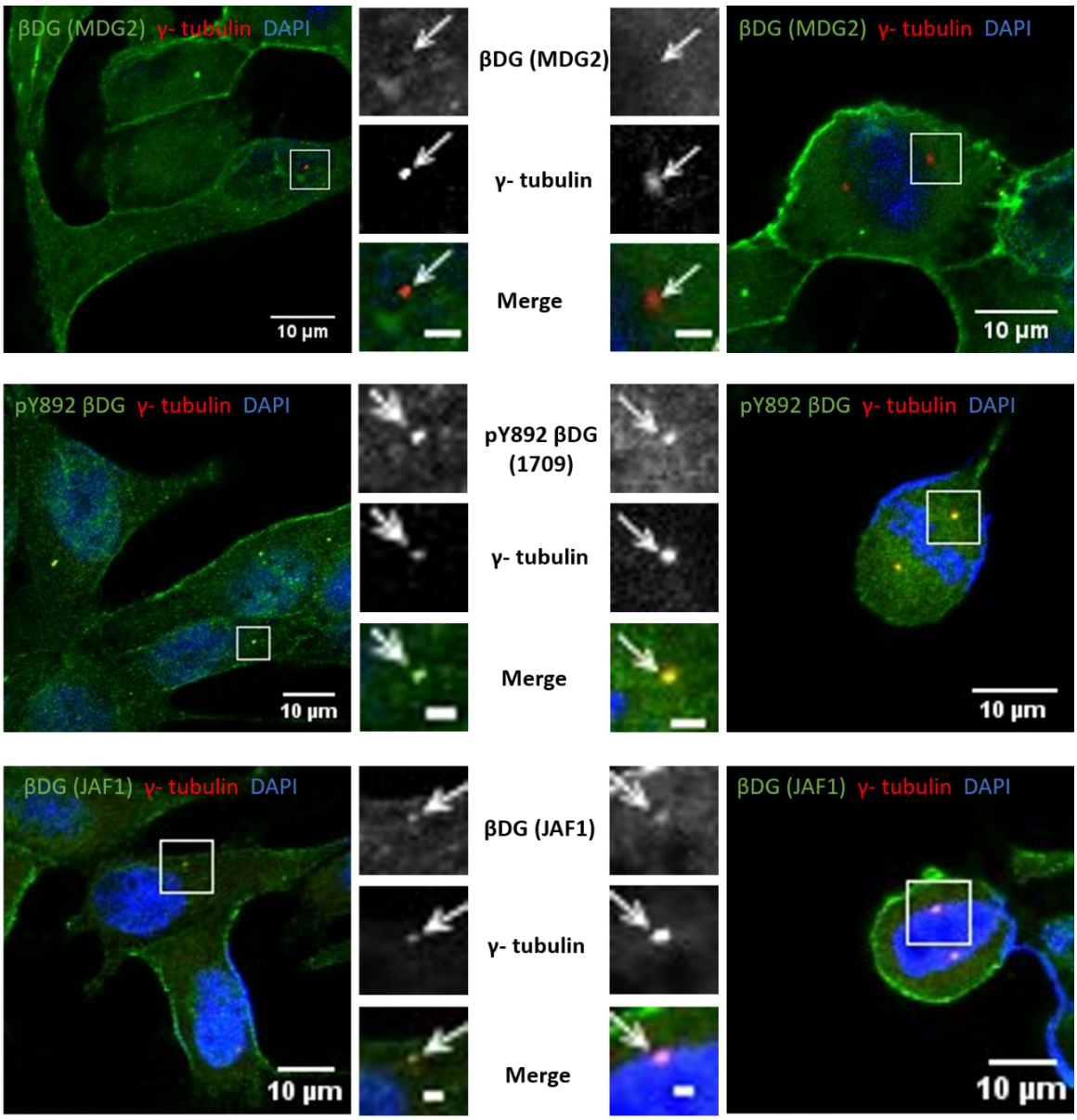

Figure 6.3 anti-βDG antibodies 1709 and JAF1 localise at the centrosomes in interphase and mitotic cells. LNCaP cells were fixed with MeOH and stained for βDG with two different antibodies (MDG2) (top) and JAF1 (bottom) or pY890 βDG (1709) (middle) (Green). Cells were costained for gamma tubulin (red) and the nuclei counterstained with DAPI (blue). Images are Z slices from confocal microscopy taken at the clearest Z slice of the centrosome. Images were taken at 60 x magnification. Scale bar is 10 μm. Enlarged images of the centrosome (white box) are included. Arrow indicates the centrosome. Scale bar is 2 μm.

6.2.3 TAGGED FORMS OF βDG DO NOT LOCALISE TO THE CENTROSOME

A problem when studying the proteins at the centrosomes is the false positive detection of proteins as a consequence of antibody cross-reactivity or non-specificity (Moudjou, et al. 1996). In order to ascertain if βDG truly localises to the centrosome, tagged versions of βDG were analysed via co-immunostaining and confocal microscopy to determine if the tagged versions could be detected at the centrosome independent of the βDG antibodies.

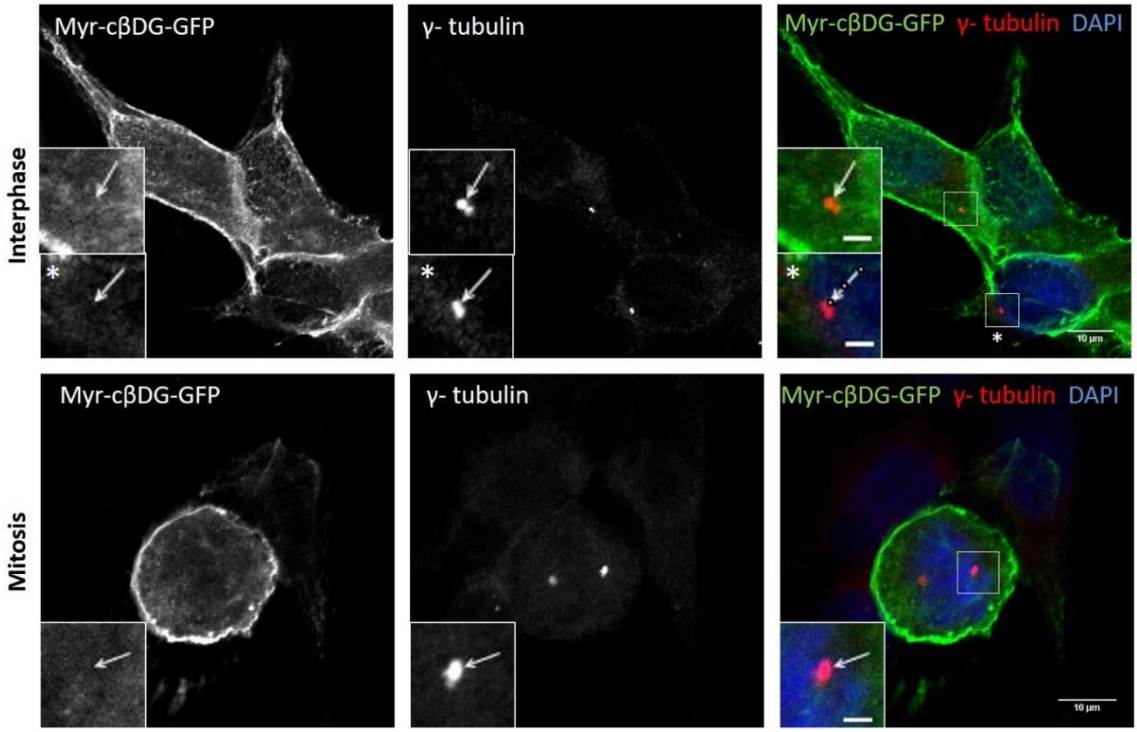

Figure 6.4 Myr-CβDG-GFP does not colocalises to the centrosomes in LNCaP cells. LNCaP cell lines stably expressing Myr-CβDG-GFP (green) were fixed and co-stained with γ- tubulin (red). DNA was counterstained with DAPI (blue). Z slice Images of interphase (top) and mitotic (bottom) cells were taken via confocal microscopy. Scale bar is 10 µm. Inset are enlarged regions of the white box. Asterisk denotes which box is enlarged. Arrows indicate the centrosome. Scale bar is 2 µm. Images were taken at 60x magnification.

6.2.3.1 Myr-cβDG-GFP does not localise to the centrosome

One well studied tagged βDG construct available in the Winder lab is a myristoylated cytoplasmic fragment of βDG with a c-terminal GFP (Myr- cβDG-GFP) (Batchelor et al., 2007, Mathew et al., 2013). Stable LNCaP cells expressing this construct were fixed and co-stained with γ-tubulin and imaged via confocal microscopy. Despite a clear localisation to the PM as expected (Batchelor et al, 2007) Myr- cβDG-GFP did not colocalise with γ-tubulin in either interphase or mitotic cells (Fig 6.4). There a few caveats to consider when using this construct. Firstly, although Myr- cβDG-GFP has been shown to localise βDG efficiently to the plasma membrane and the nucleus, partly facilitated by the myristoyl tag, it is unknown if the construct fully mirrors wildtype βDG localisation. Indeed, it should be considered that the myristoyl tag may be targeting βDG to membranes and could therefore affect its potential localisation to the centrosome. Furthermore is only a fragment of βDG which may have unknown consequences on βDG behaviour or localisation. Secondly, Myr- cβDG-GFP contains a c-terminal GFP which has been reported to perturb βDG phosphorylation at Y890 and potentially other functional properties of the crowded C-terminal tail of βDG (D. Leocadio, 2014). This may be particularly relevant in the context of this experiment given the strong localisation of pY890 specific antibody 1709 to the centrosome. As such the localisation of a second tagged-version of βDG at the centrosome was also investigated.

6.2.3.2 αβDG flag does not localise to the centrosome in LNCaP cells

LNCaP cells were transiently transfected with αβDG-flag and immunostained with anti-flag and γ-tubulin. The αβDG-flag construct has been described in previous chapters of this thesis. αβDG-flag did not colocalise with γ-tubulin in the interphase LNCaP cells (Fig 6.5). Unfortunately, no mitotic cells were observed as a consequence of the low proliferation seen in the transfected cells (Chapter 5, Fig 5.21). The flag tag is not thought to interfere with any known or putative interactions of βDG however there is the possibility of the tag interfering with as yet undescribed modifications or interactions that may perturb its function. Together these results suggest that βDG does not localise to the centrosome.

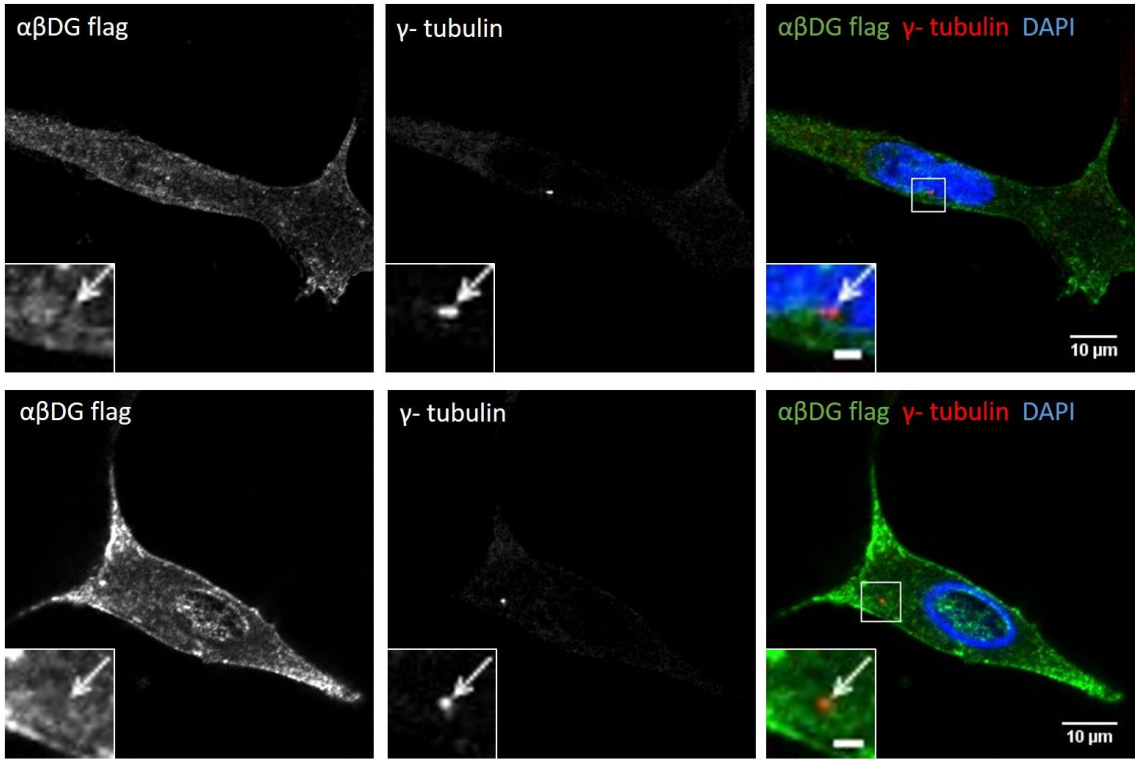

Figure 6.5 αβDG flag does not colocalises to the centrosomes in LNCaP cells. LNCaP cells were transiently transfected with αβDG flag fixed and co-stained anti-flag (green) and γ- tubulin (red). DNA was counterstained with DAPI (blue). Z slice Images of interphase cells were taken via confocal microscopy. Scale bar is 10 µm. Inset are enlarged regions of the white box. Arrows indicate the centrosome. Scale bar is 2 µm. Images were taken at 60x magnification.

6.2.4 B-DG ANTIBODIES STAIN THE CENTROSOMES IN DAG1 NULL SYSTEMS

A complementary approach to assess if the localisation of βDG at the centrosome is specific or an artefact of the antibody is to look at the expression pattern of the antibodies in a system lacking βDG protein expression.

6.2.4.1 1709 colocalises with γ-tubulin in DAG1$^{-/-}$ zebrafish embryos

One available DAG null system that has previously described in this thesis and elsewhere is the *DAG1* zebrafish line. *DAG1* fish have a point mutation in the DAG1 gene and do not express βDG protein (Lin et al 2011, Gupta et al 2011). DAG1$^{-/-}$ fish have a dystrophic phenotype and this was used to sort the zebrafish embryos via birefringence into populations of DAG1$^{+/+}$ and DAG1$^{+/-}$ fish or DAG1$^{-/-}$ at 4 d.p.f. Zebrafish embryos from each group were then immunostained with 1709 and γ-tubulin and viewed via confocal microscopy. In both the DAG^{sib} and DAG $^{-/-}$ zebrafish embryos 1709 was detected colocalised with γ-tubulin (Fig 6.6).

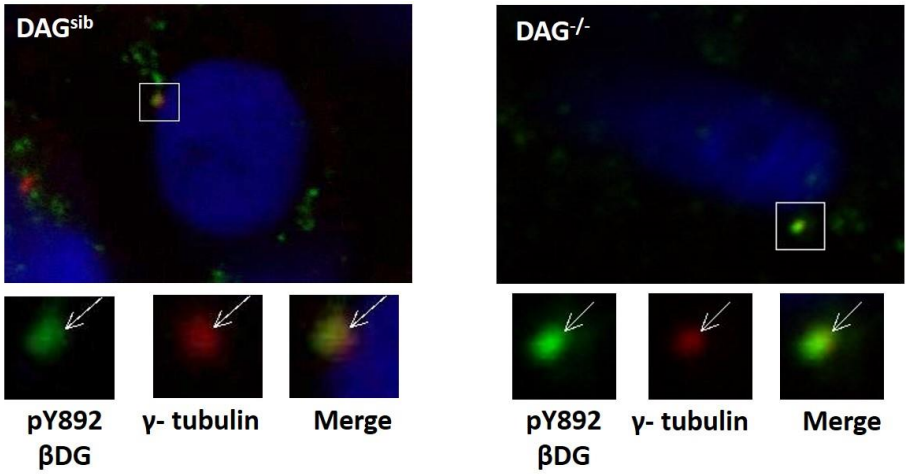

Figure 6. 6. 1709 antibody localises to the centrosomes in DAG$^{-/-}$ zebrafish embryos. At 4 d.p.f zebrafish embryos were identified as DAG^{sib} or DAG$^{-/-}$, fixed and stained for pY892 βDG (1709) (green) and γ-tubulin (red). Nuclei were counterstained with DAPI (blue). Confocal images at 60 x magnification were taken with a water- dipping lens. Enlarged images of the white box are included, arrows indicate the centrosomes.

6.2.4.2 1709 and JAF1 localise to the centrosomes in DAG null fibroblasts

The recent isolation of DAG null fibroblasts from a patient with Walker-Warburg syndrome (Riemersma et al. 2015) presents a second DAG null system in which to assess if βDG localisation at the centrosome is an artefact of the antibodies. HDF control cells and DAG null fibroblasts were co-stained with 1709 or JAF1 alongside γ-tubulin. In interphase cells 1709 and JAF1 colocalised with γ-tubulin in the HDF controls but also the DAG null fibroblasts (Fig 6.7 A, B). As there is no βDG in the DAG null cells to be detected, this clearly demonstrates an artefactual staining of the antibodies at the centrosome. A secondary antibody control shows very faint background staining, showing that it is an artefact of the primary antibody and not the secondary antibodies (Fig 6.7 C).

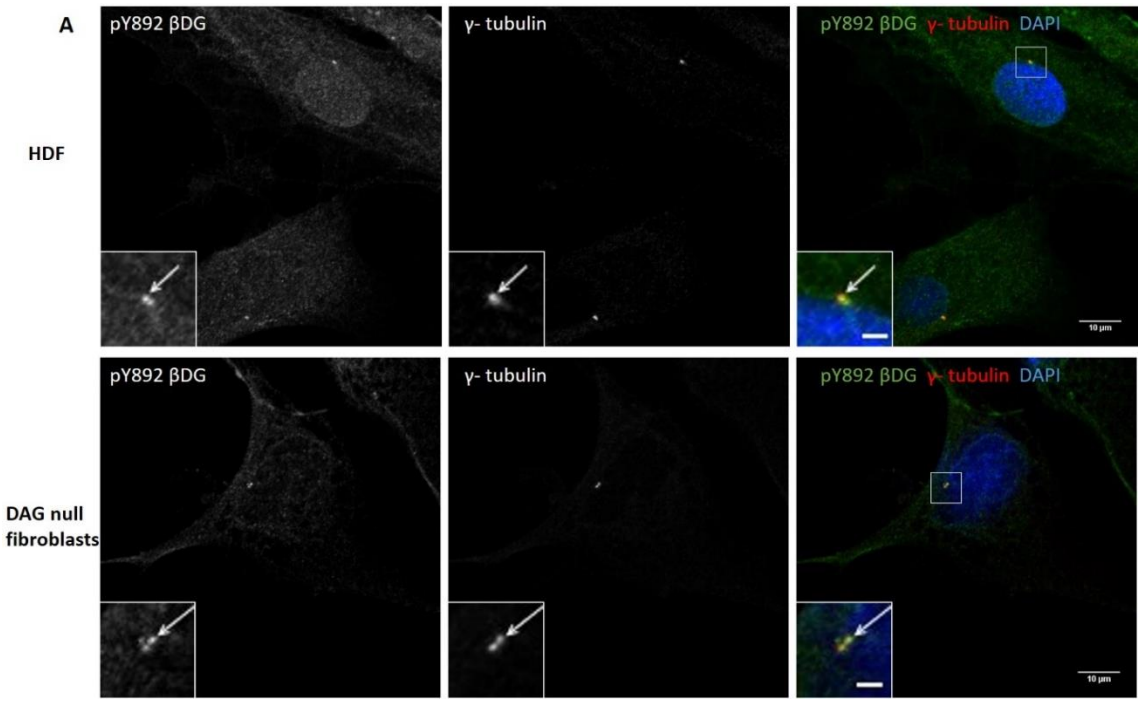

Figure 6.7 βDG antibodies localise to the centrosome in HDF and DAG null fibroblasts. HDF and DAG null fibroblasts were fixed with MeOH/ Acetone and stained for pY890 βDG (1709) (A) or βDG (Jaf1) (B) (green). Centrosomes were stained with γ-tubulin (red) and the nuclei counterstained with DAPI (blue). Images are z slices taken via confocal microscopy at 60x magnification. Scale bar 10 µm. Inset are enlarged images of the white box. Arrows indicate centrosome location. Scale bar 2 µm. C) Secondary antibody control. DAG null fibroblasts were immunostained with secondary antibodies Alexa 488 and Alexa 594 with no primary antibody. Nuclei counterstained with DAPI. Conditions as above.

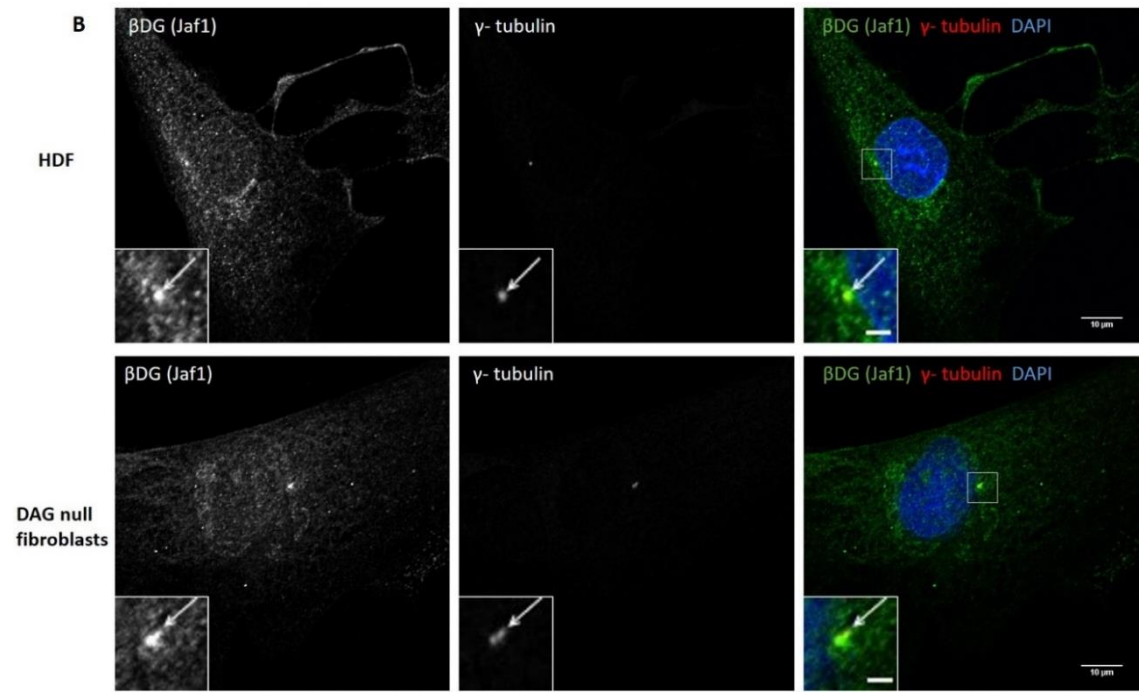

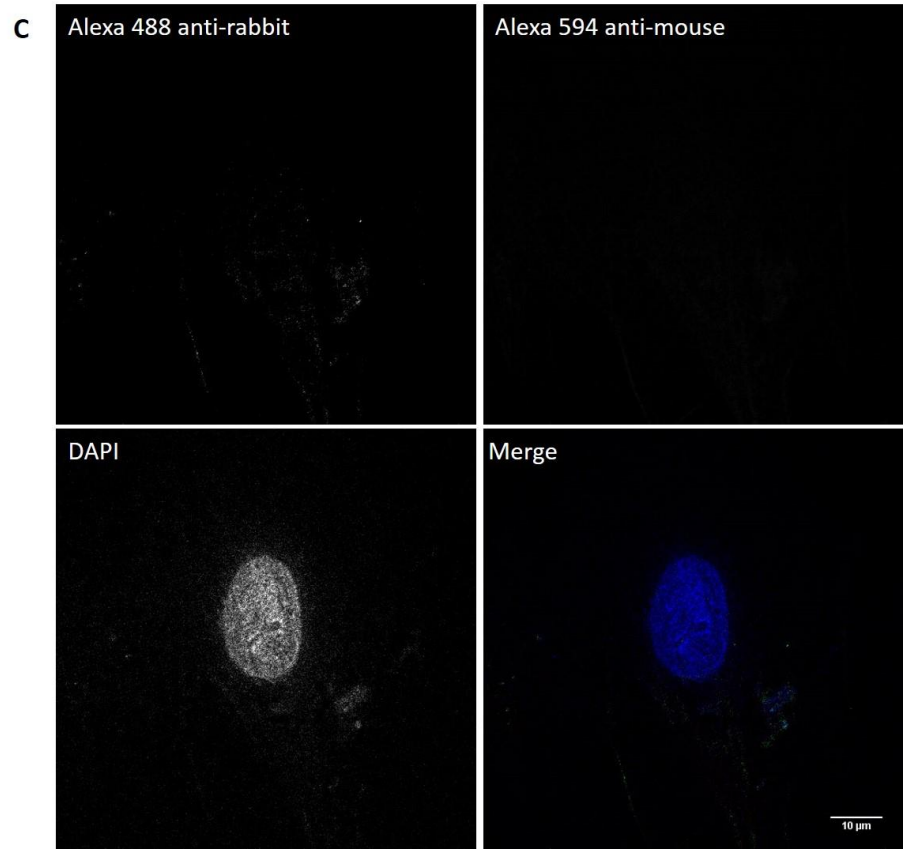

6.2.5 CENTROSOME POSITION AND NUMBER IN DAG NULL FIBROBLASTS

Although the above results indicate that βDG does not localise at the centrosomes, there is still the potential for a role for βDG in regulating centrosome function or localisation indirectly. βDG has been proposed to interact with the LINC complex at the nuclear envelope (Personal communication S. Winder and M. Laredo), a complex with roles in tethering the centrosome to the nuclear lamina. Moreover, Martinez-Vieyra et al. reported an increased nucleus-centrosome distance and centrosome duplication in DG RNAi C2C12 cells in which nuclear morphology and nuclear envelope proteins were disrupted (Martinez- Vieyra et al. 2013). Nuclear morphology is severely disrupted in the DAG null fibroblasts (Section 4.2.1), we therefore investigated if centrosome amplification and positioning was also affected in these cells.

6.2.5.1 Centrosome to nucleus distance

HDF and DAG null fibroblasts were fixed and the centrosome stained for γ-tubulin and the nucleus counterstained with DAPI (Fig 6.8, A-F). The distance between the centrosome (measured from the closest centriole) to the nuclear envelope was measured in Fiji. The mean distance was 1.795µm in HDF cells compared to 2.483 µm in the DAG null fibroblasts but this was not statistically significant as determined by a Mann Whitney U test (Fig 6.8 G, H).

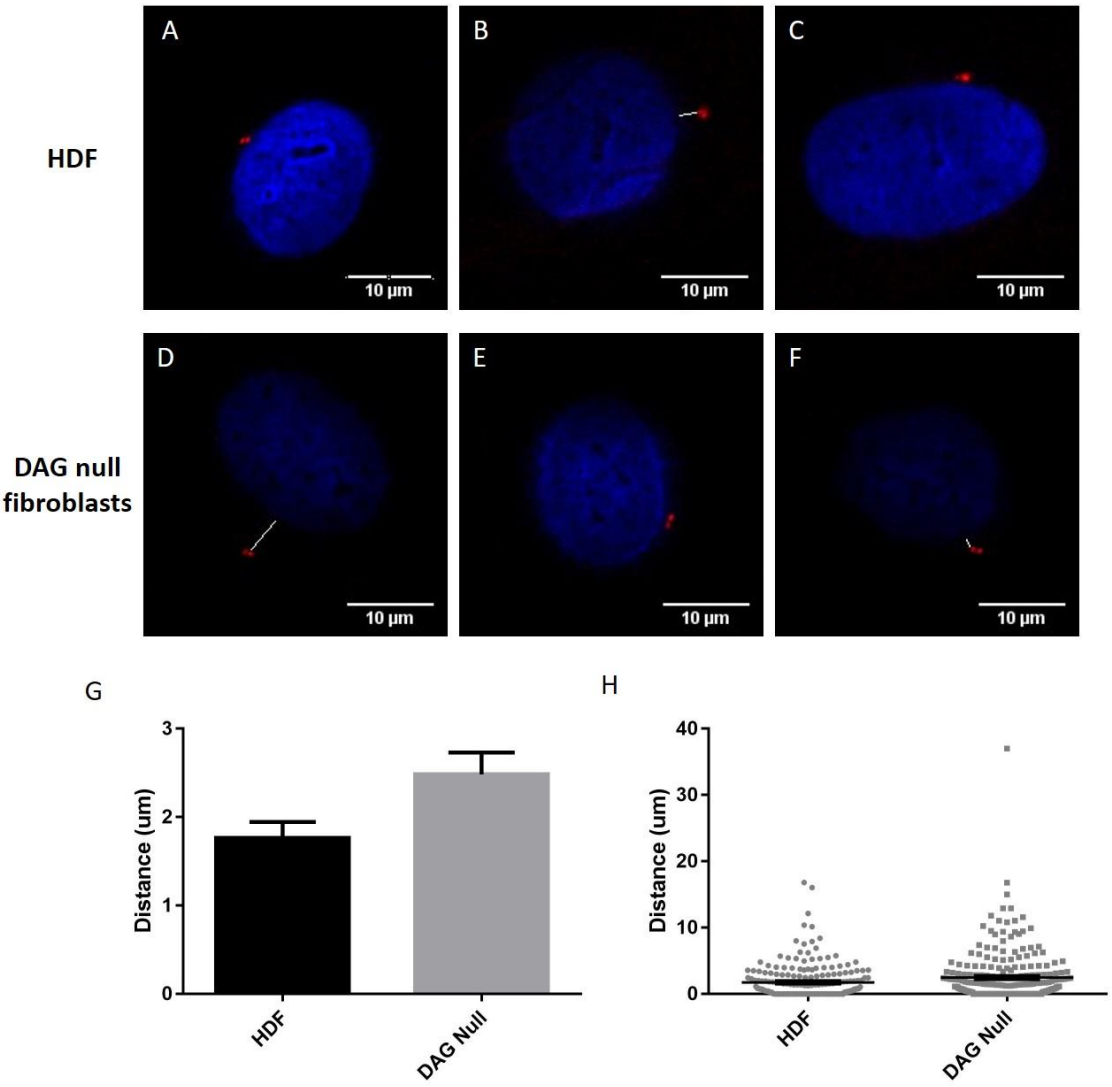

Figure 6.8. Centrosome to nucleus distance in HDF and DAG null fibroblasts. Representative confocal images of HDF (A-C) and DAG null fibroblasts (D-E). Nuclei (blue) are stained with DAPI and the centrosomes are stained with γ-tubulin (red). The distance between the centrosome and the nuclear envelope were measured using image J. (white line). Scale bar 10um. G) Mean distance ± SEM of 2 replicates each with at least n=100 per cell type. Mann-Whitney U test, P=0.0592. H) Scatter plot of total distance ± SEM between the centrosome and the nucleus. 2 replicates, each with at least n=100 per cell type

6.2.5.2 Centrosome number

Centrosome amplification was also analysed from the experiments described above. γ-tubulin antibodies detect the centriole pair within the centrosome (Fuller et al. 1995), thus one centrosome is detected as two centrioles. No HDF cells were observed with multiple centrosomes whilst a small number of DAG null fibroblasts at 1.57 ±0.84 % had multiple centrosomes (3 or more) (Fig 6.9 A-C). The majority of cells of both HDF and DAG null fibroblasts had 1 centrosome with a small percentage of cells with 2 centrosomes as would be

expected from a population of dividing cells. These results show a trend towards increased nucleus to centrosome distance and centrosome amplification in the DAG null fibroblasts, however the results are not statistically significant (Fig 6.9 B, C).

A

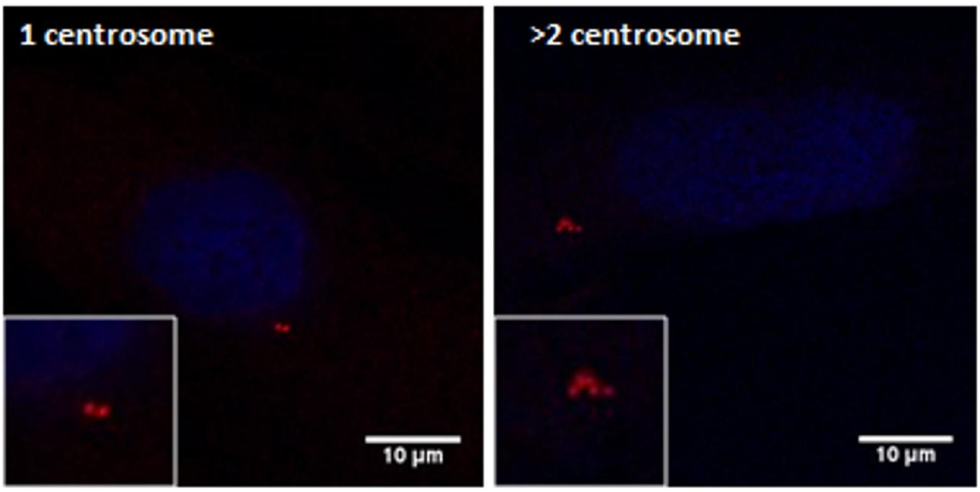

B

Centrosome Number	1		2		>2	
	HDF	DG Null	HDF	DG Null	HDF	DG Null
Percentage of cells	96.67	91.68	3.34	6.77	0.00	1.57
SD	±0.83	±0.83	±0.59	±1.42	0.00	±0.84

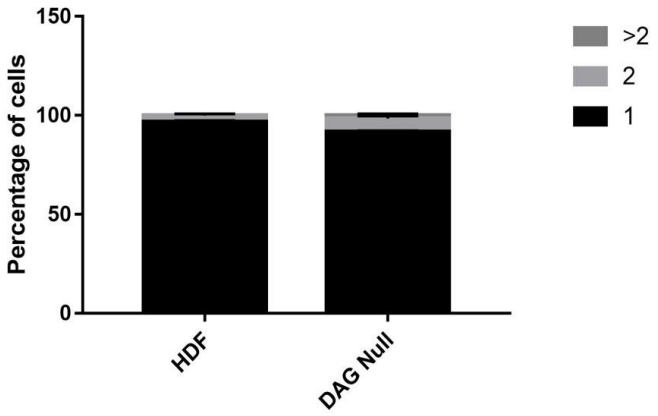

Figure 6.9. Centrosome number in HDF and DAG null cells (A)Representative confocal images of DG null nuclei with 1 (left) or >2 centrosomes (right) stained with DAPI and the centrosomes stained with γ-tubulin (red). Inset; enlarged centrosome image. Scale bar is 10 µm. 2 replicates, each with at least n=100 per cell type. (B, C) the percentage of number of centrosomes per cell in HDF and DG null fibroblasts.

6.3 DISCUSSION

The centrosome is an important organelle regulating a number of cellular processes including cell polarity, migration and division (Azimzadeh *et al.* 2007, Luders *et al.* 2007). A functional centrosome requires the cooperation of a large number of diverse proteins in the PCM (Andersen, et al. 2003, Lawo et al. 2012) but also of interacting partners that regulate centrosome positioning and interaction with other organelles, such as the nucleus (Burakov et al. 2013). The functions and mechanisms of these proteins are gradually resolving however are not completely understood. It has been reported that centrosome number and distance from the nucleus are disrupted in C2C12 myoblast cells treated with DG RNAi (Martinez- Vieyra et al. 2013). Furthermore, βDG interacts with, and modulates the localisation of emerin and lamin (Martinez- Vieyra et al. 2013), components of the nuclear envelope that are established as key proteins in the tethering of the centrosome to the nucleus (Salpingidou et al. 2008, Hale et al. 2008). We have also observed the localisation of βDG antibodies to punctate foci within a variety of cells, hypothesised to be the centrosome or primary cilia (Fig 6.2). In light of these observations we set out to investigate the localisation or functional roles for βDG with the centrosome.

6.3.1 THE LOCALISATION OF BDG AT THE CENTROSOME IS AN ARTEFACT OF THE PRIMARY ANTIBODIES

We have shown that βDG antibodies 1709 and JAF1, but not MDG2, localise to the centrosomes in both interphase and mitotic cells (Fig 6.3). However subsequent investigation has shown this to be an artefact of the antibodies rather than βDG localisation at the centrosomes. This was concluded from two different experimental approaches. Firstly, two different tagged forms of βDG, a cytoplasmic fragment (Myr-CβDG-GFP) (Fig 6.4) and a flag tagged full length βDG (αβDGflag) (Fig 6.5) did not localise to the centrosomes. Although there are arguments that tags can affect the behaviour of proteins and that the fragment may not localise to the centrosome endogenously, the artefactual staining of the antibodies was supported by analysis in DAG null systems. In two different DAG null systems, the *DAG1*$^{-/-}$ zebrafish embryos (Lin et al. 2011, Gupta et al. 2011) (Fig 6.6) and DAG null fibroblasts from a patient with Walker Warburg syndrome (Riemersma et al. 2015) (Fig 6.7), the DG antibodies 1709 and JAF1 stained the centrosomes. The staining of the centrosomes in the absence of DG confirms that the localisation at the centrosome of these antibodies is not specific to βDG.

The artefactual staining of the centrosomes by antibodies, especially with those derived from rabbit sera as is the case with 1709 and JAF1, is a notorious problem in the study of

centrosomal proteins (Moudjou et al. 1996). Sera from rabbits can contain pre-immune activity against proteins in centrosomes and basal bodies. This is best demonstrated in a study in which a γ-tubulin antibody was being developed where the detection of the centrosome via immunofluorescence was observed in the preimmune sera of all 12 rabbits used Moudjou et al. 1996. In fact, the discovery of a number of centrosomal proteins has stemmed from the activity of autoimmune sera. For example, the rabbit 0013 serum (Gosti-Testu et al. 1986) led to the identification of AKAP350, a protein kinase A anchoring protein found in the centrosomes (Keryer et al. 1993) whilst human autoimmune sera 5051 (Calarco-Gilam et al. 1983) led to the identification of pericentrin (Doxsey et al. 1994). Alternatively, there may be epitope similarity of 1709 and JAF1 in other proteins that are localised at the centrosome. Thus, the direct interaction of a protein at the centrosome should always be confirmed through biochemical techniques. The non-specific staining at the centrosome and the now apparent problems of broader non-specific staining of 1709 and JAF1 (as discussed in Chapter 3) highlights the necessity of rigorous controls for antibodies for their use in various techniques. Affinity purification of the antibodies 1709 and JAF1 with their respective antigens should be conducted to reduce the non- βDG specific detection of these antibodies for use in future applications.

6.3.2 CENTROSOME TO NUCLEUS DISTANCE AND AMPLIFICATION IN DAG NULL FIBROBLASTS

It is not necessarily surprising that βDG does not localise at the centrosome itself and it is perhaps more intuitive that βDG may exert its influence over the centrosomes through its localisation and roles at the nuclear membrane. A number of components of the nuclear envelope such as emerin, Lamins, nesprins and SUN proteins have all been implicated in centrosome positioning near to the nucleus (Burakov et al 2013, Salpingidou et al. 2008, Hale et al. 2008, Malone et al. 2003, King et al. 2008, Zhang et al. 2009). The contribution of these proteins to centrosome positioning can be through their interaction with the microtubule or actin cytoskeleton or their roles in maintaining localisation of other components of the nuclear envelope which in turn interact with the centrosome through the cytoskeleton or microtubule motors such as dynein (Burakov et al 2013). Depletion of DG via RNAi in C2C12 cells led to both mislocalisation of nuclear envelope components emerin and lamin A/C but also an increase in the distance from the centrosome to the nucleus and centrosome number in cells, likely as a consequence of the disrupted nuclear envelope (Martinez- Vieyra et al. 2013). In this study we asked if nucleus to centrosome distance was also increased in the human patient primary DAG null fibroblasts. In this instance, although there was a trend towards an increase in the distance (Fig 6.8) and a small number of cells with amplified centrosomes (Fig 6.9), it was not statistically significant. In the report by Martinez-Vieyra et al. the number of cells with

amplified centrosomes increased from 2% to 17% whilst the distance between the centrosome and the nucleus increased from 0.75µm to 1.8µm from wildtype C2C12 to DG RNAi C2C12 cells (Martinez- Vieyra et al. 2013). The difference between the significance of the results may be due to the cell types in which the experiments were conducted, although the importance of nuclear envelope proteins in tethering the centrosome has been seen in multiple cell types. It is also important to consider whether HDF cells are the best controls for the DAG null fibroblasts as they are from a different source and may be of a different age, thus a subtle change in distance may not be detected between these cells. It would be better to compare the DAG null fibroblasts to the same cells in which DG has been reexpressed.

The nuclear morphology of the DAG null fibroblasts is clearly disrupted (Section 4.2.1) it, would therefore be interesting to fully investigate the localisation of emerin, lamins and LINC complex components in these cells, which may shed light on both the nuclear morphology and centrosome positioning. It will also be important to investigate these localisations and interactions in a number of different cell types which have different adhesion and migration properties, which may have different contributions to nucleus and centrosome positioning.

DG can directly bind f-actin (Chen et al. 2003), it would therefore be interesting to investigate if DG influences centrosome position through emerin or another NE protein or itself through its cytoskeleton binding abilities. For example, this could be addressed through the expression of DG mutants with the inability to bind F-actin. As discussed in chapter 4, it is however, difficult to dissect roles of DG on the cytoskeleton from its localisation at the plasma membrane, from its roles in the nucleus.

Investigating the proteins contributing to nucleus- cytoskeletal connections at the centrosome is also important for our understanding of a number of diseases. There are a number of diseases stemming from mutations of nuclear envelope proteins, including laminopathies such as Hutchinson- Gilford progeria syndrome (HGPS) or emerin deficient X-linked EDMD (Worman 2012). Centrosome detachment from the nucleus and subsequent loss of the ability to polarise has been reported in mice models of these diseases (Hale et al. 2008). Centrosome amplification and abnormalities have also been reported with carcinogenesis (Boveri, 1914, D'Assoro et al. 2002, Ro et al, 2004). Thus understanding the mechanisms of centrosome function and position may have relevance for multiple diseases.

6.3.3 SUMMARY

1. Anti- βDG antibodies 1709 and JAF1 localise to the centrosome in interphase and mitotic cells.

2. The localisation of 1709 and JAF1 at the centrosome is an artefact of the primary antibodies as determined by studies of tagged βDG protein and DAG null systems.

-Myr-cβDG-GFP and αβDGflag do not localise to the centrosomes

-1709 and JAF1 detect the centrosomes in *DAG1*$^{-/-}$ zebrafish embryos and DAG null fibroblasts.

3. There is a small but not statistically significant increase in the distance between the nucleus and the centrosome in DAG null fibroblasts compared to HDF cells and a very small number of cells with increased number of centrosomes.

7. Discussion

The data presented in this thesis concur with and expand upon the current knowledge of a dynamic localisation of βDG within the nucleus and its mechanisms of regulation and functions therein. βDG is localised to multiple nuclear compartments including the NE, nucleoplasm and nucleoli in cancerous and 'normal' prostate cell lines and primary fibroblasts and, in conjunction with previous reports in the literature, indicates a role for βDG within the nucleus across multiple cell types (Oppizzi et al. 2008, Lara-Chacon et al. 2010, Martinez-Vieyra et al. 2013, Mathew et al. 2013). The severely disrupted nuclear morphology seen in DG null fibroblasts supports the hypothesis of a structural function of βDG within the nucleus which, although not addressed directly in this study, is potentially a consequence of the loss of the reported interactions of βDG with structural components of the NE including emerin and lamins (Martinez-Vieyra et al. 2013). Disruptions to the nuclear envelope organisation and proteins can result in mislocalised centrosomes. However, in contrast to a report in myoblasts, depleted levels of DG did not cause a significant increase in the NE to centrosome distance or centrosome number in the DG null fibroblasts. The disparity may be a consequence of differing contributions of DG to the role in different cell types cell types, migration status of the cells, or experimental caveats as addressed in chapter 6. Furthermore, it was shown that βDG does not localise to the centrosome itself and that the staining observed at the centrosomes with two separate anti- βDG antibodies was artefactual. Therefore, any potential role for DG in centrosome regulation could be through dystroglycan's interactions within other cellular structures such as the nuclear envelope or the cytoskeletal network.

Phosphorylation and the cell cycle were also investigated as potential regulatory mechanisms of the dynamic nuclear localisation of βDG. The phosphorylation status of residue T788 βDG did not appear to affect its nuclear localisation although may have roles in protein stability, thus opening an avenue for future research into the behaviour and regulation of βDG. Although DG regulation and the cell cycle are undoubtedly linked, a role for the cell cycle in the nuclear localisation of βDG remains inconclusive, although there is some evidence to suggest fluctuating levels of βDG at different stages of the cell cycle. Some caveats and further implications of the data obtained in this project are discussed below.

PTM are crucial regulators of protein localisation, including nuclear targeting. Antibodies raised against unphosphorylated and phosphorylated Y892 βDG epitopes detected βDG within the nucleus, suggesting that this modification is not essential for its nuclear targeting, in support of observations from previous studies in which Y892 has been mutated (Lara-Chacon et al. 2010,

Leocadio. 2015). Phosphorylation at residue T788(mouse)/ T790 (human) was hypothesised as a candidate for the nuclear targeting of βDG however neither phospho-mimetic or phospho-null mutations at this site altered the nuclear localisation of βDG, however there is preliminary evidence to suggest that a phospho-mimetic mutation at this site increases the protein's stability.

Phosphorylation involvement in the regulated degradation of proteins is widely reported and can be via phosphodegrons, in which phosphorylation of a short motif promotes subsequent ubiquitination and degradation, or alternatively phosphorylation can prevent degradation by modifying a constitutively active degradation motif (Ravid et al. 2008, Holt et al. 2012). Ubiquitination of βDG has been reported by multiple groups and, interestingly, the E3 ligase NEDD4L has been identified as interacting with βDG via both mass spectrometry and Y2H screens (Leocadio 2015 and S. Winder personal communication). Moreover, using in vitro studies with peptide arrays and recombinant proteins, an interaction between the WW domains on NEDD4L and the peptide sequence LEDQATFIKKGVPI, corresponding to residues 883-896 of βDG, was identified (Piggott, 2014). The T788 phosphorylation site lies within this sequence and it could therefore be possible that phosphorylation at this site could modulate an interaction between βDG and the E3 ligase and ultimately the proteasome mediated degradation of βDG. However, further in vivo studies in H2K cells and pull downs with recombinant fragments of NEDD4L and βDG did not demonstrate an interaction. It is possible that NEDD4L is interacting at different sites of βDG for example with one of the three PEST (Pro, Asp, Ser, Thr) motifs within its sequence or it may not be a direct interaction between the two proteins (Piggott, 2014). An avenue of future research could aim to assess the role of phosphorylation at T788 on the degradation of βDG via cell lines stably expressing the T788 mutant constructs in parallel with proteasome inhibitors, ubiquitin-specific resins such as Mdsk and interaction studies with E3 ligases.

Whilst it is important to understand the mechanisms of nuclear translocation, this project also aimed at identifying the cellular cues that result in a fluctuating level of nuclear DG. Although by no means conclusive, there is some evidence to suggest a role for the cell cycle in regulating the nuclear levels of βDG. There was a slight correlation between the percentage of cells in S phase and an increase in the quantified levels of total DG, this seemingly agrees with two separate reports in which DG increased in proliferating cells, particularly at S phase (Sgambato et al. 2006, Hosokawa et al. 2001). However, as previously discussed there are caveats regarding the quantification and variability of the expression of βDG in the thymidine synchronised populations and thus the potential slight fluctuation of βDG should be interpreted with caution requires further investigation. The reports by Sgambato et al and

Hosokawa et al. indicate that the cell cycle dependent regulation is at the level of transcription, through as yet unknown mechanisms (Sgambato et al. 2006, Hosokawa et al. 2001). Furthermore, in this study, βDG species with different Y892 phosphorylation statuses displayed varying degrees of fluctuation in their nuclear levels and correlation to cell cycle phases.

One can suggest a scenario in which the total levels of βDG are increased at a certain point in the cell cycle, seemingly S phase. There is a corresponding increase in the levels of phosphorylated Y892 βDG. pY892 promotes the internalisation of βDG from the membrane (Sotgia et al. 2003, Miller et al. 2012) the observed increased in this modified form of βDG may simply be a consequence of an increased level of DG substrate for the kinase or actively increased phosphorylation in response to a cellular cue. For example, an increase in phosphorylation at Y892 might be important in reducing the amount of βDG within cell adhesions at the cell surface when the cell rounds up and reduces adhesions during mitosis. Internalisation from the membrane is presumably a necessary step in the process of nuclear translocation of βDG if the source is the plasma membrane. In this scenario there would therefore be an increased intracellular pool of βDG available for interaction with nuclear import proteins. Once internalised there are likely specific PTM promoting or disrupting interactions with proteins that regulate nuclear transport or cytoplasmic or nuclear retention. The nature of the PTM or interactions promoting nuclear translocation at this time point and whether they are actively regulated by the cell cycle or just increased activity of the basal machinery as a consequence of increased internalised levels of DG is unclear. The fate of the nuclear DG is yet to be determined and it may be targeted for degradation or may play a role in cell cycle or nuclear processes. Any hypothetical role for DG in the cell cycle is clearly not vital as in DG null or knockdown systems cell still progress through the cell cycle, albeit with delays (Higginson et al. 2008, Sgambato et al. 2006).

The non-nuclear levels of pY892 βDG do not fluctuate significantly in the synchronised populations or decrease at the time point corresponding to increased levels in the nuclear fraction, a result which could suggest that the excess internalised βDG is targeted to the nucleus. Conversely a significant correlation with S phase is seen in the non-nuclear but not the nuclear levels of non-phosphorylated Y892 βDG. This observation may support the hypothesis that the nuclear translocation follows an increased internalisation from the PM as a result of its phosphorylation, whilst the non-phosphorylated population remains largely at the cell surface. Unfortunately, the dynamic localisation of pY892 βDG could not be validated via immunofluorescence analysis studies due to the artefactual staining demonstrated by the 1709 antibody in this technique.

A useful tool in the study of the behaviour of proteins in a dynamic process such as the cell cycle is live cell imaging. This process ideally requires a fluorescent tag. Whilst live cell analysis has been carried out with βDG before, the focus was not on the nuclear levels of βDG and moreover there are important caveats with the system. A C-terminal GFP tag impairs Y892 phosphorylation, and therefore interferes with an important regulatory site of interactions and localisation (Leocadio, 2014). Unfortunately, it is difficult to propose a site within βDG to insert a tag without disrupting a functional or regulatory site. A key caveat with this project was the inability to achieve higher purity or synchronised populations of cells for cell cycle analysis and the results should be analysed critically accordingly as discussed in detail in chapter 5. Future work in this field will require investigation with alternative cell cycle analysis techniques with optimised synchronised or sorting. An attractive alternative option is to use a protocol combining immunofluorescence staining, with biochemical fractionation of isolated nuclei that are then analysed on the flow cytometer to determine cell cycle phase (Rosner et al. 2013). This approach has been reportedly successful in the study of nucleocytoplasmic shuttling of proteins in the unperturbed mammalian cell cycle of multiple cell lines (Rosner et al. 2013).

Whilst neither phosphorylation at Y892 (human) and T788 (mouse) appear to have clear direct roles in the nuclear translocation of βDG there are multiple other PTM which may regulate the nuclear localisation of βDG. Given the potential for cell cycle regulation, putative sites of CDK phosphorylation remain interesting candidates, however it is not immediately clear how phosphorylation at the predicted residues could affect the nuclear transport as the sites do not overlap with sites of known interactions (Moore et al. 2010). However, it is possible that phosphorylation disrupts an unknown interaction involved in nuclear or cytoplasmic retention or transport.

Phosphorylation by CDK1 is an important regulator of chromatin organisation, cytoskeletal rearrangements and NEBD and reformation during mitosis (Foisner 2003, Enserink et al. 2010). There are multiple reports in the literature of specific localisation of DG and other DAPC components at distinct locations at the cell periphery, forming cleavage furrow and midbody during mitosis and cytokinesis (Higginson et al 2008, Villareal-Silva et al. 2011), which is supported by the data presented in chapter 5. These distinct localisations suggest a specific regulation of DG during this phase of the cell cycle, as is the case with many cytoskeletal interacting or NE proteins and one could hypothesise that CDK1 phosphorylation may play a role in the regulation or localisation of βDG. An obvious first step would be to validate if βDG is a target of CDKs whilst site specific mutations might provide functional clues.

An example of CDK1 activity mediating cytoskeletal regulation in mitosis is the CDK1 mediated phosphorylation of filamin-A, an actin cross-linking protein. Phosphorylation regulates the

actin binding ability of filamin-A, moreover, mutations at the sites of CDK1 phosphorylation of filamin-a disrupt daughter cell separation in cytokinesis (Cukier et al. 2007, Szeto et al. 2015). βDG can also bind to actin via its C-terminal tail and it remains a possibility that phosphorylation at residues within this domain may modulate its actin binding ability and ultimately modulate actin dynamics (Chen et al. 2003). However, studies in which DG has been depleted by RNAi and the DAG null fibroblasts show normal cytoskeletal features (Batchelor et al. 2007, Higginson et al. 2008), and it is difficult to reconcile these observations with a role for βDG in cytoskeletal rearrangements in mitosis.

Of particular interest in terms of this project is the regulation of NE proteins in mitosis. NE proteins including SUN1, emerin and Man1 as well as nuclear lamins are regulated in NEBD and NE reformation in part through their phosphorylation by CDKs and other mitotic kinases (Foisner 2003, Patel et al. 2014, Ottaviano et al. 1985, Nikolakaki et al. 1997). Whilst immunoblot analysis of mitotic enriched populations did not identify an altered phosphorylation status of DG in mitotic cells this technique might not have been sensitive enough. Mass spectrometry of mitotic enriched populations might identify specific sites of mitotic phosphorylation. Indeed, a number of the entries of phosphorylated βDG in the phosphosite database are as a consequence of studies of the global phospho profile of mitotic populations of cells (Hornbeck et al. 2104, Kettenbach et al. 2011). In addition to its strong localisation at the cell periphery in mitotic cells the non-phosphorylated Y892 form of βDG was faintly dispersed in the cytoplasm. The reformation of the NE is a hierarchical process (Foisner 2003, Haraguchi et al. 2000). The fact that NE are reformed in DG null cells hints that DG is not vital in this process, on the other hand some of the severe morphological defects observed in DG null cells may be a consequence of disruptions in the NE assembly process. Analysis in live cell imaging of NE markers in mitotic DG null cells might highlight if this is indeed the case.

Key to understanding the behaviour of DG in the nucleus will be the identification of its nuclear binding partners. At the plasma membrane βDG has been shown to interact with a plethora of proteins, thus broadening our knowledge of the varying pathways and functions in which βDG is involved (Moore et al. 2010). However, unravelling the interactions of βDG within the nucleus is unlikely to be a simple task. In proteomics studies a vast number of nuclear membrane proteins have been identified (Wilkie et al. 2007, Worman et al. 2015). Whilst some of these NE proteins are ubiquitously expressed, such as emerin and lamins, their functionality is modulated by specific PTM but also the temporal expression and tissue specificity of their binding partners (Worman et al. 2015). It is not unreasonable to predict that nuclear DG is a ubiquitous phenomenon given its ubiquitous expression profiles in tissues and its widespread reports of its presence in the nucleus (Ibraghimov-Beskronaya et al. 1993, Oppizzi et al. 2008,

Lara-Chacon et al. 2010, Mitchell et al. 2013, Mathew et al. 2013). It is also likely to form multiple interactions, especially given its diverse nuclear localisation at the NE, nucleoplasm and other nuclear organelles (Martinez-Vieyra et al. 2013). Indeed, studies of DAPC components within the nucleus revealed slightly different members in different cell types (Villarreal-Silva et al. 2010, Gonzalez-Ramirez et al. 2008, Fuentes-Mera et al. 2006). Immunoprecipitation experiments have already indicated interactions with the important nuclear proteins lamins, emerin (Martinez-Vieyra et al. 2013) and potentially SUN1 (M. Laredo and S. Winder, personal communication) through which βDG may contribute to both structural and signal transduction pathways in the nucleus. Analogous to the behaviour of βDG at the PM, DG may interact with signalling pathway components such as ERK and adaptor proteins in the nucleus. Mass spectrometry studies of nuclear samples have been conducted in LNCaP cells indicating a range of PTM and binding partners that remain to be validated (Leocadio, 2014). Further insights may well be gained through similar mass spectrometry approaches in samples from different tissue types or enriched for cell cycle phases.

An important βDG interaction not addressed in this study is whether αDG is also found in the nucleus and moreover if it interacts with nuclear βDG and regulates its function? αDG is a secreted protein and contains no TM domain or predicted NLS, furthermore a functional role for this protein in the nucleus is difficult to conceive, however it cannot be dismissed. αDG is difficult to detect because of its many glycosylation moieties and indeed some of the perceived loss of αDG from the PM in cancer studies may be as a consequence of loss of specific glycosylation epitopes rather than core protein. A study by Oppizzi et al. did not detect αDG in the nucleus, although this study used the aforementioned glycosylation dependent antibodies (Oppizzi et al. 2008). A different study has detected the presence of an exogenously expressed myc tagged αDG in the nucleus of LNCaP cells following fractionation however if this is true of endogenous αDG remains unclear (Leocadio, 2015).

To expand upon the findings from this project it would be important to investigate nuclear DG in different experimental systems. Whilst cells in 2D culture are easy to manipulate and study, providing valuable insights into the function and regulation of a protein and its subsequent role in cellular behaviour, it is important to recognise their limitations. *In vivo* a cell is highly influenced by its 3D microenvironment via ECM-interactions, cell-cell interactions and differing nutrient profiles (Edmondson et al. 2014, Hakkinen et al. 2011, Loessner et al. 2010). Typically cells in 3D culture grow as aggregates or spheroids with a hierarchical structure and heterogeneity demonstrating a closer resemblance of cell morphology, functions and interactions to cells *in vivo* (Kim et al. 2005, Lin et al. 2008). It has been shown that cells in 3D systems can display a different spatial organisation of surface receptors than in 2D and can

show different expression patterns of proteins (Hakkinen et al. 2011, Luca et al. 2013). βDG localisation in LNCaP, PC3 and PNT1A cells in 3D cultures has been characterised previously, broadly demonstrating a peripheral localisation and variable levels within the nuclei within a spheroid structure (Mathew, 2011). In light of the observations that nuclear levels of βDG may fluctuate in a cell cycle dependent manner it would be interesting to readdress the nuclear localisation of βDG in the 3D populations with regards to proliferation status of the cells to validate this observation in more representative conditions. A 3D system may be of particular interest in understanding the distribution of βDG in tumours as the cell aggregates or spheroids grown in culture often mimic tumour organisation with more proliferating cells in the outer layers with increased numbers of quiescent cells in inner layers and a necrotic core (Laurent et al. 2013, Kim et al. 2005, Edmondson et al. 2014). In a similar vein it should be acknowledged that the majority of the work in this project was conducted in cancer cell lines, therefore to ascertain the 'normal' processing of DG would require repeats in non-neoplastic cell lines.

Beyond cell culture systems it could be useful to assess the role of βDG in the nucleus using the available *DAG1* null or mutant DG animal models available. The aberrant nuclear morphology seen in the *DAG1* null fibroblasts and other reports in DG KD cell systems (Martinez- Vieyra et al. 2013) has not been reported in the studies of *DAG1* null tissues of chimeric mice, nor in the null zebrafish or fly models. However, it should be noted that the majority of these studies focussed at the tissue not the subcellular level. Investigations in animal models would also allow enable the investigation of how a nucleus absent for DG fares under the more dynamic mechanical stresses experienced in a living animal.

In the models addressed so far it is difficult to dissect the roles of DG at the PM from the nuclear population of DG on nuclear structure but also signalling. These studies have been hindered by the lack of a full knockout cell model. Expression of βDG with mutations in the NLS or of fragments which target strongly to the nucleus in systems such as the DG null fibroblasts could help in identifying the consequences of nuclear DG in the absence of endogenous protein. Furthermore, the exogenous protein could be expressed without a tag thus limiting potential interference with interacting partners. The development of a CRISPR/Cas9 model to produce cells lacking DG would also provide a useful experimental system to investigate the roles of nuclear DG.

The localisation of βDG in the nucleus and its emerging role in maintaining nuclear structure could have broad disease implications. A number of nuclear envelope proteins and lamins have been implicated in a range of diseases from muscular dystrophy to accelerated aging disorders (Worman et al. 2010). For example, different forms of EDMD can arise as a consequence of

mutations in lamins A and C, emerin and nesprin1 (Bonne et al. 1999, Bione et al. 1994, Zhang et al. 2007). Multiple molecular mechanisms have been proposed to underlie the pathology of NE diseases including mechanical instability by perturbing interactions between the nucleus and cytoskeleton, altered gene expression as a consequence of disrupted NE and disruption of the cell cycle (Wilkie et al. 2011, Worman et al. 2010). Disruption of individual components of the DAPC can result in the dissociation of the complex with reduced localisation at the PM and a reduction in the levels of the proteins, including DG (Villarreal-Silva et al. 2010). Given the evidence for a nuclear DAPC and its NE localisation reported elsewhere (Martinez- Vieyra et al. 2013, Leocadio et al. 2016) and in this study, it is not unreasonable to hypothesise that the nuclear DAPC could also be disrupted upon mutations or reduced levels of an individual component. Subsequent loss of nuclear DAPC components and their interactions with NE proteins, such as DG with lamins, emerin and the LINC complex could contribute to disease pathology through any of the aforementioned mechanisms. The aberrant nuclear morphology seen upon loss of DG is similar to that seen in cells deficient in lamins or emerin (Lammerding et al. 2005, Fidzianska et al. 1998, Funkhouser et al. 2013), reinforcing the role for DG in NE structure. It is not known if the interactions with NE proteins play a role in retaining DG within the nucleus, however it is also possible that disruption to the levels or correct functioning of NE proteins such as emerin and lamins could also perturb nuclear DG localisation, thus exacerbating the instability of the NE in a range of diseases.

The data presented throughout this thesis supports the presence of βDG in the nucleus of cancer cells as well as non-cancerous cells. Loss of α and βDG from the PM have been reported as early steps in the EMT and metastatic process in epithelial cancers including breast and prostate, with reexpression in tumours at secondary sites (Cross et al. 2008, Mitchell et al. 2013, Mathew et al. 2013). The loss of DG from cells correlating with cancer progression is similar to that seen with other adhesion molecules such as E-cadherin and catenins. Prostate cancers with lower expression of α-catenin correlated with higher mitotic indexes, higher S phase factions and reduced survival (Aaltomaa et al. 1999, Morita et al. 1999). Whilst potential mechanisms of DG contribution to cancer progression at the PM are perhaps more intuitive given its roles in adhesion, migration and proliferation, a potential nuclear contribution remains less clear. The 31 and 26Kda fragments of βDG have been reported in cancer cells (Singh et al. 2004, Cross et al. 2008, Mitchell et al. 2013, Leocadio et al. 2016), and pY892 βDG has been identified in the nucleus of prostate tissue microarrays (TMA) (Mathew et al. 2013) however a further in depth analysis of nuclear DG in patient tissue samples at different stages of disease progression or at different stages in animal cancer models may provide further insight into nuclear levels of DG at different stages of cancer progression. Differential regulation of βDG at the PM is likely a consequence of cancer but can also then contribute to

disease phenotypes and this scenario possibly extends to βDG within the nucleus. A potential correlation between proliferating cells and nuclear DG levels may result in an increased level of nuclear DG in the inherently highly proliferative tumour cells, in combination with increased nuclear targeting as a result of aberrant glycosylation and increased proteolytic cleavage at the cell surface. As to contribution to disease progression, although at this stage purely speculative, one may hypothesise that βDG could modulate signalling pathways by sequestering pathway components in the nucleus, in this way βDG could influence the regulation of a variety of target genes which may ultimately contribute to disease progression, including early cell cycle genes through the ERK pathway or ETV1 in prostate cancers.

Research into the role of DG at the PM has long been a focus for multiple groups, however the localisation of DG at internal structures should not be ignored. Whilst this study has demonstrated that the localisation of DG at the centrosomes is artefactual, the nuclear functions and mechanisms of regulation of βDG are still emerging. Many questions remain with regards to nuclear DG however this thesis has addressed PTM that were hypothesised to play a role in the nuclear localisation of βDG, providing a basis for future studies in understanding the complex regulation of DG. Furthermore, the investigation of the nuclear levels of DG in the cell cycle expands the knowledge of the relationship between this fundamental cellular process and DG, although further work is required to validate a specific mechanism linking the nuclear localisation of DG to the cell cycle. Given the many roles of DG in normal and disease processes it is important to continue research to improve the understanding of the cellular biology of this dynamic protein.

Appendix A: Buffers and Recipes

Buffer	Components	Notes/ Reference
Blocking Buffer (immunofluorescence)	5% FBS (v/v), 3% BSA (w/v)	Made in 1x PBS pH7.4
Blocking Buffer (Western Blot)	5% (w/v) skimmed milk or BSA	Dissolve in 1x TBST
Buffer I (Cell Fractionation)	0.32M Sucrose, 10mM Tris-HCl pH 8.0, 3mM Calcium Chloride, 2mM Magnesium actetate, 0.1mM EDTA, 0.5% NP-40 (v/v), 1mM DTT	Sterile Filter. Add protease and phosphatase inhibitors as needed. (Mathew et al. 2013)
Buffer II (Cell Fractionation)	2M Sucrose, 10mM Tris-HCl ph 8.0, 5mM Magnesium Acetate, 0.1mM EDTA, 1mM DTT	Sterile Filter. Add protease and phosphatase inhibitors as needed. (Mathew et al. 2013)
Coomassie Safe Stain	60-80mg Coomassie brilliant blue G250, 3ml Concentrated HCl	
E3 Embryo Medium (Zebrafish)	5mM NaCl, 0.17mM KCl, 0.33mM $CaCl_2$, 0.33mM $MgSO_4$, 0.0001% methylene blue.	
ECL Solution I	100 mM Tris-HCl pH8.5, 25mM Luminol, 396µM p-Coumaric Acid	
ECL Solution II	100 mM Tris-HCl pH8.5, 0.02% (v/v) H_2O_2	

Laemmli SDS-PAGE Loading Buffer (2x)	20% Glycerol (v/v), 100mM Tris-HCl pH 6.8, 4% SDS (w/v), 0.2% Bromophenol Blue (w/v), 2% β-2-mercaptoetanol (v/v)	Concentration can be adjusted to prepare a 5x concentrated buffer (Laemmli, 1970)
Laemmli SDS-PAGE Resolving Buffer	1.5 M Tris-HCl pH 8.8, 0.4% SDS (w/v)	(Laemmli, 1970)
Laemmli SDS-PAGE Running Buffer (10 x)	250 mM Tris, 1.92 M Glycine	(Laemmli, 1970)
Laemmli SDS-PAGE Stacking Buffer	0.5 M Tris-HCl pH 6.8, 0.4% SDS (w/v)	(Laemmli, 1970)
10x Loading Dye (DNA)	0.25% Bromophenol Blue (w/v), 0.25% Xylene cyanol FF (v/v), 30% glycerol (v/v)	
Mild Lysis Buffer (IP)	50 mM Tris-HCl pH 7.4, 150 mM NaCl, 1 mM EDTA, 1% Triton X-100 (v/v)	
Mild Stripping Buffer (1L)	15g Glycine, 1g SDS, 1 ml Tween 20	Adjust the pH to 2.2
Mounting Medium	10 ng/ml DAPI, 2.5% DABCO (w/v)	Dissolve in Hydromount (National Diagnostics)
PDB (Zebrafish immunofluorescence)	PBS, 0.2% (v/v) tween-20, 1% BSA (w/v) 0.01% DMSO (v/v)	
10 x Phosphate Buffered Saline (10x PBS)	1.37 M NaCl, 0.027 M KCl, 0.1 M Na_2HPO_4, 0.018M KH_2HPO_4	Adjust pH to 7.4 with HCl
PBST	PBS, 0.2% (v/v) tween-20	
Propidium iodide stain	20µg/ml Propidium Iodide, 200µg/ml RNAse A	Made in PBS pH7.4 and stored in the dark

Radio Immunoprecipitation Assay Buffer (RIPA Buffer)	50mM Tris- HCl pH 7.5, 150 mM NaCl, 1 mM EGTA, 1 mM EDTA, 1% Triton X-100 (v/v), 0.5% Sodium Deoxycholate (w/v), 0.1% SDS (w/v)	Add protease and phosphatase inhibitors as required (James et al. 2000).
SDS Running Buffer	200 mM Glycine, 25mM Tris, 0.01% SDS	
1x TAE buffer	40mM Tris-Acetate, 1mM EDTA	
Tris Buffered Saline (TBS) (1x)	50 mM Tris-HCl pH 7.4, 150 mM NaCl	
Tris Buffered Saline Tween (TBST) (1x)	50 mM Tris-HCl pH 7.4, 150 mM NaCl, 0.5% Tween 20 (v/v)	
Towbin Buffer	25 mM Tris, 192 mM Glycine, 20 % Methanol (v/v), 0.02% SDS (w/v)	Towbin et al. 1979
2x YT	1% yeast extract (w/v, 1.6% tryptone (w/v), 0.5% NaCl (w/v)	

Appendix B: Methods Tables and Figures

B.1 Plasmid Table

Plasmid	Function	Antibiotic Resistance	Reference/ Source
pcDNA3.1 (+) αβDGflag	Encodes full length mouse αβDGflag	Ampicillin	D.L.Victoria
pcDNA3.1 (+) αβDGflagT788A	Encodes full length mouse αβDGflag with the T788A mutation	Ampicillin	This study
pcDNA3.1 (+) αβDGflagT788D	Encodes full length mouse αβDGflag with the T788D mutation	Ampicillin	This study

B.2 Oligonucleotide table

Oligonucleotide	Sequence (5'-3')	Function
αβDGflagT788A F	CCCCTTCTTAATAAAGGCGGCCTGG TCCTCAAG	Site directed mutagenesis of T788 to A in the αβDGflag sequence. Forward primer.
αβDGflagT788A R	CTTGAGGACCAGGCCGCCTTTATTA AGAAGGGG	Site directed mutagenesis of T788 to A in the αβDGflag sequence. Reverse primer.
αβDGflagT788D F	CACCCCCTTCTTAATAAAGTCGGCCT GGTCCTCAAG	Site directed mutagenesis of T788 to D in the αβDGflag sequence. Forward primer.
αβDGflagT788D R	CTTGAGGACCAGGCCGACTTTATTA AGAAGGGGGTG	Site directed mutagenesis of T788 to D in the αβDGflag sequence. Reverse primer.
BGH Reverse Primer (Source Bioscience stock primer)	TAGAAGGCACAGTCGAGG	BGH reverse primer used to sequence the plasmid pcDNA3.1 (+) containing the αβDGflagT788A and αβDGflagT788D sequences
T7 promoter (F) (Source Bioscience stock promoter)	TAATACGACTCACTATAGGG	T7 promoter forward primer used to sequence the plasmid pcDNA3.1 (+) containing the αβDGflagT788A and αβDGflagT788D sequences

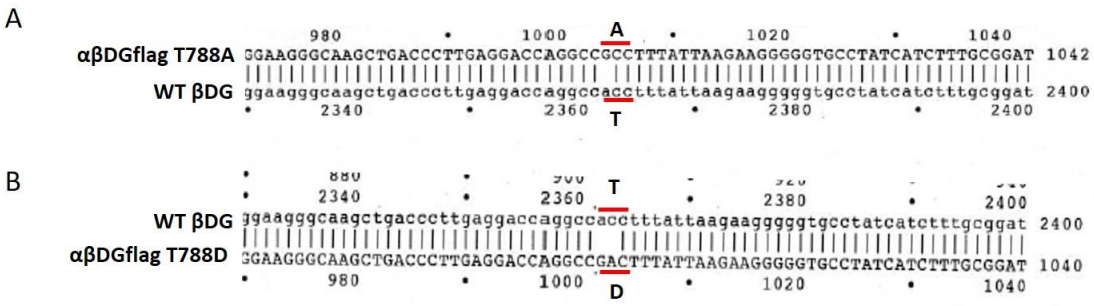

FigureB.1: DNA Sequence alignment of αβDGflag T788A and αβDGflagT788. Following Site-directed mutagenesis of (A) αβDGflag T788A and (D) αβDGflagT788 plasmids were sent for DNA sequencing at Source Bioscience for verification. Bovine growth hormone (BGH) and T7 stock primers were used. The subsequent DNA sequences were aligned with the sequence of wt βDG using DNA Strider software. Sites of SDM are underlined in red.

B.3 Protease and Phosphatase inhibitors

Enzyme	Target	Final Concentration
Sodium Orthovanadate	Tyrosine phosphatases and alkaline phosphatases	1 mM
PMSF	Serine proteases	1 mM
TPCK	Serine proteases	10 µM
Leupeptin	Serine and cysteine proteases	10 µM
Pepstatin	Aspartic acid proteases	1 µM
Aprotinin	Serine proteases	10 µg/ml
Benzamidine	Serine proteases	10 µg/ml
NaF	Serine, threonine and acidic phosphatases	10 mM
Roche Complete Protease inhibitor mix	Serine and cysteine proteases	1X

B.4. SDS-PAGE resolving and stacking mini Gel recipes

	Resolving Gel (10 ml for 2 gels)			Stacking gel (5ml for 2 gels)
Concentration	**7.5 %**	**10 %**	**12.5%**	**5%**
Acrylamide	2.5	3.35	4.15	0.8
Gel stock	3.75	3.75	3.75	0.625
Water	3.65	2.85	2.0	3.525
TEMED	5 µl	5 µl	5 µl	15 µl
10% APS	100 µl	100 µl	100 µl	50µl

B.5 PRIMARY ANTIBODIES

Antibody Name	Epitope/ Target	Species/ Class	Dilutions		Reference/ Source
			WB	IF	
βDG MANDAG2	βDG, carboxy terminus, residues 881-895 (KNMTPYRSPPPYVPP)	Mouse monoclonal	1:300	1:100	Thi Man and G. Morris (Gift) Pereboev *et al.* 2001
βDG 1709	βDG, carboxy terminus residues 881-895 phosphorylated at Y890 (mouse) /Y892 (human) (KNMTPYRSPPPpYVPP)	Rabbit IgG Polyclonal	1:500	1:200	In house (Ilsley et al. 2001)
βDG JAF1	βDG, carboxy terminus, 7 amino acid residues	Rabbit Polyclonal	1:500	1:200	D. Mornet (Gift) (Rivier et al. 1999)
βDG C-20	βDG, carboxy terminus 20 residues	Goat IgG Polyclonal	1:250	1:75	Santa Cruz (sc-16165)
α- tubulin (B512)	α- tubulin, Carboxy terminus	Mouse IgG1	1:2500	1:1000	Sigma (T5168)
Actin	Actin, carboxy terminus	Goat	1:1000	N/A	Santa Cruz (sc-1616)
β- tubulin	β- tubulin, amino terminus	Rabbit IgG monoclonal	N/A	1:3000	Cell Signalling Technology (2128)
Anti-BrdU (BMC 9318)	Bromodeoxyuridine	Mouse IgG1 monoclonal	N/A	1:100	Roche (11170376001)
Calnexin (C5C9)	Total Calnexin	Rabbit IgG monoclonal	1:1000	1:100	Cell Signalling Technology (2679)
Cyclin A2 (F683)	Cyclin A2, recombinant human protein	Mouse IgG2b monoclonal	1:750	N/A	Cell Signalling Technology (4656)
Cyclin B1	Cyclin B1, amino terminus	Rabbit IgG	1:750	N/A	Cell Signalling Technology (4138)
Cyclin D3 (DCS22)	Cyclin D3, residues 241-260	Mouse IgG1 monoclonal	1:750	N/A	Cell Signalling Technology (2936)
Cyclin E1 (ME12)	Cyclin E1, recombinant human protein	Mouse IgG1 monoclonal	1:750	N/A	Cell Signalling Technology (4129)
Fibrillarin (C13C3)	Fibrillarin, synthetic peptide surrounding Thr298 of human fibrillarin	Rabbit IgG, monoclonal	1:1000	N/A	Cell Signalling Technology (2639)
Flag M2	Flag epitope DYKDDDDK	Mouse IgG1	1:3000	1:1000	Sigma (F3165)

rFLAG	Flag epitope DYKDDDDK	Rabbit IgG	1:3500	1:1500	Sigma (F7425)
γ- tubulin	γ- tubulin amino terminus residues 38-53	Mouse IgG1 monoclonal	N/A	1:800	Sigma (T5326)
	γ- tubulin amino terminus residues 38-53	Rabbit polyclonal	N/A	1:1000	Sigma (T5192)
GAPDH (GA1R)	GAPDH	Mouse IgG1 monoclonal	1:10000	N/A	ThermoScientific (MA5-15738)
Phospho-histone H3 (HTA28)	Histone H3 phosphorylated at S28, residues 23-35	Rat IgG2a monoclonal	1:1000	1:1000	Abcam (ab10543)
Ki67 (MM1)	Ki67 fragment	Mouse IgG1	N/A	1:200	Novocastra (NCL-Ki67-MM1)
Lamin A/C (4311)	Lamins A and C, recombinant fragment of lamin A protein	Mouse monoclonal	1:1000	1:200	Cell Signalling Technology (4777)
Lamin B1 (H-90)	Lamin B1, C- terminus, residues 401-490	Rabbit IgG polyclonal	N/A	1:200	Santa Cruz (sc-20682)
Nucleolin C23 (MS-3)	Nucleolin, full length residues 1-706	Mouse IgG1	1:2500	N/A	Santa Cruz (sc-8031)

B.6 SECONDARY ANTIBODIES

Antibody Name	Epitope/ Target	Species/ Class	Dilutions		Reference/ Source
			WB	IF	
Anti-Mouse IgG peroxidase conjugate	Mouse IgG	Goat	1: 10000	N/A	Sigma (A4416)
Anti-sheep/goat IgG peroxidase conjugate	Sheep/Goat IgG	Mouse	1:10000	N/A	Sigma (A9452)
Anti-Rabbit IgG peroxidase conjugate	Rabbit IgG	Goat	1: 15000	N/A	Sigma (A0545)
Anti-Rat IgG peroxidase conjugate	Rat IgG	Goat	1:10000	N/A	Sigma (A9037)
AlexaFluor 488	Mouse IgG	Goat/ Donkey	N/A	1:500	Life technologies (A11029/ A21202)
	Rabbit IgG	Goat/ Donkey			Life technologies (A11008/ A21206)
	Goat IgG	Donkey			Life technologies (A11012)
AlexaFluor 594	Mouse IgG	Goat	N/A	1:500	Life technologies (A11005)
	Rabbit IgG	Goat			Life technologies (A11012)
Anti-Rat Texas Red	Rat IgG	Goat	N/A	1:100	Vector (T1-9400)
Anti-Sheep Fluorescein	Sheep IgG	Rabbit	N/A	1:100	Vector (F1-6000)

Appendix C: Supplementary Figures

A

Length of thymidine treatment	% of Popuation		
	G1	S	G2M
Control 1 (18hr)	75.8	13.2	10.1
18 hrs	73.9	19.8	6.0
20 hrs	74.2	19.8	5.6
22 hrs	68.6	25.6	5.8
24 hrs	66.7	27.1	6.0
26 hrs	65.3	28.7	5.9
28 hrs	62.7	31.1	6.3
30 hrs	61.2	32.2	6.7
32hrs	60.9	33.4	5.8
Control 2 (32hr)	79.8	9.3	10.5

B

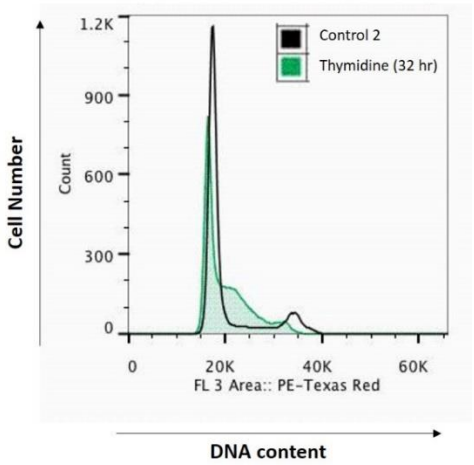

Figure C.1 Thymidine synchronisation of LNCaP cells optimisation. LNCaP cells were seeded at a density of 5 x 10^5 per 100mm dish and grown for 48 hours. Cells were treated with 2mM thymidine or PBS control. Over 18 to 32 hours of thymidine treatment cells were collected and ethanol fixed every two hours. Control 1 and control 2 were collected at the first and last time points, 18 and 32 hours respectively. Samples were then stained with propidium iodide and analysed on the CyAn ADP and DNA histograms produced. The percentage of the population of cells in G1, S and G2/M phases of the cell cycle were calculated via manual gating using flow jo software (A). Histogram overlay of C2 (black) and 32 hours thymidine treatment (green) shows an increased number of cells in S phase.

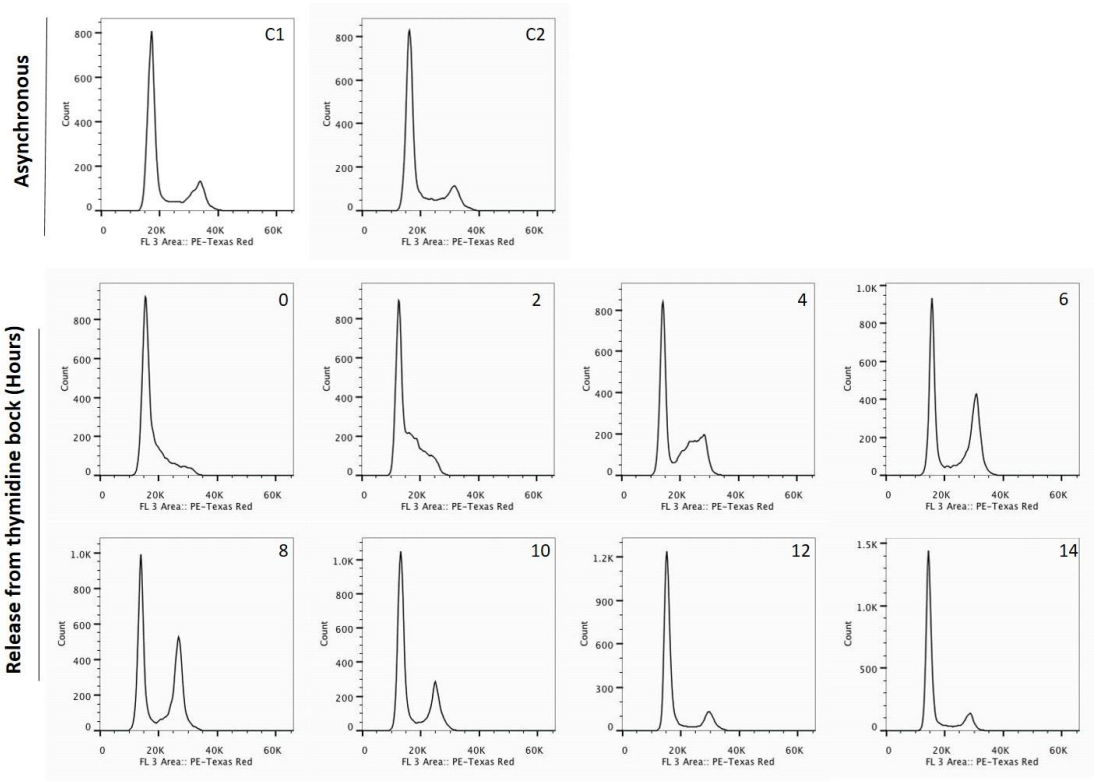

Figure C.2. Cell cycle progression of LNCaP cells released from a double thymidine block. LNCaP cells were grown for 48 hours and then treated with 2mM Thymidine for 32 hours. Cells were released by addition of fresh media for 9 hours and then blocked for a further 22 hours with 2mM Thymidine. Cells were released into the cell cycle via the addition of fresh media and collected every two hours over 14 hours. Control 1 and control 2 were PBS control treatments at 0 hr and 14 hours respectively. The collected cells were harvested for lysate collection or ethanol fixed, stained with propidium iodide and analysed for cell cycle distribution via flow cytometry. Representative DNA histograms from one experiment are shown.

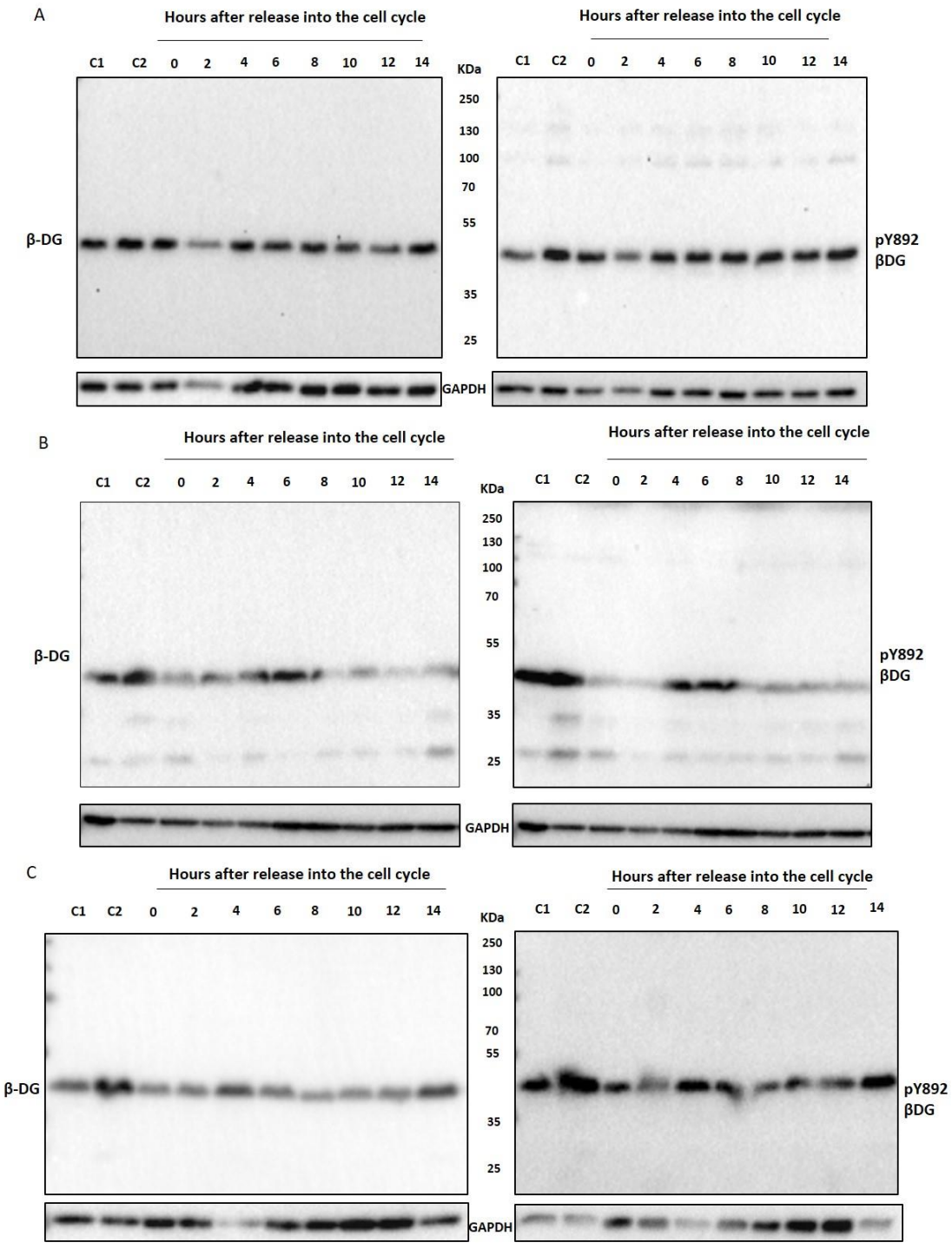

Figure C.3. Replicate immunoblots of βDG and pY892 βDG in total cell lysates from thymidine synchronised LNCaP cells. Independent repeats (A, B,C) of immunoblot of total cell lysates collected from double thymidine block synchronised LNCaP cells at each time point and immunoblotted for βDG and pY892 βDG and a GAPDH loading control.

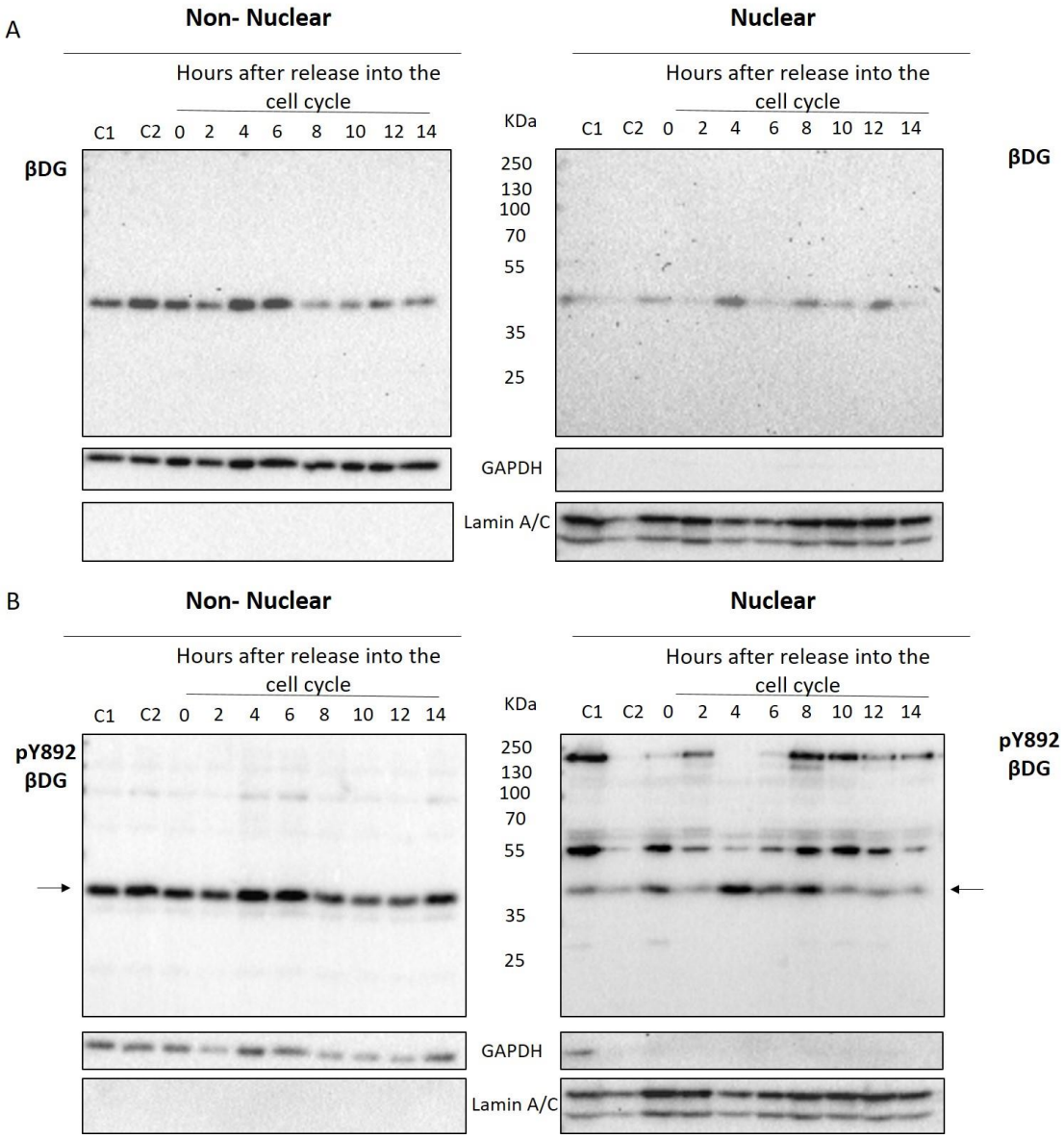

Figure C.4. Replicate immunoblots of βDG and pY892 βDG in non- nuclear and nuclear fractions of thymidine synchronised LNCaP cells. Immunoblot of non-nuclear (left) and nuclear (right) lysates collected from double thymidine block synchronised LNCaP cells at each time point and immunoblotted for (A) βDG or (B) pY892 βDG. GAPDH and Lamin A/C were included as purity markers of the fractionation and loading controls of the non-nuclear and nuclear fractions respectively. Arrows indicate the full length 43 KDa pY892 βDG

A

Predicted trypsin cleavage sites
Transmembrane domain
NLS

$_{654}$SIVVEWTNNTLPLEPCPKEQIAGLSRRIAEDDGKPRPAFSNALEPDFKATSITV
TGSGSCRHLQFIPVVPPRRVPSEAPPTEVPDRDPEKSSEDDVYLHTVIPAVVVAA
ILLIAGIIAMICYRKKRKGKLTLEDQATFIKKGVPIIFADELDDSKPPPSSSMPLILQE
EKAPLPPPEYPNQSVPETTPLNQDTMGEYTPLRDEDPNAPPYQPPPPFTAPME
GKGSRPKNMTPYRSPPPYVPP$_{895}$

B

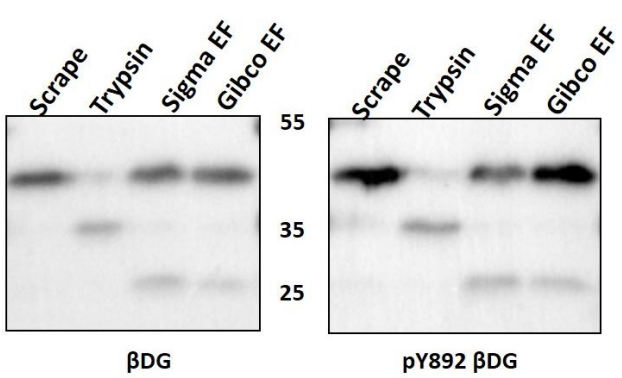

Figure C.5. βDG detection after FACS and trypsin cleavage of βDG. A) The amino acid sequence of βDG was analysed using the ExPASy Peptide cutter program (http://web.expasy.org/peptide_cutter/) to analyse for trypsin cleavage sites. Identified predicted cleavage sites in the extracellular domain of βDG are highlighted in purple. The transmembrane domain of βDG is highlighted in green and the NLS in red. B) LNCaP cells were detattched from the culture vessel via manual scrapping, trypsin incubation or incubation with two different enzyme free dissociation buffers. Total cell lysates from each treatment were immunoblotted for βDG and pY892 βDG.

Length of Treatment	Treatment	% Cells		
		G1	S	G2M
12hr	DMSO	83.3	8.18	8.51
	50ng/ml	64.8	7.47	27.2
	100ng/ml	61.3	7.16	32
	500ng/ml	65.7	7.58	26.1
18hr	DMSO	69	17.9	12.3
	50ng/ml	43.7	21.2	35
	100ng/ml	45.2	14.1	39.2
	500ng/ml	57.5	12.7	28.3
24hr	DMSO	63.6	13.1	22.4
	50ng/ml	24.7	13.2	60.5
	100ng/ml	30.1	13.9	54.5
	500ng/ml	39.9	15.5	42.7
30hr	DMSO	69.8	9.17	19.8
	50ng/ml	16.8	9.39	71.6
	100ng/ml	17.4	9.83	72.2
	500ng/ml	24	11.8	62.4

Table C.1 Optimisation of Nocodazole treatment for arrest of LNCaP cells at mitosis. LNCaP cells were grown for 48 hours and then treated with either DMSO, 50ng/ml, 100ng/ml, 500ng/ml Nocodazole for 12, 18, 24 and 30 hours. Cells were fixed with ethanol, stained with propidium iodide and the cell cycle distribution assessed on the FACF CyAN. Population percentages were calculated with MoFlow.

Bibliography

AALTOMAA, S., LIPPONEN, P., ALA-OPAS, M., ESKELINEN, M., KOSMA, V.M. 1999. α-catenin expression has prognostic value in local and locally advanced prostate cancer. *British Journal of Cancer.* 80, 477-482.

ADAMS, J.C. AND BRANCACCIO, A. 2015. The evolution of the dystroglycan complex, a major mediator of muscle integrity. *Biology Open*. 4, 1163-1179.

AGUILAR, A., WAGSTAFF, K.M., SUAREZ-SANCHEZ, R., ZINKER, S., JANS, D.A., CISNEROS, B. 2015. Nuclear localization of the dystrophin-associated protein α-dystrobrevin through importin α2/β1 is critical for interaction with the nuclear lamina/ maintenance of nuclear integrity. *FASEB.* 29, 1842- 1858.

AKHAVAN, A., GRIFFITH, O.L., SOROCEANU, L., LEONOUDAKIS, D., LUCIANI-TORRES, M.G., DAEMEN, A., GRAY, J.W., MUSCHLER, J.L. 2012. Loss of cell-surface laminin anchoring promotes tumor growth and is associated with poor clinical outcomes. *Cancer Res.* 72, 2578-2588.

ALBER, F., DOKUDOVSKAYA, S., VEENHOFF, L.M., ZHANG, W., KIPPER, J., DEVOS, D., SUPRAPTO, A., KARNI-SCHMIDT, O., WILLIAMS, R., CHAIT, B.T., SALI, A., ROUT, M.P. 2007. The molecular architecture of the nuclear pore complex. *Nature.* 450, 695-701.

ALTSCHUL, S.F., GISH, W., MILLER, W., MYERS, E.W., LIPMAN, D.J. 1990. Basic local alignment search tool. *J.Mol. Biol.* 215, 403-410.ANASTASI, G., CUTRONEO, G., GAETA, R., DI MAURO, D., ARCO, A., CONSOLO, A., SANTORO, G., TRIMARCHI, F., FAVALORO, A. 2009. Dystrophin-glycoprotein complex and vinculin-talin-integrin system in human adult cardiac muscle. *Int. J. Mol. Med.* 23, 149-159.

ANDERSON, C., WINDER, S.J., BORYCKI, A.G. 2007. Dystroglycan protein distribution conincides with basement membranes and muscle differentiation during mouse embryogenesis. *Developmental Dynamics,* 236, 2627-2635.

ANDERSEN, J.S., WILKINSON, C.J., MAYOR, T., MORTENSEN, P., NIGG, E.A., MANN, M. 2003. Proteomic characterization of the human centrosome by protein correlation profiling. *Nature*. 426, 570-574.

ANGELONI, D. 2007. Molecular analysis of deletions in human chromosome 3p21 and the role of resident cancer genes in disease. *Brief Funct. Genomic Proteomic.* 6, 19-39

ARQUINT, C., GABRYJONCZYK, A.M., NIGG, E.A. 2014. Centrosomes as signalling centres. *Phil. Trans. R. Soc. B.* 369: 20130464.

AZIMZADEH, J. AND BORNENS, M. 2007. Structure and duplication of the centrosome. *J. Cell Sci.* 120, 2139-2142.

AZIMZADEH, J. AND MARSHALL, W.F. 2010. Building the centriole. *Curr. Biol.* 20, R816-R825.

BAE, Y.H., MUI, K.L., HSU, B.Y., LIU, S.L., CRETU, A., RAZINIA, Z., XU, T., PURE, E., ASSOIAN, R.K. 2014.
A FAK-Cas-Rac-Lamellipodin Signaling Module Transduces Extracellular Matrix Stiffness into Mechanosensitive Cell Cycling. *Sci. Signal.* 7, ra57.

BAKER, A.M., BIRD, D., LANG, G., COZ, T.R., ERLER, J.T. 2013. Lysyl oxidase enzymatic function increases stiffness to drive colorectal cancer progression through FAK. *Oncogene,* 32, 1863-1888.

BALK, S.P. AND KNUDSEN, K.E. 2008. AR, the cell cycle, and prostate cancer. *Nuclear Receptor Signalling.* 6, DOI: 10.1621/nrs.06001.

BAO, X., KOBAYASHI, M., HATAKEYAMA, S., ANGATA, K., GULLBERG, D., NAKAYAMA, J., FUKUDA, M. N. & FUKUDA, M. 2009. Tumor suppressor function of laminin-binding alpha-dystroglycan requires a distinct beta3-N-acetylglucosaminyltransferase. *Proc Natl Acad Sci U S A,* 106, 12109-14.

BAR, S., BARNEA, E., LEVY, Z., NEUMAN, S., YAFFE, D., NUDEL, U. 1990. A novel product of the Duchenne muscular dystrophy gene which greatly differs from the known isoforms in its structure and tissue distribution. *Biochem. J.* 272, 557-560.

BARR, A.R., KILMARTIN, J.V., GERGELY, F. 2010. CDK5RAP2 functions in centrosome spindle pole attachment and DNA damage response. *J. Cell. Biol.* 189, 23-39.

BARRESI, R. AND CAMPBELL, K.P. 2006. Dystroglycan: from biosynthesis to pathogenesis of human disease. *J. Cell Sci.* 119, 199-207.

BATCHELOR, C.L., HIGGINSON, J.R., CHEN, Y.J., VANNI, C., EVA, A., WINDER, S.J. 2007. Recruitment of Dbl by ezrin and dystroglycan drives membrane proximal Cdc42 activation and filopodia formation. *Cell Cycle.* 6, 353-363.

BEATTIE, J., MCINTOSH, L., VAN DER WALLE, C.F. 2010. Cross-talk between the insulin-like growth factor (IGF) axis and membrane integrins to regulate cell physiology. *J. Cell. Physiol.* 224, 605-611.

BEATY. B.T. AND CONDEELIS, J. 2014. Digging a little deeper: The stages of invadopodium formation and maturation. *Eur. J. Cell. Biol.* 93, 438-444.

BEATY, B.T., SHARMA, V.P., BRAVO-CORDERO, J.J., SIMPSON, M.A., EDDY, R.J., KOLESKE, A.J., CONDEELIS, J. 2013. β1 integrin regulates Arg to promote invadopodial maturation and matrix degradation. *Mol. Biol. Cell.* 24, 1661-1675.

BEAUDOUIN, J., GERLICH, D., DAIGLE, N., EILS, R., ELLENBERG, J. 2002. Nuclear envelope breakdown proceeds by microtubule-induced tearing of the lamina. *Cell.* 108, 83-96.

BERK, J.M., TIFFT, K.E., WILSON, K.L. 2013. The nuclear envelope LEM-domain protein emerin. *Nucleus.* 4, 298-314.

BHAT, H.F., ADAMS, M.E., KHANDAY, F.A. 2013. Syntrohin proteins as Santa Claus: Role(s) in cell signal transduction. *Cell Mol. Life Sci.* 70, 2533-54.

BIES, R.D., FREIDMAN, D., ROBERTS, R., PERRYMAN, M.B., CASKEY, C.T. 1992. Expression and localisation of dystrophin in human cardiac Purkinje fibres. *Circulation.* 86, 147-153.

BIONE, S., MAESTRINI, E., RIVELLA, S., MANCINI, M., REGIS, S., ROMEO, G., TONIOLO, D. 1994. Identification of a novel X-linked gene responsible for Emery-Dreifuss muscular dystrophy. *Nat. Genet.* 8, 39-41.

BODOOR, K., SHAIKH, S., SALINA, D., RAHARJO, W.H., BASTOS, R., LOHKA, M., BURKE, B. 1999. Sequential recruitment of NPC proteins to the nuclear periphery at the end of mitosis. *J. Cell Sci.* 112, 2253-2264.

BONNE, G., BARLETTA, M.R., VARNOUS, S., BECANE, H.M., HAMMOUDA, E.H., MERLINI, L., MUNTONI, F., GREENBERG, C.R., GARY, F., URTIZBEREA, J.A., DUBOC, D., FARDEAU, M., TONIOLO, D., SCHWARTZ, K. 1999. Mutations in the gene encoding lamin A/C cause autosomal dominant Emery-Dreifuss muscular dystrophy. *Nat Genet.* 21, 285-288.

BONUCCELLI, G., SOTGIA, F., SCHUBERT, W., PARK, D.S., FRANK, P.G., WOODMAN, S.E., INSABATO, L., CAMMER, M., MINETTI, C., LISANTI, M.P. 2003. Proteasome inhibitor (mg-132) treatment
of mdx mice rescues the expression and membrane localization of dystrophin and dystrophin-associated proteins. *The American journal of pathology.* 163, 1663-1675.

BOOTSMA, D., BUDKE, L., VOS, O. 1964. Studies on synchronous division of tissue culture cells initiated by excess thymidine. *Exptl. Cell Res.* 33, 301-309.

BORDEAUX, J., WELSH, A.W., AGARWAL, S., KILLIAM, E., BAQUERO, M.T., HANNA, J.A., ANAGNOSTOU, V.K., & RIMM, D.L. 2010. Antibody validation. *Biotechniques,* 43, 197-209.

BORREGO-PINTO, J., JEGOU, T., OSORIO, D.S., AURADE, F., GORJANACZ, M., KOCH, B., MATTAJ, I.W., GOMES, E.R. 2012. Samp1 is a component of TAN lines and is required for nuclear movement. *J. Cell Sci.* 125, 1099-1105.

BOSTOCK, C.J., PRESCOTT, D.M., KIRKPATRICK, J.B. 1971. An evaluation of the double thymidine block for synchronising mammalian cells and the G1-S border. *Exp. Cell Res.* 68, 163-168.

BOVERI, T., 1914. *Zur Frage der Entstehung Maligner Tumoren.* Jena: Fischer Verlag. 1929 English translation by M Boveri reprinted as '*The Origin of Malignant Tumors*' Baltimore: Williams and Wilkins Co.

BOWE, M.A., DEYST, K.A., LESZYK, D., FALLON, J.R. 1994. Identification and purification of an agrin receptor from Torpedo postsynaptic membranes: a heteromeric complex related to the dystroglycans. *Neuron.* 12, 1173-1180.

BOWE, M.A., MENDIS, D.B., FALLON, J.R. 2000. The small leucine-rich repeat proteoglycan biglycan binds to alpha-dystroglycan and is upregulated in dystrophic muscle. *J. Cell Biol.* 148, 801-810.

BOZIC, D., SCIANDRA, F., LAMBA, D., & BRANCACCIO, A. 2004. The structure of the N-terminal region of murine skeletal muscle α-dystroglycan discloses a modular architecture. *Journal of Biological Chemistry,* 279, 44812-44816.

BOZZI, M., BIANCHI, M., SCIANDRA, F., PACI, M., GIARDINA, B., BRANCACCIO, A., CICERO, D.O. 2003. Structural characterization by NMR of the natively unfolded extracellular domain of beta-dystroglycan: toward the identification of the binding epitope for alpha-dystroglycan. *Biochemistry.* 42. 13717-31724.

BOZZI, M., INZITARI, R., SBARDELL, D., MONACO, S., PAVONI, E., GIOIA, M., MARINI, S., MORLACCHI, S., SCIANDRA, F., CASTAGNOLA, M., GIARDINA, B., BRANCACCIO, A., COLETTA, M. 2009. Enzymatic processing of β-dystroglycan recombinant ectodomain by MMP-9: Identification of the main cleavage site. *IUBMB Life*. 61, 1143-1152.

BOZZI, M., MORLACCHI, S., BIGOTTI, M. G., SCIANDRA, F. & BRANCACCIO, A. 2009. Functional diversity of dystroglycan. *Matrix Biol,* 28, 179-87.

BRANCACCIO, A., SCHULTHESS, T., GESEMANN, M., ENGEL, J. 1995. Electron microscopic evidence for a mucin-like region in chick muscle alpha-dystroglycan. *FEBS Lett.* 368, 139-142.

BRANCACCIO, A., SCHULTHESS, T., GESEMANN, M., ENGEL, J. 1997. The N-terminal region of alpha-dystroglycan is an autonomous globular domain. *Eur. J. Biochem.* 246, 166-172.

BRENNAN, P.A., JING, J., ETHUNANDAN, M., GORECKI, D. 2004. Dystroglycan complex in cancer. *Eur. J. Surg. Oncol.* 30, 589-592.

BROOKS, P.C., STROMBLAD, S., SANDERS, L.C., SCHALSCHA, T.L., AIMES, R.T., STETLER-STEVENSON, W.G., QUIGLEY, J.P., CHERESH, D.A. 1996. Localization of matrix metalloproteinase MMP-2 to the surface of invasive cells by interaction with integrin alpha v beta 3. *Cell*. 85. 683-693.

BROWN, S.C., TORELLI, S., BROCKINGTON, M., YUVA, Y., JIMENEZ, C., FENG, L., ANDERSON, L., USG, I., KROGER, S., BUSHBY, K., VOIT, T., SEWRY, C., MUNTONI, F. 2004. Abnormalities in alpha-dystroglycan expression in MDC1C and LGMD2I muscular dystrophies. *Am. J. Pathol.* 164, 727-737.

BUCH, C., LINDBERG, R., FIGUEROA, R., GUDISE, S., ONISCHENKO, E., HALBERG, E. 2009. An integral protein of the inner nuclear membrane localises to the mitotic spindle in mammalian cells. *J. Cell Sci.* 122, 2100-2107.

BUCK, S.B., BRADFORD, J., GEE, K.R., AGNEW, B.J., CLARKE, S.T., SALIC, A. 2008. Detection of S-phase cell cycle progression using 5-ethynyl-2'-deoxyuridine incorporation with click chemistry, an alternative to using 5-bromo-2'-deoxyuridine antibodies. *Biotechniques*. 44, 927-929.

BUDIRAHARDJA, Y. AND GONCZY. P. 2009. Coupling the cell cycle to development. *Development.* 136, 2861-2872.

BURAKOV, A.V., NADEZHDINA, E.S., SLEPCHENKO, B., RODIONOV, V. 2003. Centrosome positioning in interphase cells. *J. Cell Biol.* 162, 963-969.

BURAKOV, A.V., NADEZHDINA, E.S. 2013. Association of the nucleus and centrosome: magnet or Velcro? *Cell Biol. Int.* 37, 95-104.

CAI, C., HSIEH, C. L., OMWANCHA, J., ZHENG, Z., CHEN, S. Y., BAERT, J. L. & SHEMSHEDINI, L. 2007. ETV1 is a novel androgen receptor-regulated gene that mediates prostate cancer cell invasion. *Mol Endocrinol,* 21, 1835-46.

CAI, H., BABIC, I., WEI, X., HUANG, J., WITTE, O. 2011. Invasive prostate carcinoma driven by c-Src and androgen receptor synergy. *Cancer Res.* 71, 862-872.

CAI, M., HUANG, Y., GHIRLANDO, R., WILSON, K.L., CRAIGIE, R., CLORE, G.M. 2001. Solution structure of the constant region of nuclear envelope protein LAP2 reveals 2 LEM-domain structures: one binds BAF and the other binds DNA. *EMBO J.* 20, 4399-4407.

CALDON, C. E., SUTHERLAND, R.L., MUSGROVE, E.A. 2010. Cell cycle proteins in epithelial differentiation: implications for breast cancer. *Cell Cycle.* 9, 1918- 1928.

CAMPBELL, K.P. 1995. Three muscular dystrophies: loss of cytoskeleton-extracellular matrix linkage. *Cell.* 5, 675-679.

CAO, W., HENRY, M.D., BORROW, P., YAMADA, H., ELDER, J.H., RAVKOV, E.V., NICHOL, S.T., COMPANS, R.W., CAMPBELL, K.P., OLDSTONE, M.B. 1998. Identification of alpha-dystroglycan as a receptor for lymphocytic choriomeningitis virus and Lassa fever virus. *Science.* 282, 2079-2081.

CASSWELL, P.T., SPENCE, H.J., PARSONS, M., WHITE, D.P., CLARK, K., CHENG, K.W., MILLS, G.B., HUMPHRIES, M.J., MESSENT, A.J., ANDERSON, K.L.M MCCAFFREY, M.W., OZANNE, B.W., NORMAN, J.C. 2007. Rab25 associates with alpha5beta1 integrin to promote invasive migration in 3D microenvironments. *Dev. Cell.* 13, 496-510.

CAUTAIN, B., HILL, R., DE PEDRO, N., LINK, W. 2015. Components and regulation of nuclear transport processes. *FEBS J.* 282, 445-462.

CAVALCANTI-ADAM, E.A., MICOULET, A., BLUMMEL, J., AURENHEIMER, J., KESSLER, H., SPATZ, J.P. 2006. Lateral spacing of integrin ligands influences cell spreading and focal adhesion assembly. *Eur. J. Cell Biol.* 85, 219-224.

CHAMBARD, J.C., LEFLOCH, R., POUYSSEGUR, J., LENORMAND, P. 2007. ERK implication in cell cycle regulation. *Biochim. Biophys. Acta.* 1773, 1299-1310.

CHANG, W., ANTOKU, S., OSTLUND, C., WORMAN, H.J., GUNDERSEN, G.G. 2015. Linker of nucleoskeleton and cytoskeleton (LINC) complex- mediated actin-dependent nuclear positioning orients centrosomes in migrating myoblasts. *Nucleus.* 6, 77-88.

CHANG, W., FOLKER, E.S., WORMAN, H.J., GUNDERSEN, G.G. 2013. Emerin organises actin flow for nuclear movement and centrosome orientation in migrating fibroblasts. *Mol. Biol. Cell.* 24, 3869-3880.

CHAUMET, A., WRIGHT, G.D., SEET, S.H., THAM, K.M., GOUNKO, N.V., BARD, F. 2015. Nuclear envelope-associated endosomes deliver surface proteins to the nucleus. *Nat. Comm.* 6: 8218.

CHEN, R., SARNECKI, C, BLENIS, J. 1992. Nuclear Localization and Regulation of Erk and rsk-Encoded Protein Kinases. *Mol. Cell. Biol.* 12, 915-927.

CHEN, YJ, SPENCE, H. J., CAMERON, J. M., JESS, T., ILSLEY, J. L., WINDER, S. J. 2003. Direct interaction of beta-dystroglycan with F-actin. *Biochem. J.* 375, 329-337.

CHEN, M.K., AND HUNG, M.C. 2015. Proteolytic cleavage, trafficking, and functions of nuclear receptor tyrosine kinase. *FEBS J.* 282, 3693-3721.

CHEN, Z.J., WANG, W.P., CHEN, Y.C., WANG, J.Y., LIN, W.H., TAI, L.A., LIOU, G.G., YANG, C.S., CHI, Y.H. 2014. Dysregulated interaction between lamin A and SUN1 induce abnormalities in the nuclear envelope and endoplasmic reticulum in progeric laminopathies. *J. Cell Sci.*125, 1729-1704.

CHENG, K.W., LAHAD, J.P., KUO, W.L., LAPUK, A., YAMADA, K., AUERSPERG, N., LIU, J., SMITH-MCCUNE, K., LU, K.H., FISHMAN, D., GRAY, J.W., MILLS, G.B. 2004. The RAB25 small GTPase determines aggressiveness of ovarian and breast cancers. *Nat. Med.* 10, 1251-1256.

CHUAN, Y., PANG, S., CEDAZO-MINGUEZ, A., NORSTEDT, G., POUSETTE, A., FLORES-MORALES, A. 2006. Androgen induction of prostate cancer invasion is mediated by ezrin. *J. Biol. Chem.* 281, 29938-29948.

CHUNG, H., MULTHAUPT, H.A., OH, E.S., COUCHMAN, J.R. 2016. Minireview: Syndecans and their crucial roles during tissue regeneration. *FEBS Lett.*

CHIBA, A., MATSUMURA, K., YAMADA, H., INAZU, T., SHIMIZU, T., KUSUNOKI, S., KANAZAWA, I., KOBATA, A., ENDO, T. 1997. Structures of sialylated O-linked oligosaccharides of bovine peripheral nerve alpha-dystroglycan. The role of a novel O-mannosyl-type oligosaccharide in the binding of alpha-dystroglycan with laminin. *J. Biol. Chem.* 272, 2156-2162

CIFUENTES, E., CROXEN, R., MENON, M., BARRACK, E.R., REDDY, G.P. 2003. Synchronised prostate cancer cells for studying androgen regulated events in cell cycle progression from G1 into S phase. *J. Cell Physiol.* 195, 337-345.

COHEN, M.W., JACOBSON, C., YURCHENCO, P.D., MORRIS, G.E., CARBONETTO, S. 1997. Laminin-induced clustering of dystroglycan on embryonic muscle cells: comparison with agrin-induced clustering. *J. Cell Biol*. 136, 1047-1058.

COHEN, M. W., MOODY-CORBETT, F. & GODFREY, E. W. 1995. Former neuritic pathways containing endogenous neural agrin have high synaptogenic activity. *Dev Biol,* 167, 458-68.

COLLINS, B., GORELICK, G., SCHNEIDER, A. 2001. Dystroglycan is present in rat thyroid and rat thyroid cells and responds to Thyrotropin. *Endocrinology.* 142, 3152- 3162.

COMBS, A.C. AND ERVASTI, J.M. 2005. Enhanced laminin binding by α-dystroglycan after enzymatic deglycosylation. *Biochem. J.* 390, 303-309.

CONSTANTIN, B. 2014. Dystrophin complex functions as a scaffold for signalling proteins. *Biochim. Biophys. Acta.* 1838, 635-642.

CORRADO, K., MILLS, P.L., CHAMBERLAIN, J.S. 1994. Deletion analysis of the dystrophin-actin binding domain. *FEBS Letters.* 344, 255-260.

CÔTÉ, P.D., MOUKHLES, H., LINDENBAUM, M., CARBONETTO, S. 1999. Chimaeric mice deficient in dystroglycans develop muscular dystrophy and have disrupted myoneural synapses. *Nat. Genet.* 23, 338-342.

COUMOU, J., NARASIMHAN, S., TRENTELMAN, J.J., WAGEMAKERS, A., KOETSVELD, J., ERSOZ, J.I., OEI, A., FIKRIG, E., HOVIUS, J.W. 2016. Ixodes scapualris dystroglycan-like proteins promotes Borrelia burgdorferi migration from the gut. *J. Mol. Med.* 94, 361-370.

CRISP, M., LIU, Q., ROUX, K., RATTNER, J.B., SHANAHAN, C., BURKE, B., STAHL, P.D., HODZIC, D. 2006. Coupling of the nucleus and cytoplasm role of the LINC complex. *J. Cell Biol.* 172, 41-53.

CROSBIE, R.H., LEBAKKEN, C.S., HOLT, K.H., VENZKE, D.P., STRAUB, V., LEE, J.C., GRADY, R.M., CHAMBERLAIN, J.S., SANES, J.R., CAMPBELL, K.P. 1999. Membrane targeting and stabilisation of sarcospan is mediated by the sarcoglycan subcomplex. *J. Cell Biol.* 145, 153-165.

CROSS, S. S., LIPPITT, J., MITCHELL, A., HOLLINGSBURY, F., BALASUBRAMANIAN, S. P., REED, M. W., EATON, C., CATTO, J. W., HAMDY, F. & WINDER, S. J. 2008. Expression of beta-dystroglycan is reduced or absent in many human carcinomas. *Histopathology,* 53**,** 561-6.

CUKIER, I.H., LI, Y., LEE, J.M. 2007. Cyclin B1/Cdk1 binds and phosphorylates Filamin A and regulates its ability to cross-link actin. *FEBS Letters.* 581, 1661-1672.

CUNNINGHAM, D. AND YOU, Z. 2015. In vitro and in vivo model systems used in prostate cancer research. *J. Biol. Methods.* 2, doi:10.14440/jbm.2015.63.

D'ASSORO, A.B., LINGLE, W.L., SALISBURY, J.L. 2002. Centrosome amplification and the development of cancer. *Oncogene.*21, 6146-6153.

DABAUVALLE, M.C., MULLER, E., EWALD, A., KRESS, W., KROHNE, G., MULLER, C.R. 1999. Distribution of emerin during the cell cycle. *EJCB.* 78, 749-756.

DE BERNABE, D.B., VAN BOKHOVEN, H., VAN BEUSEKOM, E., VAN DEN AKKER, W., KANT, S., DOBYNS, W.B., CORMAND, B., CURRIER, S., HAMEL, B., TALIM, B., TOPALOGLU, H., BRUNNER,

H.G. 2003. A homozygous nonsense mutation in the fukutin gene causes a Walker-Warburg syndrome phenotype. *J. Med. Genet.* 40, 845-848.

DE BRABANDER, M.J., VAN DE VEIRE, R.M., AERTS, F.E., BORGERS, M., JANSSEN, P.A. 1976. The effects of methyl (5-(2-thienylcarbonyl)-1H-benzimidazol-2-yl) carbamate, (R 17934; NSC 238159), a new synthetic antitumoral drug interfering with microtubules, on mammalian cells cultured in vitro. *Cancer Res.* 36, 905-916.

DENG, W.M., SCHNEIDER, M.,FROCK, R., CASTILLEJO-LOPEZ, C., GAMAN, E.A., BAUMGARTNER, A., RUOHOLA-BAKER, H. 2003. Dystroglycan is required for polarizing the epithelial cells and the oocyte in Drosophila. *Development.* 130, 173-184.

DESGROSELLIER, J.S. AND CHERESH, D.A. 2010. Integrins in cancer: biological implications and therapeutic opportunities. *Nat. Rev. Cancer.* 10, 9-21.

DESTAING, O., PLANUS, E., BOUVARD, D., ODDOU, C., BADOWSKI, C., BOSSY, V., RADUCANU, A., FOURCADE, B., ALBIQES-RIZO, C., BLOCK, M.R. 2010. β1A integrin is a master regulator of invadosome organisation and function. *Mol. Biol. Cell.* 21, 4108-4119.

DEYST, K.A., BOWE, M.A., LESZYK, J.D., FALLON, J.R. 1995. The α-dystroglycan-β-dystroglycan complex membrane organisation and relationship to an agrin receptor. *J. Bio. Chem.* 270, 25956-25959.

DI STASIO, E., SCIANDRA, F., MARAS, B., DI TOMMASO, F., PETRUCCI, T.C., GIARDINA, B., BRANCACCIO, A. 1999. Structural and Functional Analysis of the N-Terminal Extracellular Region of β-Dystroglycan. *Biochem. Biophys. Res. Comm.* 266, 274-278.

DORNER, D., GOTZMANN, J., FOISNER, R. 2007. Nucleoplasmic lamins and their interaction partners, LAP2α, Rb, and BAF in transcriptional regulation. *FEBS J.* 274, 1362-1373.

DOXSEY, S.J., STEIN, P., EVANS, L., CALARCO, P.D., KIRSCHNER, M. 1994. Pericentrin, a highly conserved centrosome protein involved in microtubule organisation. *Cell.* 76, 639-650.

DURBEEJ, M. AND CAMPBELL, K.P. 1999. Biochemical characterization of the epithelial dystroglycan complex. *J. Biol. Chem.* 274, 26609–26616.

DURBEEJ, M., HENRY, M.D., CAMPBELL, K.P. 1998. Dystroglycan in development and disease. *Curr. Opin. Cell Biol.* 10, 594-601.

DURBEEJ, M., HENRY, M.D., FERLETTA, M., CAMPBELL, K.P., EKBLOM, P. 1998. Distribution of Dystroglycan in normal adult mouse tissues. *J. Histochem. Cytochem.* 46, 449-457.

DURBEEJ, M., LARSSON, E., IBRAGHIMOV-BESKROVNAYA, O., ROBERDS, S.L., CAMPBELL, K.P., EKBLOM, P. 1995. Non-muscle alpha-dystroglycan is involved in epithelial development. *J. Cell. Biol.* 130, 79–91.

DURBEEJ, M., TALTS, J.F., HENRY, M.D., YURCHENCO, P.D., CAMPBELL, K.P., EKBLOM, P. 2001. Dystroglycan binding to laminin a1LG4 module influences epithelial morphogenesis of salivary gland and lung in vitro. *Differentiation.* 69, 121-134.

DURONIO, R.J., XIONG, Y. 2013. Signaling pathways that control cell proliferation. *Cold Spring Harb. Perspect. Biol.* 5, a008904.

EDMONDSON, R., JENKINS-BROGLIE, J., ADCOCK, A.F., YANG, L. 2014. Three-dimensional cell culture systems and their applications in drug discovery and cell-based biosensors. *Assay and drug development technologies.* 12, 207-218.

ELLENBERG, J., SIGGIA, E.D., MOREIRA, J.E., SMITH, C.L., PRESLEY, J.F., WORMAN, H.J., LIPPINCOTT-SCHWARTZ, J. 1997. Nuclear membrane dynamics and reassembly in living cells: targeting of an inner nuclear membrane protein in interphase and mitosis. *J. Cell Biol.* 138, 1193-1206.

ENSERINK, J.M. AND KOLODNER, R.D. 2010. An overview of Cdk1-controlled targets and processes. *Cell Division.* 5, 11

ERIKSSON, M., BROWN, W.T., GORDON, L.B., GLYNN, M.W., SINGER, J., SCOTT, L., ERDOS, M.R., ROBBINS, C.M., MOSES, T.Y., BERGLUND, P., DUTRA, A., PAK, E., DURKIN, S., CSOKA, A.B., BOEHNKE, M., GLOVER, T.W., COLLINS, F.S. 2003. Recurrent de novo point mutations in lamin A cause Hutchinson-Gilford progeria syndrome. *Nature.* 423, 293-298.

ERVASTI, J. M. & CAMPBELL, K. P. 1991. Membrane organization of the dystrophin-glycoprotein complex. *Cell,* 66, 1121-31.

ERVASTI, J.M. AND CAMPBELL, K.P. 1993. A role for the dystrophin-glycoprotein complex as a transmembrane linker between laminin and actin. *J. Cell Biol.* 122, 809-823.

ERVASTI, J.M., OHLENDIECK, K., KAHL, S.D., GAVER, M.G., CAMPBELL, K.P. 1990. Deficiency of a glycoprotein component of the dystrophin complex in dystrophic muscle. *Nature.* 345, 315-319.

ESSER, K.A., MILLER, M. R., HUANG, Q., MEIER, M. M., BELTRAN-VALERO DE BERNABE, D., STIPP, C. S., CAMPBELL, K. P., LYNCH,C. F., SMITH, B. J., COHEN, M. B., HENRY, M. D. 2013. Loss of LARGE2 Disrupts Functional Glycosylation of α-Dystroglycan in Prostate Cancer. *J Biol. Chem.* 288, 2132- 2142.

EYERMANN, C., CZAPLINSKI, K., COLOGNATO, H. 2012. Dystroglycan promotes filopodial formation and process branching in differentiating oligodendroglia *J. Neurochem.* 120, 928-947.

FEHON, R.G., MCCLATCHEY, A.I., BRETSCHER, A. 2010. Organising the cell cortex: the role of ERM proteins. *Nat. Rev. Mol. Cell Biol.* 11, 276-287.

FELDMAN, B.J. and FELDMAN, D. 2001. The development of androgen-independent prostate cancer. *Nat. Rev. Cancer.* 1, 34-45.

FERLETTA, M., KIKKAWA, Y., YU, H., TALTS, J.F., DURBEEJ, M., SONNENBERG, A., TIMPL, R., CAMPBELL, K.P., EKBLOM, P., GENERSCH, E. 2003. Opposing roles of integrin α6Aβ1 and dystroglycan in laminin-mediated extracellular signal-regulated kinase activation. *Mol. Biol. Cell*. 14, 2088-2103.

FIDZIANSKA, A., TONIOLO, D., HAUSMANOWA-PETRUSEWICZ, I. 1998. Ultrastructural abnormality of sarcolemmal nuclei in Emery-Dreifuss muscular dystrophy (EDMD). *J. Neurol. Sci*. 159, 88–93.

FLOTHO, A., MELCHOIR, F. 2013. Sumoylation: A regulatory protein modification in health and disease. *Ann. Rev. Biochem.* 82, 357-385.

FORNEROD, M., OHNO, M., YOSHIDA, M., MATTAJ, I.W. 1997. CRM1 is an export receptor for leucine-rich nuclear export signals. *Cell.* 90, 1051-1060.

FOISNER, R. 2003. Cell cycle dynamics of the nuclear envelope. *TheScientificWorldJOURNAL.* 3, 1-20.

FOISNER, R., AND GERACE, L. 1993. Integral membrane proteins of the nuclear envelope interact with lamins and chromosomes, and DNA binding is modulated by mitotic phosphorylation. *Cell.* 73, 1267-1279.

FONTES, M.R., TEH, T., TOTH, G., JOHN, A., PAVO, I., JANS, D.A., KOBE, B. 2003, Role of flanking sequences and phosphorylation in the recognition of the simian-virus-40 large T-antigen nuclear localization sequences by importin-alpha. *Biochem. J.* 375, 339-349.

FORSBURG, S.L. 2004. Eukaryotic MCM proteins: Beyond replication initiation. *Microbiol. Mol. Biol. Rev.* 68, 109-131.

FRISCH, S.M. AND FRANCIS, H. 1994. Disruption of epithelial cell-matrix interactions induces apoptosis. *J. Cell Biol.* 124, 619-626.

FRISCH, S.M. AND SCREATON, R.A. 2001. Anoikis mechanisms. *Curr. Op. Cell Biol.* 13, 555-562.

FROST, A.R., BOHM, S.V., SEWDUTH, R.N., JOSIFOVA, D., OGILIVE, C.M., IZATT, L., ROBERTS, R.G. 2010. Heterozygous deletion of a 2-Mb region including the dystroglycan gene in a patient with mild myopathy, facial hypotonia, oral-motor dyspraxia and white matter abnormalities. *Eur J Hum Genet.* 18, 852-855.

FUENTES-MERA, L., RODRIGUEZ-MUNOZ, R., GONZALEZ-RAMIREZ, R., GARCIA-SIERRA, F., GONZALEZ, E., MORNET, D., CISNEROS, B. 2006. Characterization of a novel Dp71 dystrophin-associated protein complex (DAPC) present in the nucleus of HeLa cells: members of the nuclear DAPC associate with the nuclear matrix. *Exp. Cell Res.* 312, 3023-3035.

FULLER, S.D., GOWEN, B.E., REINSCH, S., SAWYER, A., BUENDIA, B., WEPF, R., KARSENTI, E. 1995. The core of the mammalian centriole contains gamma-tubulin. *Curr. Biol.* 5, 1384-1393.

FUNKHOUSER, C.M., SKNEPNEK, R., TAKESHI, S., GOLDMAN, A.E., GOLDMAN, R.D., OLVERA DE LA
CRUZ, M. 2013. Mechanical model of blebbing in nuclear lamin meshworks. *PNAS.* 110, 3248-3253.

GALVAGNI, F., NARDI, F., MAIDA, M., BARNARDI, G., VANNUCCINI, S., PETRAGLIA, F., SANTUCCI, A., ORLANDINI, M. 2016. CD93 and dystroglycan cooperation in human endothelial cell adhesion and migration adhesion and migration. *Oncotarget.* 7, 10090-10103.

GANEM, N.J., GODINHO, S.A., PELLMAN, D. 2009. A mechanism linking extra centrosomes to chromosomal instability. *Nature.* 460, 278- 282.

GAUTIER, T., ROBERT-NICOUD, M., GUILLY, M.N., HERNANDEZ-VERDUN, D. 1992. Relocation of nucleolar proteins around the chromosomes at mitosis. A study by confocal laser scanning microscopy. *J. Cell Sci.* 102, 729-737.

GE, X., FRANK, C.L., CALDERON DE ANDA, F., TSAI, L.H. 2010. Hook3 interacts with PCM1 to regulate pericentriolar matrix assembly and the timing of neurogenesis. *Neuron.* 65, 191-203.

GEE, S.H., BLACHER, R.W., DOUVILLE, P.J., PROVOST, P.R., YURCHENCO, P.D., CARBONETTO, S. 1993. Laminin-binding protein 120 from brain is closely related to the dystrophin associated glycoprotein, dystroglycan, and binds with high affinity to the major heparin binding domain of laminin. *J. Biol. Chem.* 268, 14972-14980.

GEIS, T., MARQUARD, K., RODL, T., REIHLE, C., SCHRMER, S., VON KALLE, T., BORNEMANN, A., HEHR, U., BLANKENBURG, M. 2013. Homozygous dystroglycan mutation associated with a

novel muscle-eye-brain disease-like phenotype with multicystic leucodystrophy. *Neurogenetics.* 14, 205-213.

GEORGE, S.J., AND DWIVEDI, A. 2004. MMPs, cadherins, and cell proliferation. *Trends Cardiovasc. Med.* 14, 100-105.

GIANCOTTI, F.G. 1997. Integrin signalling: specificity and control of cell survival and cell cycle progression. *Curr. Op. Cell Biol.* 9, 691-700.

GILLE, H., KORTENJANN, M., THOMAE, O., MOOMAW, C., SLAUGHTER, C., COBB, M.H., SHAW, P.E. 1995. ERK phosphorylation potentiates Elk-1-mediated ternary complex formation and transactivation. *EMBO. J.* 14, 951-962.

GODFREY, C., FOLEY, A.R., CLEMENT, E., MUNTONI, F. 2011. Dystroglycanopathies: coming into focus. *Curr. Opin. Genet. Dev.* 21, 278-285.

GOMES, E.R., JANI, S., GUNDERSEN, G.G. 2005. Nuclear movement regulated by Cdc42, MRCK, myosin, and actin flow establishes MTOC polarization in migrating cells. *Cell*. 121, 451-63.

GONZALEZ-RAMIREZ, R., MORALES-LAZARO, S. L., TAPIA-RAMIREZ, V., MORNET, D. & CISNEROS, B. 2008. Nuclear and nuclear envelope localization of dystrophin Dp71 and dystrophin-associated proteins (DAPs) in the C2C12 muscle cells: DAPs nuclear localization is modulated during myogenesis. *J Cell Biochem,* 105, 735-45.

GONCZY, P. 2002. Nuclear envelope: torn apart at mitosis. *Curr. Biol.* 12, R242-244.

GONCZY, P. 2012. Towards a molecular architecture of centriole assembly. *Nat. Mol. Cell Biol.* 13, 425-435.

GONCZY, P., PICHLER, S., KIRKHAM, M., HYMAN, A.A. 1999. Cytoplasmic dynein is required for distinct aspects of MTOC positioning, including centrosome separation in one cell stage *Caenorhabditis elegans* embryo. *Mol. Biol. Cell.* 147, 135-150.

GORECKI, D.C., DERRY, J.M.J., BARNARD, E.A. 1994. Dystroglycan: brain localisation and chromosome mapping in the mouse. *Hum. Mol. Genet.* 3, 1589-1597.

GORECKI, D.C., MONACO, A.P., DERRY, J.M., WALKER, A.P., BARNARD, E.A., BARNARD, P.J. 1992. Expression of four alternative dystrophin transcripts in brain regions regulated by different promoters. *Hum. Mol. Genet.* 1, 505-510.

GORLICH, D., PANTE, N., KUTAY, U., AEBI, U., BISCHOFF, F.R. 1996. Identification of different roles for RanGDP and RanGTP in nuclear protein import. *EMBO J.* 15, 5584-5594.

GOSS, V.L., HOCEVAR, B.A., THOMPSON, L.J., STRATTON, C.A., BURNS, D.J., FIELDS, A.P. 1994. Identification of nuclear beta II protein kinase C as a mitotic lamin kinase. *J. Biol. Chem.* 269, 19074-19080.

GOSTI-TESTU, F., MARTY, M.C., BERGES, J., MAUNORY, R., BORNENS, M. 1986. Identification of centrosomal proteins in a human lymphoblastic cell line. *EMBO J.* 5, 2545-2550.

GOULD, C. M., DIELLA, F., VIA, A., PUNTERVOLL, P., GEMUND, C., CHABANIS-DAVIDSON, S., MICHAEL, S., SAYADI, A., BRYNE, J. C., CHICA, C., SEILER, M., DAVEY, N. E., HASLAM, N., WEATHERITT, R. J., BUDD, A., HUGHES, T., PAS, J., RYCHLEWSKI, L., TRAVE, G., AASLAND, R., HELMER-CITTERICH, M., LINDING, R. & GIBSON, T. J. 2010. ELM: the status of the 2010 eukaryotic linear motif resource. *Nucleic Acids Res,* 38, D167-80.

GRUENBAUM, Y., MARGALIT, A., GOLDMAN, R.D., SHUMAKER, D.K., WILSON, K.L. 2005. The nuclear lamina comes of age. *Nat. Rev. Mol. Cell Biol.* 6, 21-31.

GUPTA, V., KAWAHARA, G., GUNDRY, S.R., CHEN, A.T., LENCER, W.I., ZHOU, Y., ZON, L.I., KUNKEL, L.M., BEGGS, A.H. 2011. The zebrafish DAG1 mutant: a novel genetic model for dystroglycanopathies. *Hum. Mol. Genet.* 20, 1712-1725.

GURUHARSHA, K.G., KANKEL, M.W., ARTAVANIS-TSAKONAS, S. 2012. The Notch signalling system: recent insights into the complexity of a conserved pathway. *Nat. Rev. Genet.* 13, 654-666.

HAKKINEN, K.M., HARUNAGA, J.S., DOYLE, A.D., YAMADA, K.M. 2011. Direct Comparisons of the Morphology, Migration, Cell Adhesions, and Actin Cytoskeleton of Fibroblasts in Four Different Three-Dimensional Extracellular Matrices. *Tissue Engineering.* 17, 713-724.

HALE, C.M., SHRESTHA, A.L., KHATAU, S.B., STEWART-HUTCHINSON, P.J., HERNANDEZ, L., STEWART, C.L., HODZIC, D., WIRTZ, D. 2008. Dysfunctional connections between the nucleus and the actin and microtubule networks in laminopathic models. *Biophysical J.* 95, 5462-5475.

HAMARATOGLU, F., WILLECKE, M., KANGO-SINGH, M., NOLO, R., HYUN, E., TAO, C., JAFAR-NEJAD, H., HALDER, G. 2006. The tumour-suppressor genes NF2/ Merlin and Expanded act through Hippo signalling to regulate cell proliferation and apoptosis. *Nat. Cell Biol.* 8, 27-36.

HANDWERGER, K.E., AND GALI, J.G. 2006. Subnuclear organelles: new insights into form and function. *Trends Cell Biol.* 16, 19-26.

HAQUE, F., MAZZEO, D., PATEL, J.T., SMALLWOOD, D.T., ELLIS, J.A., SHANAHAN, C.M., SHACKLETON, S. 2010. Mammalian SUN protein interaction networks at the inner nuclear membrane and their role in laminopathy disease processes. *J. Biol. Chem.,* 29, 3487-3498.

HAQUE, F., LLOYD, D.J., SMALLWOOD, D.T., DENT, C.L., SHANAHAN, C.M., FRY, A.M., TREMBATH, R.C., SHACKLETON, S. 2006. SUN1 interacts with nuclear lamin A and cytoplasmic nesprins to provide a physical connection between the nuclear lamina and the cytoskeleton. *Mol. Cell Biol.* 26, 3738-3751.

HARA, Y., BALCI-HAYTA, B., YOSHIDA-MORIGUCHI, T., KANAGAWA, M., BELTRAN-VALERO DE BERNABE, D., GUNDESLI, H., WILLER, T., SATZ, J.S., CRAWFORD, R.W., BURDEN, S.J., KUNZ, S., OLDSTONE, M.B., ACCARDI, A., TALIM, B., MUTONI, F., TOPALOGLU, H., DINCER, P., CAMPBELL, K.P. 2011. A dystroglycan mutation associated with limb-girdle muscular dystrophy. *N Engl J Med.* 364, 939-946.

HARA, Y., KANAGAWA, M., KUNZ, S., YOSHIDA-MORIGUCHI, T., SATZ, J.S., KOBAYASHI, Y.M., ZHU, Z., BURDEN, S.J., OLDSTONE, M.B., CAMPBELL, K.P. 2011. Like-acetylglucosaminyltransferase (LARGE)-dependent modification of dystroglycan at Thr-317/319 is required for laminin binding and arena virus infection. *Proc. Natl. Acad. Sci. USA.* 108, 17426-17431.

HARAGUCHI, T., KOUJIN, T., HAYAKAWA, T., KANEDA, T., TSUTSUMI, C., IMAMOTO, N., AKAZAWA, C., SUKEGAWAJ., YONEDA, Y., HIRAOKA, Y. 2000. Live fluorescent imaging reveals early recruitment of emerin, LBR, RanBP2, and Nup153 to reforming, functional nuclear envelopes. *J. Cell Sci.* 113, 779-794.

HARAGUCHI, T., KOUJIN, T., SEGURA-TOTTEN, M., LEE, K.K., MATSUOKA, Y., YONEDA, Y., WILSON, K.L., HIRAOKA, Y. 2001. BAF is required for emerin assembly into the reforming nuclear envelope. *J. Cell Sci.* 114, 4574-4585.

HELLIWELL, T.R., MAN, N., MORRIS, G.E. 1994. Expression of the 43 kD dystrophin-associated glycoprotein in human neuromuscular disease. *Neuromusc. Disord.* 4, 101-113.

HEMMING, M.L., ELIAS, J.E., GYGI, S.P., SELKOE, D.J. 2008. Proteomic profiling of gamma-secretase substrates and mapping of substrate requirements. *PLoS Biol.* 6, e257.

HENRY, M. D. & CAMPBELL, K. P. 1998. A role for dystroglycan in basement membrane assembly. *Cell,* 95, 859-70.

HENRY, M. D., COHEN, M. B. & CAMPBELL, K. P. 2001a. Reduced expression of dystroglycan in breast and prostate cancer. *Hum Pathol,* 32, 791-5.

HENRY, M.D., SATZ, J.S., BRAKEBUSCH, C., COSTELL, M., GUSTAFSSON, E., FASSLER, R., CAMPBELL, K.P. 2001b. Distinct roles for dystroglycan, beta1 integrin and perlecan in cell surface laminin organization. *J Cell Sci*. 114, 1137-1144.

HERNANDEZ-IBARRA, J.A., LAREDO-CISNEROS, M.S., MONDRAGO-GONZALEZ, R., SANTAMARIA-GUAYASAMIN, N., CISNEROS, B. 2015. Localization of α-Dystrobrevin in Cajal bodies and the nucleoli: A new role for α-dystrobrevin in the structure/stability of the Nucleolus. *J. Cell Biochem.* 116, 2755-2765.

HERNANDEZ-VERDUN, D. 2011. Assembly and disassembly of the nucleolus during the cell cycle. *Nucleus.* 2, 189-194.

HERRMANN, R., STRAUB, V., BLANK, M., KUTZICK, C., FRANKE, N., JACOBS, N.E., HANS-GERD, L., KRÖGER, S., VOIT, T. 2000. Dissociation of the Dystroglycan complex in caveolin-3-deficient limb girdle muscular dystrophy. *Hum. Mol. Genet.* 9, 2335- 2340.

HERZOG, C., HAS, C., FRANZKE, C. W., ECHTERMEYER, F. G., SCHLOTZER-SCHREHARDT, U., KROGER, S., GUSTAFSSON, E., FASSLER, R. & BRUCKNER-TUDERMAN, L. 2004. Dystroglycan in skin and cutaneous cells: beta-subunit is shed from the cell surface. *J Invest Dermatol,* 122, 1372-80.

HETZER, M.W. 2010. The nuclear envelope. *Cold Spring Harbor Perspectives in Biology.* 2, a000539.

HETZER, M., BILBAO-CORTES, D., WALTHER, T.C., GRUSS, O.J., MATTAJ, I.W. 2000. GTP hydrolysis by Ran is required for nuclear envelope assembly. *Mol. Cell.*5, 1013-1024.

HIGGINSON, J. R., THOMPSON, O. & WINDER, S. J. 2008. Targeting of dystroglycan to the cleavage furrow and midbody in cytokinesis. *Int J Biochem Cell Biol,* 40, 892-900.

HOHENESTER, E., TISI, D., TALTS, J.F., TIMPL, R. 1999. The crystal structure of a laminin G-like module reveals the molecular basis of alpha-dystroglycan binding to laminins, perlecan, and agrin. *Mol. Cell.* 4, 783-792.

HOLT, K.H. AND CAMPBELL, K.P. 1998. Assembly of the sarcoglycan complex. Insights for muscular dystrophy. *J. Biol. Chem.* 273, 34667-34670.

HOLT, K.H., CROSBIE, R.H., VENZKE, D.P., CAMPBELL, K.P. 2000. Biosynthesis of Dystroglycan: processing of a precursor propeptide. *FEBS Letters.* 468, 79-83.

HOLT, L.J. 2012. Regulatory molecules: coupling protein stability to phospho regulation during cell division. *FEBS Letters.* 586, 2773-2777.

HORNBECK, P.V., ZHANG, B., MURRAY, B., KORNHAUSER, J. M., LATHAM, V., SKRZYPEK, E. 2014. PhosphoSitePlus, 2014: mutations, PTMs and recalibrations. *Nucleic Acids Res,* 43, D512-20. URL : http://www.phosphosite.org/homeAction.action

HOROSZEWICZ, J. S., LEONG, S. S., KAWINSKI, E., KARR, J. P., ROSENTHAL, H., CHU, T. M., MIRAND, E. A. & MURPHY, G. P. 1983. LNCaP model of human prostatic carcinoma. *Cancer Res,* 43, 1809-18.

HOSOKAWA, H., NINOMIYA, H., KITAMURA, Y., FUJIWARA, K., MASAKI, T. 2001. Vascular endothelial cells that express dystroglycan are involved in angiogenesis. *J. Cell Sci.* 115, 1487-1496.

HOYTE, K., JAYASINHA, V., XIA, B., MARTIN, P.T. 2004. Transgenic overexpression of dystroglycan does not inhibit muscular dystrophy in mdx mice. *Am. J. Pathol*. 164,711-718.

HSU, T., TROJANOWSKA, M., WATSON, D.K. 2004 Ets proteins in biological control and cancer. *J Cell Biochem* 91,896–903

HU, M. AND POLYAK, K. 2008. Microenvironmental regulation of cancer development. *Curr. Opin. Genet. Dev.* 18, 27-34.

HUA, Q., KNUDSON, C.B., KNUDSON, W. 1993. Internalization of hyaluronan by chondrocytes occurs via receptor-mediated endocytosis. *J. Cell. Sci.* 365-375.

HUANG, X., POY, F., ZHANG, R., JOACHIMIAK, A., SUDOL, M. & ECK, M.J. 2000. Structure of a WW domain containing fragment of dystrophin in complex with β-dystroglycan. *Nature Structural Biology,* 7, 634-638.

HUANG, Q., MILLER, M.R., SCHAPPET, J., HENRY, M.D. 2015. The glycosyltransferase LARGE2 is repressed by Snail and ZEB1 in prostate cancer. *Cancer Biol. Ther.* 16, 125-136.

HUMPHREY, E.L., LACEY, E., LE, L.T., FENG, L., SCIANDRA, F., MORRIS, C. R., HEWITT, J. E., HOLT, I., BRANCACCIO, A., BARRESI, R., SEWRY, C.A., BROWN, S. C., MORRIS, G.E. 2015. A new monoclonal antibody DAG-6F4 against human alpha-dystroglycan reveals reduced core protein in some, but not all, dystroglycanopathy patients. *Neuromuscular Disorders,* 25, 32-42.

IWATA, Y., NAKAMURA, H., FUJIWARA, K., SHIGEKAWA, M. 1993. Altered membrane-dystrophin association in the cardiomyopathic hamster heart muscle. *Biochem. Biophys. Res. Commun.* 190, 589-595.

IBRAGHIMOV-BESKROVNAYA, O., ERVASTI, J. M., LEVEILLE, C. J., SLAUGHTER, C. A., SERNETT, S. W. & CAMPBELL, K. P. 1992. Primary structure of dystrophin-associated glycoproteins linking dystrophin to the extracellular matrix. *Nature,* 355, 696-702.

IBRAGHIMOV-BESKROVNAYA, O., MILATOVICH, A., OZCELIK, T., YANG, B., KOEPNICK, K., FRANCKE, U. & CAMPBELL, K. P. 1993. Human dystroglycan: skeletal muscle cDNA, genomic structure, origin of tissue specific isoforms and chromosomal localization. *Hum Mol Genet,* 2, 1651-7.

ILSLEY, J. L., SUDOL, M. & WINDER, S. J. 2002. The WW domain: linking cell signalling to the membrane cytoskeleton. *Cell Signal,* 14, 183-189

ILSLEY, J. L., SUDOL, M. & WINDER, S. J. 2001. The interaction of dystrophin with beta-dystroglycan is regulated by tyrosine phosphorylation. *Cell Signal,* 13, 625-32

ISGRO, T.A., AND SCHULTEN, K. 2005. Binding dynamics of isolated nucleoporin repeat regions to importin-beta. *Structure.* 13, 1869-1879.

ITO, N., RUEGG, U.T., KUDO, A., MIYAGOE-SUZUKI, Y., TAKEDA, S. 2013. Activation of calcium signalling through Trpv1 by nNOS and peroxynitrite as a key trigger of skeletal muscle hypertrophy. *Nat. Med.* 19. 101-106.

JACOBSON, C., MONTANARO, F., LINDENBAUM, M., CARBONETTO, S., FERNS, M. 1998. alpha-Dystroglycan functions in acetylcholine receptor aggregation but is not a coreceptor for agrin-MuSK signaling. *J. Neurosci.* 18, 6340-6348.

JAE, L.T., RAABEN, M., RIEMERSMA, M., VAN BEUSEKOM, E., BLOMEN, V.A., VELDS, A., KERKHOVEN, R.M., CARETTE, J.E., TOPALOGLU, H., MEINECKE, P., WESSELS, M.W., LEFEBER, D.J., WHELAN, S.P., VAN BOKHOVEN, H., BRUMMELKAMP, T.R. 2013. Deciphering the glycosylome of dytroglycaopathies using haploid screens for Lassa virus entry. *Science.* 340, 479-483.

JAMES, M., MAN, N.G., WISE, C.J., JONES, G.E., MORRIS, G.E. 1996. Utrophin-dystroglycan complex in membranes of adherent cultured cells. *Cell Motil. Cytoskel.* 33, 163-174.

JAMES, M., NUTTALL, A., ILSLEY, J. L., OTTERSBACH, K., TINSLEY, J. M., SUDOL, M. & WINDER, S. J. 2000. Adhesion-dependent tyrosine phosphorylation of (beta)-dystroglycan regulates its interaction with utrophin. *J Cell Sci,* 113, 1717-1726

JANS, D.A., AND HASSAN, G. 1998. Nuclear targeting by growth factors, cytokines, and their receptors: a role in signaling? *Bioessays.* 20, 400-411.

JIMENEZ-MALLEBRERA, C., TORELLI, S., FENG, L., KIM, J., GODFREY, C., CLEMENT, E., MEIN, R., ABBS, S., BROWN, S.C., CAMPBELL, K.P., KROGER, S., TALIM, B., TOPALOGLU, H., QUINLIVAN, R., ROPER, H., CHILDS, A.M., KINALI, M., SEWRY, C.A., MUNTONI, F. 2009. A comparative study of alpha-dystroglycan glycosylation in dystroglycanopathies suggests that the hypoglycosylation of alpha-dystroglycan does not consistently correlate with clinical severity. *Brain Pathol.* 19. 596-611.

JING, J., LIEN, C. F., SHARMA, S., RICE, J., BRENNAN, P. A. & GORECKI, D. C. 2004. Aberrant expression, processing and degradation of dystroglycan in squamous cell carcinomas. *Eur J Cancer,* 40, 2143-51.

JORDAN, M.A., THROWER, D., WILSON, L. 1992. Effects of vinblastine, podophyllotoxin and nocodazole on mitotic spindles Implications for the role of microtubule dynamics in mitosis. *J. Cell Sci.* 102, 401-416.

JUNG, D., YANG, B., MEYER, J., CHAMBERLAIN, J.S., CAMPBELL, K.P. 1995. Identification and characterisation of the dystrophin anchoring sire on beta-dystroglycan. *J. Biol. Chem.*270, 27305-27310.

KAHL, J., CAMPANELLI, J.T. 2003. A role for the juxtamembrane domain of beta-dystroglycan in agrin-induced acetylcholine receptor clustering. *J. Neurosci.* 23, 392-402.

KAKU, N., MATSUDA, K., TSUJIMURA, A., KAWATA, M. 2008. Characterization of nuclear import of the domain-specific androgen receptor in association with the importin α/β and ran-guanosine 5'-triphosphate systems. *Endocrinology.* 149, 3960-3969.

KALDERON, D., ROBERTS, B.L., RICHARDSON, W.D., SMITH, A.E. 1984. Sequence requirements for nuclear location of simian virus 40 large-T antigen. *Nature.* 311, 33-38.

KANAGAWA, M., SAITO, F., KUNZ, S., YOSHIDA-MORIGUCHI, T., BARRESI, R., KOBAYASHI, Y.M., MUSCHLER, J., DUMANSKI, J.P., MICHELE, D.E., OLDSTONE, M.B., CAMPBELL, K.P. 2004. Molecular recognition by LARGE is essential for expression of functional dystroglycan. *Cell.* 117, 953-964.

KANG, R., WAN, J., ARSTIKAITIS, P., TAKAHASHI, H., HUANG, K., BAILEY, A .O., THOMPSON, J.X., ROTH, A.F., DRISDEL, R.C., MASTRO, R., GREEN, W.N., YATES, J.R., DAVIS, N.G., EL-HUSSEINI, A. 2008. Neural palmitoyl-proteomics reveals dynamic synaptic palmitoylation. *Nature.* 456, 904-909.

KASAHARA, K., NAKAYAMA, Y., NAKAZATO, Y., IKEDA, K., KUGA, T., YAMAGUCHI, N. 2007. Src signalling regulates completion of abscission in cytokinesis through ERK/ MAPK activation at the midbody. *J. Biol. Chem.* 282, 5327-5339.

KELLY, T., MUELLER, S.C., YEH, Y., CHEN, W.T. 1994. Invadopodia promote proteolysis of a wide range of extracellular matrix proteins. *J. Cell Physiol.* 158, 299-308.

KENNEDY, B.K., BARBIE, D.A., CLASSON, M., DYSON, N., HARLOW, E. 2000. Nuclear organization of DNA replication in primary mammalian cells. *Genes and Dev.* 14, 2855-2868.

KERYER, G., RIOS, R.M., LANDMARK, B, F., SKALHEGG, B., LOHMANN, S.M., BORNENS. M. 1993. A high-affinity binding protein for the regulatory subunit of cAMP-dependent protein kinase II in the centrosome of human cells. *Exp. Cell Res.*204, 230-240.

KETTENBACH, A.N., SCHWEPPE, D.K., FAHERTY, B.K., PECHENICK, D., PLETNEV, A.A., GERBER, S.A. 2011. Quantitative Phosphoproteomics Identifies Substrates and Functional Modules of Aurora and Polo-Like Kinase Activities in Mitotic Cells. *Sci. Signal.* 4, rs5. doi: 10.1126/scisignal.2001497.

KIM, J,B. 2005. Three-dimensional tissue culture models in cancer biology. *Semin. Cancer Biol.* 15, 365-377.

KIM, W., BENNETT, E.J., HUTTLIN, E.L., GUO, A., LI, J., POSSEMATO, A., SOWA, M.E., RAD, R., RUSH, J., COMB, M.J., HARPER, J.W., GYGI, S.P. 2011. Systematic and quantitative assessment of the ubiquitin-modified proteome. *Mol. Cell.* 44, 325-340.

KING, M.C., DRIVAS, T.G., BLOBEL, G. 2008. A network of nuclear envelope membrane proteins linking centromeres to microtubules. *Cell.* 134, 427-438.

KINOSHITA, E., KINOSHITA-KIKUTA, E., TAKIYAMA, K., KOIKE, T. 2005. Phosphate-binding Tag, a New Tool to Visualise Phosphorylated Proteins. *Molecular & Cellular Proteomics,* 749-757.

KITAMURA, R., SEKIMOTO, T., ITO, S., HARADA, S., YAMAGATA, H., MASAI, H., YONEDA, Y., YANAGI,
K. 2006. Nuclear import of Epstein-Barr virus nuclear antigen 1 mediated by NPI-1 (Importin alpha5) is up- and down-regulated by phosphorylation of the nuclear localization signal for which Lys379 and Arg380 are essential. *J. Virol.* 80, 1979-1991.

KNUDSEN, B. S., MIRANTI, C. K. 2006. The impact of cell adhesion changes on proliferation and survival during prostate cancer development and progression. *J. Cell. Biochem.* 99, 345-361.

KOBAYASHI, K., NAKAHORI, Y., MIYAKE, M., MATSUMURA, K., KONDO-LIDA, E., NOMURA, Y., SEGAWA, M., YOSHIOKA, M., SAITO, K., OSAWA, M., HAMANO, K., SAKAIHARA, Y., NONAKA, I., NAKAGOME, Y., KANAZAWA, I., NAKAMURA, Y., TOKUNAGA, K., TODA, T. 1998. An

ancient retrotransposal insertion causes Fukuyama-type congenital muscular dystrophy. *Nature.* 394, 388-392.

KOENIG, M., HOFFMAN, E.P., BERTELSON, C.J., MONACO, A.P., FEENER, C., KUNKEL, L.M. 1987. Complete cloning of the Duchenne muscular dystrophy (DMD) cDNA and preliminary genomic organization of the DMD gene in normal and affected individuals. *Cell*. 50, 509–517.

KOENIG, M.M BEGGS, A.G., MOYER, M., SCHERPF, S., HEINDRICH, K., BETTECKEN, T., MULLER, C.R., LINDLOF, M., KAARIAINEN, H. 1989. The molecular basis for Duchenne versus Becker muscular dystrophy: correlation of severity with type of deletion. *Am. J. Hum. Genet*. 45, 498–506.

KOLE, R., AND KRIEG, A.M. 2015. Exon skipping therapy for Duchenne muscular dystrophy. *Adv Drug Deliv Rev.* 87, 104-107.

KORYAKINA, Y., KNUDSEN, K. E., GIOELI, D. 2015. Cell cycle dependent regulation of androgen receptor function. *Endocr. Relat. Cancer.* 22, 249-264.

KRUDE, T., MUSAHL, C., LASKEY, R.A., KNIPPERS, R. 1996. Human replication proteins hCdc21, hCdc46 and P1Mcm3 bind chromatin uniformly before S-phase and are displaced locally during DNA replication. *J. Cell Sci.* 109. 309-318,

KUNDA, P., AND BAUM, B. 2009. The actin cytoskeleton in spindle assembly and positioning. *Trends Cell Biol.* 19, 174-179.

KUNZ, S., ROJEK, J.M., KANAGAWA, M., SPIROPOULOU, C.F., BARRESI, R., CAMPBELL, K.P., OLDSTONE, M.B. 2005. Posttranslational modification of alpha-dystroglycan, the cellular receptor for arenaviruses, by the glycosyltransferase LARGE is critical for virus binding. *J. Virol.* 79, 14282-14296.

KUTAY, U., BISCHOFF, F.R., KOSTKA, S., KRAFT, R., GORLICH, D. 1997. Export of importin alpha from the nucleus is mediated by a specific nuclear transport factor. *Cell.* 90, 1061-1071.

LA COUR, T., KIEMER, L., MOLGAARD, A., GUPTA, R., SKRIVER, K., BRUNAK, S. 2004. Analysis and prediction of leucine-rich nuclear export signals. *Protein Eng. Des. Sel.* 17, 527-536.

LAEMMLI, U.K. 1970. Cleavage of structural proteins during the assembly of the head of bacteriophage T4. *Nature.* 227, 680-685.

LAI, Y., THOMAS, G.D., YUE, Y., YANG, H.T., LI, D., LONG, C., JUDGE, L., BOSTICK, B., CHAMBERLAIN, J.S. TERJUNG, R.L. 2009. Dystrophins carrying spectrin-like repeats 16 and 17 anchor nNOS to the sarcolemma and enhance exercise performance in a mouse model of muscular dystrophy. *J. Clin. Invest.* 119, 624-635.

LAM, M.H., HOUSE, C.M., TIGANIS, T., MITCHELHILL, K. I., SARCEVIC, B., CURES, A., RAMSAY, R., KEMP, B.E., MARTIN, T.J., GILLESPIE, M.T. 1999. Phosphorylation at the cyclin-dependent kinases site (Thr85) of parathyroid hormone-related protein negatively regulates its nuclear localization. *J, Biol. Chem.* 274, 18559-18566.

LAMMERDING, J., HSAIO, J., SCHULZE, P.C., KOZLOV, S., STEWART, C.L., LEE, R.T. 2005. Abnormal nuclear shape and impaired mechanotransduction in emerin-deficient cells. *J. Cell Biol.* 170, 781-791.

LANGE, A., MILLS, R.E., LANGE, C.J., STEWART, M., DEVINE, S.E., CORBETT, A.H. 2007. Classical nuclear localisation signals: definition, function, and interaction with importin alpha. *J. Biol. Chem.* 282, 5101-5105.

LANGE, A., MCLANE, L.M., MILLS, R.E., DEVINE, S.E., CORBETT, A. H. 2010. Expanding the definition of the classical bipartite nuclear localisation signal. *Traffic*. 11, 311-323.

LANGENBACH, K.J. AND RANDO, T.A. 2002. Inhibition of dystroglycan binding to laminin disrupts the PI3k/AKT pathway and survival signalling in muscle cells. *Muscle Nerve.* 26, 644-653.

LARA-CHACON, B., DE LEON, M. B., LEOCADIO, D., GOMEZ, P., FUENTES-MERA, L., MARTINEZ-VIEYRA, I., ORTEGA, A., JANS, D. A. & CISNEROS, B. 2010. Characterization of an Importin alpha/beta-recognized nuclear localization signal in beta-dystroglycan. *J Cell Biochem,* 110, 706-17.

LAURENT, J., FROGIA, C., CAZALES, M., MONDESERT, O., DUCOMMUN, B., LOBJOIS, V. 2013. Multicellular tumor spheroid models to explore cell cycle checkpoints in 3D. *BMC Cancer.* 13

LAWO, S., HASEGAN, M., GUPTA, G.D., PELLETIER, L. 2012. Subdiffraction imaging of centrosomes reveals higher-order organizational features of pericentriolar material. *Nat. Cell Biol.* 14, 1148-1158.

LEE. K. A., HAMMERLE, L. P., ANDREWS, P.S., STOKES, M.P., MUSTELIN, T., SILVA, J.C., DOEDENS, J.R. (2011). Ubiquitin ligase substrate identification through quantitative proteomics at both the protein and peptide levels. *J. Biol Chem.*, 286, 41530-41538.

LEE, K.K., HARAGUCHI, T., LEE, R.S., KOUJIN, T., HIRAOKA, Y., WILSON, K.L. 2001. Distinct functional domains in emerin bind lamin A and DNA-bridging protein BAF. *J. Cell Sci.* 114, 4567-4573.

LEI, M. 2005. The MCM complex: Its role in DNA replication and implications for cancer therapy. *Curr. Cancer Drug targets.* 5, 365-380.

LEI, K., ZHU, X., XU, R., XU, T., ZHUANG, Y., HAN, M. 2012. Inner nuclear envelope proteins SUN1 and SUN2 play a prominent role in the DNA damage response. *Curr. Biol.* 22, 1609-1615.

LEOCADIO, D. 2014. Post-Translational Modifiation And Nuclear Targeting Of Beta-Dystroglycan. PhD Thesis. The University of Sheffield.

LEOCADIO, D., MITCHELL, A., WINDER, S.J. 2016. γ-secretase dependent nuclear targeting of Dystroglycan. *J Cell. Biochem.*117, 2149-2157.

LEONOUDAKIS, D., HUANG, G., AKHAVAN, A., FATA, J.E., SINGH, M., GRAY, J.W., MUSCHLER, J.L. 2014. Endocytic trafficking of laminin is controlled by dystroglycan and is disrupted in cancers. *J. Cell Sci.* 127, 4894-4903.

LEVENTAL, K.R., YU, H., KASS, L., LAKINS, J.N., EGEBALD, M., ERLER, J.T., FONG, S.F., CSISZAR, K., GIACCIA, S., WENWINGER, W., YAMAUCHI, M., GASSER, D.L., WEAVER, V.M. 2009. Matrix crosslinking forces tumour progression by enhancing integrin signalling. *Cell.* 139, 891-906.

LIDOV, H.G., SELIG, S., KUNKEL, L.M. 1995. Dp140: a novel 140 kDa CNS transcript from the dystrophin locus. *Hum. Mol. Genet.* 4, 77-81.

LIN, R.Z. AND CHANG, H.Y. 2008. Recent advances in three-dimensional multicellular spheroid culture for biomedical research. *Biotechnol. J.* 3, 1172-1184.

LIN, Y. Y., WHITE, R.J., TORELLI, S., CIRAK, S., MUNTONI, F., STEMPLE, D.L. 2011. Zebrafish fukutin family proteins link the unfolded protein response with dystroglycanopathies. *Hum. Mol. Genet.* 20, 1763-1775.

LINDER, M.E., DESCHENES, R.J.2007. Palmitoylation: policing protein stability and traffic. *Nat Rev Mol Cell Biol*.8, 74-84.

LINDSAY, M.E., HOLASKA, J.M., WELCH, K., PASCHAL, B.M., MACARA, I.G. 2001. Ran-binding protein 3 is a cofactor for Crm1-mediated nuclear protein export. *J. Cell Biol.* 153, 1391-1402.

LIPSCOMB, L., PIGGOTT, R.W., EMMERSON, T., WINDER, S.J. 2016. Dasatinib as a treatment for Duchenne muscular dystrophy. *Hum. Mol. Genet.* 25, 266-274.

LIU, X., DU, L., FENG, R. 2013. c-Src regulates cell cycle proteins expression through protein kinase B/glycogen synthase kinase 3 beta and extracellular signal-regulated kinases 1/2 pathways in MCF-7 cells. *Acta. Biochim. Biophys.* 45, 586-592.

LO, H.W., ALI-SEYED, M., WU, Y., BARTHOLOMEUSZ, G., HSU, S.C., HUNG, M.C. 2006. Nuclear-cytoplasmic transport of EGFR involves receptor endocytosis, importin β1 and CRM1. *J. Cell Biochem.* 98, 1570-1583.

LO, H.W., XIA, W., WEI, Y., ALI-SEYED, M., HUANG, S.F., HUNG, M.C. 2005. Novel prognostic value of nuclear epidermal growth factor receptor in breast cancer. *Cancer Res.* 65, 338-348.

LOESSNER, D., STOK, K.S., LUTOLF, M.P., HUTMACHER, D.W., CLEMENTS, J.A., RIZZI, S.C. 2010. Bioengineered 3D platform to explore cell-ECM interactions and drug resistance of epithelial ovarian cancer cells. *Biomaterials.* 31, 8494-8506.

LOMBARDI, M.L., JAALOUK, D.E., SHANAHAN, C.M., BURKE, B., ROUX, K.J., LAMMERDING, J. 2011. The interaction between nesprins and sun proteins at the nuclear envelope is critical for force transmission between the nucleus and cytoskeleton. *J Biol Chem.* 286, 26743–26753

LOSASSO, C., DI TOMMASO, F., SGAMBATO, A., ARDITO, R., CITTADINI, A., GIARDINA, B., PETRUCCI, T. C. & BRANCACCIO, A. 2000. Anomalous dystroglycan in carcinoma cell lines. *FEBS Lett,* 484, 194-8.

LOUVET-VALLEE, S. 2000. ERM proteins: from cellular architecture to cell signalling. *Biol. Cell* 92, 305-316.

LOVISA, SL, LEBLEU, V.S., TAMPE, B., SUGIMOTO, H., VADNAGARA, K., CARSTENS, J.L., WU, C.C., HAGOS, Y., BURCKHARDT, B.C., PENTCHEVA-HOANG, T., NISCHAL, H., ALLISON, J.P., ZEISBERG, M., KALLURI, R. 2015. Epithelial-to-mesenchymal transition induces cell cycle arrest and parenchymal damage in renal fibrosis. *Nat. Med.* 21, 998-1009.

LUCA, A.C., MERSCH, S., DEENEN, R.et al. 2013. Impact of the 3D microenvironment on phenotype, gene expression, and EGFR inhibition of colorectal cancer cell lines. *PLoS One.* 8, e59689.

LUDERS, J. AND STEARNS, T. 2007. Microtubule-organising centres: a re-evaluation. *Nat. Rev. Mol. Cell Biol.* 8, 161-167.

LUKE, Y. H., ZAIM, I., KARAKESISOGLOU, V.M., JAEGER, L., SELLIN, W., LU, M., SCHNEIDER, S., NEUMANN, A., BEIJER, A., MUNCK. M. 2008. Nesprin-2 Giant (NUANCE) maintains nuclear envelope architecture and composition in skin. *J. Cell Sci.* 121, 1887-1898.

LUMENG, C., PHELPS, S., CRAWFORD, G.E., WALDEN, P.D., BARALD, K., CHAMBERLAIN, J.S. 1999. Interactions between beta-2-syntrophin and a family of microtubule-associated serine/threonine kinases. *Nat. Neurosci.*2, 611-617.

LUXTON, G.W., GOMES, E.R., FOLKER, E. S., VINTINNER, E., GUNDERSEN, G.G. 2010. Linear arrays of nuclear envelope proteins harness retrograde actin flow for nuclear movement. *Science.* 329, 956-959.

LUXTON, G.W., AND GUNDERSON, G.G. 2011. Orientation and function of the nuclear-centrosomal axis during cell migration. *Curr. Opin. Cell Biol.* 23, 579-588.

LUZHNA, L., KATHIRIA, P., KOVALCHUK, O. 2013. Micronuclei in genotoxicity assessment: from genetics to epigenetics and beyond. *Front. Genet.* 4, 131.

MAISON, C., HORSTMANN, H., GEORGATOS, S.D. 1993. Regulated docking of nuclear membrane vesicles to vimentin filaments during mitosis. *J. Cell Biol.* 123, 133-144.

MALONE, C.J., MISNER, L., LE BOT, N., TSAI, M.C., CAMPBELL, J.M., AHRINGER, J., WHITE, J.G. 2003. The *C. elegans* Hook protein, ZYG-12, mediates the essential attachment between the centrosome and the nucleus. *Cell.* 115, 825-836.

MALUMBRES, M., AND BARBACID, M. 2009. Cell Cycle, CDKs and cancer: a changing paradigm. *Nat. Rev. Cancer.* 9, 153-166.

MANILAL, S., THI MAN, N., MORRIS, G.E. 1998. Colocalization of emerin and lamins in interphase nuclei and changes during mitosis. *Biochem. And Biophys. Res. Comm.* 249, 643-647.

MANSUR, N. R., MEYER-SIEGLER, J.C., WURZER, J.C. AND SIROVER, M.A. 1993. Cell cycle regulation of the glyceraldehyde-3-phosphate dehydrogenase/ uracil DNA glycosylase gene in normal human cells. *Nucleic Acids Res.* 21, 993-998.

MARTIN, C., CHEN, S., MAYA-MENDOZA, A., LOVRIC, J., SIMS, P.F.G., JACKSON, D.A. 2009. Lamin B1 maintains the functional plasticity of the nucleoli. *J. Cell Sci.* 122, 1551-1562.

MARTINEZ-VIEYRA, I. A., VASQUEZ-LIMETA, A., GONZALEZ-RAMIREZ, R., MORALES-LAZARO, S. L., MONDRAGON, M., MONDRAGON, R., ORTEGA, A., WINDER, S. J., CISNEROS, B. 2013. A role for β-Dystroglycan in the organisation and structure of the nucleus in myoblasts. *Biochem. Biophys. Acta.*1833 (3), 698-711.

MARTINS, R.P., FINAN, J.D., GUILAK, F., LEE, D.A. 2012. Mechanical regulation of nuclear structure and function. *Annu. Rev. Biomed. Eng.* 14, 431-455.

MASCKAUCHAN, T. N., SHAWBER, C.J., FUNAHASHI, Y., LI, C.M., KITAJEWSKI, J. 2005. Wnt/Beta-catenin signalling induces proliferation, survival and interleukin-8 in human endothelial cells. *Angiogenesis.* 8, 43-51.

MATHEW, G. 2011. The nuclear function of dystroglycan in prostate cancer. PhD Thesis. The University of Sheffield.

MATHEW, G., MITCHELL, A., DOWN, J.M., JACOBS, L. A., HAMDY, F.C., EATON, C., ROSARIO, D.J., CROSS, S.S., WINDER, S.J. 2013. Nuclear targeting of Dystroglycan promotes the expression of androgen regulated transcription factors in prostate cancer. *Sci. Rep.* 30, 2792

MATSUMURA, K., ZHONG, D., SAITO, F., ARAI, K., ADACHI, K., KAWAI, H., HIGUCHI, I., NISHINO, I, SHIMIZU, T. 2005. Proteolysis of beta-dystroglycan in muscular diseases. *Neuromuscul. Disord.* 15, 336-341.

MEIER, J., AND GEORGATOS, S.D. 1994. Type B lamins remain associated with the integral nuclear envelope protein p58 during mitosis: implications for nuclear reassembly. *EMBO J.* 13, 1888-1898.

MEJAT, A. AND MISTELI, T. 2010. LINC complexes in health and disease. *Nucleus.* 1, 40-52.

MERCURI, E. AND MUNTONI, F. 2013. Muscular Dystrophies. *Lancet.* 381, 845-860.

MEYER, A.J., ALMENDRALA, D.K., GO, M. M., WALD KRAUSS, S. 2010. Structural protein 4.1R is integrally involved in nuclear envelope protein localization, centrosome-nucleus association and transcriptional signalling. *J. Cell Sci.* 124, 1433-1444.

MEYER, T., BEGITT, A., LODIGE, I., VAN ROSSUM, M., VINKEMEIER, U. 2002. Constitutive and IFN gamma-induced nuclear import of STAT1 proceed through independent pathways. *Embo. J.* 21, 344354.

MEYERZON, M., FRIDOLFSSON, H.N., LY, N., MCNALLY, F.J., STARR, D.A. 2009. UNC-83 is a nuclear -specific cargo adaptor for kinesin-1-mediated nuclear migration. *Development.* 136, 2725-2733.

MILLER, G., MOORE, C. J., TERRY, R., LA RIVIERE, T., MITCHELL, A., PIGGOTT, R., DEAR, T. N., WELLS, D. J., WINDER, S. J. 2012. Preventing phosphorylation of dystroglycan ameliorates the dystrophic phenotype in MDX mouse. *Hum.Mol. Genet.* 21, 4508-4520.

MILLER, G., WANG, E.L., NASSAR, K.L., PETER, A.K., CROSBIE, R.H. 2007. Structural and functional analysis of the sarcoglycan-sarcospan subcomplex. *Exp. Cell Res.* 313, 639-651.

MILLER, M.R., MA, D., SCHAPPET, J., BREHENY, P., MOTT, S.L., BANNICK, N., ASKELAND, E., BROWN, J., HENRY, M.D. 2015. Downregulation of dystroglycan glycosyltransferases LARGE2 and ISPD associate with increased mortality in clear cell renal cell carcinoma. *Molecular Cancer.* 14, 141.

MINN, I. L., ROLLS, M. M., HANNA-ROSE, W., MALONE, C.J. 2009. SUN-1 and ZYG-12, mediators of centrosome nucleus attachment, are a functional SUN/ KASH pair in *Caenorhabditis elegans. Mol. Biol. Cell.* 20, 4586-4595.

MITCHELL, A., MATHEW, G., JIANG, T., HAMDY, F.C., CROSS, S.S., EATON, C.L., WINDER, S.J. 2013, Dystroglycan function is a novel determinant of tumor growth and behaviour in prostate cancer. *Prostate.*73, 389-408.

MIURA, P. AND JASMIN, B.J. 2006. Utrophin upregulation for treating Duchenne or Becker muscular dystrophy: how close are we? *Trends Mol. Med.*12, 122-129

MOIR, R.D., SPANN, T. P., LOPEZ-SOLER, R.I., YOON, M., GOLDMAN, A.E., KHUON, S., GOLDMAN, R.D. 2000a. Review: The dynamics of the nuclear lamins during the cell cycle-relationship between structure and function. *J. Struct. Biol.* 129, 324-334.

MOIR, R.D., YOON, M., KHUON, S., GOLDMAN, R.D. 2000b. Nuclear lamins A and B1: different pathways of assembly during nuclear envelope formation in living cells. *J. Cell Biol.* 151, 1155-1168.

MOIR, R.D., SPANN, T., HERRMANN, H., GOLDMAN, R.D. 2000c. Disruption of nuclear lamin organisation blocks the elongation phase pf DNA replication. *J. Cell Biol.* 149, 1179-1192.

MOORE, C. J. & WINDER, S. J. 2010. Dystroglycan versatility in cell adhesion: a tale of multiple motifs. *Cell Commun Signal,* 8, 3.

MOORE, C.J. & WINDER, S.J. 2012.The inside and out of dystroglycan post-translational modification. *Neuromusc. Disord.* 22, 959-965.

MOORE, M. S. 1998. Ran and nuclear transport. *J. Biol. Chem.* 273, 22857-22860.

MORAZ, M. L., PYTHOUD, C., TURK, R., ROTHENBERGER, S., PASGUATO, A., CAMPBELL, K.P., KUNZ, S.2013. Cell entry of Lassa virus induces tyrosine phosphorylation of dystroglycan. *Cell Microbiol.*15, 689-700.

MORENO-LAYSECA, P., STREULI, C.H. 2014. Signalling pathways linking integrins with cell cycle progression. *Matrix Biology.* 34, 144-153.

MORGAN, J.T., PFEIFFER, E.R., THIRKILL, T.L., KUMAR, P., PENG, G., FRIDOLFSSON, H.N., DOUGLAS, G.C., STARR, D.A., BARAKAT, A.I. 2011. Nesprin-3 regulates endothelial cell morphology, perinuclear cytoskeletal architecture, and flow-induced polarization. *Mol. Biol. Cell.* 22, 4324-4334.

MORGIA, G., FALASAPERLA, M., MALAPONTE G., MADONIA, M., INDELICATO, G., TRAVALI,S., MAZZARINO, M. C. 2005. Matrix metalloproteinases as diagnostic (MMP-13) and prognostic (MMP-2, MMP-9) markers of prostate cancer. *Urol. Res.* 33, 44-50.

MORITA, N., UEMURA, H., TSUMATANI, K., CHO, M., HIRAO, Y., OKAJIMA, E., KONISHI, N., HIASA, Y. 1999. E-cadherin and α-, β-, and γ-catenin expression in prostate cancers: correlation with tumour invasion. *British Journal of Cancer.* 79, 1879-1883.

MORITZ, M., BRAUNFELD, M.B., SEDAT, J.W., ALBERTS, B., AGARD, D.A. 1995. Microtubule nucleation by gamma-tubulin-containing rings in the centrosome. *Nature*. 378, 638–640.

MORO, L., VENTURINO, M., BOZZO, C., SILENGO, L., ALTRUDA, F., BEGUINOT, L., TARONE, G., DEFILIPPI, P. 1998. Integrins induce activation of EGF receptor: role in MAP kinase induction and adhesion-dependent cell survival. *EMBO J.* 17, 6622-6632.

MORRIS, G.E., MAN, N., PEREBOEV, A., KENDRICK-JONES, J., WINDER, S.J. 1999. Disruption of the utrophin-actin interaction by monoclonal antibodies and prediction of an acti-binding surface of utrophin. *Biochem. J.* 337, 119-123.

MOUDJOU, M., BORDES, N., PAINTRAND, M., BORNENS, M. 1996. γ-tubulin in mammalian cells: the centrosomal and cytosolic forms. *J. Cell Sci.* 109, 875-887.

MUCHIR, A., BONNE, G., VAN DER KOOI, A.J., VAN MEEGEN, M., BAAS, F., BOLHUIS, P.A., DE VISSER, M., SCHWARTZ, K. 2000. Identification of mutations in the gene encoding lamins A/C in autosomal dominant limb girdle muscular dystrophy with atrioventricular conduction disturbances (LGMD1B). *Hum. Mol. Genet.* 9, 1453-1459.

MULHOLLAND, D.J., CHENG, H., REID, K. RENNIE, P.S., NELSON, C.C. 2002. The androgen receptor can promote beta-catenin nuclear translocation independently of adenomatous polyposois coli. *J. Biol. Chem.* 17, 17933-17943.

MUNTONI, F., TORELLI, S., FERLINI, A. 2003. Dystrophin mutations: one gene, several proteins, multiple phenotypes. *Lancet Neurol.* 2, 731-740.

MURANEN, T., GRÖNHOLM, M., RENKEMA, G.H., CARPEN, O. 2005. Cell cycle-dependent nucleocytoplasmic shuttling of the neurofibromatosis 2 tumour suppressor merlin. *Oncogene.* 24, 1150-1158.

MURPHY, L.O., MACKEIGAN, J.P., BLENIS, J. 2004. A network of immediate early gene products propagates subtle differences in mitogen-activated protein kinase signal amplitude and duration. *Mol. Cell Biol.* 24, 144-153.

MURTHY, S., WU, M., BAI, V.U., HOU, Z., MENON, M., BARRACK, E.R., KIM, S.H., REDDY, G.P.R. 2013. Role of androgen receptor in progression of LNCaP prostate cancer cells from G_1 to S phase. *PLOS ONE.* e56692.

MUSACCHIO, A. AND SLAMON, E.D. 2007. The spindle-assembly checkpoint in space and time. *Nature Rev. Mol. Cell. Biol.* 8, 379-393.

MUSCHLER, J., LEVY, D., BOUDREAU, R., HENRY, M., CAMPBELL, K., BISSELL, M.J. 2002. A role for dystroglycan in epithelial polarization loss of function in breast tumor cells. *Cancer Res.* 62, 7102-7109.

MYERS, J.M., MARTINS, G.G., OSTROWSKI, J., STACHOWIAK, M.K. 2003. Nuclear trafficking of FGFR1: a role for the transmembrane domain. *J. Cell Biochem.* 88, 1273-1291.

NADEZHDINA, E.S., FAIS, D., CHENTSOV, Y.S. 1979. On the association of centrioles with the interphase nucleus. *Eur. J. Cell Biol.* 19, 109- 115.

NARDOZZI, J. D., LOTT, K. L., CINGOLANI, G. 2010. Phosphorylation meets nuclear import: a review. *Cell Commun Signal,* 8, 32.

NAWROTZKI, R., LOH, N.Y., RUEGG, M.A., DAVIES, K.E., BLAKE, D.J. 1998. Characterization of alpha-dystrobrevin in muscle. *J. Cell Sci.* 111, 2595-2605.

NEGI, S.S. AND OLSON, M.O. 2006. Effects of interphase and mitotic phosphorylation on the mobility and location of the nucleolar protein B23. *J. Cell Sci.* 119, 3676-3685.

NELSON, C.M. AND CHEN, C.S. 2002. Cell-cell signalling by direct contact increases cell proliferation via a PI3K-dependent signal. *FEBS Letters.* 514, 238-242.

NEWEY, S.E., HOWMAN, E.V., PONTING, C.P., BENSON, M.A., NAWROTZKI, R., LOH, N.Y., DAVIES, K.E., BLAKE, D.J. 2000. Alternative splicing of dystrobrevin regulates the stoichiometry of syntrophin binding to the dystrophin protein complex. *Curr. Biol.* 10, 1295-1298.

NEWPORT, J., AND YAN, H. 1996. Organization of DNA into foci during replication. *Curr. Op. Cell Biol.* 8, 365-368.

NIGG, E.A., STEARNS, T. 2011. The centrosome cycle: centriole biogenesis, duplication and inherent asymmetries. *Nat. Cell Biol.* 13, 1154-1160.

NIKOLAKAKI, E., MEIER, J., SIMOS, G., GEORGATOS, S.D., GIANNAKOUROS, T. 1997. Mitotic phosphorylation of the lamin B receptor by a serine/arginine kinase and p34(cdc2). *J. Biol. Chem.* 272, 6208-6213.

NIWA, T., SAITO, H., IMAJOH-OHMI, S., KAMINISHI, M., SETO, Y., MIKI, Y., NAKANISHI, A. 2009. BRCA2 interacts with the cytoskeletal linker protein plectin to form a complex controlling centrosome localization. *Cancer Sci.* 100, 2115- 2125.

NOBES, C.D. AND HALL, A. 1995. Rho, rac, and cdc42 GTPases regulate the assembly of multimolecular focal complexes associated with actin stress fibres, lamellipodia, and filopodia. *Cell.* 81, 53-62.

NURSE, P., THURIAX, P., NASMYTH, K. 1976. Genetic control of the cell division cycle in the fission yeast Schizosaccharomyces pombe. *Mol. Gen. Genet.* 146, 167-178.

NÜSSLEIN-VOLHARD, C. AND DAHM, R. 2002. Zebrafish: a practical approach. New York: Oxford University Press, 303.

OAK, S.A., RUSSO, K., PETRUCCI, T.C., JARRET, H.W. 2002. Mouse α1-syntrophin binding to Grb2: Further evidence of a role for syntrophin in cell signalling. *Biochemistry.* 40, 11270-11278.

OAKLEY, B.R., OAKLEY, C.E., YOON, Y., JUNG, K. 1990. γ-tubulin is a component of the spindle pole body that is essential for microtubule function is Aspergillus nidulans. *Cell.* 61, 1289-1301.

OBINO, D., FARINA, F., MALBEC, O., SAEZ, P.J., MAURIN, M., GAILLARD, J., DINGLI, F., LOEW, D., GAUTREAU, A., YUSEFF, M. A., BLANCHOIN, L., THERY, M., LENNON-DUMENIL, A.M. 2015. Actin nucleation at the centrosome controls lymphocyte polarity. *Nat. Comm.* 7:10969 doi: 10.1038/ncomms10969.

OLSEN, J.V., ONG, S., MANN, M. 2004. Trypsin cleaves exclusively C-terminal to arginine and lysine residues. *Mol. & Cell Proteomics.* 3, 608-614.

OLSON, M.F. AND SAHAI, E. 2009. The actin cytoskeleton in cancer cell motility. *Clin. Exp. Metastasis.* 26. 273-287.

OPPIZZI, M. L., AKHAVAN, A., SINGH, M., FATA, J. E. & MUSCHLER, J. L. 2008. Nuclear translocation of beta-dystroglycan reveals a distinctive trafficking pattern of autoproteolyzed mucins. *Traffic,* 9, 2063-72.

OTTAVIANO, Y., AND GERACE, L. 1985. Phosphorylation of the nuclear lamins during mitosis and interphase. *J. Biol. Chem.* 260, 624-632.

OXLEY, C.L., ANTHIS, N.J., LOWE, E.D., VAKONAKIS, I, CAMPBELL, I.D., WEGENER, K.L. 2008. An integrin phosphorylation switch: the effect of beta3 integrin tail phosphorylation of Dok1 and talin binding. *J. Biol. Chem.* 283, 5420-5426.

PAINTRAND, M., MOUDJOU, M., DELACROIX, H., BORNENS, M. 1992. Centrosome organisation and centriole architecture: their sensitivity to divalent cations. *J. Struct. Biol.* 108, 107-128.

PARBERRY-CLARK, C., BURY, J. P., CROSS, S. S. & WINDER, S. J. 2011. Loss of dystroglycan function in oesophageal cancer. *Histopathology,* 59, 180-7.

PATEL, J.T., BOTTRILL, A., PROSSER., S.L., JAYARAMAN, S., STRAATMAN, K., FRY, A.M., SHACKELTON, S. 2014. Mitotic phosphorylation of SUN1 loosens its connection with the nuclear lamina while the LINC complex remains intact. *Nucleus.* 5, 462-73.

PEARCE, M., BLAKE, D.J., TINSLEY, J.M., BYTH, B.C., CAMPBELL, L., MONACO, A.P., DAVIES, K.E. 1993. The utrophin and dystrophin genes share similarities in genomic structure. *Hum. Mol. Genet*. 2, 1765–1772.

PENG, H.B., ALI, A.A., DAGGETT, D.F., RAUVALA, H., HASSELL, J.R., SMALHEISER, N.R. 1998. The relationship between perlecan and dystroglycan and its implication in the formation of the neuromuscular junction. *Cell Adhes. Commun.* 5, 475-489.

PEREBOEV, A.V., AHMED, N., MAN, N., MORRIS, G.E. 2001. Epitopes in the interacting regions of β-dystroglycan (PPxY motif) and dystrophin (WW domain). *BBA,* 1527, 54-60.

PETROF, B.J. 1998. The molecular basis of activity-induced muscle injury in Duchenne muscular dystrophy. *Mol. Cell. Biochem.*179, 111-123.

PIEL, M., MEYER, P., KHODJAKOV, A., RIEDER, C.L., BORNENS, M. 2000. The respective contributions of the mother and daughter centrioles to centrosome activity and behaviour in vertebrate cells. *J. Cell Biol.* 149, 317-329.

PINTO, L.C., FAVARO, W.J., CAGNON, V.H.A. 2010. Proliferative, structural and molecular features of the *Mdx* mouse prostate. *Int. J. Exp. Path.* 91, 408-419.

PLANQUE, N. 2006. Nuclear trafficking of secreted factors and cell surface receptors: new pathways to regulate cell proliferation and differentiation and involvement in cancers. *Cell Comm. and Sig.*4

POLLICE, A.A., MCCOY, J. P., SHACKNEY, S.E., SMITH, C.A., AGARWAL, J., BURHOLT, D.R., JANOCKO, L.E., HORNICEK, F.J., SINGH, S.G., HARTSOCK, R.J. 1992. Sequential paraformaldehyde and methanol fixation for simultaneous flow cytometric analysis of DNA, cell surface proteins, and intracellular proteins. *Cytometry.*13, 432-444.

POZAROWSKI, P. AND DARZYNKIEWICZ, Z. 2004. Analysis of cell cycle by flow cytometry. *Methods Mol. Biol.* 281, 301-311.

PROKOCIMER, M., DAVIDOVICH, M., NISSIM-RAFINIA, M., WIESEL-MOTIUK, N., BAR, D.Z., BARKAN, R., MESHORER, E., GRUENBAUM, Y. 2009. Nuclear lamins: key regulators of nuclear structure and activities. *J. Cell Mol. Med.* 13, 1059- 1085.

PROVENZANO, P.P., ELICEIRI, K.W., CAMPBELL, J.M., INMAN, D.R., WHITE, J.G., KEELEY, P.J. 2006. Collagen reorganisation at the tumour-stroma interface facilitates local invasion. *BMC Med.* 4, 38.

PRUNUSKE, A.J. AND ULLMAN, K.S. 2006. The nuclear envelope: form and reformation. *Curr. Opin. Cell Biol.* 18, 108-116.

PUCKETT, R.L., MOORE, S.A., WINDER, T.L., WILLER, T., ROMANSKY, S.G., COVAULT, K.K., CAMPBELL, W.P., ABDENUR, J.E. 2009. Further evidence of Fukutin mutations as a cause of childhood onset limb-girdle muscular dystrophy without mental retardation. *Neuromuscul Disord.* 19, 352-356.

PUGACHEVA, E. N., ROEGIERS, F. & GOLEMIS, E. A. 2006. Interdependence of cell attachment and cell cycle signalling. *Curr Opin Cell Biol,* 18, 507-15.

RABE, B., VLACHOU, A., PANTE, N., HELENIUS, A., KANN, M. 2003. Nuclear import of hepatitis B virus caspids and release of the viral genome. *PNAS.* 100, 9849-9854.

RADU, A., NEUBAUER, V., AKAGI, T., HANAFUSA, H., GEORGESCU, M. 2003. PTEN induces cell cycle arrest by decreasing the level and nuclear localization of cyclin D1. *Mol. Cell Biol.* 23, 6139- 6149.

RAMASWAMY, S., NAKAMURA, N., VAZQUEZ, F., BATT, D.B., PERERA, S., ROBERTS, T.M., SELLERS, W.R. 1999.Biology Regulation of G1 progression by the PTEN tumor suppressor protein is linked to inhibition of the phosphatidylinositol 3-kinaseyAkt pathway. *Proc. Natl. Acad. Sci.* 96, 2110-2115.

RAMBUKKANA, A., YAMADA, H., ZANAZZI, G., MATHUS, T., SALZER, J.L., YURCHENCO, P.D., CAMPBELL, K.P., FISCHETTI, V.A. 1998. Role of alpha-dystroglycan as a Schwann cell receptor for Mycobacterium leprae. *Science.* 282, 2076-2079.

RASKA, I., SHAW, P.J., CMARKO, D. 2006. New insights into nucleolar architecture and activity. *Int. Rev. Cytol.* 255, 177-235.

RAVID, T. AND HOCHSTRASSER, M. 2008. Diversity of degradation signals in the ubiquitin-proteasome system. *Nat. Rev. Mol. Cell Biol.* 9, 679-689.

RAZAFSKY, D., HODZIC, D. 2009. Bringing KASH under the SUN: the many faces of nucleo-cytoskeletal connections. *J. Cell Biol.* 186, 461-472.

REILLY, J.F., AND MAHER, P.A. 2001. Importin beta-mediated nuclear import of fibroblast growth factor receptor: role in cell proliferation. *J. Cell Biol.* 152, 1307-1312.

RENTSCHLER, S., LINN, H., DEININGER, K., BEDFORD, M.T., ESPANEL, X., SUDOL, M. 1999. The WW domain of dystrophin requires EF-hands region to interact with β-dystroglycan. *Biological Chemistry.* 380, 431-442.

RIDLEY, A.J., SCHWARTZ, M.A., BURRIDGE, K., FIRTEL, R.A., GINSBERG, M.H., BORISY, G., PARSONS, J.T., HORWITZ, A.R. 2003. Cell migration: integrating signals from front to back. *Science.* 302, 1704-1709.

RIEMERSMA, M., MANDEL, H., VAN BEUSEKOM, E., GAZZOLI, I., ROSCIOLI, T., ERAN, A., GERSHONI-BARUCH, R., GERSHONI, M., PIETROKOVSKI, S., VISSERS, L.E., LEFEBER, D.J., WILLEMSEM, M.A., WEVERS, R.A., VAN BOKHOVEN, H. 2015. Absence of α- and β-dystroglycan is associated with Walker-Warburg syndrome. *Neurology.* 28, 2177-2182.

RIVIER, F., ROBERT, A., ROYUELA, M., HUGON, G., BONET-KERRACHE, A., MORNET, D. 1999. Dystrophin and utrophin complexed with different associated proteins in cardiac purkinje fibers. *Histochem. J.* 31, 425-432.

RO, S. AND YANG, L.X. 2004, Centrosomes- Their role in Tumors and cancer therapy. *Anticancer Res.* 24, 3269-3273.

ROBBINS, E., JENTZSCH, G., MICALI, A. 1968. The centriole cycle in synchronized HeLa cells. *J. Cell Biol*. 36, 329–39.

ROBERDS, S.L., ERVASTI, J.M., ANDERSON, R.D., OHLENDIECK, K., KAHL, S.D., ZOLOTO, D., CAMPBELL, K.P. 1993. Disruption of the dystrophin-glycoprotein complex in the cardiomyopathic hamster. *J. Biol. Chem.* 268, 11496-11499.

ROSNER, M., SCHIPANY, K., HENGSTSCHLAGER, M. 2013. Merging high-quality biochemical fractionation with a refined flow cytometry approach to monitor nucleocytoplasmic protein expression throughout the unperturbed mammalian cell cycle. *Nature Protocols,* 8, 602-626.

RUSSO, K., DI STASIO, E., MACCHIA, G., ROSA, G., BRANCACCIO, A., PETRUCCI, T.C. 2000. Characterization of the beta-dystroglycan-growth-factor receptor 2 (Grb2) interaction. *Biochem. Biophys. Res. Commun.* 274, 93-98.

SAITO, F., MOORE, S.A., BARRESI, R., HENRY, M.D., MESSING, A., ROSS-BARTA, S.E., COHN.R.D., WILLIAMSON, R.A., SLUKA, K.A., SHERMAN, D.L., BROPHY, P.J., SCHMELZER, J.D., LOW, P.A., WRABETZ, L., FELTRI, M.L., CAMPBELL, K.P. 2003. Unique Role of Dystroglycan in Peripheral Nerve Myelination, Nodal Structure, and Sodium Channel Stabilization. *Neuron.* 38, 747-758.

SAKAKI, M., KOIKE, H., TAKAHASHI, N., SASAGAWA, N., TOMIOKA, S., ARAHATA, K., ISHIURA, S. 2001. Interaction between emerin and the nuclear lamins. *J. Biochem* . 129, 321-327.

SAKAUE-SAWANO, A., KUROKAWA, H., MORIMURA, T., HANYU, A., HAMA, H., OSAWA, H., KASHIWAGI, S., FUKAMI, K., MIYATA, T., MIYOSHI, H., IMAMURA, T., OGAWA, M., MASAI, H., MIYAWAKI, A. 2008. Visualizing spatiotemporal dynamics of multicellular cell-cycle progression. *Cell.* 132, 487-498.

SALINA, D., BODOOR, K., ECKLEY, D.M., SCHROER, T.A., RATTNER, J.B., BURKE, B. 2002. Cytoplasmic dynein as a facilitator of nuclear envelope breakdown. *Cell.* 108, 97-107.

SALPINGIDOU, G., SMERTENKO, A., HAUSMANOWA-PETRUCEWICZ, I., HUSSEY, P.J., HUTCHISON, C.J. 2007. A novel role for the nuclear membrane protein emerin in association of the centrosome to the outer nuclear membrane. *J. Cell Biol.* 178, 897-904.

SCALTRITI, M. AND BASELGA, J. 2006. The epidermal growth factor receptor pathway: A model for targeted therapy. *Clin. Cancer Res.* 12, 5268-5272

SCHAFER, K. AND BRAUN, T. 1995. Monoclonal anti-FLAG antibodies react with a new isoform of rat MG2+ dependent protein phosphatase beta. *Biochem. Biophys. Res Commun.* 207, 708-714.

SCHAUSBERGER, E., EFERL, R., PARZEFALL W., CHABICOVSKY, M., BREIT, P., WAGNER, E. F., SCHULTE-HERMANN, R., GRASL-KRAUPP, B. 2003. Induction of DNA synthesis in primary mouse hepatocytes is associated with nuclear pro-transforming growth factor alpha and ERBB-1 and is independent of C-Jun. *Carcinogenesis.* 24, 835-841.

SCHRODER, J.E., TEGELER, M.R., GROβHANS, U., PORTEN, E., BLANK, M., LEE, J., ESAPA, C., BLAKE, D.J., KRÖGER, S. 2007. Dystroglycan regulates structure, proliferation and differentiation of neuroepithelial cells in the developing vertebrate CNS. *Dev. Biol.* 307, 62-78.

SCHNEIDER, M., KHALIL, A.A., POULTON, J., CASTILLEJO-LOPEZ, C., EGGER-ADAM, D., WODARZ, A., DENG, W.M., BAUMGARTNER, S. 2006. Perlecan and Dystroglycan act at the basal side of the Drosophila follicular epithelium to maintain epithelial organization. *Development.* 133, 3805-3815.

SCIANDRA, F., SCHNEIDER, M., GIARDINA, B., BAUMGARTNER, S., PETRUCCI, T.C., BRANCACCIO, A. 2001. Identification of the β-dystroglycan binding epitope within the C-terminal region of α-dystroglycan. *Eur. J. Biochem.* 268, 4590- 4597.

SGAMBATO, A. AND BRANCACCIO, A. 2005. The dystroglycan complex: from biology to cancer. *J. Cell Physiol.* 205, 163-169.

SGAMBATO, A., CAMERINI, A., AMOROSO, D., GENOVESE, G., DE LUCA, F., CECCHI, M., MIGALDI, M., RETTINO, A., VALSUANI, C., TARTARELLI, G., DONATI, S., SICLARI, O., ROSSI, G. & CITTADINI, A. 2007a. Expression of dystroglycan correlates with tumor grade and predicts survival in renal cell carcinoma. *Cancer Biol Ther,* 6, 1840-6.

SGAMBATO, A., CAMERINI, A., FARAGLIA, B., PAVONI, E., MONTANARI, M., SPADA, D., LOSASSO, C., BRANCACCIO, A. & CITTADINI, A. 2004. Increased expression of dystroglycan inhibits the growth and tumourigenicity of human mammary epithelial cells. *Cancer Biol Ther,* 3, 967-75.

SGAMBATO, A., CAMERINI, A., GENOVESE, G., DE LUCA, F., VIACAVA, P., MIGALDI, M., BONINSEGNA, A., CECCHI, M., SEPICH, C. A., ROSSI, G., ARENA, V., CITTADINI, A. & AMOROSO, D. 2010. Loss of nuclear p27(kip1) and alpha-dystroglycan is a frequent event and is a strong predictor of poor outcome in renal cell carcinoma. *Cancer Sci,* 101, 2080-6.

SGAMBATO, A., DE PAOLA, B., MIGALDI, M., DI SALVATORE, M., RETTINO, A., ROSSI, G., FARAGLIA, B., BONINSEGNA, A., MAIORANA, A. & CITTADINI, A. 2007b. Dystroglycan expression is reduced during prostate tumorigenesis and is regulated by androgens in prostate cancer cells. *J Cell Physiol,* 213, 528-39.

SGAMBATO, A., DI SALVATORE, M. A., DE PAOLA, B., RETTINO, A., FARAGLIA, B., BONINSEGNA, A., GRAZIANI, C., CAMERINI, A., PROIETTI, G. & CITTADINI, A. 2006. Analysis of dystroglycan regulation and functions in mouse mammary epithelial cells and implications for mammary tumorigenesis. *J Cell Physiol,* 207, 520-9.

SGAMBATO, A., MIGALDI, M., MONTANARI, M., CAMERINI, A., BRANCACCIO, A., ROSSI, G., CANGIANO, R., LOSASSO, C., CAPELLI, G., TRENTINI, G. P. & CITTADINI, A. 2003. Dystroglycan expression is frequently reduced in human breast and colon cancers and is associated with tumor progression. *Am J Pathol,* 162, 849-60.

SGAMBATO, A., TARQUINI, E., RESCI, F., DE PAOLA, B., FARAGLIA, B., CAMERINI, A., RETTINO, A., MIGALDI, M., CITTADINI, A., ZANNONI, G.F. 2006. Aberrant expression of alpha-dystroglycan in cervical and vulvar cancer. *Gynecol. Oncol.* 103, 397-404.

SHAH, S.P., ROTH, A., GOYA, R., OLOUMI, A., HA, G., ZHAO, Y., TURASHVILI, G., DING, J., TSE, K., HAFFARI, G., BASHASHATI, A., PRENTICE, L.M..APARICIO, A. ET AL. 2012.
The clonal and mutational evolution spectrum of primary triple-negative breast cancers. *Nature.* 486, 395-399.

SHANG, Z.J., ETHUNANDAN, M., GORECKI, D.C., BRENNAN, P.A. 2008. Aberrant expression of beta-dystroglycan may be due to processing by matrix metalloproteinases-2 and -9 in oral squamous cell carcinoma. *Oral Oncol.* 44, 1139-1146.

SHAY, J.W., PORTER, K.R., PRESCOTT, D.M. 1974. The surface morphology and fine structure of CHO (Chinese Hamster Ovary) cells following enucleation. *PNAS.* 71, 3059-3063.

SHCHERBATA, H.R., YATSENKO, A.S., PATTERSON, L., SOOD, V.D., NUDEL, U., YAFFE, D., BAKER, D., RUOHOLA-BAKER, H. 2007. Dissecting muscle and neuronal disorders in a drosophila model of muscular dystrophy. *EMBO J.* 26, 481-493.

SHEN, T. AND GUAN, J. 2001. Differential regulation of cell migration and cell cycle progression by FAK complexes with Src, PI3K, Grb7 and Grb2 in focal contacts. *FEBS Letters.* 499, 176-181.

SHEN, J. G., XU, C. Y., LI, X., DONG, M. J., JIANG, Z, N., WANG, J., WANG, L. B. 2012.
Dystroglycan is associated with tumour progression and patient survival in gastric cancer. *Pathol. Oncol. Res.* 18, 79-84.

SHERR, C.J. 1996. Cancer cell cycle. *Science.* 274, 1672-1677.

SHERR, C.J. AND ROBERTS, J.M. 1999. CDK-inhibitors: positive and negative regulators of G1-Phase progression. *Genes Dev.* 13, 1501-1512.

SHIMI, T., BUTIN-ISRAELI, V., ADAM, S.A., HAMANAKA, R.B., GOLDMAN, A.E., LUCAS, C.A., SHUMAKER., D.A., KOSAK, S.T., CHANDEL., N.S., GOLDMAN, R.D. 2011. The role of nuclear lamin B1 in cell proliferation and senescence. *Genes & Development.* 25, 2579-2593.

SHIMI, T., KITTISOPIKUL, M., TRAN, J., GOLDMAN, A.E., ADAM, S.A., ZHENG, Y., JAGAMAN, K., GOLDMAN, R.D. 2015. Structural organization of nuclear lamins A, C, B1, and B2 revealed by superresolution microscopy. *Mol. Biol. Cell.* 26, 4075-4086.

SHIMOJO, H., KOBAYASHI, M., KAMIGAITO, T., SHIMOJO, Y., FUKUDA, M. & NAKAYAMA, J. 2011. Reduced glycosylation of alpha-dystroglycan on carcinoma cells contributes to formation of highly infiltrative histological patterns in prostate cancer. *Prostate,* 71, 1151-1157.

SINGH, J., ITAHANA, Y., KNIGHT-KRAJEWSKI, S., KANAGAWA, M., CAMPBELL, K. P., BISSELL, M. J. & MUSCHLER, J. 2004. Proteolytic enzymes and altered glycosylation modulate dystroglycan function in carcinoma cells. *Cancer Res,* 64, 6152- 6159.

SOLINET, S., MAHMUD, K., STEWMAN, S.F., EL KADHI, K.B., DECELLE, B., TALJE, L., MA, A., KWOK, B.H., CARRENO, S. 2013. The actin-binding ERM protein moesin binds to and stabilises microtubules at the cell cortex. *J. Cell Biol.* 202, 251-260.

SONGYANG, Z., BLECHNER, S., HOAGLAND, N., HOEKSTRA, M.F., PIWNICA-WORMS, H., CANTLEY, L.C. 1994. Use of an oriented peptide library to determine the optimal substrates of protein kinases. *Curr. Biol.* 4, 973-982.

SOROKIN, S. 1962. Centrioles and the formation of rudimentary cilia by fibroblasts and smooth muscle cells. *J. Cell Sci.* 3, 207- 230.

SOTGIA, F., LEE, J.K., DAS, K., BEDFORD, M., PETRUCCI, T.C., MACIOCE, P., SARGIACOMO, M., BRICARELLI, F.D., MINETTI, C., SUDOL, M., LISANTI, M.P. 2000. Caveolin-3 directly interacts with the C-terminal tail of beta-dystroglycan. Identification of a central WW-like domain within caveolin family members. *J. Biol. Chem.* 275, 38048-38058.

SOTGIA, F., BONUCCELLI, G., BEDFORD, M., BRANCACCIO, A., MAYER, U., WILSON, M. T., CAMPOS-GONZALEZ, R., BROOKS, J. W., SUDOL, M. & LISANTI, M. P. 2003. Localization of phospho-beta-dystroglycan (pY892) to an intracellular vesicular compartment in cultured cells and skeletal muscle fibres in vivo. *Biochemistry,* 42, 7110-23.

SOTGIA, F., LEE, H., BEDFORD, M. T., PETRUCCI, T., SUDOL, M. & LISANTI, M. P. 2001. Tyrosine phosphorylation of beta-dystroglycan at its WW domain binding motif, PPxY, recruits SH2 domain containing proteins. *Biochemistry,* 40, 14585-92.

SPANN, T.P., MOIR, R.D., GOLDMAN, A.E., STICK. R. AND GOLDMAN, R.D. 1997. Disruption of nuclear lamina organisation alters the distribution of replication factors and inhibits DNA synthesis. *J. Cell Biol.* 136, 1201-1212.

SPENCE, H.J., CHEN, Y.J., BATCHELOR, C.L., HIGGINSON, J.R., SUILA, H., CARPEN, O., WINDER, S.J. 2004. Ezrin-dependent regulation of the actin cytoskeleton by beta-dystroglycan. *Hum. Mol. Genet.* 13, 1657-1668.

SPENCE, H. J., DHILLON, A. S., JAMES, M. & WINDER, S. J. 2004. Dystroglycan, a scaffold for the ERK-MAP kinase cascade. *EMBO Rep,* 5, 484-9.

STALNAKER, S.H., HASHMI, S., LIM, J.M., AOKI, K., PORTERFIELD, M., GUTIERREZ-SANCHEZ, G., WHEELER, J., ERVASTI, J.M., BERGMANN, C., TIEMEYER, M., WELLS, L. 2010. Site mapping and characterization of O-glycan structures on alpha-dystroglycan isolated from rabbit skeletal muscle. *J. Biol Chem.* 285: 24882-24891.

STEWART-HUTCHINSON, P.J., HALE, C.M., WIRTZ, D., HODZIC, D. 2008. Structural requirements for the assembly of LINC complexes and their function in cellular mechanical stiffness. *Exp. Cell. Res.* 314, 1892-1905.

STOKER, M., O'NEILL, C., BERRYMAN, S., WAXMAN, V. 1968. Anchorage and growth regulation in normal and virus-transformed cells. *Int. J. Cancer.* 3, 683-693.

STUURMAN, N., HEINS, S., AEBI, U. 1998. Nuclear lamins: their structure, assembly, and interactions. *J. Struct. Biol.* 122, 42-66.

SUAREZ-SANCHEZ, R., AGUILAR, A., WAGSTAFF, K.M., VELEZ, G., AZUARA-MEDINA, P.M., GOMEZ, P., VASQUEZ-LIMETA, A., HERNANDEZ-HERNANDEZ, O., LIEU, K.G., JANS, D.A., CISNEROS, B. 2014. Nucleocytoplasmic shuttling of the Duchenne muscular dystrophy gene product dystrophin Dp71 is dependent on the importin α/β and CRM1 nuclear transporters and microtubule motor dynein. *Biochim. Biophys. Acta.* 1843, 985-1001.

SUEL, K.E., GU, H., COOK, Y.M. 2008. Modular organization and combinatorial energetics of proline-tyrosine nuclear localization signals. *PLoS Biol.* 6, e137.

SUZUKI, A., YOSHIDA, M., YAMAMOTO, H., OZAWA, E. 1992. Glycoprotein-binding site of dystrophin is confined to the cysteine-rich domain and the first half of the carboxy-terminal domain. *FEBS Letters.* 308, 154-160.

SUZUKI, A., YOSHIDA, M., OZAWA, E. 1995. Mammalian alpha1- and beta1- syntrophin bind to the alternative splice-prone region of the dystrophin COOh terminus. *J. Cell Biol.* 128, 373-381.

SZETO, S.G., WILLIAMS, E.C., RUDNER, A.D., LEE, J.M. 2015. Phosphorylation of filamin A by Cdk1 regulates filamin A localization and daughter cell separation. *Exp. Cell Res.* 330, 248-266.

TADAYONI, R., RENDON, A., SORIA-JASSO, CISNEROS, B. 2012. Dystrophin Dp71: The smallest but multifunctional product of the Duchenne Muscular Dystrophy gene. *Mol. Neurobiol.* 45, 43-60.

TAKAYAMA, S., ISHII, S., IKEDA, T., MASAMURA, S., DOI, M., KITAJIMA, M. 2005. The relationship between bone metastasis from human breast cancer and integrin alpha (v) beta 3 expression. *Anticancer Res.*25, 79-83.

TALTS, J.F., ANDAC, Z., GOHRING, W., BRANCACCIO, A., TIMPL, R. 1999. Binding of the G domains of laminin alpha1 and alpha2 chains and perlecan to heparin, sulfatides, alpha-dystroglycan and several extracellular matrix proteins. *EMBO J.* 18, 863-870.

TANIGUCHI-IKEDA, M., MORIOKA, I, IIJIMA, K., TODA, T. 2016. Mechanistic aspects of the formation of α-dystroglycan and therapeutic research for the treatment of α-dystroglycanopathy: A review. *Mol. Aspects. Med.* 16, 30043-30047

TANG, X., FALLS, D.L., LI, X., LANE, T., LUSKIN, M.B. 2007. Antigen-retrieval procedure for bromodeoxyuridine immunolabeling with concurrent labelling of nuclear DNA and antigens damaged by HCl pretreatment. *J. Neurosci.* 27, 5837-5844.

TEIXIDO-TRAVESA, N., ROIG, J., LUDERS, J. 2012. The where, when and how of microtubule nucleation- one ring to rule them all. *J. Cell Sci.* 125, 4445-4456.

TERRIN, A., MONTERISI, S., STANGHERLIN, A., ZOCCARATO, A., KOSCINSKI, A., SURDO, N.C., MONGILLO, M., SAWA, A., JORDANIDES, N.E., MOUNTFORD, C., ZACCOLO, M. 2012. PKA and PDE4D3 anchoring to AKAP9 provides distinct regulation of cAMP signals at the centrosome. *J. Cell Biol.* 198, 607-621.

TETSU, O. AND MCCORMICK, F. 1999. Beta-catenin regulates expression of cyclin D1 in colon carcinoma cells. *Nature.* 398, 422-426.

THALMANN, G. N., ANEZINIS, P, E., CHANG, S., ZHAU, H. E., KIM, E., HOPWOOD, V. L., PATHAK, S., VON ESCHENBACH, A. C., CHUNG, L. W. K. 1994. Androgen-independent Cancer Progression and Bone Metastasis in the LNCaP model of Human Prostate Cancer. *Cancer Res,* 54, 2577-2581.

THI MAN, N., HELLIWELL, T.R., SIMMONS, C., WINDER, S.J., KENDRICK-JONES, J., DAVIES, K.E., MORRIS, G.E. 1995. Full-length and short forms of utrophin, the dystrophin-related protein. *FEBS Letters.* 358, 262–266.

THOMAS, D.B. AND LINGWOOD, C.A. 1975. A model of cell cycle control: effects of thymidine on synchronous cell cultures. *Cell*. 5, 37-42.

THOMSON, A. A., CUNHA, G. R., MARKER, P. C. 2008. Prostate development and pathogenesis. *Differentiation.* 76, 559-564.

THOMPSON, L.J., BOLLEN, M., FIELDS, A.P. 1997. Identification of protein phosphatase 1 as a mitotic lamin phosphatase. *J. Biol. Chem.* 272, 29639-29697.

THOMPSON, O., MOORE, C. J., HUSSAIN, S. A., KLEINO, I., PECKHAM, M., HOHENESTER, E., AYSCOUGH, K. R., SAKSELA, K. & WINDER, S. J. 2010. Modulation of cell spreading and cell-substrate adhesion dynamics by dystroglycan. *J Cell Sci,* 123, 118-27.

THOMPSON, O., KLEINO, I., CRIMALDI, L., GIMONA, M., SAKSELA, K., WINDER, S.J. 2008. Dystroglycan, Tks5 and Src mediated assembly of podosomes in myoblasts. *PLoS One.* 3, e3638

TISI, D., TALTS, J.F., TIMPL, R., HOHENESTER, E. 2000. Structure of the C-terminal laminin G-like domain pair of the laminin alpha2 chain harbouring binding sites for alpha-dystroglycan and heparin. *EMBO J,* 19, 1432-1440.

TOMLINS, S. A., RHODES, D. R., PERNER, S., DHANASEKARAN, S. M., MEHRA, R., SUN, X. W., VARAMBALLY, S., CAO, X., TCHINDA, J., KUEFER, R., LEE, C., MONTIE, J. E., SHAH, R. B., PIENTA, K. J., RUBIN, M. A. & CHINNAIYAN, A. M. 2005. Recurrent fusion of TMPRSS2 and ETS transcription factor genes in prostate cancer. *Science,* 310, 644-8.

TORELLI, S., FERLINI, A., OBICI, L., SEWRY, C., MUNTONI, F. 1999. Expression, regulation and localisation of dystrophin isoforms in human foetal skeletal and cardiac muscle. *Neuromusc. Disord.* 9, 541-551.

TORII, S., YAMAMOTO, T., TSUCHIYA, Y., NISHIDA, E. 2006. ERK MAP kinase in G_1 cell cycle progression and cancer. *Cancer Sci.* 97, 697-702.

TOWBIN, H., STAEHELIN, T., GORDON, J. 1979. Electrophoretic transfer of proteins from polyacrylamide gels to nitrocellulose sheets: procedure and some applications. *Proc. Natl. Acad. Sci. USA.* 76, 4350-4354.

TRAN, T.D., LIM, J.M., LIU, M., STALNAKER.S.H., WELLS, L., TEN HAGEN, K.G., LIVE, D. 2012. Glycosylation of α-Dystroglycan: O- mannosylation influences the subsequent addition of GalNAc by UDP-GalNAc polypeptide N-acetylgalactosaminyltransferases. *J. Bio. Chem.* 287, 20967-20974.

TSAI, R.Y.L., AND PEDERSON, T. 2014. Connecting the nucleolus to the cell cycle and human disease. *FASEB J.* 28, 3290-3296.

TSOU, M.F., AND STEARNS, T. 2006. Mechanism limiting centrosome duplication to once per cell cycle. *Nature.* 442, 947-951.

VAN DIJK, M., GORANSSON, S.A., STROMBLAD, S. 2013. Cell to extracellular matrix interactions and their reciprocal nature in cancer. *Exp. Cell. Res.* 319, 1663-1670.

VAN STEENBRUGGE, G.J., VAN UFFELEN, C.J.C., BOLT, J., SCHRODER, F.H. 1991. The human prostatic cancer cell line LNCaP and its derived sublines: an in vitro model for the study of androgen sensitivity. *J. Steroid Biochem. Molec. Biol.* 40, 207-214.

VASQUEZ-LIMETA, A., WAGSTAFF, K.M., ORTEGA, A., CROUCH, D.H., JANS, D.A., CISNEROS, B. 2014. Nuclear import of β-dystroglycan is facilitated by Ezrin-mediated cytoskeleton reorganization. *PLOS one,* 9, e90629.

VILLARREAL-SILVA, M., CENTENO-CRUZ, F., SUAREZ-SANCHEZ, R., GARRIDO, E. & CISNEROS, B. 2011. Knockdown of dystrophin dp71 impairs PC12 cells cycle: localization in the spindle and cytokinesis structures implies a role for dp71 in cell division. *PLoS One,* 6, e23504.

VILLARREAL-SILVA, M., SUAREZ-SANCHEZ, R., RODRIGUEZ-MUNOZ, R., MORNET, D. & CISNEROS, B. 2010. Dystrophin Dp71 is critical for stability of the DAPs in the nucleus of PC12 cells. *Neurochem Res,* 35, 366-73.

WALKER, J.L., AND ASSOIAN, R.K. 2005. Integrin-dependent signal transduction regulating cyclin D1 expression and G1 phase cell cycle progression. *Cancer Metastasis Rev.* 24, 383-393.

WALKER, J.L., FOURNIER, A.K., ASSOIAN, R.K. 2005. Regulation of growth factor signalling and cell cycle progression by cell adhesion and adhesion-dependent changes in cellular tension. *Cytokine & Growth Factor Reviews.* 16, 395-405.

WALTER, J., SUN, L., NEWPORT, J. 1998. Regulated chromosomal DNA replication in the absence of a nucleus. *Mol. Cell.* 1, 519-529.

WANG, Y.N. and HUNG, M.C. 2012. Nuclear functions and subcellular trafficking mechanisms of the epidermal growth factor receptor family. *Cell and Bioscience.* 2:13.

WANG, Y.N., LEE, H.H., LEE, H.J., DU, Y., YAMAGUCHI, H., HUNG, M.C. 2012. Membrane-bound trafficking regulates nuclear transport of integral epidermal growth factor receptor (EGFR) and ErbB-2. *J. Biol. Chem.* 287, 16869-16879.

WANG, Y.N., WANG, H., YAMAGUCHI, H., LEE, H.J., LEE, H.H., HUNG, M.C. 2010a. COPI-mediated retrograde trafficking from the golgi to the ER regulates EGFR nuclear transport. *Biochem. Biophys. Res. Commun.* 399, 498-504.

WANG, Y.N., YAMAGUCHI, H., HUO, L., DU, Y., LEE, H.J., LEE, H.H., WANG, H., HSU, J.M., HUNG, M.C. 2010b. The translocon sec61β localised in the inner nuclear membrane transports membrane-embedded EGF receptor to the nucleus. *J. Biol. Chem.* 285. 38720-38729.

WEILING, H., XIAOWEN, Y., CHUNMEI, L., JIANPING, X. 2013. Function and evolution of ubiquitous bacterial signalling adapted phosphopeptide recognition domain FHA. *Cell Signal.* 25, 660- 665.

WEIR, M. L., OPPIZZI, M. L., HENRY, M. D., ONISHI, A., CAMPBELL, K. P., BISSELL, M. J. & MUSCHLER, J. L. 2006. Dystroglycan loss disrupts polarity and beta-casein induction in mammary epithelial cells by perturbing laminin anchoring. *J Cell Sci,* 119, 4047-58.

WEISE, C., AND ZHENG, Y.A. 2000. A new function for the γ-tubulin ring complex as a microtubule minus end cap. *Nat. Cell Biol.* 2, 358-364.

WEN, W., MEINKOTH, J.L., TSIEN, R.Y., TAYLOR, S.S. 1995. Identification of a signal for rapid export of proteins from the nucleus. *Cell.* 82, 463-473.

WILHELMSEN, K., LITJENS, S.H.M., KUIKMAN, I., TSHIMBALANGA, N., JANSSEN, H., VAN DEN BOUT, I., RAYMOND, K., SONNENBERG, A. 2005. Nesprin-3, a novel outer nuclear membrane protein, associates with the cytoskeletal linker protein plectin. *J. Cell Biol.* 171, 799-810.

WILKIE, G.S., KORFALI, N., SWANSON, S.K., MALIK, P., SRSEN, V., BATRAKOU, D.G., DE LAS HERAS, J., ZULEGER, N., KERR, A.R.W., FLORENS, L., SCHIRMER, E.C. 2011. Several novel nuclear envelope transmembrane proteins identified in skeletal muscle have cytoskeletal associations. *Mol. And Cell. Proteomics.* 10, 1-16

WILLIAMS, C.C., ALLISON, J.G., VIDAL, G.A., BURROW, M.E., BECKMAN, B.S., MARRERO, L., JONES, F.E. 2004. The ERBB4/HER4 receptor tyrosine kinase regulates gene expression by functioning as a STAT5A nuclear chaperone. *J. Cell Biol.* 167, 469-478.

WILLIAMSON, R.A., HENRY, M.D., DANIELS, K.J., HRSTKA, R.F., LEE, J.C., SUNADA, Y., IBRAGHIMOV-BESKROVNAYA, O., CAMPBELL, K.P. 1997. Dystroglycan is essential for early embryonic development: distribution of Reichert's membrane in Dag1-null mice. *Hum. Mol. Genet.* 6, 831-841.

WILSON, M.D., SOPONARO, M., LEIDL, M.A.., SVEJSTRUP, J.Q. (2012) MultiDsk: A Ubiquitin-Specific Affinity Resin. PLOS One, 7 (10), e6398.

WINDER, S.J. 2001. The complexities of Dystroglycan. *Trends Biochem Sci.* 26, 118-124.

WINDER, S.J., AND KENDRICK-JONES, J. 1995. Calcium/calmodulin-dependent regulation of the NH2-terminal F-actin binding domain of utrophin. *FEBS Letters.* 357, 125–128.

WOLFE, M.S. 2010. Structure, mechanism and inhibition of gamma-secretase and presenilin-like proteases. *Biol. Chem.* 391, 839-847.

WORMAN, H.J. 2012. Nuclear lamins and laminopathies. *J. Pathol.* 226, 316-325.

WORMAN, H.J., OSTLUND, C., WANG, Y. 2010. Diseases of the nuclear envelope. *Cold Spring Harb. Perspect. Biol.* 2, a000760.

WORMAN, H.J., YUAN, J., BLOBEL, G., GEORGATOS, S.D. 1988. A lamin B receptor in the nuclear envelope. *Proc. Natl. Acad. Sci. USA.* 85, 8531-8534.

WU, J., MISRA, G., RUSSELL, R.J., LADD, A.J., LELE, T.P., DICKINSON, R.B. 2011, Effects of dynein on microtubule mechanics and centrosome positioning. *Mol. Biol. Cell.* 22, 4834-4841.

XU, J., RODRIGUEZ, D., PETITCLERC, E., KIM, J.J., HANGAI, M., MOON, Y.S., DAVIS, G.E., BROOKS, P.C. 2001. Proteolytic exposure of a cryptic site within collagen type IV is required for angiogenesis amd tumor growth in vivo. *J. Cell Biol.* 154, 1069-1079.

XU, L.N., XU, B.N., CAI, J., YANG, J.B., LIN, N. 2013. Tumor-associated fibroblast-conditioned medium promotes tumor cell proliferation and angiogenesis. *Genetics and Molecular Research.* 12, 5863- 5871.

YAMADA, H., SAITO, F., FUKUTA-OHI, H., ZHONG, D., HASE, A., ARAI, K., OKUYAMA, A., MAEKAWA, R., SHIMIZU, T., MATSUMURA, K. 2001. Processing of b-dystroglycan by matrix metalloproteinase disrupts the link between the extracellular matrix and cell membrane via the Dystroglycan complex. *Hum. Mol. Genet.* 10, 1563-1569.

YAMADA, H., SHIMIZU, T., TANAKA, T., CAMPBELL, K.P., MATSUMURA, K. 1994. Dystroglycan is a binding protein of laminin and merosin in peripheral nerve. *FEBS Lett.* 352, 49-53.

YAMAKITA, Y., TOTSUKAWA, G., YAMASHIRO, S., FRY, D., ZHANG, X., HANKS, S.K., MATSUMURA, F. 1999. Dissociation of FAK/p130(CAS)/c-Src complex during mitosis: role of mitosis specific serine phosphorylation of FAK. *J. Cell Biol.* 144, 315-324.

YANG, B., JUNG, D., MOTTO, D., MEYER, J., KORETZKY, G., CAMPBELL, K.P. 1995. SH3 domain mediated interaction of dystroglycan and Grb2. *J. Biol. Chem.* 270, 11711-11714.

YANG, L., GUAN, T., GERACE, L. 1997. Integral membrane proteins of the nuclear envelope are dispersed throughout the endoplasmic reticulum during mitosis. *J. Cell Biol.* 137, 1199-1210.

YATSENKO, A.S., KUCHERENKO, M.M., PANTOJA, M., FISCHER, K.A., MADEOY, J., DENG, W.M., SCHNEIDER, M., BAUMGARTNER, S., AKEY, J., SHCHERBATA, H.R., RUOHOLA-BAKER, H. 2009. The conserved WW-domain binding sites in Dystroglycan C-terminus are essential but partially redundant for Dystroglycan function*. BMC Dev Biol* .9, 18.

YE, Q., AND WORMAN, H. J. 1994. Primary structure analysis and lamin B and DNA binding of human LBR, an integral protein of the nuclear envelope inner membrane. *J. Biol. Chem.* 269, 11306-11311.

YONEMURA, S., HIRAO, M., DOI, Y., TAKAHASHI, N., KONDO, T., TSUKITA. S., TSUKITA, S. 1998. Ezrin/ Radixin/ Moesin (ERM) proteins bind to a positively charged amino acid cluster in the juxta-membrane cytoplasmic domain of CD44, CD43, and ICAM-2. *J. Cell Biol.* 140, 885-895.

YONEMURA, S., NAGAFUCHI, A., SATO, N., TSUKITA, S. 1993. Concentration of an integral membrane protein, CD43 (Leukosialin, sialophorin), in the cleavage furrow through the interaction of its cytoplasmic domain with actin-based cytoskeletons. *J. Cell Biol.* 120, 437-449.

YONGMIN, X., YANWEN, Z., HARRY, W.J. 2009. Dystrophin glycoprotein complex-associated Gbetagamma subunits activate phosphatidylinositol-3-kinase/Akt signaling in skeletal muscle in a laminin-dependent manner. *J Cell Physiol*. 219, 402-414.

YOSHIDA, M. AND OZAWA, E. 1990. Glycoprotein complex anchoring dystrophin to sarcolemma. *J. Biochem.* 108, 748-752.

YOSHIDA, M., HAMA, H., ISHIKAWA-SAKURAI, M., IMAMURA, M., MIZUNO, Y, ARAISHI, K., WAKABAYASHI-TAKAI, E., NOGUCHI, S., SASAOKA, T., OZAWA, E. 2000. Biochemical evidence for association of dystrobrevin with the sarcoglycan-sarcospan complex as a basis for understanding sarcoglycanopathy. *Hum. Mol. Genet.* 9, 1033-1040.

YOSHIDA, M., SUZUKI, A., YAMAMOTO, H., NOGUCHI, S., MIZUNO, Y., OZAWA, E. 1994. Dissociation of the complex of dystrophin and its associated proteins into several unique groups by n-octyl-D-glucoside. *Eur. J. Biochem.* 222, 1055-1061.

YOSHIDA-MORIGUCHI, T., YU, L., STALNAKER, S.H., DAVIS, S., KUNZ, S., MADSON, M., OLDSTONE, M.B., SCHACHTER, H., WELLS, L., CAMPBELL, K.P. 2010. O-mannosyl phosphorylation of alpha-dystroglycan is required for laminin binding. *Science.* 327, 88-92.

YOSHIDA-MORIGUCHI, T., AND CAMPBELL, K.P. 2015. Matriglycan: a novel polysaccharide that links dystroglycan to the basement membrane. *Glycobiology.* 7, 702-713.

YUAN, X., LI, T., WANG, H., ZHANG, T., BARUA, M., BORGESI, R.A., BUBLEY, G.J., LU, M.L., BALK, S.P. 2006. Androgen receptor remains critical for cell cycle progression in androgen-independent CWR22 prostate cancer cells. *AJP.* 169, 682-696.

YUAN, X., WU, H., XU, H., XIONG, H., CHU, Q., YU, S., WU, G.S., WU, K. 2015. Notch signaling: an emerging therapeutic target for cancer treatment. *Cancer Lett.* 369, 20-27.

ZHANG, Q., BETHMANN, C., WORTH, N.F., DAVIES, J.D., WASNER, C., FEUER, A., RAGNAUTH, C.D., YI, Q., MELLAD, J.A., WARREN, D.T., WHEELER, M.A., ELLIS, J.A., SKEPPER, J.N., VORGERD, M., SCHLOTTER-WEIGEL, B., WEISSBERG, P.L., ROBERTS, R.G., WEHNERT, M., SHANAHAN, C.M. 2007. Nesprin-1 and -2 are involved in the pathogenesis of Emery-Dreifuss muscular dystrophy and are critical for nuclear envelope integrity. *Hum. Mol. Genet.* 16, 2816-2833.

ZHANG, Q., RAGNAUTH, C., GREENER, M.J., SHANAHAN, C.M., ROBERTS, R.G. 2002. The nesprins are giant actin-binding proteins, orthologous to Drosophila melanogaster muscle protein MSP-300. *Genomics.* 80, 473-481.

ZHANG, W. AND LIU, H. T. 2002, MAPK signal pathways in the regulation of cell proliferation in mammalian cells. *Cell Research.* 12, 9-18.

ZHANG, X., LEI, K., YUAN, X., WU, X., ZHUANG, Y., XU, T., XU, R., HAN, M. 2009. SUN1/2 and Syne/Nesprin-1/2 complexes connect centrosome to the nucleus during neurogenesis and neuronal migration in mice. *Neuron.* 64, 173-187.

ZHONG, D., SAITO, F., SAITO, Y., NAKAMURA, A., SHIMIZU, T. & MATSUMURA, K. 2006. Characterization of the protease activity that cleaves the extracellular domain of beta-dystroglycan. *Biochem Biophys Res Commun,* 345**,** 867-71.

ZHOU, K., ROLLS, M.M., HALL, D.H., MALONE, C.J., HANNA-ROSE, W. 2009. A ZYG-12 dynein interaction at the nuclear envelope defines cytoskeletal architecture in the *C. elegans* gonad. *J. Cell Biol.* 186, 229-241.

ZIELINSKA, D.F., GNAD, F., WISNIEWSKI, J.R., MANN, M. 2010. Precision mapping of an in vivo N-glycoproteome reveals rigid topological and sequence constraints. *Cell.* 141, 897-907.

ZIEVE, G.W., TURNBULL, D., MULLINS, J.M., MCINTOSH, J.R. 1980. Production of large numbers of mitotic mammalian cells by use of the reversible microtubule inhibitor nocodazole: nocodazole accumulated mitotic cells. *Exp. Cell Res.* 126, 397-405.

ZUTTER, M.M., SANTORO, S.A., STAATZ, W.D., TSUNG, Y.L. 1995. Re-expression of the alpha 2 beta 1 integrin abrogates the malignant phenotype of breast carcinoma cells. *Proc Natl Acad Sci U S A.*, 92, 7411-7415.